STUDIES ON SLOW RELEASE ANTIBIOTIC MIDDLE EAR PELLETS

Emma Hoskison MA MB BChir

Thesis submitted to the University of Nottingham for the degree of Doctor of Philosophy

May 2018

ABSTRACT

Otitis Media with Effusion (OME) is the commonest cause of paediatric hearing impairment globally. Antibiotic laden pellets placed in the middle ear (ME) present a potential novel treatment strategy for OME disrupting the middle ear biofilm and avoiding systemic side effects. *In vitro* studies of *Staphylococcus Aureus* biofilm eradication with pellets laden with rifampicin and clindamycin demonstrate a future potential OME treatment and this study aims to establish the safety of these pellets *in vivo*.

Rifampicin (1.8mM) and clindamycin (35.3mM) loaded pellets made of poly lactic-co-glycolic acid and pluronic were surgically placed in guinea pig middle ears.

Auditory Brainstem Responses (ABRs) thresholds between 8-30 kHz were tested over 16 weeks alongside controls to assess for ototoxicity; amplitudes and latencies studied to assess for neurotoxicity. At one week post insertion of antibiotic laden pellets, marked ABR threshold elevation (15-40 dB) was observed and persisted (25-40 dB) at week 16 without accompanying changes in ABR wave amplitudes and latencies. This pattern therefore does not support a neurotoxic mechanism.

Representative cytocochleograms and immunofluorescence of the cochleas did not exhibit any appreciable frank outer or inner hair cell loss from the guinea pigs loaded with rifampicin and clindamycin pellets. This suggests that the pellets are not causing threshold elevation via an ototoxic mechanism.

ME histology revealed pellet remnants causing a moderate inflammatory response persisting at 16 weeks. With evidence of chronic inflammation in the middle ear, an associated ME effusion which has been undetected experimentally may underlie the ABR threshold elevation seen with rifampicin and clindamycin laden pellets. Confined to the middle ear, this may also explain the lack of IHC and OHC damage.

As a delivery vehicle to the ME, PLGA and Pluronic pellets have potential, but further studies are required on their antibiotic carriage to the middle ear before *in vivo* use.

PUBLICATIONS

Hoskison, E., Daniel, M., Al-Zahid, S., Shakesheff, KM., Bayston, R., Birchall, J.P. Drug Delivery to the ear *Ther Deliv* 2013;4:115-24

CONFERENCE PRESENTATIONS

ORS Liverpool (9/10/2015). Studies to establish the safety of middle ear pellets using ABR, cytocochleograms and histology. Hoskison E, Daniel M, Mulheran M, Furness D, Bayston R, Birchall JP

CHOLE Edinburgh (5/6/2016): Studies to establish the safety of middle ear pellets Hoskison E, Daniel M, Mulheran M, Furness D, Bayston R, Birchall JP

ACKNOWLEDGEMENTS

I would like to sincerely thank my supervisors for their help, support and guidance at every stage during this PhD. My original supervisors Professor JP Birchall and Dr Mike Mulheran were instrumental in setting up the PhD, guiding the scientific work, encouraging the progression of the experimental work and initial stages of write up. During the final year of my PhD I would like to acknowledge the great help and support given to me by Professor David Baguley and Professor Doug Hartley. Without their intervention I would not have progressed and for that I am immensely grateful.

There have been numerous colleagues who I have had the pleasure of meeting and working with throughout this PhD. The OME research group in Nottingham allowed open discussion of the results at stages during the experimental work. The group consisted of Professor Roger Bayston, Dr Mat Daniel, Professor Kevin Shakesheff, Dr Saif Al-Zaid and Katie Belfield.

Dr Mat Daniel, Mr Ali Qureishi and Mr Saif Al-Zahid were instrumental in pellet design and manufacture at the University of Nottingham and I am grateful for the provision of the pellets for the *in vivo* work.

The experiments were kindly hosted by Professor Ian Forsythe in the department of neurosciences in Leicester. I worked alongside many helpful and supportive colleagues there including Dr Emmanuelle Schiavon and Dr Deborah Linley. Dr Jennifer Edwards also kindly helped with her expertise in preparing and processing the histology slides.

Deborah Bursnall assisted me with the experiments as did the other staff members at the Clinical Research Facility and I appreciate their support and expertise.

At the University of Keele, Professor David Furness kindly allowed me to visit and use the Nomarski microscope for the cytocochleogram stage of the analysis. He also added his valuable expertise in the preparation of the slides and cell analysis.

During my PhD I have not only developed as a scientist, but as a mother of three wonderful boys: Thomas, Michael and Edward. I hope that the skills and knowledge that I have developed during this PhD will one day be inspirational to the next generation of scientists and I shall encourage all three of them to follow a similar academic pathway.

My father Ian has been unwavering in his support and taught me to follow my ambitions and my late mother, Eileen showed me there are no limits of what can be achieved with hard work and determination - attributes also passed onto my brother Peter.

Most of all, I dedicate this thesis to my husband David Byrne who I am blessed to have at my side as my critic, motivator and best friend.

"Remember to look up at the stars and not down at your feet" Stephen Hawking (1942-2018)

FINANCIAL SUPPORT

This PhD was supported by financial awards from the Midlands Institute of Otology (2012) and Action on Hearing Loss (2013).

The research was awarded the Otorhinolaryngological Research Society Xomed-Treace Prize which allowed me to attend the American Academy in Orlando 2014.

DECLARATION

I certify that this is my own work, except where indicated by referencing. No part of this thesis has been submitted elsewhere for any other degree or qualification

---

E E Hoskison Date

CONTENTS

Abstract.....i
Acknowledgements.....iv
Financial Support.....vi
Declaration.....vii
List of Figures.....xviii
List of Tables.....xxv
Abbreviations.....xxvii

Contents

Chapter 1: Introduction 30
1.1 Understanding the transduction of sound on developing therapeutic intervention to OME 30
1.1.1 The Sense of Hearing 31
1.1.2 Overview of anatomy and hearing 32
1.1.3 Specialised features of sound transduction 38
1.1.4 Trapdoor model theory 38
1.1.5 Adaptation 40
1.1.6 Frequency selectivity 41
1.1.7 Amplification 41
1.1.8 Innervation 42
1.1.9 Summary of signal transduction 43
1.2 Otitis Media with Effusion 44
1.2.1 Symptoms 44
1.2.2 Prevalence 45
1.2.3 Aetiology 46
1.2.4 Pathogenesis 48
1.2.5 Mucins 53
1.2.6 Viruses 56
1.2.7 Bacteria 56
1.2.8 Atopy 58
1.2.9 Eustachian tube “ex-vacuo” theory 59
1.2.10 Prognosis of OME 60

1.3 Biofilms 62
1.3.1 Studies *in vitro* 63
1.3.2 Studies *in vivo* 64
1.3.3 Implications of biofilms on OME treatment 65
1.3.4 Biofilms in nature and disease 66
1.3.5 Adherence 67
1.3.6 Polysaccharides 67
1.3.7 Biofilm interaction with mucin 69
1.3.8 Biofilm architecture 69
1.3.9 Intercellular signalling "Quorum sensing" 70
1.3.10 Antibiotic recalcitrance 71
1.3.11 Biofilm examination and measurement in research 72
1.3.12 Clinical diagnosis of biofilm infections 72
1.3.13 Therapeutic possibilities of treating biofilms in OME 72
1.4 Treatment for OME 74
1.4.1 Medical management 74
1.4.2 Nasal topical steroids 74
1.4.3 Systemic steroids 75
1.4.4 Oral antibiotics 75
1.4.5 Other medical treatments 76
1.4.6 Surgical management 77
1.4.7 Ventilation tube surgery 78
1.4.8 Adenoidectomy 79
1.4.9 Eustachian tuboplasty 80
1.4.10 Failure of current treatment strategies 81
1.5 Drug delivery to the ear 82
1.5.1 Anatomy overview 82
1.5.2 Overview of treatments for the ear 84
1.5.3 Topical treatments 85
1.5.4 Oral treatment 85
1.5.5 Intravenous administration of drugs 88
1.5.6 Transtympanic administration of drugs without TM breech 90
1.5.7 Transtympanic administration of drugs with TM breech: injection 91
1.5.8 Transtympanic administration of drugs with TM breech: incision (VT insertion) 93
1.5.9 Transtympanic administration of drugs with TM elevation: tympanomeatal flap 93
1.5.10 Eustachian tube drug delivery 96

1.5.11 Other methods of drug delivery 97
1.5.12 Summary and future perspective 98
1.6 Animal models for middle ear experimentation 100
1.6.1 History of animal models for experimentation 100
1.6.2 Regulations of animal experimentation 100
1.6.3 Otological research and animal experimentation 101
1.6.4 Knowledge of anatomy of guinea pig and rat ear dimensions 102
1.6.5 Selection of albino vs pigmented animals 103
1.6.6 Physiological differences between animal species 104
1.6.7 Animal models and OME 106
1.7 Ototoxicity 107
1.7.1 Definition of Ototoxicity 107
1.7.2 Mechanism of ototoxicity of aminoglycosides 108
1.7.3 Mechanism of ototoxicity of cisplatin 108
1.7.4 Mechanism of ototoxicity for noise induced hearing loss 109
1.7.5 Mechanism of ototoxicity without IHC and OHC loss 109
1.7.6 Animal models used to assess for ototoxicity 110
1.7.7 Antibiotics and other drugs with known ototoxicity in rodents 111
1.7.8 Other adverse effects of antibiotics in rodents 111
1.7.9 Background of poly lactic-co-glycolic acid (PLGA) and pluronic use in rodents 113
1.7.10 *In vitro* studies testing for ototoxicity 115
1.7.11 *In vivo* studies test for ototoxicity 115
1.8 Novel treatment strategies for OME: 117
1.8.1 Pellets 117
1.8.2 Hydrogel 119
1.8.3 Biodegradable ventilation tubes 120
1.8.4 Magnetic nanoparticles 120
1.9 Auditory Brainstem Response 121
1.9.1 Auditory Brainstem Response Threshold 124
1.9.2 Auditory Brainstem Response Latency 127
1.9.3 Auditory Brainstem Response Amplitude 128
1.10 Cytocochleograms 129
1.11 Histology 130
Chapter 2: Project Aims 132
2.1 Overall aims 132
2.1.1 Selection of animal model 132
2.1.2 Development of surgical delivery to the middle ear 132

2.2.3 Testing the safety of middle ear surgery 133
2.2.4 Testing middle ear pellets made of PLGA and pluronic for safety including ototoxicity 133
2.2.5 Testing middle ear pellets made of PLGA and pluronic loaded with rifampicin and clindamycin for safety including ototoxicity 133
2.2.6 Testing middle ear pellets made of PLGA and pluronic loaded with rifampicin and clindamycin individually for safety including ototoxicity 134
Chapter 3: Experimental Methods 135
3.1 Principal Experimental Groups 135
3.2 Animal Procurement and Husbandry 136
3.3 Monitoring and maintenance of physiological function during experiments . 137
3.4 Surgical procedure 137
3.5 The use of sedation/anaesthesia in the experimental design 139
3.6 Experimental regimens 141
3.6.1 Regimen 1: ABR Recording 141
3.6.2 Regimen 2: ABR Recording and surgery 141
3.6.3 Regimen 3: ABR Recording and terminal anaesthesia 141
3.6.4 Regimen 4: Hypnorm substitution 142
3.7 Pharmacology of anaesthetic agents 143
3.7.1 Isofluorane 143
3.7.2 Midazolam (Hypnovel) 143
3.7.3 Fentanyl/Fluanisone (Hypnorm) 143
3.7.4 Medetomidine 144
3.7.5 Atipamezole 144
3.7.6 Atropine 144
3.8 Auditory Brainstem Response 145
3.8.1 ABR analysis 145
3.8.2 Acoustic Calibration 149
3.8.3 Regimen for Auditory Brainstem Response recordings 152
3.8.4 Auditory Brainstem Response recording 153
3.9 Terminal anaesthesia and preparation of specimens 155
3.9.1 Schedule 1 Animal Scientific Procedures Act euthanasia 155
3.9.2 Perfusion and fixation 155
3.10 Middle Ear Histology 156
3.10.1 Dehydration 156
3.10.2 Clearing 157
3.10.3 Wax Impregnation 157
3.10.4 Slicing 157
3.10.5 Removal of paraffin 157

3.10.6 Staining 157
3.10.7 Mounting 158
3.11 Cytocochleograms 159
3.12 Pellet manufacture and preparation 161
3.13 Cadaveric experiments 165
3.14 Statistical analysis 166
Chapter 4: Development of the animal model: results of cadaveric work comparing the middle ear of the guinea pig and rat 167
4.1 Anatomical comparison 167
4.1.1 External relations of the temporal bone 167
4.1.2 Outer ear: 168
4.1.3 Middle ear: 171
4.2 Surgical approaches to the middle ear 173
4.2.1 Transtympanic 173
4.2.2 Retrobulla 174
4.2.3 Anterobulla 174
4.2.4 Discussion of cadaveric work 175
Chapter 5: Results of Auditory Brainstem Responses 177
5.1.1 ABR threshold results analysis 177
5.1.2 Changes in ABR threshold over 8-30 kHz over weeks 0-16: biological control group 177
5.1.3 Changes in ABR threshold over 8-30 kHz over weeks 0-16: surgical control group 179
5.1.4 Changes in ABR threshold over 8-30 kHz over weeks 0-16: PLGA and pluronic pellet control group 180
5.1.5 Changes in ABR threshold over 8-30 kHz over weeks 0-16: Pellets with rifampicin and clindamycin in combination 181
5.1.6 Changes in ABR threshold over 8-30 kHz over weeks 0-16: pellets with rifampicin tested separately 182
5.1.7 Changes in ABR Threshold over 8-30 kHz over Weeks 0-16: pellets with clindamycin tested separately 184
5.1.8 Holm-Bonferroni correction for the ABR threshold data 185
5.1.9 Summary and discussion of ABR threshold results 188
5.2 ABR amplitude results analysis 190
5.2.1 Changes in ABR amplitude of biological control group over 74-94dB at 16kHz 190
5.2.2 Changes in ABR amplitude of biological control group over 74-94dB at 24kHz 192
5.2.3 Summary of changes in ABR amplitude of biological control groups at 16kHz and 24kHz 194

5.2.4 Changes in ABR amplitude of surgical control group over 74-94dB at 16kHz 195
5.2.5 Changes in ABR amplitude of surgical control group over 74-94dB at 24kHz 197
5.2.6 Summary of changes in ABR amplitude of surgical control group at 16kHz and 24kHz 199
5.2.7 Changes in ABR amplitude of PLGA and pluronic pellet control group over 74-94dB at 16kHz 200
5.2.8 Changes in amplitude of PLGA and pluronic pellet over 74-94dB at 24kHz 201
5.2.9 Summary of changes in amplitude of PLGA and pluronic pellet at 16kHz and 24kHz 203
5.2.10 Changes in amplitude of pellets loaded with rifampicin and clindamycin in combination over 74-94dB at 16kHz 204
5.2.11 Changes in ABR amplitude of pellets loaded with rifampicin and clindamycin over 74-94dB at 24kHz 206
5.2.12 Summary of changes in PLGA and pluronic pellet loaded with rifampicin and clindamycin in combination over 74-94dB at 16kHz and 24kHz 208
5.2.13 Changes in ABR amplitude of pellet loaded with rifampicin over 74-94dB at 16kHz 209
5.2.14 Changes in ABR amplitude of pellet loaded with rifampicin over 74-94dB at 24kHz 211
5.2.15 Summary of changes in amplitude of Pellet loaded with Rifampicin at 16kHz and 24kHz 213
5.2.16 Changes in ABR amplitude of pellet loaded with clindamycin over 74-94dB at 16kHz 214
5.2.17 Changes in ABR amplitude of pellet loaded with clindamycin over 74-94dB at 24kHz 216
5.2.18 Summary of changes in amplitude of pellet loaded with clindamycin at 16kHz and 24kHz 218
5.2.19 Summary of amplitude results 219
5.2.20 Amplitude results using Friedman's two way analysis of variance 221
5.2.21 Summary of Friedman's two way analysis of amplitude 225
5.2.22 Holm- Bonferroni correction for the ABR amplitude data 225
5.2.23 Discussion of ABR amplitude results 232
5.3 ABR latency results analysis 234
5.3.1 Changes in latency of biological control group over 74-94dB at 16kHz 234
5.3.2 Changes in latency of biological control group over 74-94kHz at 24kHz 236
5.3.3 Summary of latency results of biological control group at 16kHz and 24kHz 237
5.3.4 Surgical control group latency over time at 16kHz 238
5.3.5 Surgical control group latency over time at 24kHz 240

5.3.6 Summary of latency results of surgical control group at 16kHz and 24kHz 242
5.3.7 Pellet control group latency over time at 16kHz 243
5.3.8 Pellet control group latency over time 24kHz 244
5.3.9 Summary of changes in latency results of PLGA and pluronic pellet control group at 16kHz and 24kHz 246
5.3.10 Changes in ABR latency of PLGA and pluronic pellet with rifampicin and clindamycin in combination over 74-94dB at 16kHz 247
5.3.11 Changes in ABR latency of PLGA and pluronic pellet with rifampicin and clindamycin in combination over 74-94dB at 24kHz 249
5.3.12 Summary of changes in latency results of pellet with rifampicin and clindamycin pellets at 16kHz and 24kHz 251
5.3.13 Changes in ABR latency of PLGA and pluronic pellet with rifampicin over 74-94dB at 16kHz 251
5.3.14 Changes in ABR latency of PLGA and pluronic pellet with rifampicin over 74-94dB at 24kHz 253
5.3.15 Summary of latency results pellet loaded with rifampicin 16kHz and 24kHz 254
5.3.16 Changes in ABR latency of PLGA and pluronic pellet with clindamycin pellet over 74-94dB at 16kHz 255
5.3.17 Changes in ABR latency of PLGA and pluronic pellet over 74-94dB at 24kHz 257
5.3.18 Summary of changes in latency results of PLGA and pluronic pellet loaded with clindamycin over 16kHz and 24kHz 258
5.3.19 Summary of overall ABR latency results 259
5.3.20 Latency results using Friedman's two way analysis 260
5.3.21 Summary of Friedman's two way analysis of latency 263
5.3.22 Holm- Bonferroni correction for the ABR latency data 264
5.3.23 Discussion of ABR latency results 270
5.4.0 Weight changes seen during ABR testing 272
5.4.1 Guinea pig weight change with treatment 272
5.4.2 Biological control, surgical control and pellet control groups. 273
5.4.3 Pellets loaded with Rifampicin and Clindamycin in combination 273
5.4.4 Pellets loaded with Rifampicin or Clindamycin separately 274
5.4.5 Dominant boars 274
Chapter 6: Cytocochleograms and IHC and OHC morphology studies 275
6.1.1 Cytocochleogram of the biological control group 275
6.1.2 Cytocochleogram of PLGA and pluronic pellet group 279
6.1.3 Cytocochleogram of PLGA and pluronic pellet loaded with rifampicin and clindamycin 283
6.1.4 Summary of cytocochleogram results 287

6.2 IHC and OHC morphological studies using immunofluorescence 288
6.2.1 Surgical Control morphological studies of IHC and OHC 289
6.2.2 PLGA and pluronic pellet control 292
6.2.3 PLGA and pluronic pellet loaded with rifampicin and clindamycin in combination 295
6.2.4 Summary of immunofluorescence studies 298
Chapter 7: Temporal bone histology results 300
7.1.1 Histology of surgical control group 300
7.1.2 Histology of the pellet loaded with rifampicin and clindamycin 303
7.1.3 Discussion of histology results 305
Chapter 8: Discussion 307
8.1 Experimental limitations and homeostasis 308
8.1.1 Limitations of pellets 308
8.1.2 Limitations of anaesthetic regimen 308
8.1.3 Importance of temperature homeostasis 310
8.1.4 Importance of oxygen saturation homeostasis 311
8.2 Guinea pig animal welfare 312
8.2.1 Guinea pig housing 312
8.2.2 Complications of surgery: wound infection, haemorrhage, facial nerve injury 314
8.2.3 Complications of recovery 317
8.3 Technical challenges with ABR recordings 318
8.4 Guinea pig dimensions and suitability as a middle ear experimental model .. 320
8.5 ABR results 322
8.5.1 ABR threshold results 322
8.5.2 Round window and oval window permeabilities 329
8.5.3 ABR amplitude results 332
8.5.4 Factors causing ABR amplitude elevation 334
8.5.5 Factors causing ABR amplitude reduction 335
8.5.6 Explanation for no correlation of ABR amplitude changes 336
8.5.7 ABR latency results 338
8.5.8 Factors causing ABR latency elevation 340
8.5.9 Factors causing ABR latency reduction 342
8.5.10 Explanation for no correlating ABR latency changes 343
8.5.11 ABR threshold elevation without changes in amplitude and latency 344
8.5.12 Discussion of lack of weight gain from pellet loaded with rifampicin and clindamycin 345
8.6 Cytocochleogram studies 346
8.7 Immunofluorescence studies 349

8.8 Histology studies 350
8.9 Potential sites of action of rifampicin and clindamycin 353
8.9.1 Stria vascularis 353
8.9.2 Spiral ganglion cells 354
8.9.3 OHC 354
8.9.4 IHC 355
8.9.5 Synaptopathy 355
8.10 Summary 356
8.10.1 Summary of experimental regimen 356
8.10.2 Summary of experimental findings 357
8.10.3 Possible explanation for ABR threshold elevation 358
8.11 Future studies 360
References 362

Index of Figures

FIGURE 1: *CORONAL VIEW OF THE LEFT MIDDLE EAR SHOWING THE OSSICULAR CHAIN: MALLEUS, INCUS AND STAPES (ILLUSTRATION BY E HOSKISON USING PAINT)*..... 34

FIGURE 2: *SCHEMATIC DIAGRAM SHOWING THE TAPERED BASILAR MEMBRANE INCREASING IN WIDTH FROM THE BASE TO THE APEX (FROM WEBNODE.COM)* 35

FIGURE 3: *CROSS SECTION OF THE COCHLEA SHOWING THE COCHLEAR DUCT OR SCALA MEDIA (ENCYCLOPEDIA BRITANNICA INC 1997)* 36

FIGURE 4: *SCHEMATIC DIAGRAM OF THE "TRAPDOOR" MODEL SHOWING HAIR CELL EXCITATION WITH POSITIVE DISPLACEMENT MEDIATED BY THE TIP LINKS (GILLESPIE ET AL., 1995)*..... 39

FIGURE 5: *HISTOLOGY OF MIDDLE EAR MUCOSA IN OME SHOWING METAPLASIA (HILTON 2011)* 52

FIGURE 6: *INFLAMMATORY CASCADE PRODUCING MUCIN (ADAPTED FROM KUBBA ET AL., 2000)* 56

FIGURE 7: *DIAGRAM TO SHOW STRUCTURE OF A) N-ACETYL GLUCOSAMINE AND B) POLYSACCHARIDE INTERCELLULAR ADHESIN (LEUNG 2009)* 68

FIGURE 8: *THE HEARING RANGES OF SOME COMMON LABORATORY ANIMALS TAKEN FROM HEFFNER ET AL., 2007.* 105

FIGURE 9 *GRAPH SHOWING THE SENSITIVITY TO VARIOUS FREQUENCIES OF EIGHT DIFFERENT SPECIES INCLUDING COMMONLY USED LABORATORY ANIMALS AND HUMANS (TURNER ET AL., 2005). THE DATA HAS BEEN ADAPTED FROM FAY ET AL., 1988* 123

FIGURE 10: *AN EXAMPLE OF A "CLEAN" ABR WAVEFORM SHOWING THE PEAKS (P1-P5) AND TROUGHS (N1-N5) OF THE FIVE WAVES (I-V)*..... 125

FIGURE 11. *ABR RECORDINGS MAY MISREPRESENT THE BEHAVIOURAL THRESHOLDS OF HEARING IN ANIMALS (HEFFNER ET AL., 2003)* 126

FIGURE 12. *DIAGRAM OF SURGICAL APPROACH TO GUINEA PIG MIDDLE EAR BULLA (HIGHLIGHTED YELLOW) WITH RETRACTION OF THE POSTERIOR DIGASTRIC. LEVEL OF CERVICAL SKIN INCISION INDICATED (RED DOTTED LINE)* 138

FIGURE 13: *SCHEMATIC DIAGRAM OF SIGNAL GENERATOR AND RECORDING SYSTEM*..... 145

FIGURE 14: *EXAMPLE OF CUMULATIVE VIEWS OF ABR RECORDING SHOWING PEAKS P1 (RED), P2 (YELLOW), P3 (GREEN), P4 (TURQUOISE) AND P5 (BLUE).* 148

FIGURE 15: *EXAMPLE OF SELECTION OF PEAKS P1-P5 WITH CIRCLES AND TROUGHS N1-N5 (TRIANGLES). THRESHOLD FOR THIS ABR RECORDING WOULD BE AT 30DB* 149

FIGURE 16*: THE ACOUSTIC COUPLER SET UP.* 150

FIGURE 17: *MAXIMAL DRIVER OUTPUT (DB SPL) AFTER CLOSED FIELD STIMULUS AT 8,16,24 AND 30KHZ*.... 152

FIGURE 18: *IMAGE OF THREE ELECTRODES POSITIONED ON GUINEA PIG (RED: MIDLINE LIVE ELECTRODE, BLACK: PRE-AURICULAR REFERENCE ELECTRODE, WHITE: RUMP GROUND ELECTRODE)* 154

FIGURE 19: *IMAGE OF TWO PELLETS LADEN WITH RIFAMPICIN WITH CM SCALE* 163

FIGURE 20: *GRAPH TO SHOW THE RELATIONSHIP BETWEEN THE HIGHEST FREQUENCY OF HEARING (HZ) AND MASS OF MALLEUS AND INCUS (MG) FOR DIFFERENT SPECIES: HUMAN, GUINEA PIG AND RAT* 170

FIGURE 21: *BIOLOGICAL CONTROL SHOWING NO SIGNIFICANT CHANGES IN MEAN ABR THRESHOLDS OVER 0-16 WEEKS* 178
FIGURE 22: *SURGICAL CONTROL GROUP SHOWING ONLY ONE SIGNIFICANT CHANGE IN ABR THRESHOLD AT 16 KHZ AT WEEK 1 (MARKED WITH A *).* 179
FIGURE 23: *PLGA AND PLURONIC PELLET ALONE SHOWING ONE SIGNIFICANT CHANGE IN THRESHOLD OF 10 DB AT 30 KHZ AT WEEK 16 (MARKED WITH A *)* 180
FIGURE 24: *RIFAMPICIN AND CLINDAMYCIN LOADED PLGA AND PLURONIC PELLETS. HIGHLY SIGNIFICANT CHANGES AT VIRTUALLY ALL FREQUENCIES OVER WEEKS 1-16. NOT ALL SIGNIFICANCE LEVELS INDICATED.* 181
FIGURE 25: *PLGA AND PLURONIC PELLETS LOADED WITH RIFAMPICIN ALONE (N=8).* 183
FIGURE 26: *PLGA AND PLURONIC PELLETS LOADED WITH CLINDAMYCIN ALONE (N=8).* 184
FIGURE 27: *CHANGES IN AMPLITUDE OVER TIME FOR BIOLOGICAL CONTROL GROUP AT 16KHZ ANALYSING THE P1 WAVE. SIGNIFICANCE IS DENOTED BY A *.* 190
FIGURE 28: *CHANGES IN AMPLITUDE AGAINST TIME BIOLOGICAL CONTROL GROUP AT 16KHZ ANALYSING THE P2 WAVE. SIGNIFICANCE IS DENOTED BY A *.* 191
FIGURE 29: *CHANGES IN AMPLITUDE AGAINST TIME BIOLOGICAL CONTROL GROUP AT 16KHZ ANALYSING THE P3 WAVE. SIGNIFICANCE IS DENOTED BY A *.* 191
FIGURE 30: *CHANGES IN AMPLITUDE AGAINST TIME BIOLOGICAL CONTROL GROUP AT 24KHZ ANALYSING THE P1 WAVE. SIGNIFICANCE IS DENOTED BY A *.* 192
FIGURE 31: *CHANGES IN AMPLITUDE AGAINST TIME BIOLOGICAL CONTROL GROUP AT 24KHZ ANALYSING THE P2 WAVE. SIGNIFICANCE IS DENOTED BY A *.* 193
FIGURE 32: *CHANGES IN AMPLITUDE AGAINST TIME FOR BIOLOGICAL CONTROL GROUP AT 24KHZ ANALYSING THE P3 WAVE. SIGNIFICANCE IS DENOTED BY A *.* 193
FIGURE 33: *CHANGES IN AMPLITUDE AGAINST TIME FOR SURGICAL CONTROL GROUP AT 16KHZ ANALYSING THE P1 WAVE. SIGNIFICANCE IS DENOTED BY A *.* 195
FIGURE 34: *CHANGES IN AMPLITUDE AGAINST TIME FOR SURGICAL CONTROL GROUP AT 16KHZ ANALYSING THE P2 WAVE. SIGNIFICANCE IS DENOTED BY A *.* 196
FIGURE 35: *CHANGES IN AMPLITUDE AGAINST TIME FOR SURGICAL CONTROL GROUP AT 16KHZ ANALYSING THE P3 WAVE. SIGNIFICANCE IS DENOTED BY A *.* 196
FIGURE 36: *CHANGES IN AMPLITUDE AGAINST TIME FOR SURGICAL CONTROL GROUP AT 24KHZ ANALYSING THE P1 WAVE. SIGNIFICANCE IS DENOTED BY A *.* 197
FIGURE 37: *CHANGES IN AMPLITUDE AGAINST TIME FOR SURGICAL CONTROL GROUP AT 24KHZ ANALYSING THE P2 WAVE. SIGNIFICANCE IS DENOTED BY A *.* 198
FIGURE 38: CHANGES IN AMPLITUDE AGAINST TIME FOR SURGICAL CONTROL GROUP AT 24KHZ ANALYSING THE P3 WAVE. SIGNIFICANCE IS DENOTED BY A * 198
FIGURE 39: *CHANGES IN AMPLITUDE AGAINST TIME PLGA AND PLURONIC PELLET CONTROL GROUP AT 16KHZ ANALYSING THE P1 WAVE. SIGNIFICANCE IS DENOTED BY A *.* 200

FIGURE 40: *CHANGES IN AMPLITUDE AGAINST TIME PLGA AND PLURONIC PELLET CONTROL GROUP AT 16KHZ ANALYSING THE P2 WAVE. SIGNIFICANCE IS DENOTED BY A *.* 200
FIGURE 41: *CHANGES IN AMPLITUDE AGAINST TIME PLGA AND PLURONIC PELLET CONTROL GROUP AT 16KHZ ANALYSING THE P3 WAVE. SIGNIFICANCE IS DENOTED BY A *.* 201
FIGURE 42: *CHANGES IN AMPLITUDE AGAINST TIME PLGA AND PLURONIC PELLET CONTROL GROUP AT 24KHZ ANALYSING THE P1 WAVE. SIGNIFICANCE IS DENOTED BY A *.* 201
FIGURE 43: *CHANGES IN AMPLITUDE AGAINST TIME PLGA AND PLURONIC PELLET CONTROL GROUP AT 24KHZ ANALYSING THE P1 WAVE. SIGNIFICANCE IS DENOTED BY A *.* 202
FIGURE 44: *CHANGES IN AMPLITUDE AGAINST TIME PLGA AND PLURONIC PELLET CONTROL GROUP AT 24KHZ ANALYSING THE P1 WAVE. SIGNIFICANCE IS DENOTED BY A *.* 202
FIGURE 45: *CHANGES IN AMPLITUDE AGAINST TIME PLGA AND PLURONIC PELLET WITH RIFAMPICIN AND CLINDAMYCIN AT 16KHZ ANALYSING THE P1 WAVE. SIGNIFICANCE IS DENOTED BY A *.* 204
FIGURE 46: *CHANGES IN AMPLITUDE AGAINST TIME PLGA AND PLURONIC PELLET WITH RIFAMPICIN AND CLINDAMYCIN AT 16KHZ ANALYSING THE P2 WAVE. SIGNIFICANCE IS DENOTED BY A *.* 205
FIGURE 47: *CHANGES IN AMPLITUDE AGAINST TIME PLGA AND PLURONIC PELLET WITH RIFAMPICIN AND CLINDAMYCIN AT 16KHZ ANALYSING THE P3 WAVE. SIGNIFICANCE IS DENOTED BY A *.* 205
FIGURE 48: *CHANGES IN AMPLITUDE AGAINST TIME PLGA AND PLURONIC PELLET WITH RIFAMPICIN AND CLINDAMYCIN AT 24KHZ ANALYSING THE P1 WAVE. SIGNIFICANCE IS DENOTED BY A *.* 206
FIGURE 49: *CHANGES IN AMPLITUDE AGAINST TIME PLGA AND PLURONIC PELLET WITH RIFAMPICIN AND CLINDAMYCIN AT 24KHZ ANALYSING THE P2 WAVE. SIGNIFICANCE IS DENOTED BY A *.* 207
FIGURE 50*: CHANGES IN AMPLITUDE AGAINST TIME PLGA AND PLURONIC PELLET WITH RIFAMPICIN AND CLINDAMYCIN AT 24KHZ ANALYSING THE P3 WAVE. SIGNIFICANCE IS DENOTED BY A *.* 207
FIGURE 51*: CHANGES IN AMPLITUDE AGAINST TIME PLGA AND PLURONIC PELLET WITH RIFAMPICIN AT 16KHZ ANALYSING THE P1 WAVE. SIGNIFICANCE IS DENOTED BY A *.* 209
FIGURE 52*: CHANGES IN AMPLITUDE AGAINST TIME PLGA AND PLURONIC PELLET WITH RIFAMPICIN AT 16KHZ ANALYSING THE P2 WAVE. SIGNIFICANCE IS DENOTED BY A *.* 210
FIGURE 53: *CHANGES IN AMPLITUDE AGAINST TIME PLGA AND PLURONIC PELLET WITH RIFAMPICIN AT 16KHZ ANALYSING THE P3 WAVE. SIGNIFICANCE IS DENOTED BY A *.* 210
FIGURE 54*: CHANGES IN AMPLITUDE AGAINST TIME PLGA AND PLURONIC PELLET WITH RIFAMPICIN AT 24KHZ ANALYSING THE P1 WAVE. SIGNIFICANCE IS DENOTED BY A *.* 211
FIGURE 55*: CHANGES IN AMPLITUDE AGAINST TIME PLGA AND PLURONIC PELLET WITH RIFAMPICIN AT 24KHZ ANALYSING THE P2 WAVE. SIGNIFICANCE IS DENOTED BY A *.* 212
FIGURE 56: *CHANGES IN AMPLITUDE AGAINST TIME PLGA AND PLURONIC PELLET WITH RIFAMPICIN AT 24KHZ ANALYSING THE P3 WAVE. SIGNIFICANCE IS DENOTED BY A *.* 212
FIGURE 57: CHANGES IN AMPLITUDE AGAINST TIME PLGA AND PLURONIC PELLET WITH CLINDAMYCIN AT 16KHZ ANALYSING THE P1 WAVE. SIGNIFICANCE IS DENOTED BY A *. 214
FIGURE 58*: CHANGES IN AMPLITUDE AGAINST TIME PLGA AND PLURONIC PELLET WITH CLINDAMYCIN AT 16KHZ ANALYSING THE P2 WAVE. SIGNIFICANCE IS DENOTED BY A *.* 214

FIGURE 59: CHANGES IN AMPLITUDE AGAINST TIME PLGA AND PLURONIC PELLET WITH CLINDAMYCIN AT 16KHZ ANALYSING THE P3 WAVE. SIGNIFICANCE IS DENOTED BY A *. 215
FIGURE 60: *CHANGES IN AMPLITUDE AGAINST TIME PLGA AND PLURONIC PELLET WITH CLINDAMYCIN AT 24KHZ ANALYSING THE P1 WAVE. SIGNIFICANCE IS DENOTED BY A *.* 216
FIGURE 61: *CHANGES IN AMPLITUDE AGAINST TIME PLGA AND PLURONIC PELLET WITH CLINDAMYCIN AT 24KHZ ANALYSING THE P2 WAVE. SIGNIFICANCE IS DENOTED BY A *.* 216
FIGURE 62*: CHANGES IN AMPLITUDE AGAINST TIME PLGA AND PLURONIC PELLET WITH CLINDAMYCIN AT 24KHZ ANALYSING THE P3 WAVE. SIGNIFICANCE IS DENOTED BY A *.* 217
FIGURE 63: EXAMPLE OF ABR TRACE WITH POOR DEFINITION OF WAVEFORMS. Y AXIS: AMPLITUDE/MV, X AXIS TIME/MSECS 220
FIGURE 64: EXAMPLE OF ABR TRACE WITH GOOD DEFINITION OF WAVEFORMS. Y AXIS: AMPLITUDE/MV, X AXIS TIME/MSECS 220
FIGURE 67: *CHANGES IN LATENCY OVER TIME FOR BIOLOGICAL CONTROL GROUP AT 16KHZ ANALYSING THE P3 WAVE. SIGNIFICANCE IS DENOTED BY A *.* 235
FIGURE 68: *CHANGES IN LATENCY OVER TIME FOR BIOLOGICAL CONTROL GROUP AT 24KHZ ANALYSING THE P1 WAVE. SIGNIFICANCE IS DENOTED BY A *.* 236
FIGURE 69: *CHANGES IN LATENCY OVER TIME FOR BIOLOGICAL CONTROL GROUP AT 24KHZ ANALYSING THE P2 WAVE. SIGNIFICANCE IS DENOTED BY A *.* 236
FIGURE 70: *CHANGES IN LATENCY OVER TIME FOR BIOLOGICAL CONTROL GROUP AT 16KHZ ANALYSING THE P3 WAVE. SIGNIFICANCE IS DENOTED BY A *.* 237
FIGURE 71: *CHANGES IN LATENCY OVER TIME FOR SURGICAL CONTROL GROUP AT 16KHZ ANALYSING THE P1 WAVE. SIGNIFICANCE IS DENOTED BY A *.* 238
FIGURE 72: CHANGES IN LATENCY OVER TIME FOR SURGICAL CONTROL GROUP AT 16KHZ ANALYSING THE P2 WAVE. SIGNIFICANCE IS DENOTED BY A *. 239
FIGURE 73: CHANGES IN LATENCY OVER TIME FOR SURGICAL CONTROL GROUP AT 16KHZ ANALYSING THE P3 WAVE. SIGNIFICANCE IS DENOTED BY A *. 239
FIGURE 74: *CHANGES IN LATENCY OVER TIME FOR SURGICAL CONTROL GROUP AT 24KHZ ANALYSING THE P1 WAVE. SIGNIFICANCE IS DENOTED BY A *.* 240
FIGURE 75: *CHANGES IN LATENCY OVER TIME FOR SURGICAL CONTROL GROUP AT 24KHZ ANALYSING THE P2 WAVE. SIGNIFICANCE IS DENOTED BY A *.* 241
FIGURE 76: *CHANGES IN LATENCY OVER TIME FOR SURGICAL CONTROL GROUP AT 24KHZ ANALYSING THE P3 WAVE. SIGNIFICANCE IS DENOTED BY A *.* 241
FIGURE 77: *CHANGES IN LATENCY OVER TIME FOR PLGA AND PLURONIC CONTROL GROUP AT 16KHZ ANALYSING THE P1 WAVE. SIGNIFICANCE IS DENOTED BY A *.* 243
FIGURE 78: *CHANGES IN LATENCY OVER TIME FOR PLGA AND PLURONIC CONTROL GROUP AT 16KHZ ANALYSING THE P2 WAVE. SIGNIFICANCE IS DENOTED BY A *.* 243
FIGURE 79: *CHANGES IN LATENCY OVER TIME FOR PLGA AND PLURONIC CONTROL GROUP AT 16KHZ ANALYSING THE P3 WAVE. SIGNIFICANCE IS DENOTED BY A *.* 244

FIGURE 80: *CHANGES IN LATENCY OVER TIME FOR PLGA AND PLURONIC CONTROL GROUP AT 16KHZ ANALYSING THE P1 WAVE. SIGNIFICANCE IS DENOTED BY A *.* 245
FIGURE 81: *CHANGES IN LATENCY OVER TIME FOR PLGA AND PLURONIC CONTROL GROUP AT 24KHZ ANALYSING THE P2 WAVE. SIGNIFICANCE IS DENOTED BY A *.* 245
FIGURE 82: *CHANGES IN LATENCY OVER TIME FOR PLGA AND PLURONIC CONTROL GROUP AT 24KHZ ANALYSING THE P3 WAVE. SIGNIFICANCE IS DENOTED BY A *.* 246
FIGURE 83: *CHANGES IN LATENCY OVER TIME FOR PLGA AND PLURONIC PELLET WITH RIFAMPICIN AND CLINDAMYCIN IN COMBINATION AT 16KHZ ANALYSING THE P1 WAVE. SIGNIFICANCE IS DENOTED BY A *.* 247
FIGURE 84: *CHANGES IN LATENCY OVER TIME FOR PLGA AND PLURONIC PELLET WITH RIFAMPICIN AND CLINDAMYCIN IN COMBINATION AT 16KHZ ANALYSING THE P2 WAVE. SIGNIFICANCE IS DENOTED BY A *.* 247
FIGURE 85: *CHANGES IN LATENCY OVER TIME FOR PLGA AND PLURONIC PELLET WITH RIFAMPICIN AND CLINDAMYCIN IN COMBINATION AT 16KHZ ANALYSING THE P3 WAVE. SIGNIFICANCE IS DENOTED BY A *.* 248
FIGURE 86: *CHANGES IN LATENCY OVER TIME FOR PLGA AND PLURONIC CONTROL WITH RIFAMPICIN AND CLINDAMYCIN IN COMBINATION AT 24KHZ ANALYSING THE P1 WAVE. SIGNIFICANCE IS DENOTED BY A *.* 249
FIGURE 87: *CHANGES IN LATENCY OVER TIME FOR PLGA AND PLURONIC PELLET WITH RIFAMPICIN AND CLINDAMYCIN IN COMBINATION AT 24KHZ ANALYSING THE P2 WAVE. SIGNIFICANCE IS DENOTED BY A *.* 250
FIGURE 88: *CHANGES IN LATENCY OVER TIME FOR PLGA AND PLURONIC PELLET WITH RIFAMPICIN AND CLINDAMYCIN IN COMBINATION AT 24KHZ ANALYSING THE P3 WAVE. SIGNIFICANCE IS DENOTED BY A *.* 250
FIGURE 89: *CHANGES IN AMPLITUDE OVER TIME FOR PLGA AND PLURONIC CONTROL WITH RIFAMPICIN AND CLINDAMYCIN IN COMBINATION AT 16KHZ ANALYSING THE P1 WAVE. SIGNIFICANCE IS DENOTED BY A *.* 251
FIGURE 90*: CHANGES IN AMPLITUDE OVER TIME FOR PLGA AND PLURONIC PELLET WITH RIFAMPICIN AT 16KHZ ANALYSING THE P2 WAVE. SIGNIFICANCE IS DENOTED BY A *.* 252
FIGURE 91: *CHANGES IN AMPLITUDE OVER TIME FOR PLGA AND PLURONIC PELLET WITH RIFAMPICIN AT 16KHZ ANALYSING THE P3 WAVE. SIGNIFICANCE IS DENOTED BY A *.* 252
FIGURE 92: *CHANGES IN AMPLITUDE OVER TIME FOR PLGA AND PLURONIC PELLET WITH RIFAMPICIN AT 24KHZ ANALYSING THE P1 WAVE. SIGNIFICANCE IS DENOTED BY A *.* 253
FIGURE 93: *CHANGES IN AMPLITUDE OVER TIME FOR PLGA AND PLURONIC PELLET WITH RIFAMPICIN AT 24KHZ ANALYSING THE P2 WAVE. SIGNIFICANCE IS DENOTED BY A *.* 253
FIGURE 94: *CHANGES IN AMPLITUDE OVER TIME FOR PLGA AND PLURONIC PELLET WITH RIFAMPICIN AT 24KHZ ANALYSING THE P3 WAVE. SIGNIFICANCE IS DENOTED BY A *.* 254

FIGURE 95: *CHANGES IN LATENCY OVER TIME FOR PLGA AND PLURONIC PELLET WITH RIFAMPICIN AT 16KHZ ANALYSING THE P1 WAVE. SIGNIFICANCE IS DENOTED BY A *.* 255
FIGURE 96: *CHANGES IN AMPLITUDE OVER TIME FOR PLGA AND PLURONIC PELLET WITH CLINDAMYCIN AT 16KHZ ANALYSING THE P2 WAVE. SIGNIFICANCE IS DENOTED BY A *.* 255
FIGURE 97: *CHANGES IN LATENCY OVER TIME FOR PLGA AND PLURONIC PELLET WITH CLINDAMYCIN AT 16KHZ ANALYSING THE P3 WAVE. SIGNIFICANCE IS DENOTED BY A *.* 256
FIGURE 98: *CHANGES IN LATENCY OVER TIME FOR PLGA AND PLURONIC PELLET WITH CLINDAMYCIN AT 24KHZ ANALYSING THE P1 WAVE. SIGNIFICANCE IS DENOTED BY A *.* 257
FIGURE 99: *CHANGES IN CLINDAMYCIN OVER TIME FOR PLGA AND PLURONIC PELLET WITH RIFAMPICIN AT 24KHZ ANALYSING THE P2 WAVE. SIGNIFICANCE IS DENOTED BY A *.* 257
FIGURE 100: *CHANGES IN LATENCY OVER TIME FOR PLGA AND PLURONIC PELLET WITH CLINDAMYCIN AT 24KHZ ANALYSING THE P3 WAVE. SIGNIFICANCE IS DENOTED BY A *.* 258
FIGURE 101: *WEIGHT CHANGE (GRAMS) OVER TIME (WEEKS) FOR DIFFERENT TREATMENT GROUPS.* 273
FIGURE 102: *CYTOCOCHLEOGRAM OF BIOLOGICAL CONTROL GROUP INNER HAIR CELL ROWS FROM APEX (ROW 0) TO BASE.* 276
FIGURE 103: *CYTOCOCHLEOGRAM OF BIOLOGICAL CONTROL GROUP OHC ROW 1 (INNERMOST ROW) FROM APEX (ROW 0) TO BASE.* 276
FIGURE 104: *CYTOCOCHLEOGRAM OF BIOLOGICAL CONTROL GROUP OHC ROW 2 (MIDDLE ROW) FROM APEX (ROW 0) TO BASE.* 277
FIGURE 105: *CYTOCOCHLEOGRAM OF BIOLOGICAL CONTROL GROUP OUTER HAIR CELL ROW 3 (OUTERMOST ROW) FROM APEX (ROW 0) TO BASE.* 278
FIGURE 106: *SCHEMATIC DIAGRAM OF TYPICAL SEGMENT OF COCHLEA (A ROW) FROM BC GROUP SHOWING THE DISTRIBUTION OF HAIR CELLS PRESENT ○ AND ABSENT ●. TEMPLATE PROVIDED BY PROFESSOR DAVID FURNESS (SEE ACKNOWLEDGEMENTS).* 278
FIGURE 107: *CYTOCOCHLEOGRAM OF PLGA AND PLURONIC PELLET CONTROL GROUP IHC FROM APEX (ROW 0) TO BASE.* 280
FIGURE 108: *CYTOCOCHLEOGRAM OF PLGA AND PLURONIC PELLET CONTROL GROUP INNERMOST ROW OF OHC FROM APEX AT 0 TO BASE.* 281
FIGURE 109: *CYTOCOCHLEOGRAM OF PLGA AND PLURONIC PELLET CONTROL GROUP MIDDLE ROW OF OHC FROM APEX AT 0 TO BASE.* 281
FIGURE 110: *CYTOCOCHLEOGRAM OF PLGA AND PLURONIC PELLET CONTROL GROUP OUTERMOST ROW OF OHC FROM APEX AT 0 TO BASE.* 282
FIGURE 111: *CYTOCOCHLEOGRAM OF PLGA AND PLURONIC PELLET LOADED WITH RIFAMPICIN AND CLINDAMYCIN IHC FROM APEX ROW 0 TO BASE.* 283
FIGURE 112: *CYTOCOCHLEOGRAM OF PLGA AND PLURONIC PELLET LOADED WITH RIFAMPICIN AND CLINDAMYCIN INNERMOST ROW OF OHC FROM APEX ROW 0 TO BASE.* 284
FIGURE 113: *CYTOCOCHLEOGRAM OF PLGA AND PLURONIC PELLET LOADED WITH RIFAMPICIN AND CLINDAMYCIN MIDDLE ROW OF OHC FROM APEX ROW 0 TO BASE.* 285

FIGURE 114: CYTOCOCHLEOGRAM OF PLGA AND PLURONIC PELLET LOADED WITH RIFAMPICIN AND CLINDAMYCIN OUTERMOST ROW OF OHC FROM APEX (ROW 0) TO BASE..... 286
FIGURE 115: *PREPARATION OF ORGAN OF CORTI USING DAPI AND PHALLOIDIN STAINING. BAR = 50MM IN A BIOLOGICAL CONTROL SPECIMEN.* 288
FIGURE 116: *SURGICAL CONTROL APICAL SECTION OF COCHLEA WITHOUT AND WITH DAPI AND PHALLOIDIN IMMUNOFLUORESCENCE. BAR = 50MM*..... 289
FIGURE 117: *SURGICAL CONTROL MIDDLE SECTION OF COCHLEA WITHOUT AND WITH DAPI AND PHALLOIDIN IMMUNOFLUORESCENCE. BAR = 50MM*..... 290
FIGURE 118: *SURGICAL CONTROL BASAL SECTION OF COCHLEA WITHOUT AND WITH DAPI AND PHALLOIDIN IMMUNOFLUORESCENCE. BAR = 50MM* 291
FIGURE 119: *PLGA AND PLURONIC PELLET CONTROL APICAL SECTION OF COCHLEA WITHOUT AND WITH DAPI AND PHALLOIDIN IMMUNOFLUORESCENCE. BAR = 50MM* 292
FIGURE 120: *PLGA AND PLURONIC PELLET CONTROL MIDDLE SECTION OF COCHLEA WITHOUT AND WITH DAPI AND PHALLOIDIN IMMUNOFLUORESCENCE. BAR = 50MM* 293
FIGURE 121: *PLGA AND PLURONIC PELLET CONTROL BASAL SECTION OF COCHLEA WITHOUT AND WITH DAPI AND PHALLOIDIN IMMUNOFLUORESCENCE. BAR = 50MM*..... 294
FIGURE 122: *PLGA AND PLURONIC PELLET LOADED WITH RIFAMPICIN AND CLINDAMYCIN APICAL SECTION OF COCHLEA WITHOUT AND WITH DAPI AND PHALLOIDIN IMMUNOFLUORESCENCE. BAR = 50MM*..... 295
FIGURE 123: *PLGA AND PLURONIC PELLET LOADED WITH RIFAMPICIN AND CLINDAMYCIN MIDDLE SECTION OF COCHLEA WITHOUT AND WITH DAPI AND PHALLOIDIN IMMUNOFLUORESCENCE. BAR = 50MM*..... 296
FIGURE 124: *PLGA AND PLURONIC PELLET LOADED WITH RIFAMPICIN AND CLINDAMYCIN BASAL SECTION OF COCHLEA WITHOUT AND WITH DAPI AND PHALLOIDIN IMMUNOFLUORESCENCE. BAR = 50MM*..... 297
FIGURE 126: *COCHLEA FROM PLGA AND PLURONIC GUINEA PIG SHOWING ULTRASTRUCTURE IN A) COCHLEA B) COCHLEA C) ORGAN OF CORTI – INTACT REISSNER'S MEMBRANE, DISRUPTED TECTORIAL MEMBRANE D) SPIRAL GANGLION E) STRIA VASCULARIS AND F) ORGAN OF CORTI X 40.* 302
FIGURE 127: *COCHLEA FROM PLGA AND PLURONIC GUINEA PIG LOADED WITH RIFAMPICIN AND CLINDAMYCIN SHOWING ULTRASTRUCTURE IN A) MIDDLE EAR WITH PELLET B) PELLET AND ME EPITHELIUM C) PELLET AND ME EPITHELIUM D) PELLET MARGIN AND CENTRE X 40 E) PELLET MARGIN AND CENTRE X 40 AND F) BONE WAX REACTION X 40.* 304

Tables:

TABLE 1: *COMPONENTS OF MIDDLE EAR SECRETIONS AND THEIR ROLE ON DEFENCE AGAINST PATHOGENS* 50
TABLE 2: *SUMMARY OF DRUG DELIVERY TO THE EAR* 100
TABLE 3: *THE KNOWN SIDE EFFECTS OF DIFFERENT ANTIBIOTIC GROUPS IN RODENTS* 113
TABLE 4: *SUMMARY OF ABR LATENCY AND AMPLITUDE CHANGES WITH DIFFERENT STIMULI PRESENTED TO THE COCHLEA* 129
TABLE 5: *DRUG DOSES USED IN EXPERIMENTAL REGIMENS ACCORDING TO ANIMAL WEIGHT* 142
TABLE 6: *MEASUREMENTS OF THE EXTERNAL AUDITORY CANAL AND TYMPANIC MEMBRANE IN THE GUINEA PIG AND RAT* 169
TABLE 7: *MEASUREMENTS OF THE VENTRAL BULLA OF THE GUINEA PIG AND MIDDLE EAR OF THE RAT* 169
TABLE 8: *BIOLOGICAL CONTROL THRESHOLD P VALUES AND THE HOLM BONFERRONI CORRECTION. VALUES WHERE THE NULL HYPOTHESIS IS REJECTED ARE HIGHLIGHTED RED.* 185
TABLE 9: *SURGICAL CONTROL THRESHOLD P VALUES AND THE HOLM BONFERRONI CORRECTION. VALUES WHERE THE NULL HYPOTHESIS IS REJECTED ARE HIGHLIGHTED RED.* 186
TABLE 10: *PELLET CONTROL THRESHOLD P VALUES AND THE HOLM BONFERRONI CORRECTION. VALUES WHERE THE NULL HYPOTHESIS IS REJECTED ARE HIGHLIGHTED RED.* 186
TABLE 11: *PELLET WITH RIFAMPICIN AND CLINDAMYCIN THRESHOLD P VALUES AND THE HOLM BONFERRONI CORRECTION. VALUES WHERE THE NULL HYPOTHESIS IS REJECTED ARE HIGHLIGHTED RED.* 186
TABLE 12: *PELLET WITH RIFAMPICIN THRESHOLD P VALUES AND THE HOLM BONFERRONI CORRECTION. VALUES WHERE THE NULL HYPOTHESIS IS REJECTED ARE HIGHLIGHTED RED.* 187
TABLE 13: *PELLET WITH CLINDAMYCIN THRESHOLD P VALUES AND THE HOLM BONFERRONI CORRECTION. VALUES WHERE THE NULL HYPOTHESIS IS REJECTED ARE HIGHLIGHTED RED.* 187
TABLE 14: *CHANGES IN AMPLITUDE FOR WAVES P1-P3 MEASURED AT 16KHZ AND 24KHZ FOR THE BIOLOGICAL CONTROL GROUP.* 194
TABLE 15: *CHANGES IN AMPLITUDE FOR WAVES P1-P3 MEASURED AT 16KHZ AND 24KHZ FOR THE SURGICAL CONTROL GROUP* 199
TABLE 16: *CHANGES IN AMPLITUDE FOR WAVES P1-P3 MEASURED AT 16KHZ AND 24KHZ FOR THE PLGA AND PLURONIC PELLET CONTROL GROUP.* 203
TABLE 17*: CHANGES IN AMPLITUDE FOR WAVES P1-P3 MEASURED AT 16KHZ AND 24KHZ FOR THE PLGA AND PLURONIC LOADED WITH RIFAMPICIN AND CLINDAMYCIN IN COMBINATION* 208
TABLE 18: *CHANGES IN AMPLITUDE FOR WAVES P1-P3 MEASURED AT 16KHZ AND 24KHZ FOR THE PLGA AND PLURONIC LOADED WITH RIFAMPICIN GROUP.* 213
TABLE 19*: CHANGES IN AMPLITUDE FOR WAVES P1-P3 MEASURED AT 16KHZ AND 24KHZ FOR THE PLGA AND PLURONIC LOADED WITH CLINDAMYCIN GROUP.* 218
TABLE 20: *SUMMARY OF THE CHANGES IN AMPLITUDE FOR WAVES P1-P3 MEASURED AT 16KHZ AND 24KHZ FOR ALL EXPERIMENTAL GROUPS.* 219
TABLE 21: *RESULTS OF FRIEDMAN'S TWO WAY ANALYSIS OF AMPLITUDE OF WAVE P1. SIGNIFICANCE DENOTED AS P<0.05 MARKED WITH *.* 222

TABLE 22: *RESULTS OF FRIEDMAN'S TWO WAY ANALYSIS OF AMPLITUDE WAVE P2. SIGNIFICANCE DENOTED AS P<0.05 MARKED WITH *.* 223
TABLE 23: *RESULTS OF FRIEDMAN'S TWO WAY ANALYSIS OF AMPLITUDE OF WAVE P3. SIGNIFICANCE DENOTED AS P<0.05 MARKED WITH *.* 224
TABLE 24: *BIOLOGICAL CONTROL AMPLITUDE P VALUES AT 16KHZ AND THE HOLM BONFERRONI CORRECTION. VALUES WHERE THE NULL HYPOTHESIS IS REJECTED ARE HIGHLIGHTED RED.* 226
TABLE 25: *BIOLOGICAL CONTROL AMPLITUDE P VALUES AT 24KHZ AND THE HOLM BONFERRONI CORRECTION. VALUES WHERE THE NULL HYPOTHESIS IS REJECTED ARE HIGHLIGHTED RED.* 226
TABLE 26: *SURGICAL CONTROL AMPLITUDE P VALUES AT 16KHZ AND THE HOLM BONFERRONI CORRECTION. VALUES WHERE THE NULL HYPOTHESIS IS REJECTED ARE HIGHLIGHTED RED.* 227
TABLE 27: *SURGICAL CONTROL AMPLITUDE P VALUES AT 24KHZ AND THE HOLM BONFERRONI CORRECTION. VALUES WHERE THE NULL HYPOTHESIS IS REJECTED ARE HIGHLIGHTED RED.* 227
TABLE 28: *PELLET CONTROL AMPLITUDE P VALUES AT 16KHZ AND THE HOLM BONFERRONI CORRECTION. VALUES WHERE THE NULL HYPOTHESIS IS REJECTED ARE HIGHLIGHTED RED.* 228
TABLE 29: *PELLET CONTROL AMPLITUDE P VALUES AT 24KHZ AND THE HOLM BONFERRONI CORRECTION. VALUES WHERE THE NULL HYPOTHESIS IS REJECTED ARE HIGHLIGHTED RED.* 228
TABLE 30: *PELLET WITH RIFAMPICIN AND CLINDAMYCIN AMPLITUDE P VALUES AT 16KHZ AND THE HOLM BONFERRONI CORRECTION. VALUES WHERE THE NULL HYPOTHESIS IS REJECTED ARE HIGHLIGHTED RED.* . 229
TABLE 31: *PELLET WITH RIFAMPICIN AND CLINDAMYCIN AMPLITUDE P VALUES AT 24KHZ AND THE HOLM BONFERRONI CORRECTION. VALUES WHERE THE NULL HYPOTHESIS IS REJECTED ARE HIGHLIGHTED RED.* . 229
TABLE 32: *PELLET WITH RIFAMPICIN AMPLITUDE P VALUES AT 16KHZ AND THE HOLM BONFERRONI CORRECTION. VALUES WHERE THE NULL HYPOTHESIS IS REJECTED ARE HIGHLIGHTED RED.* 230
TABLE 33: *PELLET WITH RIFAMPICIN AMPLITUDE P VALUES AT 24KHZ AND THE HOLM BONFERRONI CORRECTION. VALUES WHERE THE NULL HYPOTHESIS IS REJECTED ARE HIGHLIGHTED RED.* 230
TABLE 34: *PELLET WITH CLINDAMYCIN AMPLITUDE P VALUES AT 16KHZ AND THE HOLM BONFERRONI CORRECTION. VALUES WHERE THE NULL HYPOTHESIS IS REJECTED ARE HIGHLIGHTED RED.* 231
TABLE 35: *PELLET WITH RIFAMPICIN CLINDAMYCIN AMPLITUDE P VALUES AT 24KHZ AND THE HOLM BONFERRONI CORRECTION. VALUES WHERE THE NULL HYPOTHESIS IS REJECTED ARE HIGHLIGHTED RED.* 231
TABLE 36: *THE CHANGES IN LATENCY FOR WAVES P1-P3 MEASURED AT 16KHZ AND 24KHZ FOR THE BIOLOGICAL CONTROL GROUP.* 237
TABLE 37: *CHANGES IN LATENCY FOR WAVES P1-P3 MEASURED AT 16KHZ AND 24KHZ FOR THE SURGICAL CONTROL GROUP.* 242
TABLE 38: *CHANGES IN LATENCY FOR WAVES P1-P3 MEASURED AT 16KHZ AND 24KHZ FOR THE PLGA AND PLURONIC PELLET CONTROL GROUP.* 246
TABLE 39: *THE CHANGES IN LATENCY FOR WAVES P1-P3 MEASURED AT 16KHZ AND 24KHZ FOR THE PLGA AND PLURONIC LOADED WITH RIFAMPICIN AND CLINDAMYCIN GROUP.* 251
TABLE 40: *CHANGES IN LATENCY FOR WAVES P1-P3 MEASURED AT 16KHZ AND 24KHZ FOR THE PLGA AND PLURONIC LOADED WITH RIFAMPICIN GROUP.* 254

TABLE 41: *CHANGES IN LATENCY FOR WAVES P1-P3 MEASURED AT 16KHZ AND 24KHZ FOR THE PLGA AND PLURONIC LOADED WITH CLINDAMYCIN GROUP.* 258
TABLE 42: *SUMMARY OF THE CHANGES IN LATENCY FOR WAVES P1-P3 MEASURED AT 16KHZ AND 24KHZ FOR ALL EXPERIMENTAL GROUPS.* 259
TABLE 43: *RESULTS OF FRIEDMAN'S TWO WAY ANALYSIS OF LATENCY OF WAVE P1. SIGNIFICANCE IS DENOTED BY A *.* 261
TABLE 44: *RESULTS OF FRIEDMAN'S TWO WAY ANALYSIS OF LATENCY OF WAVE P2. SIGNIFICANCE IS DENOTED BY A *.* 262
TABLE 45: *RESULTS OF FRIEDMAN'S TWO WAY ANALYSIS OF LATENCY OF WAVE P3. SIGNIFICANCE IS DENOTED BY A *.* 263
TABLE 46: *BIOLOGICAL CONTROL LATENCY P VALUES AT 16KHZ AND THE HOLM BONFERRONI CORRECTION. VALUES WHERE THE NULL HYPOTHESIS IS REJECTED ARE HIGHLIGHTED RED.* 264
TABLE 47: *BIOLOGICAL CONTROL LATENCY P VALUES AT 24KHZ AND THE HOLM BONFERRONI CORRECTION. VALUES WHERE THE NULL HYPOTHESIS IS REJECTED ARE HIGHLIGHTED RED.* 265
TABLE 48: *SURGICAL CONTROL LATENCY P VALUES AT 16KHZ AND THE HOLM BONFERRONI CORRECTION. VALUES WHERE THE NULL HYPOTHESIS IS REJECTED ARE HIGHLIGHTED RED.* 265
TABLE 49: *SURGICAL CONTROL LATENCY P VALUES AT 24KHZ AND THE HOLM BONFERRONI CORRECTION. VALUES WHERE THE NULL HYPOTHESIS IS REJECTED ARE HIGHLIGHTED RED.* 266
TABLE 50: *PELLET CONTROL LATENCY P VALUES AT 16KHZ AND THE HOLM BONFERRONI CORRECTION. VALUES WHERE THE NULL HYPOTHESIS IS REJECTED ARE HIGHLIGHTED RED.* 266
TABLE 51: *PELLET CONTROL LATENCY P VALUES AT 24KHZ AND THE HOLM BONFERRONI CORRECTION. VALUES WHERE THE NULL HYPOTHESIS IS REJECTED ARE HIGHLIGHTED RED.* 267
TABLE 52: *PELLET WITH RIFAMPICIN AND CLINDAMYCIN LATENCY P VALUES AT 16KHZ AND THE HOLM BONFERRONI CORRECTION. VALUES WHERE THE NULL HYPOTHESIS IS REJECTED ARE HIGHLIGHTED RED.* . 267
TABLE 53: *PELLET WITH RIFAMPICIN AND CLINDAMYCIN LATENCY P VALUES AT 24KHZ AND THE HOLM BONFERRONI CORRECTION. VALUES WHERE THE NULL HYPOTHESIS IS REJECTED ARE HIGHLIGHTED RED.* . 268
TABLE 54: *PELLET WITH RIFAMPICIN LATENCY P VALUES AT 16KHZ AND THE HOLM BONFERRONI CORRECTION. VALUES WHERE THE NULL HYPOTHESIS IS REJECTED ARE HIGHLIGHTED RED.* 268
TABLE 55: *PELLET WITH RIFAMPICIN LATENCY P VALUES AT 24KHZ AND THE HOLM BONFERRONI CORRECTION. VALUES WHERE THE NULL HYPOTHESIS IS REJECTED ARE HIGHLIGHTED RED.* 269
TABLE 56: *PELLET WITH CLINDAMYCIN LATENCY P VALUES AT 16KHZ AND THE HOLM BONFERRONI CORRECTION. VALUES WHERE THE NULL HYPOTHESIS IS REJECTED ARE HIGHLIGHTED RED.* 269
TABLE 57: *PELLET WITH CLINDAMYCIN LATENCY P VALUES AT 24KHZ AND THE HOLM BONFERRONI CORRECTION. VALUES WHERE THE NULL HYPOTHESIS IS REJECTED ARE HIGHLIGHTED RED.* 270
TABLE 58: *TABLE TO SHOW THE GUINEA PIGS HOUSED AT RANDOM (INITIALLY WITH 4 PER CAGE)* 313
TABLE 59: *TABLE TO SHOW COMPOUNDS WITH THEIR MOLECULAR WEIGHT, HEARING LOSS PROFILE AND MECHANISMS OF CAUSATION OF OTOTOXICITY.* 325

Abbreviations

ABR	Auditory Brainstem Response
AHL	N-acetyl homocysteine lactones
AOM	Acute otitis media
ASPA	Animals and Scientific Procedures Act 1986
cGMP	cyclic guanosine monophosphate
CRS	chronic rhinosinusitis
CSLM	confocal scanning laser microscopy
CSOM	chronic supporative otitis media
DAPI	4', 6-diamidino-2-phenylindole (fluorescent stain binding to A-T)
dB	decibels
DNA	Deoxyribonucleic acid
DPX	Distrene – tri cresyl phosphate in xylene
EAC	External auditory canal
EDTA	Ethylenediaminetetra-acetic acid
EEG	electroencephalograph
ENT	ear, nose, throat
EPS	extracellular polymeric substance
H and E	Haematoxylin and Eosin
Hz	Hertz
IHC	inner hair cells
IID	interaural intensity difference
ITD	interaural time difference
LPS	Lipo polysaccharide

ME	middle ear
MRC	medical research council
NACWO	Named animal care and welfare officer
NHS	National Health Service
NICE	National Institute of Clinical Excellence
NIHL	Noise induced hearing loss
NO	Nitric oxide
OAE	Otoacoustic emissions
OHC	outer hair cells
OME	otitis media with effusion
P	PLGA and pluronic pellet
PA	PLGA and pluronic pellet with antibiotics
PClind	PLGA and pluronic pellet with clindamycin
PCR	polymerase chain reaction
PIA	polysaccharide intracellular adhesion
PIP2	phosphatidylinositol 4,5 bisphosphonate
PLGA	poly-lacto-co-glycolic acid
PRif	PLGA and pluronic pellet with rifampicin
PVA	polyvinyl alcohol
RW	round window
SC	surgical control
SCV	small colony variants
SEM	scanning electron microscopy
SNHL	sensorineural hearing loss
SSNHL	sudden sensorineural hearing loss
SPL	sound pressure level

SM	scala media
ST	scala tympani
SV	scala vestibuli
TARGET	Trial of alternative regimens in Glue Ear treatment
TDT	Trucker-Davis Technologies
TM	tympanic membrane
TMPA	trimethylphenylammonium
UK	United Kingdom
USA	United States of America
UV	ultra violet
WHO	World Health Organisation

Chapter 1: Introduction

1.1 Understanding the transduction of sound on developing therapeutic intervention to OME

Otitis Media with Effusion (OME) is the commonest cause of paediatric hearing impairment in the developed world (Mandel *et al*., 2008). Current treatment strategies include ventilation tube insertion (NICE 2008). This has approximately 25% of patients requiring a repeat surgical procedure within two years of the first procedure (Gates *et al*., 1987) and with a mean number of procedures per person of 2.1 (Daniel *et al.,* 2006). The ideal treatment strategy should therefore be to treat OME and prevent recurrence with a single therapeutic intervention. A putative new treatment for OME is insertion of an antibiotic laden pellet into the middle ear allowing topical antibiotic delivery in a sustained release fashion. Such pellets have been designed using polylactic glycolic acid (PLGA) and pluronic and when loaded with rifampicin and clindamycin demonstrate biofilm eradication *in vitro* (Daniel *et al*., 2010). Inserting these pellets into the middle ear of animal models is an important step to establish the safety of potential new OME treatments.

Before understanding the potential harmful effects of drug pellets on inner ear function, it is first necessary to consider the middle and inner ear function in normal hearing individuals and the overall impact of impaired hearing.

1.1.1 The Sense of Hearing

The sense of hearing influences all aspects of life (Barker *et al*., 2017). Sound is a key component to human survival throughout evolution (Manley *et al*., 2017); through detection of prey by predators and hence has a vital role in danger avoidance and prolonging life. Hearing is also a key component of communication with other individuals, contributing to life's overall enjoyment (Bakhos *et al*., 2017). Human progress throughout the millennia with the development of language and subsequent learning and passing on knowledge has been greatly influenced by hearing and communication (Manley *et al*., 2017). Hearing is a component of many hobbies including music. This is evidenced from Beethoven's Heiligenstadt Testament at the age of 31 when he describes his decreased appreciation for his music and subsequent desperation and reclusiveness due to progressive hearing loss (Van Beethoven 1802).

Impaired hearing in childhood can affect language development (Samelli *et al*., 2017). This is seen in conditions such as Otitis Media with Effusion (OME) which is the commonest cause of paediatric hearing impairment in the developed world (Mandel *et al*., 2008). OME causes a conductive hearing loss due to fluid accumulation in the middle ear (Venekamp *et al*., 2016) and is common in the 2-6 year age group during language acquisition (Qureishi *et al*., 2014). Understanding the detailed mechanisms of sound transmission through the ear is a key component to developing therapeutic interventions to treat OME and hence prevent the long term sequelae of speech and language delay and missed academic potential.

1.1.2 Overview of anatomy and hearing

Sound is a compressive wave in an elastic medium. It is a form of mechanical energy and is caused by changes in air pressures which are detected by the ear. Molecules of air are constantly moving and colliding. This is described as Brownian motion of air molecules in contact with the tympanic membrane (Harris *et al*., 1968). Compression of air molecules creates a sound, which travels in the form of a sinusoidal compressive wave to the pinna. The EAC (external auditory canal) channels the sound wave to the tympanic membrane (Szymanski *et al*., 2018) causing vibrations at the frequencies of the component sounds. The tympanic membrane vibrations in turn cause ossicular chain vibrations (malleus, incus and stapes) which results in the stapes footplate vibrating the oval window (O'Connor *et al*., 2017) (Figure 1).

Vibrations of the oval window are transmitted to the scala vestibuli in the cochlea (Rask-Andersen *et al*., 2018). The cochlea has three main components (Zou *et al*., 2015); the SV (scala vestibuli), SM (scala media) and ST (scala tympani). Acoustic energy is transferred from the air containing middle ear to the fluid filled cochlea (Greene *et al*., 2015) and then from the oval window to the round window (Figure 2). The wave travels through the scala vestibuli first, then the flexible partition of the cochlea, called the basilar membrane, vibrates (Warren *et al*., 2016). This vibration is characteristic for the sound's frequency, creating a tonotopic organisation of the sound (Warren *et al*., 2016). Vibration of the OHC (outer hair cells) and IHC (inner hair cells) in the Organ of Corti then contribute to signal transduction as channels on the apical portion of the inner hair cells are mechanically opened via the tip links creating

a depolarising current (Fettiplace *et al*., 2017). Inward flux of K^+ and Ca^{2+} ions cause depolarisation and generation of an action potential which results in release of glutamate on to spiral ganglion processes (Fettiplace *et al*., 2017). Here, action potentials are generated in response to the glutamate induced depolarisation. These action potentials are propagated to the brain stem via afferent neurons (Fettiplace *et al*., 2017).

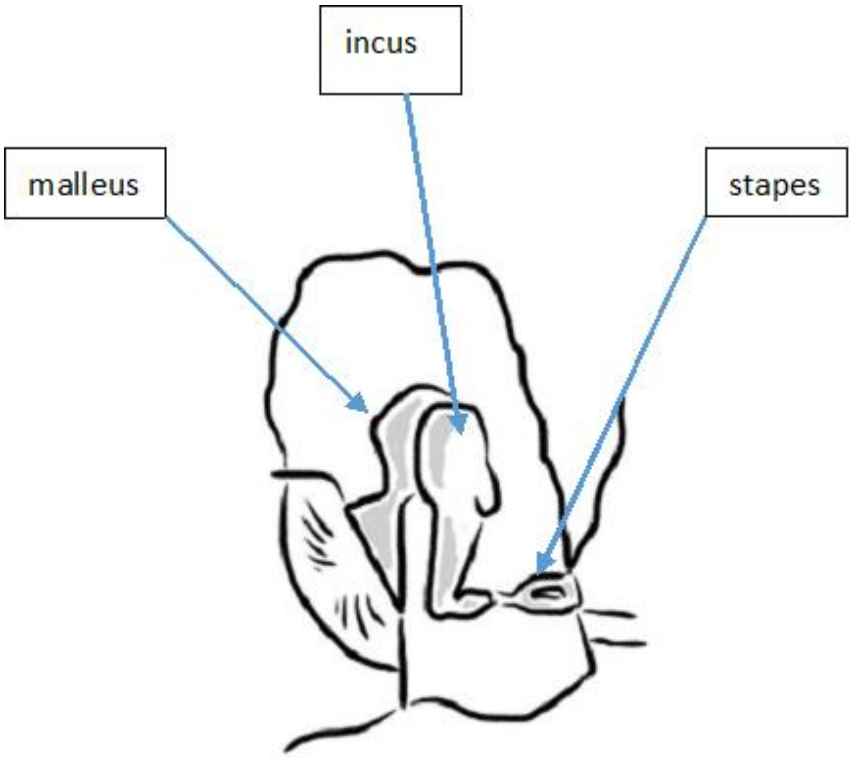


Figure 1: ***Coronal view of the left middle ear showing the ossicular chain: malleus, incus and stapes (Illustration by E Hoskison using Paint)***

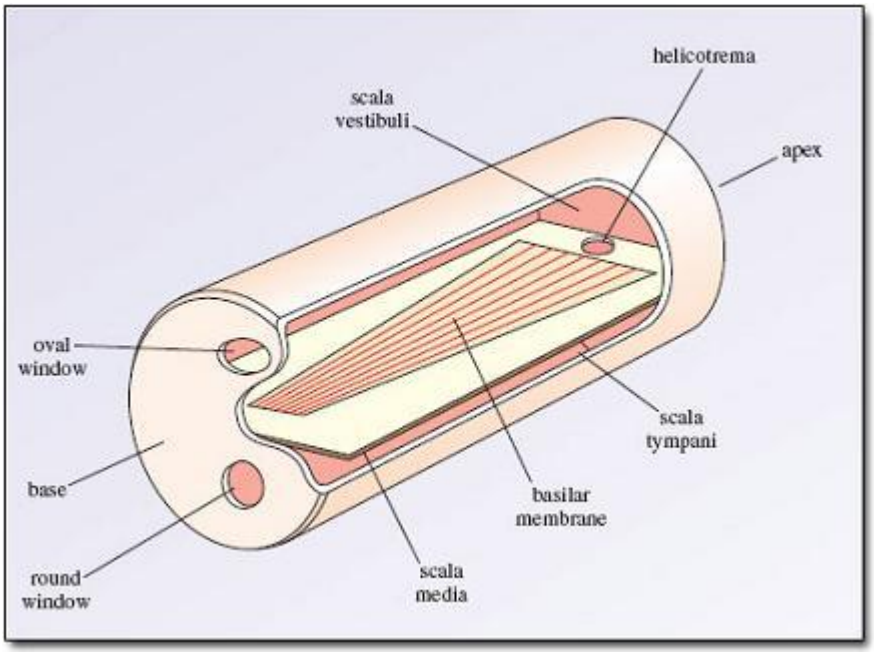


Figure 2: ***Schematic diagram showing the tapered basilar membrane increasing in width from the base to the apex (from webnode.com)***

A cross section of the cochlea (Figure 3) showing separation into three main compartments (ST, SM and SV) and the separation of the perilymph and the endolymph. This allows for the maintenance of a resting potential in the Organ of Corti, known as endocochlear potential, before depolarisation and action potential generation.

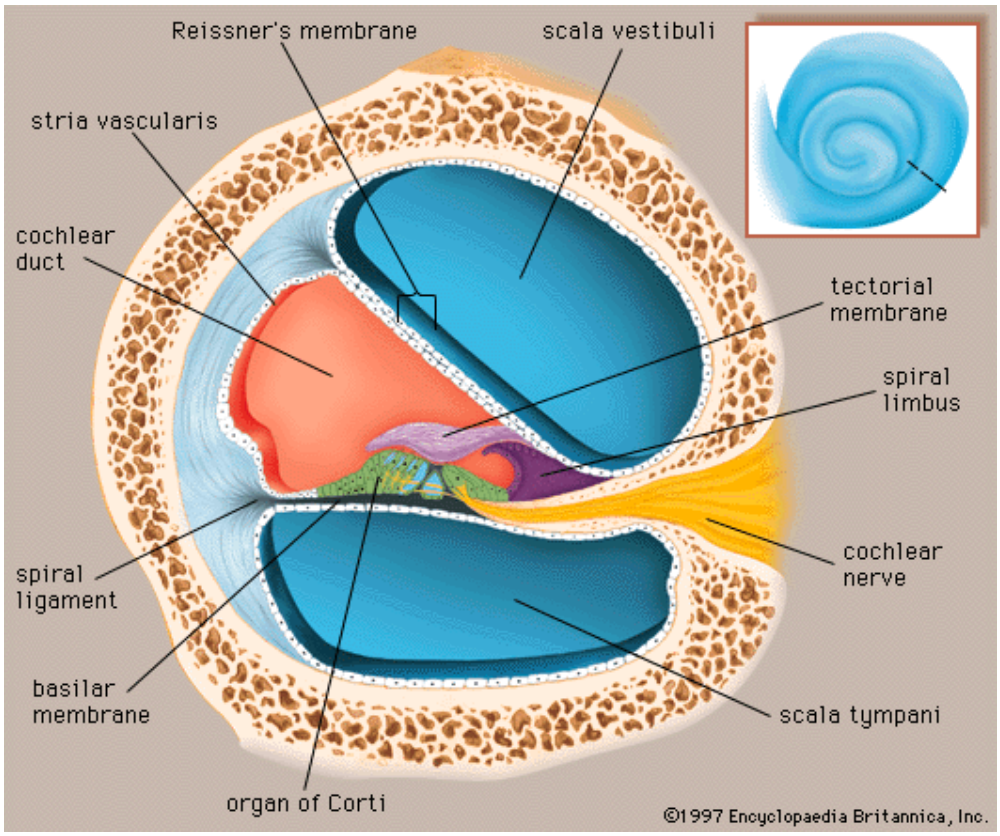


Figure 3: ***Cross section of the cochlea showing the cochlear duct or scala media (Encyclopedia Britannica Inc 1997)***

The cochlea is adapted for the transduction of mechanical energy into electrical energy whilst preserving the sound wave's temporal structure, intensity and amplitude. The ear has several adaptive mechanisms which ensure that minimal energy is wasted in transmission of the sounds to the cochlea. This is especially important due to the impedance mismatch of the air-water interface from the middle to the inner ear (Withnell *et al*., 2013). Without the middle ear acting as energy transformer, over 99.9% of incident sound energy would be reflected at the air-fluid interface at the junction of the air in the middle ear and fluid filled inner ear. This would be the equivalent of approximately 30dB hearing loss.

Amplification mechanisms include channelling the sound's energy at the pinna. Animals such as cats are designed to rotate their ears to the direction of the sound to improve linearity of the acoustic axis and hence sound detection and spatial awareness of its source (Musicant *et al*., 1990). Humans, however do not have this adaptation. The binaural design allows analysis of the time delay as sound reaches the two ears separately and the intensity difference between the two ears is analysed and processed by the brain – this is the interaural time difference (ITD). The head shadow effect creates the interaural intensity difference (IID) and assists directionality coding of sounds (Parisa *et al*., 2017). Such information is encoded in a complex signal allowing accurate temporal and spatial information of the sound to be analysed by the brain. In humans, the accuracy of sound localisation is 1.5 degrees (Durlach *et al*., 1978).

The air-fluid interface at the oval window creates an impedance mismatch which the ear has adapted to overcome using two mechanisms. The surface area of the tympanic membrane is 20 times greater than the oval window. The oval window is located at the stapes footplate allowing amplification of signal. The ossicular chain also acts as a fulcrum with a lever ratio of 1.3 in humans (Guinan *et al*., 1967) amplifying the mechanical vibrations and limiting dissipation of energy. As a result of these two mechanisms, hydraulic press and lever arm, approximately 30dB of sound energy is gained, compensating for the losses from the air/fluid interface impedance mismatch (Withnell *et al*., 2013).

The sound amplification and impedance mismatch function of the middle ear is important to understand when attempting to address pathology of the middle ear such as OME (otitis media with effusion). The preservation of middle ear function is also important when considering any therapeutic intervention for middle ear disease such as OME. Tympanic membrane and ossicular chain integrity are important to maintain optimal middle ear function.

1.1.3 Specialised features of sound transduction

Von Békésy's experiments on cochlea physiology demonstrated that, when using a vibrating electrode to record from the basilar membrane, the cochlea monophonic wave was proportional to the basilar membrane displacement and not velocity (Békésy *et al*., 1974). His work also showed properties of the basilar membrane which set up the tonotopic mapping along its length - the apex is wider and has resonance with low frequency sounds. Vibrations of the basilar membrane in a sound specific location contribute to tuning of the sound. The basilar membrane has a central role in signal transduction. Energy is transmitted to a specific locus allowing hair cell vibrations resulting in signal transduction.

1.1.4 Trapdoor model theory

Vibration of the OHC in the organ of Corti at frequency specific longitudinal distance along the basilar membrane has led to the "trapdoor model" for ion channel opening. The tectorial membrane acts as a spring on top of the OHC. As the basilar membrane is deflected down, the tectorial membrane is stretched and the vibrations are

transferred to the OHC. The hair cells are central to signal transduction of mechanical energy into electrical signals. As the OHC vibrate in an excitable fashion, the "trapdoor" model of ion channel opening and hair cell excitation causes a depolarising current by K^+ and Ca^{2+} ion influx (Gillespie *et al*., 1995) (Figure 4). The tip links connecting the OHC are an essential component of this motion detection. Tip link destruction by proteolytic enzyme elastase (Preyer *et al*., 1995) or removal of the Ca^{2+} ions (Assad *et al*., 1991) shows a loss of signal transduction, supporting this model. Studies on the frog saccular hair cells have shown that whole bundle stiffness is a property of the open probabilities of transduction channels (Hudspeth *et al*., 1988) which is evidence that this mechanism transcends across vertebrates. Stretch on the tip links has been shown experimentally to be directly proportional to the angle of stereocilia deflection (Geisler *et al*., 1998) emphasising the accuracy and effectiveness of the tip links as sensors (Geisler *et al*., 1993) and their role in transduction of the sound into an electrical signal.

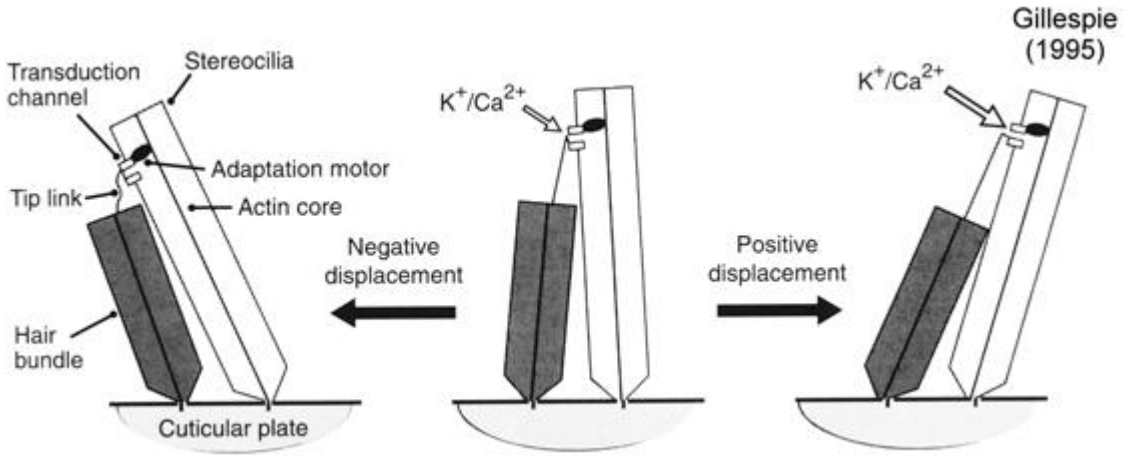


Figure 4: ***Schematic diagram of the "trapdoor" model showing hair cell excitation with positive displacement mediated by the tip links (Gillespie et al., 1995)***

Current flow has also been shown to be proportional to stereocilia displacement in the direction of the kinocilium (Fettiplace 1992) with a sensitivity of up to 0.3nm (Hudspeth *et al*., 1988).

1.1.5 Adaptation

The cochlea is also able to undergo adaptation to a stimulus; a property which is function of the stereocilia. Adaptation occurs during excitation when the magnitude of the transducer current slowly decreases to a new resting level. The mechanism of hair cell adaptation has been shown to be a function of calcium ion concentration - with a reduction in speed of adaptation shown in turtle hair cells when the Ca^{2+} ion concentration is decreased from 3nM to 1mM (Crawford *et al*., 1991). It has been proposed that the calcium ions interact with the transducer channels determining the state of adaptation (Fettiplace *et al*., 1992). Adaptation involves movement of the ion channel up or down the stereocilium.

The “motor” theory of adaptation was proposed by Hudspeth and Gillespie in 1994 with actin-myosin interaction causing increased tension in the tip links during excitation, gradually dragging the adaptation motor downwards and hence reducing tension until a new equilibrium is reached. Conversely, when deflected in the opposite inhibitory direction, the tip links have a reduced tension allowing the motor mechanism to climb upwards to counteract this.

1.1.6 Frequency selectivity

Hair cells are adapted to have a greater sensitivity to sinusoids of a certain frequency along the length of the basilar membrane (Fettiplace *et al*., 1992). This selectivity is a function of the tonotopic organisation of the basilar membrane due to the physical change in properties of the basilar membrane along its length. The OHC also have a role fine-tuning this mechanism by refining the signal.

1.1.7 Amplification

Measurements of basilar membrane displacement in response to sound waves were first performed by Von Békésy (Von Békésy 1974) using stroboscopic light and large amplitudes. This produced displacements in the micrometre range. Johnstone and Boyle used a Doppler shift technique in 1967 to measure basilar membrane displacements (Johnstone *et al*., 1967). Khanna and Leonard were the first to use submicron measurements of the basilar membrane using laser interferometry (Khanna *et al*., 1982). Interferometry is a technique used to detect small displacements using the principles of a coherent single beam being split into two identical beams of electromagnetic radiation. Each beam travels a separate path and then they combine at a detector. Any resulting phase difference in the beams as they arrive at the detector is analysed to determine the difference in path length or a refractive difference along the path. Such measurements show the fine tuning of the basilar membrane for frequency specific sounds and also superior accuracy for low sound levels.

The identification of sound emissions from human ears in response to brief clicks (Kemp *et al*., 1978) provided a clue to the cochlea's transduction processes. Evidence that these sounds were generated by outer hair cells was supported by Brownell (1985) with the identification of the OHC as the source of otoacoustic emissions (OAE) as they mechanically deform when stimulated with a current (Brownell *et al*., 1985). The reticular lamina and the basilar membrane were seen to move towards each other as the OHC contracted. These results showed the OHC enhancing the responses of the basilar membrane in a frequency selective manner acting as a feedback mechanism. This amplification mechanism varies in extent along the length of the basilar membrane explaining the variation in fine tuning between more basally placed high frequency and apical low frequency sounds.

1.1.8 Innervation

Signal transduction occurs at the IHC generating an action potential which is transmitted along spiral ganglia neurones to the brain. Each IHC connects with 10-30 afferent neurons with a single synapse to type I myelinated neurons and multiple synapses with type II unmyelinated neurons. Such complex innervation is required for rapid, accurate coding of temporal events (Geisler *et al*., 1998). The presence of efferent innervations, via the olivocochlear system, has a mechanism in the fine tuning and hence accurate transduction of the electrical signal. Feedback is directed to the outer hair cells or the axons which supply the IHC. This mechanism allows sharp signal generation.

1.1.9 Summary of signal transduction

Mechanical energy travelling through the middle ear is amplified to minimise energy dissipation at the air fluid interface between the middle and inner ears. This is achieved using two mechanisms: 1) reducing the surface area of the oval window relative to the TM and 2) the fulcrum mechanism of the ossicles. The cochlea utilises a number of different processes for signal transduction utilising the IHC which are situated along the basilar membrane. Tonotopic organisation of the cochlea's basilar membrane assists the organisation of transduction. The OHC and efferent feedback mechanisms have a role in signal tuning to preserve temporal, spatial, intensity and frequency information, accurate discrimination which is important to human communication, interaction and survival.

Understanding the mechanisms of signal transduction is essential prior to designing and implementing potential invasive treatments for ME conditions such as OME. This is where fluid accumulates in the ME cavity affecting the impedance-mismatch mechanism and transmission of sound to the inner ear.

1.2 Otitis Media with Effusion

OME is the commonest cause of paediatric hearing impairment in the developed world (Mandel *et al*., 2008). Understanding the detailed aetiology and pathogenesis of OME allows for design of therapeutic interventions which are safe, effective and acceptable to the paediatric population.

OME is the chronic inflammation of the middle ear mucosa associated with development and accumulation of mucus behind an intact tympanic membrane and without the symptoms and signs of acute infection (Venekamp *et al*., 2016). The mastoid air cell system may also be involved due to its anatomical connection with the ME via the mastoid antrum (Abdul-Aziz *et al*., 2017). OME has a clinical diagnosis with the presence of mucin and resultant conductive hearing loss (Schilder *et al*., 2016). If the mucus is present for a three month timescale, the effusion is considered to be chronic (Bluestone *et al*., 1984). It is common for a middle ear effusion to develop after an upper respiratory tract infection (Schilder *et al*., 2016) with a majority of these resolving naturally. Any middle ear irritation can lead to an effusion developing and hence the causes of OME are widespread including trauma (Miller *et al*., 2016), infection and inflammation (Wierzbicka *et al*., 2012).

1.2.1 Symptoms

Fluid which is either serous or mucoid in consistency can accumulate in the middle ear and affects the transmission of sound from sound waves from the external ear to the

cochlea. The fluid decreases tympanic membrane and ossicular chain vibration and hence attenuates the propagation of the sound signal through the middle ear. Children with OME therefore experience a 18-35dB conductive hearing loss (Cai *et al*., 2017) due to the impaired ME function. Presentation maybe with hearing impairment and preschool children may demonstrate speech and language delay. Although symptoms are transient in most children, a proportion require treatment because of the impact OME has on hearing and subsequent education and speech and language development (NICE 2008). Children may have a preceding history of AOM (acute otitis media) with fever and otalgia. In young infants this otalgia may manifest with ear pulling or general malaise for example being unable to sleep, irritable and unable to tolerate a normal diet. OME, AOM and recurrent AOM with three or more episodes in a six month interval are all closely related conditions (Alho *et al*., 1995). Studies of school children have shown that patients with AOM are more likely to develop OME (Martines *et al*., 2011).

1.2.2 Prevalence

Otitis Media with Effusion (OME) is the commonest cause of hearing impairment in the developed world (Mandel *et al*., 2008) with a point prevalence of 20% (proportion of patients having OME at any one time) and up to 80% of the population of children being affected before the age of 10 years (Mandel *et al*., 008; NICE 2008). OME is common in the preschool age group with two peaks of incidence seen at 2 and 5 years (Zielhuis *et al*., 1990) as seen in a study of Dutch children. A cumulative incidence of OME has been shown in preschool children in the USA with 53% incidence in the first

year and 61% in the second (Casselbrandt *et al*., 1995). A European cohort has found that 35% of children have had at least one episode of otitis media before the age of two (Brauer *et al*., 2006). A large study of n=2253 in Pittsburgh USA (Paradise *et al*., 1997) showed that 91.1% of children developed OME in the first two years of life and of these, 52.5% had bilateral effusions. These effusions in the Paradise study were due to both OME and AOM; two conditions which other studies show are interlinked (Martines *et al*., 2011).

Draining the OME with ventilation tube insertion is also one of the most common surgical procedures performed in children. This is the current treatment regimen for OME according to the NICE guidelines of 2008. However, it does not address the underlying infection and hence many children have OME recurrence. Approximately 25% of patients require a repeat surgical procedure within two years of the first procedure (Gates *et al*., 1987) and studies have shown that the mean number of procedures per person is 2.1 (Daniel *et al*., 2006). The ideal treatment strategy should therefore be to treat OME and prevent recurrence with a single therapeutic intervention.

1.2.3 Aetiology

OME is a multifactorial disease process. Risk factors for OME, however, have been identified through extensive epidemiological studies. There are still many theories regarding the aetiology of OME and hence this is an active area of ongoing research. The numerous theories underlying the pathogenesis of OME explains the multiple different treatments which are offered to patients, without a consensus for one single

effective treatment strategy. It is possible that OME is a multifactorial disease process but with different dominant factors causing OME in different individuals. This would result in treatment tailored to each separate patient to initially address the dominant factors with the aim of eliminating OME. This is the case in other multifactorial disease processes in medicine and therefore, there would be a precedent for the treatment of OME to follow a similar pattern. The challenge posed, therefore, is to determine the dominant factor in each patient and to tailor this treatment accordingly.

Genetic studies have shown that OME has a significant genetic component. A prospective twin study in Pittsburgh, USA showed a strong correlation between monozygotic sets compared to dizygotic sets experiencing middle ear effusions over a 24 month period (Casselbrant *et al*., 1999). It has been speculated that this may have an anatomical basis with a hereditability of degree of pneumatisation of the mastoid (Dahlberg *et al*., 1945) and differences in Eustachian tube dimensions and function according to race (Beery *et al*., 1980). In an attempt to further characterise genetic susceptibility, genomic scanning has been done and loci on chromosomal regions 10q, 19q and 3p have been identified as possible gene locations for chronic and recurrent OME (Daly *et al*., 1999).

OME has a seasonal prevalence with approximately twice as many cases in the winter months compared to the summer months (Rovers *et al*., 2000, Sassen *et al*., 1997). This may be due to an increase in upper respiratory tract infections and closer contact with other children during these colder months due to increased time spent indoors.

Attendance in day care with more than four children under 3.5 years of age has also been identified as a risk factor for OME (Dewey *et al*., 2000). This supports the contact theory with the main aetiological cause being a contagious environmental factor such as viruses and bacteria that may survive as a biofilm on toys and surfaces in the day-care environment (Walker *et al*., 2017).

1.2.4 Pathogenesis

The middle ear communicates with the nasopharynx via the Eustachian tube (Jufas *et al*., 2016); both have an epithelial lining. The epithelial cells are similar to those in the upper respiratory tract, acting as a defence mechanism against the environment. The epithelium of the middle ear varies depending on location (Luo *et al*., 2017). Near the Eustachian tube opening, it is cuboidal or columnar, turning into flat epithelium near the mastoid air cell system and cuboidal on the promontory. Inside the mastoid, the epithelium is squamous and the Eustachian tube is lined with tall columnar epithelial cells which are ciliated and secretory (Hentzer *et al*., 1984). This creates a mucociliary transport system carrying pathogens from the middle ear down the Eustachian tube and into the nasopharynx (Ilomäki *et al*., 2016). Insults to the cilia in the form of upper respiratory tract infections result in impaired function or destruction of the cilia causing tubal dysfunction and impaired mucociliary clearance (Ohashi *et al*., 1991).

The healthy middle ear secretes fluid from the mucosal epithelial cells. The mucosal fluid is composed of mucins (Solzbacher *et al*., 2003), antibodies (Bernstein *et al*., 1993), defensins (Underwood *et al*., 2011), protegrins (Bolintineanu *et al*., 2011), collectins (van Rozendaal *et al*., 2001), cathlecidins (Lehrer *et al*., 2002), lysozyme (Travis *et al*., 1999), histatins (Melino *et al*., 2014) and nitric oxide (Brukdorfer *et al*., 2005). All of these molecules have a defensive role acting producing a physical barrier and with their antimicrobial properties (see Table 1). The mucus secreted by the respiratory epithelium in the body has a variable thickness according to the site of secretion. For example the ear has thinner mucus than in the mucus lining the stomach. Mucus is also constantly in motion in a healthy individual due to the action of the beating respiratory cilia (Luo *et al*., 2017).

In a healthy individual, middle ear fluid does not accumulate. Clearance mechanisms which act on fluid elimination include cilia beating towards the nasopharynx via the Eustachian tube. Thus, the fluid and any accumulated debris are swallowed and the low pH of the gastric environment has a bactericidal effect eliminating contaminants of the middle ear (Schubert *et al*., 2014).

Although the healthy middle ear mucosa is constantly secreting fluid, no effusion is seen. This suggests that there may be a difference in the composition especially regarding the viscosity of the middle ear fluid in a patient with OME and/or a defective fluid clearance mechanism.

Molecule	Role in defence	Reference
Mucins	Facilitates binding bacteria to initiate mucociliary clearance/ phagocytosis/cytokine mediated destruction	Solzbacher *et al*., 2003
Antibodies	IgE mediated hypersensitivity and activation of inflammatory cascade	Bernstein *et al*., 1993
Defensins	Antimicrobial action, proinflammatory, chemoattractants	Underwood *et al*., 2011
Protegrins	Small peptides with 16-18 amino acid residues. Integrate into lipopolysaccharide in bacterial membranes and permeabilize them	Bolintineanu *et al*., 2011
Collectins	Family of collagen containing C type lectins. Soluble pattern recognition receptors which bind to micro organisms prior to phagocytosis by macrophages	van Rozendaal *et al*., 2001
Cathlecidins	Bipartite molecules with an N-terminal cathelin domain and C-terminal antimicrobial domain	Lehrer *et al*., 2002
Lysozyme	Large antimicrobial protein with action against Gram positive organisms	Travis *et al*., 1999
Histatins	Metal binding peptides with antibacterial properties	Melino *et al*., 2014
Nitric Oxide	A free radical which binds to haem and activates cGMP signalling cascade Reacts with other radicals to produce oxidants resulting in protein damage	Brukdorfer *et al*., 2005

Table 1: ***Components of middle ear secretions and their role on defence against pathogens***

In an attempt to investigate the composition of middle ear effusion in patients with OME, aspirates of the fluid have frequently been taken for scientific analysis (Brake *et al*., 2012, Daniel *et al*., 2012, Xu *et al*., 2011). This fluid is easily available from patients and has provided many research units with material to investigate to determine the components of the effusion and hence elucidate the pathogenesis of OME. There has been a huge focus on analysis of this fluid in recent years (Brake *et al*., 2012, Daniel *et al*., 2012, Xu *et al*., 2011), however it must be stated that this has been biased by the easy availability of the material and hence may not be the best source to determine the pathogenesis of OME. The composition of middle ear effusions have been shown to comprise of water, cells, cell debris, electrolytes and high molecular weight compounds of which most are mucins and a smaller number protein, lipids and deoxyribonucleic acid (DNA).

OME is caused by inflammation of the ciliated, pseudostratified columnar epithelium of the Eustachian tube and the hypotympanum. This causes mucus secretion and a differentiation into thickened pseudostratified mucus secreting epithelium (Ishii *et al*., 1980, Tos M *et al*., 1980) with a reduction in cilia number and cilia function (Takeuchi *et al*., 1990). Figure 5 demonstrates histologically the metaplasia seen in OME in a mutant mouse model labelled Islet 1 (Hilton *et al*., 2011). Examination of the middle ear histologically revealed chronic OME with an intact tympanic membrane. The mucosa was thickened with fibrocytes, granulocytes and granulation tissue. The genetic basis for this in this mouse colony was found by Hilton *et al* to be a tyrosine to

cysteine mis-sense mutation on the Islet 1 gene with further studies ongoing to detect to exact mechanisms. Islet 1 genes have previously been found in the gastric lining, suggesting a role in regulating somatostatin gene expression and hence gastric mucosal secretion.

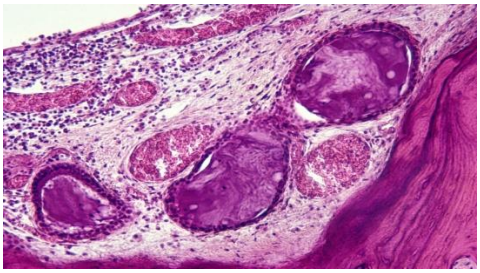


Figure 5: ***Histology of middle ear mucosa in OME showing metaplasia (Hilton 2011)***

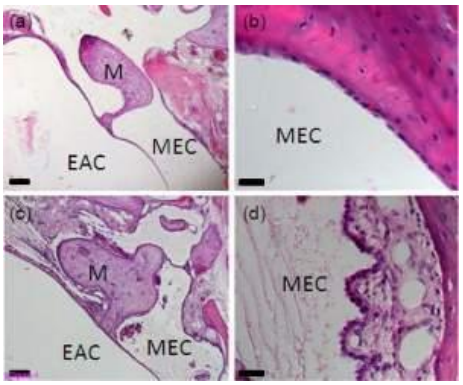


Figure taken from Hilton 2011

- a) and b) both normal mucosa of middle ear cavity (MEC) and external auditory canal (EAC) with the malleus (M)
- c) and d) from mice with *Islet 1* gene mutation. Note the thickened mucosal lining of the middle ear mucosa with mucous production, fibroblasts, granulocyte and granulation tissue

Figure 5*: Histology of middle ear mucosa in OME showing metaplasia (Hilton et al., 2011)*

Histologically, the submucosa shows blood vessel dilatation and increased number of inflammatory cells such as macrophages, plasma cells and lymphocytes. The middle ear effusion is usually mucoid or serous in nature, but its actual origins are a matter of some debate. Fluid can be secreted from the epithelial, goblet cells and mucus glands as well as an inflammatory transudate or exudate. The mucins are thought to be the

main contributing factor to the variable viscosity of the middle ear effusions (Kubba *et al*., 2000).

1.2.5 Mucins

Mucin is secreted by the middle ear epithelial cells. Mucins are glycoproteins which consist of a protein backbone, sugar side chains and interconnected disulphide bonds. Mucins allow lubrication, prevent dehydration and protect the underlying mucosa and facilitate H_2O transport. Genes expressing mucins in the middle ear are secretory gel forming, secretory non-gel forming and cell surface (Linden *et al*., 2008). Mucins located on the cell surfaces provide a barrier preventing molecules such as bacteria from attaching and invading the underlying mucosa. Other mucins have intracellular functions with a role in regulation of cell growth and apoptosis when encountering microbes or toxins (Linden *et al*., 2008).

Middle ear effusion aspirates have identified the main gel-forming mucins in the middle ear to be MUC2, MUC 5AC and MUC5B (Hutton *et al*., 1997, Ubell *et al*., 2010, Duah *et al*., 2016). Patients with OME have also been found to have defects in the MUC5AC gene which may predispose them to this condition (Ubell *et al*., 2010). In addition to bacterial pathogens, aspirates of the middle ear have been found to be composed of water, cell debris, electrolytes and high molecular weight compounds which are predominantly mucin. Mucus provides a surface for bacterial attachment to prevent bacterial adherence to the underlying mucosa causing an infection (Reddy *et al*., 1997). Mucin molecules have oligosaccharide side chains which bacteria can bind

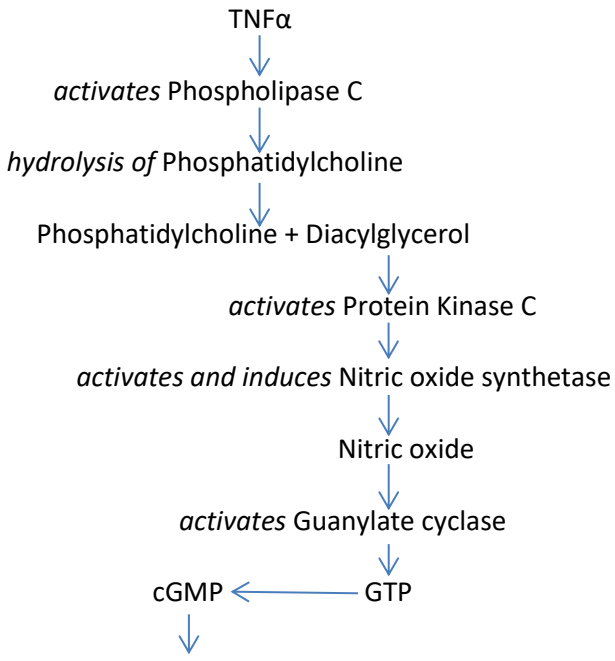
via adhesins. In a situation where the bacteria evade elimination, the mucus has the ability to proliferate in its lysozyme, lactoferrin and complement components. If the host defence systems fail in the middle ear, OME develops (Kubba *et al*., 2000).

Detailed studies of middle ear effusions has shown that there is a difference in composition of the effusions between children and also a difference in composition of effusions between left and right ears in a bilateral case of OME (Johnson *et al*., 1997). In this particular study, the levels of mucins and cytokines IL-8, TNF-α, IL-1β were analysed. Higher levels of cytokines were found in effusions with greater viscosity caused by a higher level of mucin. This suggests that inflammatory mediators may increase the production of mucin. Inflammatory mediators such as IgG and IgA have been identified in middle ear effusions in higher levels than in serum. Other features of inflammation were also identified such as vascular proliferation, infiltration of plasma cells and lymphocytes and metaplasia of the middle ear with an increase in goblet cells and mucus glands (Ishii *et al*., 1980, Sade *et al*., 1966, Jones *et al*., 1979).

Nitric oxide (NO) has been identified as an important inflammatory mediator which has cytotoxic actions when released in large quantities (Anggard *et al*., 1994). *In vitro* studies have shown that NO increases mucin production in cell cultures of goblet cells which is predominantly MUC5AC (Capper *et al*., 2003). *In vivo* models have also shown an increase in mucin with NO (Rose *et al*., 1997). Middle ear effusions have also been shown to contain NO metabolites which is further evidence that NO is an important inflammatory mediator in OME (John *et al*., 1999). Detailed genetic analysis of samples

of blood from patients with OME using PCR has shown that there is a potential susceptibility to OME with an endothelial NO synthase polymorphism (Ates *et al*., 2017). Understanding the detailed basis for OME susceptibility may help to select treatments for individuals.

Evidence of inflammatory mediators causing OME has led to proposed cascades including the flowchart from Kubba *et al*., 2000 (Figure 6). The common pathway is for mucin secretion and hence a middle ear effusion. Recent detailed analysis of mucin in OME aspirates has shown that children with MUC5B in their effusions were younger than other children undergoing ventilation tube insertion (Duah *et al*., 2016) suggesting that certain types of mucin are more pathogenic for OME, especially affecting those under 48 months. This is an important factor when considering the impact of OME on speech and language acquisition.



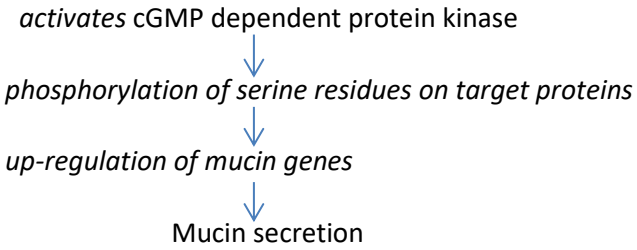


Figure 6: ***Inflammatory cascade producing mucin (adapted from Kubba et al., 2000)***

1.2.6 Viruses

Analysis of middle ear effusions has also shown that viruses have been found using reverse transcriptase polymerase chain reaction (Pitkäranta *et al*., 1998) and more recently quantitative PCR identifying viral nucleic acid in 15% of middle ear fluid samples (Slinger *et al*., 2016). Viruses detected included human rhinovirus in 63%, respiratory syncytial virus and coronavirus. Viruses activate the inflammatory cascade (Figure 6) and increase the production of mucin creating a middle ear effusion which is usually of a short duration.

1.2.7 Bacteria

Although OME is likely multifactorial (Schilder *et al*., 2016), there is a wealth of evidence for the involvement of bacteria. There is overlap between the incidence of AOM in children and the subsequent development of OME and it has been found that 50% of middle ear effusions follow an episode of AOM (Alho *et al*., 1995). Identified risk factors include attendance in day care, increased number of siblings and a low socioeconomic group. All of these factors increase the risk of infection spread and reduced hygiene. Breast feeding increases an infant's immunity due to its antimicrobial

and anti-inflammatory properties and hence is believed to be a protective factor against OME (Abrahams *et al*., 2011). Neonatal immunity is also attributable to antibodies transferred from the mother to baby *in utero*. This effect lasts 6 months, therefore breast feeding for greater than 6 months may confer additional protection. There is also likely to be synergy with the risk factors such as breastfeeding and high socioeconomic class. Adenoidal hypertrophy in the nasopharynx has been postulated as a site where bacteria are quiescent before transfer via the Eustachian tube into the middle ear. This theory is supported by evidence that there is a higher number of pathogens in the nasopharyngeal flora of children with OME (91%) compared to those without (Hemlin *et al*., 1991).

Aspirates of OME fluid which has been present for more than 2 months have shown live bacteria in 91.8% of samples (Daniel *et al*., 2012) indicating their possible role in the pathogenesis of OME. The most common was *Streptococcus pneumonia* in 8% (Jero *et al*., 1997). This study was performed on children with a wide age spectrum and the incidence of pathogens was found to be higher in younger children.

It is also worth commenting that in some studies up to 20% of effusions are sterile, emphasising the multifactorial components at play in the aetiology of OME. A recent multicentre study from Korea showed that aspirates from children receiving grommets cultured bacteria in only 13.3% of cases and of these, *Haemophilus Influenza* was the most prevalent (Yoo *et al*., 2018).

The current 13-valent conjugate pneumococcal vaccination given in the UK (Prevnar 13, Pfizer) confers protection against 13 strains of *Streptococcus*. Studies testing effusions from patients with OME requiring ventilation tube insertion have identified only serotype 19A which is covered by Prevnar suggesting that the other bacterial serotypes of Streptococcus which are found in the middle ear are not currently covered by a vaccination schedule (Slinger *et al*., 2016).

1.2.8 Atopy

There is mixed evidence that atopy has a role in the aetiology of OME. Martines *et al*., (2011) found a strong association with OME and atopy in a cohort of 2097 Sicilian schoolchildren. One theory behind this include impaired immunity and a middle ear inflammatory reaction increasing susceptibility to microbial infection (Zernotti *et al*., 2017). However, other studies contradict this (Tos *et al*., 1979). Oral antihistamines have been shown to have no benefit in the treatment of OME (Griffin *et al*., 2006) again highlighting the multifactorial nature of OME.

1.2.9 Eustachian tube “ex-vacuo” theory

A theory for the development of OME which has now been largely abandoned is the “ex-vacuo” theory. This describes blockage of the Eustachian tube which causes a negative middle ear pressure and the development of a transudate effusion. Analysis of the middle ear effusion has shown that exudates are present which contradicts this theory. Eustachian tube dysfunction may allow acid reflux to pass to the middle ear causing inflammation. In children, the Eustachian tube is more horizontal than in adults, hence facilitating acid reflux to the middle ear. This acid reflux could also aid bacterial transfer to the middle ear. Evidence for this theory of Eustachian tube dysfunction as an aetiological factor for OME includes the presence of pepsin in the middle ear fluid at concentrations of 1000 times greater than serum (Tasker *et al*., 2002). Pepsin is a component of gastric secretions and hence its presence at high concentrations in the middle ear is evidence supporting reflux. A recent study showed evidence of laryngopharyngoreflux in 67% of children with OME (Górecka-Tuteja *et al*., 2016) using pH manometry of the oesophagus. This study did not investigate the presence of reflux up to the ET and potential contribution to the pathogenesis of OME. It is also important to state that both LPR and OME are common and hence an association is therefore expected.

1.2.10 Prognosis of OME

A large proportion of patients with OME have a self-resolving condition which requires no treatment.

In the USA there is a much lower threshold for referral to see a specialist. In the UK, children referred to specialist ENT clinics are those that have significant behavioural problems and educational concerns. This variation in threshold for referral may explain any discrepancies between epidemiology between the UK as compared to the USA and differences in Health care systems (private insurance in the USA vs. National Health Service in the UK).

In the acute setting, AOM has the potential sequelae of acute mastoiditis which can lead to intracranial complications including sagittal sinus thrombosis, meningitis and intracranial abscess formation with a death rate of 5% in the cases which develop into intracranial complications (Bluestone *et al*., 2002). Chronic OME has the potential complications of deficient expressive speech, poorer concentration skills, high frequency sensorineural hearing loss, tympanic membrane atelectasis, perforation, retraction and cholesteatoma (Daly *et al*., 1999). With language delay there is a subsequent overall impact on education, career and hence earning potential in later life.

OME has a recurrent nature in some children with 25% requiring a second grommet insertion after the first (Gates *et al*., 1987). Underlying this recurrence are virulence

factors which result in the bacteria becoming difficult to eliminate including the presence of mucin. Another potential virulence factor is the bacteria in OME live in a biofilm formation in the middle ear. Understanding the formation and architecture of biofilms in greater detail may assist in treatment of OME and long term eradication, avoiding recurrence.

1.3 Biofilms

There is evidence that OME is a biofilm disease (Hall-Stoolley *et al*., 2006). A biofilm is a highly organised multicellular community (Bakaletz *et al*., 2012) which fulfils four diagnostic criteria: 1) bacteria are aggregated 2) bacteria are associated with a surface 3) bacteria are encased in a complex extracellular matrix and 4) bacteria are recalcitrant to antibiotic treatment (Hall-Stoodley *et al*., 2009, Parsek *et al*., 2003). The community of bacteria is encased in extracellular polymeric substance (EPS) that is attached to a surface. In comparison with their planktonic state, biofilms have a reduced growth rate due to the limited availability of nutrients and a distinct transcriptome (Post *et al*., 2004, Post *et al*., 2007). Biofilms also have the ability to exchange genetic material and hence develop the potential for antibiotic resistance, enhancing their survival (Slinger *et al*., 2006). These virulence factors allow biofilms to evade the host's immune response and also the action of antibiotics. The EPS also provides a physical barrier providing recalcitrance to biofilm disruption and removal (Flemming *et al*., 2010).

OME is challenging to treat with a high recurrence rate – 25% of children require a second grommet insertion (Gates *et al*., 1987). There is evidence of biofilm formation in the middle ear which explains this recalcitrance to antibiotics and recurrence of the condition. The middle ear effusions that have been collected are culture negative for bacteria. Polymerase chain reaction (PCR) however, has detected bacterial DNA (Rayner *et al*., 1998) and also messenger RNA identifying metabolically active bacteria. Special techniques are therefore required to detect biofilms as bacterial culture

appears to be insufficient. Paluch-Oles *et al* looked at effusion samples taken post ventilation tube insertion in children with OME (Paluch-Oles *et al*., 2011). Bacterial growth was demonstrated in 40% of samples using conventional culture techniques but using the method of PCR, bacteria were found in 98% of cases. Mucosal samples from children with chronic or recurrent OME also demonstrated bacterial biofilms (Homoe *et al*., 2009).

Bacteria may be transmitted to the middle ear from the adenoids which are located in the nasopharynx close to the Eustachian tube orifice. A study by Hori *et al*., in 2010 showed that children with OME have a higher percentage of their adenoidal mucosal surface covered with biofilm than that of children with obstructive sleep apnoea (Hori *et al*., 2010). Studies on 20 children with adenoidal hypertrophy and OME detected biofilms on all adenoidal specimens after surgery using scanning electron microscopy (Tawfik *et al*., 2016). This was significantly greater than 20 children with adenoidal hypertrophy who don't have OME, supporting the view that adenoidal biofilm contributes to the recurrent nature of OME.

1.3.1 Studies *in vitro*

Studies have shown that the main organisms associated with OME (*Haemophilus influenza, Streptococcus Pneumoniae and Moraxella catarrhalis*) readily form biofilms both *in vivo* (Ehrlich *et al*., 2002, van Hoecke *et al*., 2016) and *in vitro* (Murphy *et al*., 2002, Allegrucci *et al*., 2006, Pearson *et al*., 2006). In the animal model of the chinchilla,

Haemophilus influenza was shown to develop a biofilm in the middle ear cavity after five days (Ehrlich *et al*., 2002). *Haemophilus influenza* has been the most extensively studied biofilm and it has been shown that proteins expressed on the surface are unique in the biofilm format compared to the planktonic state (Murphy *et al*., 2002). In addition to the proteins identified, adhesins, enzymes and lipopolysaccharides have been located on the surface of *Haemophilus influenza* biofilms which are thought to act as a virulence factors (Webster *et al*., 2006). Sialylation of the lipopolysaccharide has also been shown to be a major virulence factor both *in vitro* and *in vivo* (Bouchet *et al*., 2003).

1.3.2 Studies *in vivo*

Analysis of specimens taken from the middle ear mucosa in children undergoing ventilation tube insertion with recurrent AOM or chronic OME has shown biofilms of *Haemophilus influenza, Streptococcus pneumonia and Moraxella catarrhalis* (Hall-Stoodley *et al*., 2006). Despite the culture negative status of the effusions, a large number of viable bacteria were seen after dead fluorescent staining using confocal scanning laser microscopy (CSLM) and 92% showed biofilms which were identified as clusters of pathogenic bacteria with a matrix attached to a surface. Evidence of Gram positive cocci infection of the middle ear mucosal epithelium has been shown in mucosal biopsies from children with OME. This may explain the persistent nature of infection and recalcitrance to antibiotic treatment (Coates *et al*., 2010). Bacterial messenger RNA has been detected in up to 35% of culture negative middle ear

effusions from children undergoing myringotomy insertion for OME (Rayner 1998). This finding reinforces the role of bacteria in the biofilm model.

1.3.3 Implications of biofilms on OME treatment

Bacteria in biofilms have been shown to be 1000 times more resistant to the action of antibiotics than in their planktonic forms (Starner *et al*., 2008, Kaji *et al*., 2008). This is due to their multiple virulence factors including the EPS and ability to exchange genetic information conferring antibiotic resistance. Biofilms therefore pose a challenge for eradication and in the treatment of OME due antibiotic recalcitrance and the persistence of pathogens (Belfield *et al*., 2015). There maybe implications of inserting a potential substrate in the form of ventilation tubes for the biofilms to grow on (Jang *et al*., 2007) creating an inflammatory reaction and chronic infection. There is also evidence that the adenoids are a reservoir for biofilms and hence when OME is eradicated, bacteria can ascend into the middle ear to reform a biofilm (Nistico *et al*., 2011, Saafan *et al*., 2012, Tawfik *et al*., 2016). This may be one of the explanations for recurrent OME. The treatment for OME has to account for the presence of biofilms and therefore antibiotic delivery should be ideally targeted to disrupt the biofilm matrix.

1.3.4 Biofilms in nature and disease

Studies of aquatic environments show that bacteria grow in communities which we know as biofilms, encased in a matrix, adherent to a surface and with a sufficient nutrient supply. It is rare to find bacteria in the free floating planktonic form. Microscopic observations and quantitative studies have shown that over 99.9% of bacteria can grow in biofilms on different surfaces (Donlan and Costerton 2002). Biofilms are a major problem in the water industry as they adhere to water pipes. Complex methods for sampling, examining and controlling the growth in this environment have been developed (Donlan and Costerton 2002). Medical specialities have since accepted the presence of biofilms in clinical infections. Microbiologists classify bacteria into mucoid and non-mucoid species depending on their ability to produce slime, which is a mucin-like layer produced by the biofilm.

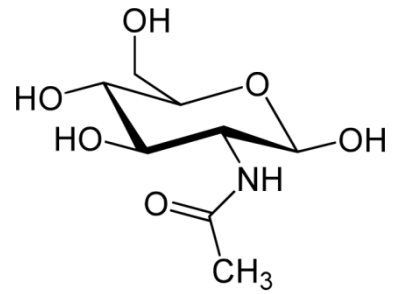
The US National Institute of Health states that biofilms contribute to over 80% of microbial infections in humans (Davies *et al*., 2003). Many clinical infections are the result of biofilm infections such as cystic fibrosis, perichondritis and infective endocarditis. Most indwelling medical devices are a substrate for biofilm adherence including catheters, prosthetic heart valves, extra ventricular devices (Bayston *et al*., 2007) which all feature in neurosurgery and in the field of Ear, Nose and Throat, tracheostomy tubes and ventilation tubes. Biofilms are also found in many ENT infections such as chronic rhinosinusitis (CRS) (Barshak *et al*., 2017), recurrent tonsillitis, chronic supporative otitis media (CSOM), middle ear cholesteatoma and implant infections (Smith A *et al*., 2011).

1.3.5 Adherence

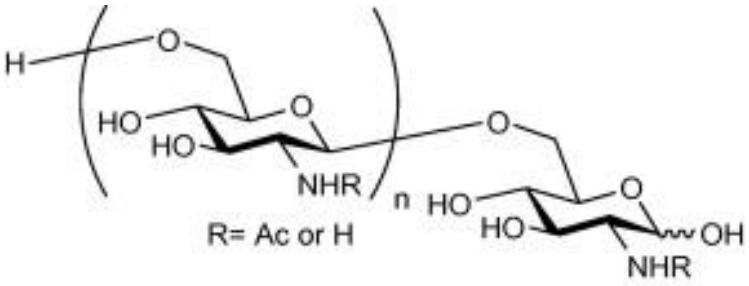
The initial step of biofilm formation is adherence to a surface which may be a cell, mucin or an artificial implant such as a ventilation tube. The surface type and bacterial characteristics both influence adherence. A solid-liquid interface and a rough textured surface are thought to be favourable mediums for microbial attachment and growth (Donlan and Costerton 2002) similar to the presence of OME in the middle ear. Bacteria which adhere strongly to a surface are better at producing biofilms. Bacteria use Brownian motion to locate a target surface. When the bacteria are in close vicinity, they use flagella or produce polysaccharides to help bridge the gap and overcome any electrostatic repulsive forces, assisting adhesion (Hori *et al*., 2010).

1.3.6 Polysaccharides

Two main groups of polysaccharides are produced by bacteria: lipopolysaccharide (LPS) and extra-cellular polymeric substance (EPS). LPS consists of lipid A, core polysaccharides and outer O antigen units. LPS is important for the initial stages of cell surface adhesion whereas EPS is the primary matrix component of biofilms. EPS exists in three forms: 1) capsular which is tightly bound to the cell wall 2) loosely bound which creates the slime of biofilms and 3) soluble form. The EPS produced from *Staphylococcus Epidermis's* is called Polysaccharide Intercellular Adhesion (PIA) and is the most widely studied. PIA has the basic unit of N-acetyl-glucosamine which is amide and has repeated units linked in a β-1, 6 formation (Figure 7). PIA residues contain up to 15% of de-N-Acetylated amino groups (Mack *et al*., 2004).



a) N-Acetyl-glucosamine



b) Polysaccharide intercellular adhesin PIA (Leung *et al*., 2009)

Figure 7: ***Diagram to show structure of a) N-acetyl glucosamine and b) Polysaccharide intercellular adhesin (Leung 2009)***

1.3.7 Biofilm interaction with mucin

The molecular structure of biofilm polysaccharides share many similarities with mucins; both are peptidoglycans. Their glycosylation allows for attraction of water molecules to form gel-like macromolecules. Mucins secreted by the body may act as a substrate for the growth of biofilms due to their large surface area for attachment. Therefore, mucins can act as a virulence factor for biofilms. Studies have demonstrated a surface coated in mucin results in growth of biofilms with increased resistance to antibiotics compared to plain glass surfaces (Landry *et al*., 2006).

Due to the similar structure of mucins and biofilms, chemical agents have been shown to breakdown both. An example of this is the mucolytic Ambroxol degrades alginates produced by *Pseudomonas Aeruginosa* biofilms (Li *et al*., 2008).

1.3.8 Biofilm architecture

After adherence to a surface, bacteria multiply to form a biofilm. They mature to form pillars and develop specialised water channels allowing nutrients to enter and waste products to leave (Donlan *et al*., 2002). Each colony has a unique structure as shown by CLSM (Tolker-Neilsen *et al*., 2000) which can vary according to the age of the colonies. For example *Pseudomonas Aeruginosa* has been shown to form ball shaped micro-colonies or loose protruding structures depending on the exact species. Bacteria were also been to be motile, leaving their colonies and joining others. This occurs

particularly if a certain size is reached allowing the biofilm to change from a compact micro-colony to loose structures.

The co-existence of planktonic and sessile populations of bacteria with a constant interchange is thought to be an adaptation to external factors. This has been demonstrated experimentally by growing *Pseudomonas* and *Burkholderia* together in a commensal environment forming mixed micro colonies. When the environment changes to non-commensal, both bacterial species form separate micro colonies (Nielsen *et al.*, 2000). This phenomenon can be explained by chemotactic signalling known as quorum sensing and allows bacteria to adapt to their environments altering to a planktonic form if the conditions for biofilm formation are unfavourable. This adaptability should be considered a virulence factor allowing biofilms to evade and survive harsh biological conditions.

1.3.9 Intercellular signalling "Quorum sensing"

Intercellular signalling is also known as a phenomenon called "quorum sensing" where bacteria in a biofilm detect local densities and co-ordinate their behaviour (Jamal *et al.*, 2017). The sensors are thought to be N-Acetyl Homoserine Lactones which control the expression of target genes. There is evidence that quorum signalling has an important role in the development of biofilms by controlling the expression of extra-cellular polymeric substances (EPS) which are central to the ability to form a biofilm (Nadell *et al.*, 2008).

1.3.10 Antibiotic recalcitrance

Bacteria in a biofilm show a marked recalcitrance to antibiotics. There are thought to be several factors behind this. The exopolysaccharide gel layer (slime) formed by the biofilm provides a protective physical barrier preventing penetration of antibiotics to bacteria (Souli *et al*., 1998). Another theory is that the biofilms have the ability to form small colony variants (SCVs) when the biofilm is so thick that oxygen and nutrients are depleted. The SCVs are subpopulations in the dormant state and have switched off many of the mechanisms that antibiotics target and hence become recalcitrant (Bayston *et al*., 2000).

In the biofilm state, cell wall synthesis inhibitors are affected, resulting in a reduction of cell wall protein production which conserves energy (Neut *et al*., 2007). As the division rate of bacterial cells in a biofilm are reduced, antibiotics which target dividing cells are less effective. Genetic information can also transfer between adjacent cells allowing mutations which may confer antibiotic resistance. This can even occur between different bacterial species (Fergie *et al*., 2004).

All of these factors combine to reduce biofilm susceptibility to antibiotic treatment and hence can cause significant problems clinically with chronic infections such as OME.

1.3.11 Biofilm examination and measurement in research

Direct imaging of biofilms is the gold standard for examination. Scanning Electron Microscopy (SEM) requires hydrated biofilms to be processed before imaging which may cause a degree of distortion. New advances in the development of CSLM have removed the processing step and allows biofilms to be examined dynamically, although the resolution is slightly less than SEM (Sugimoto *et al*., 2016).

1.3.12 Clinical diagnosis of biofilm infections

Biofilm infections are difficult to diagnose clinically. The techniques of SEM and CSLM are expensive and are impractical to use in the clinical setting. However, in most cases the surface of the biofilm is biological such as the middle ear mucosa in OME. Blood culture alone can fail to pick up sufficient quantities of bacteria as many of the bacterial are in a dormant form in the biofilm.

Future developments are required to develop a reliable biofilm detection assay that can be used clinically. This may involve measuring the metabolites such as quorum sensing signalling molecules and would have implications for the treatment of OME.

1.3.13 Therapeutic possibilities of treating biofilms in OME

Successful treatment of OME, for which there is strong evidence is a biofilm infection, should not involve increasing the antibiotic dose systemically for prolonged periods of time as this has the risk of greater side effects for the patient and a limited efficacy

due to antibiotic recalcitrance (Belfield *et al*., 2015). Disruption of the biofilm using mucolytic agents, altering the substrate surface and hence limiting bacterial adherence, formation and quorum sensing are all possible therapies. Applying this to the middle ear in the treatment of OME however is challenging as systemic drug delivery would not achieve high enough doses and the middle ear is difficult to access anatomically. Before the discussion of any novel forms of treatment for OME, it is worth considering the variety of different treatments available and the merits and disadvantages of each.

1.4 Treatment for OME

1.4.1 Medical management

Medical treatment for OME would render surgery unnecessary, which appeals considering the recurrent nature of OME and the high incidence in children. Numerous hospital visits with interventions have a potential impact on children's education and wellbeing. Different medical treatments for OME have been trialled as discussed below.

1.4.2 Nasal topical steroids

Administration of nasal steroid topically treats any potential blockage of the eustachian tube opening in the postnasal space. Steroids reduce inflammation and encourage opening of the tube. Studies, however, have not shown a significant benefit from topical nasal steroids in the treatment of OME (Shapiro *et al*., 1992, Wang *et al*., 2017). A well designed study was a double blind randomized controlled trial with 217 children aged between 4 and 11 years old taking either mometasone furoate or placebo for 3 months (Williamson *et al*., 2009). No clinical difference in the resolution of OME was found. To reinforce this, the NICE guidelines (2008) have stated that there is no proven benefit from the use of topical nasal steroids. There is also little benefit in the use of nasal topical steroids in children who have variable anatomy of the eustachian tube and hence are prone to recurrent OME such as craniofacial abnormalities including midface hypoplasia in trisomy 21.

1.4.3 Systemic steroids

Systemic steroids can be used to reduce the inflammation of the middle ear mucosa in OME. Studies to assess the efficacy of systemic steroids have had mixed results. A study comparing the effects of systemic steroids to the effect of systemic steroids and oral antibiotics showed that OME resolved quicker in the treatment group given both steroids and antibiotics (Mandel *et al*., 2002). However, this difference was only apparent for two weeks after treatment had ceased. Similarly, a systematic review by Simpson *et al.,* (2011) has shown that systemic steroids used in combination with oral antibiotics causes OME to resolve quicker, but this benefit is not long term and there is no evidence of any alleviation of hearing loss (Simpson *et al*., 2011). Systemic steroids also have considerable side effects when given for any long duration including gastric ulceration, osteopenia, suppression of the hypothalamo-pituitary axis and growth retardation which is especially relevant when considering the paediatric cohort.

1.4.4 Oral antibiotics

Systematic reviews of oral antibiotics to treat OME have found no benefit if patients are followed up for a long period (Rosenfield *et al*., 2002). This evidence is from 1966-1991. A Cochrane review published in 2012 has similar conclusions (van Zon *et al*., 2012) and the NICE guidelines do not recommend the use of oral antibiotics (NICE 2008) to treat OME.

1.4.5 Other medical treatments

No medical treatments for OME have shown efficacy to the extent that they could replace ventilation tube (VT) insertion. The use of nasal decongestants with or without antihistamine administration has not shown any clinical benefit in the management of OME (Griffin *et al*., 2006, Cantekin *et al*., 1983). Administration of oral mucolytics such as mucodyne has not shown any statistically significant increase in the resolution of OME (Commins *et al*., 2000). Treating OME with homeopathic remedies has not shown any statistically significant clinical benefit when compared to controls in a prospective double blinded randomized controlled trial (Pedrero-Escalas *et al*., 2016) although this study was based on otoscopy and tympanometry and not audiometric or clinical outcomes. Auto-inflation is a technique which increases pressure in the post nasal space and opens the Eustachian tubes, hence enhancing middle ear drainage. This manoeuvre has been shown to improve the likelihood of OME resolution over 2 weeks to 3 months (Williamson *et al*., 2011) but requires a degree of skill and dexterity which is unsuitable as a treatment of a condition which mainly affects young children. In addition, the long term effects of auto-inflation are not established.

A further understanding of immune pathways activated during OME is important when considering the development of new therapies for OME. The OME signalling pathway includes Toll-like receptors which have a dual function in OME induction and resolution. Understanding these receptors and signalling molecules is important as they are possible targets for novel OME therapies (Leichtle *et al*., 2009).

Hearing aids are a valid management option in children with OME. They are used to overcome the conductive hearing loss created by the fluid and hence impedance mismatch. Their function is to amplify sound rather than as a therapeutic intervention to treat OME. Wearing hearing aids would help to resolve the speech and language difficulties experienced by children. Hearing aids are associated with battery ingestion, which has the rare yet potential life threatening complication of oesophageal perforation (Litovitz *et al*., 1992). Hearing aids, however have the risk of noise trauma with sound amplification after OME resolution and a higher incidence of bullying at school when worn (Leff *et al*., 1999). Studies show that over 90% of children who are fitted with hearing aids wear them (Gan *et al*., 2017) despite the potential for less social acceptance. This high proportion may result from the numerous stages involved from diagnosis of OME to referral for hearing aid and eventual fitting on the NHS (National Health Service) providing potential opportunities for resolution of the OME and chance for parents to alter their decision regarding hearing aid fitting.

1.4.6 Surgical management

Following the current NICE guidance for OME, children who have a hearing loss of 25dB or worse in the better hearing ear undergo watchful waiting for three months (NICE 2008, ENT UK 2009). After this period, if there is still a hearing problem, children undergo ventilation tube (VT) insertion. This is the most common operation in Otolaryngological practice with 35,225 operations to drain the middle ear fluid in patents of all ages in the period 2015-2016 (hospital episode).

1.4.7 Ventilation tube surgery

Ventilation tubes are commonly referred to as grommets. They are inserted via a hole in the tympanic membrane called a myringotomy which also allows the surgeon to drain the middle ear of fluid. The myringotomy and hence grommet insertion is in the anterior-inferior aspect of the tympanic membrane to avoid the incudostapedial joint which is located in the superior posterior quadrant. The grommet allows the middle ear ventilation and equalises the pressure between the middle and outer ears (NICE 2008). Ventilation tubes typically last between 9 and 12 months before self-extrusion. A systematic review shows that myringotomy and aspiration without insertion of a grommet are not effective at improving hearing to an adequate level (Freemantle *et al*., 1992).

Clinical trials assessing the efficacy of grommet surgery have had the problems of randomization of ears and of non-stringent audiometric criteria. A large multi-centre trails (TARGET Trial of Alternative Regimens in Glue Ear Treatment – TARGET 2003) was set up in the UK using strict audiometric criteria and randomizing patients instead of ears. A comprehensive Cochrane meta-analysis (Browning *et al*., 2010) uses the TARGET trial results with the MRC (Medical Research Council) results and shows that grommets on average offer a 10 to 14 dB improvement 3 months post insertion. These hearing benefits last for 6 months until the OME has resolved or the grommet self-extrudes. Symptomatic hearing loss from OME is still considered to be best treated with grommet insertion (Schilder *et al*., 2017).

1.4.8 Adenoidectomy

The adenoids are located in the post nasal space and are part of Waldeyer's ring of lymphoid tissue on the upper aerodigestive tract. Adenoidectomy was previously thought to improve OME by removing Eustachian tube obstruction and hence improving ventilation of the middle ear. However, current opinion is that the adenoids are a source of bacteria in the form of biofilm which cause recurrent infection. Adenoidectomy was previously the surgical procedure of choice to treat OME before ventilation tube insertion (Browning *et al*., 2008). Adenoidectomy is normally performed as an adjunct to ventilation tube insertion conferring an additional benefit of 2.3 dB at 1 year follow up compared to ventilation tube insertion alone. The main benefit, however, is a reduction in the recurrence rate of OME from 47% to 28% percent when adenoidectomy is performed at the same time as ventilation tube insertion, compared to ventilation tubes on their own (Browning *et al*., 2008). Adenoidectomy has been shown from the TARGET trial data to improve the average hearing of children by 4.2dB over 12, 18 and 24 months (MRC Otitis Media Study Group 2012). Adenoidectomy also reduced the eligibility for revision surgery from 31% to 14% at 12 months follow up. However, adenoidectomy is not without risk of complication including hypernasal speech, velopharyngeal insufficiency and most importantly, post-operative haemorrhage which is serious enough to require a return to theatre at a rate of 0.6% (MRC Otitis Media Study Group 2012). Post-operative haemorrhage is a particularly serious complication in young children with a circulating blood volume of 80mls per kg of body weight. Therefore, the addition of adenoidectomy in the treatment of OME remains debatable (Schuler *et al*., 2017).

1.4.9 Eustachian tuboplasty

Eustachian tube dysfunction has a role in the pathogenesis of chronic ear disease including OME. This is due to the anatomical connection between the protympanum and the ME (Jufas *et al*., 2016) allowing ventilation of the ME and mucociliary clearance pathway for pathogens. If there is a dilation dysfunction of the ET, there is a potential for an effusion to develop in the ME cavity as seen in OME. A treatment strategy for OME is therefore to open the ET and improve its function. This can be achieved by insertion of a balloon down the ET from the ME as an adjunct to ME surgery (Tarabichi *et al*., 2016) or accessing this from the nasopharynx (Ashry *et al*., 2017). Results have shown a symptomatic improvement in 79% of adult cases post cartilaginous balloon tuboplasty (Ashry *et al*., 2017). Other options are laser (Kujawski *et al*., 2004) or microdebrider (Metson *et al*., 2007) treatment of the ET cartilaginous portion to increase its patency and hence prevent the development of OME. Balloon tuboplasty, however, has the additional benefit of circumferential treatment to the ET as shown histologically (Kivekas *et al*., 2015).

There are no major adverse outcomes reported to date after laser Eustachian tuboplasty with a complication rate of 4.4% reported (Miller *et al*., 2017). Eustachian tuboplasty is a relatively new treatment option for OME which has a potential therapeutic benefit for adults and children (Pau *et al*., 2015). However, future high quality evidence in the form of randomised controlled trials and are required in this area to evaluate the benefit of Eustachian tuboplasty further (Randrup *et al*., 2015).

1.4.10 Failure of current treatment strategies

Medical treatments of OME show failures and even the current gold standard of ventilation tube insertion results in a quarter of patients developing recurrent OME (Gates *et al*., 1987) after grommet extrusion. The average number of surgeries per patient has also be found to be 2.1 (Daniel *et al*., 2006), again emphasising the recurrent nature of OME. The presence of biofilms in the middle ear and persistent nature with antibiotic recalcitrance may explain this rate of recurrence as the underlying infection has not been treated sufficiently with grommet insertion. The concept of biofilms also explains why oral antibiotics are insufficient to treat OME. An effective treatment for OME which minimises recurrence therefore must target the biofilm infection and oral antibiotics do not reach adequate concentrations in the middle ear to achieve this (Belfield *et al*., 2015).

1.5 Drug delivery to the ear

In order to develop new treatments for OME, it is important to understand the different methods of drug delivery to the ear, with a focus on delivery directly to the middle ear compartment to eradicate biofilm bacteria whilst avoiding unwanted systemic side effects.

1.5.1 Anatomy overview

The ear is divided into three compartments: the outer, middle and inner ear (Gleeson *et al*., 2008). The outer ear runs from the pinna, along the external auditory canal and ends at the tympanic membrane, separating the outer ear from the middle ear. The middle ear also communicates via the eustachian tube to the space behind the nose and via the round and oval windows to the inner ear. The tympanic membrane comprises of three layers: 1. the outer skin which is five cells thick, 2. connective tissue with collagen giving the tympanic membrane its structural integrity and 3. internal mucosal lining which is one cell thick and comprises cuboidal ciliated respiratory epithelium. Drug delivery to the middle ear via the transtympanic route must cross all three layers of the tympanic membrane with or without a physical breach.

As discussed previously (Figure 1), the middle ear contains the ossicular chain comprising the malleus, incus and stapes and has a mucosal lining which maintains the moist middle ear environment. Ciliated epithelium wafts debris into the eustachian tube as a protective mucociliary clearance mechanism. The eustachian tube

replenishes the air in the middle ear cavity by letting in air at atmospheric pressure to the middle ear. The mastoid air cell complex communicates with the middle ear and infections can spread from the middle ear via the mastoid antrum causing mastoiditis.

The inner ear contains the cochlea and the semi-circular canals which are the hearing and balance organs. The inner ear is protected and surrounded by dense temporal bone. As described previously, cochlea hair cells are responsible for detection of sound and the hair cells in the semi-circular canals detect motion. The delicate inner ear structure (sensory elements) is surrounded by perilymph which is in continuity with the cerebrospinal fluid via the perilymphatic duct. Internally, the cochlea and semi-circular canals are interconnected by a system of endolymphatics. The oval window is a thin membrane which allows the vibrations of the stapes to transmit sound vibrations to the inner ear. The round window acts as a pressure buffer moving out of phase with the oval window. Both the round and oval windows facilitate the primary function of the middle ear of efficient acoustic energy transfer from the air vibrations from the outer ear to the vibrations of cochlea fluid in the inner ear. The round window ultrastructure consists of three cell layers – the outer epithelium, middle connective tissue layer and inner epithelium. The round window has been shown to have different permeabilities to particles depending on their molecular size, concentration, liposolubility, charge and thickness of the membrane (Goycoolea *et al*., 1997). Recent technology has developed vectors which are viral (Jero *et al*., 2001) and non-viral (Yin *et al*., 2014) allowing transfer of therapies to the inner ear by deliberately crossing the round window. There is a preference for non- viral vectors as these are not associated

with carcinogenesis. In addition, non-viral vectors do not have any DNA packaging difficulties and are more easily produced (Yoon *et al*., 2016). It is important to consider the transfer of drugs from the middle ear to the inner ear across the round window and oval window membranes as potential adverse side effects in the development of new therapies to treat OME.

1.5.2 Overview of treatments for the ear

Various treatments have been proposed for treating the plethora of ear conditions whether they are infective, inflammatory, metabolic or autoimmune. This is relevant in the context of OME which is considered to have both an infective and inflammatory component. Drugs can be delivered systemically or be directed to the middle ear which has the advantage of increasing the dosage and efficacy without exposing the patient to unwanted side effects. However, delivery to the middle ear requires the development of systems which allows sustained release of local high concentrations. This poses a challenge when considering absorption of drugs from the middle ear mucosa and their transit down the eustachian tube and also the potential transfer across the round window to the inner ear where damage to the hearing or balance mechanisms may occur as side effects causing vestibulotoxicity (King *et al*., 2013) and ototoxicity (Stevens *et al*., 2015).

1.5.3 Topical treatments

The application of topical treatments is used in inflammatory conditions of the outer ear which have caused secondary inflammation of the tympanic membrane (Neilson *et al*., 2008). In the clinical setting of OME, inflammation of the TM is present after potential secondary infection. Antibacterial and antifungal creams are applied to the ear canal under direct vision usually as an office procedure without the need for any anaesthetic (Rosenfeld *et al*., 2014). Care must be taken to avoid excoriation to the external auditory canal skin or trauma to the tympanic membrane which could both potentially cause the patient discomfort. Although topical medication will treat the outer layer of the intact tympanic membrane, there will be no transfer of medication to the middle ear unless there is a TM breach for example in cases of acute otitis media (AOM) (Winterstein *et al*., 2013).

1.5.4 Oral treatment

Oral medication is used in the treatment of many otological conditions including AOM. Although there is reduced bioavailability compared to systemic or topical treatments, the non-invasive approach is suitable for those patients deemed unfit for a general anaesthetic which is required for many other drug delivery systems.

Oral antibiotics are prescribed for the treatment of conditions such as AOM (SIGN Guidelines) and CSOM. Upper respiratory pathogens involved in AOM and CSOM include *Streptococcus pneumonia*, *Haemophilus influenza* and *Moraxella catarrhalis*

(Celin *et al*., 1991) and antibiotic regimens are targeted to cover these organisms with amoxicillin having the most widespread use. Disadvantages of oral antibiotics include the possibility of multidrug resistance to these upper respiratory tract organisms (Tos *et al*., 1980) with particular concern regarding increasing resistance to *Streptococcus pneumonia* (SIGN Guidelines). The side effects of oral antibiotics are mainly gastrointestinal, including *Clostridium difficile* infections which are associated with quinolones such as ciprofloxacin given for the treatment of *Pseudomonas aeruginosa* infections. Oral antibiotics have also been shown to give variable concentrations in plasma and middle ear fluid. For example, a study with amoxicillin has shown that following oral administration, 15-35% of children have no detectable amoxicillin in the middle ear fluid (Celin *et al*., 1991).

Otitis media with effusion as discussed, is the commonest cause of hearing impairment in children in the developed world and is a biofilm disease (Hall-Stoodley *et al*., 2006, Mandel *et al*., 2008, Pichichero *et al*., 2009, Woodford *et al*., 2009) requiring 10 to 1000 times higher concentrations of antibiotics to kill them in comparison with planktonic bacteria (Kubba *et al*., 2000; Belfield *et al*., 2015). Oral antibiotics therefore are less efficacious than directed topical treatment and do not achieve the higher concentrations required to eradicate a biofilm disease such as OME. Oral antibiotics are also associated with side effects including gastrointestinal disturbance and skin rash (Venekamp *et al*., 2016).

Steroids can be given orally for treatment of other otological conditions such as sudden sensorineural hearing loss (SSNHL) (Wilson *et al*., 1980) with a significant improvement in hearing if administered in the acute setting. As already mentioned in the treatment of OME, systemic effects of oral steroids include suppression of the hypothalamopituitary axis, gastric ulceration and haemorrhage, pancreatitis, psychiatric disturbance and hyperglycaemia (Gleeson 2008). Side effects are uncommon as the typical regimen is a short five days of 40mg prednisolone taken once daily.

Systemic oral treatments for Ménière's disease include diuretics which reduce the production and accumulation of endolymph (Jackson *et al*., 1981). Diuretics, such as bendroflumethiazide, however have significant side effects for the patient including hypokalaemia and postural hypotension (Santos *et al*., 1993), requiring patient monitoring.

Noise-induced hearing loss has been assessed experimentally and treated by administering patients with oral antioxidants such as N-acetyl cysteine (Lin *et al*., 2010). This has shown a protective effect in the clinical setting by reducing the hearing threshold and is a promising orally administered neuroprotective agent to preserve hearing. Further clinical trials are required before widespread implementation.

Oral drug administration therefore has a wide application to many conditions involving the middle and inner ears. Patient compliance and reliability is important especially

when drugs are to be taken long term. Side effects can be significant especially involving the gastrointestinal tract and hence can affect patient compliance. There is limited bioavailability when compared to topical drug administration and hence higher doses may be required. The duration of oral administration also depends on the underlying condition being treated. In the context of OME, although oral treatment in the form of antibiotics is non-invasive, its efficacy is debatable especially with the presence of biofilms and with considerable side effects when given to children (Venekamp *et al*., 2016).

1.5.5 Intravenous administration of drugs

Middle ear infections which spread to the mastoid bone result in conditions such as acute mastoiditis (Obringer *et al*., 2016) and chronic infections of the temporal bone known as necrotising otitis externa (Chawdhary *et al*., 2017). Acute mastoiditis treatment typically requires up to a week of intravenous antibiotics, but necrotising otitis externa requires treatment for a minimum of six weeks. Patients would require a cannula or a long intravenous line to be inserted which has a localised infection risk with subsequent cellulitis or thrombophlebitis. For both of these conditions mastoiditis and necrotising otitis externa, the treatment is targeted to pathogens in conjunction with local microbiology guidelines and consideration of immunization status. Intravenous antibiotics commenced for acute mastoiditis include ceftriaxone, beta-lactam or beta-lactamase inhibitors (Obringer *et al*., 2016). Use of aminoglycoside antibiotics will require blood samples to be taken for monitoring to minimise the side effects including nephrotoxicity and ototoxicity (Huth *et al*., 2011).

The latter is usually permanent (Greenwood *et al*., 1959). Vestibulotoxicity, which is damage to the balance system, can occur in up to 15% of patients on systemic aminoglycosides (Fee *et al*., 1980) and ototoxicity occurs between 2% and 25% (Mulheran *et al*., 2001). Symptoms of vestibulotoxicity include disequilibrium and tinnitus, and hearing loss if ototoxicity is present. Gentamicin, which is an aminoglycoside antibiotic has been found in the outer hair cells of guinea pigs within 30 minutes of intravenous administration in one experimental setting with a peak at 6 hours (Imaimura *et al*., 2003). This emphasises the importance of dose timing of these antibiotics and level monitoring. Gentamicin kills hair cells by apoptosis with the effects taking up to five days.

Intravenous steroids have also been used for sudden sensorineural hearing loss (Kakehata *et al*., 2006) in combination with hyperbaric oxygen treatment (Hosokawa *et al*., 2017) and also for the treatment of Ménière's disease (Shea *et al*., 2012). The side effects of intravenous steroids are similar to those seen when administered orally (see section 1.5.4).

Intravenous treatment is not appropriate in the context of OME as patients are typically systemically well. Expert panel opinion still considers ventilation tube insertion to be the optimal treatment for OME in the context of symptoms from the hearing loss (Schilder *et al*., 2017).

1.5.6 Transtympanic administration of drugs without TM breech

The tympanic membrane acts as a barrier to the delivery of drugs to the middle ear and therefore must be artificially breached if it is intact. The possibility of transmitting drugs across an intact tympanic membrane has being tested experimentally in the form of iontophoresis (Passali *et al*., 1984) which works on the principle of ion delivery by applying an electrical potential across cell membranes and using magnetic fields to move magnetic nanoparticles to targeted structures in the ear (Shapiro *et al*., 2010). Preliminary animal models of nanoparticle technology used to deliver prednisolone to the middle ear has shown increased inflammatory changes in rats after 30 days on a histological examination of the temporal bones (Lafond *et al*.,2018). This technology has future potential but requires more translational studies using *in vivo* models to ascertain the potential side effects and safety of this innovative new modality of treatment. Magnetic nanoparticle technology has the potential to target therapies to specific sites such as the cochlea to decrease the ototoxic effects of chemotherapeutic treatments such as cisplatin which are systemically administered (Ramaswamy *et al*., 2017). Active transport to the cochlea also avoids drug delivery to the middle ear via transtympanic delivery. Preliminary studies on mice models show the possible potential of such nanotechnology (Ramaswamy *et al*., 2017).

Application of P407-PBP, a polymer to the EAC containing 1% ciprofloxacin antibiotic in chinchilla models has shown formation of a hydrogel and flux across an intact tympanic membrane with drug delivery to the ME. This has potential as a new treatment for OME (Yang *et al*., 2016), allowing topical delivery of drugs without

systemic side effects and TM breech. Future experiments are required however in these methods which do not breech the TM for long term efficacy in humans and safety.

Peptides have also been identified which allow transportation across an intact TM and are hence a potential new treatment strategy for drug delivery to the ME in cases such as OME (Kurabi *et al*., 2017). Experiments using rat models have shown that peptides transport across an intact TM and have the potential to carry drugs to the ME without changes in the morphology of the ME and IE. Peptide transport therefore is a possible future therapeutic mechanism for drug delivery to the ME for conditions such as OME.

1.5.7 Transtympanic administration of drugs with TM breech: injection

Transtympanic injection antibiotics, local anaesthetic and steroids have the advantage of delivering greater local concentrations in the middle ear which is more efficacious and has minimal systemic side effects (Chandrasekhar *et al*., 2001, Ho *et al*., 2004) when compared to intravenous treatments. Administration of drugs by transtympanic injection is performed in the office or operating theatre setting involving usually a local anaesthetic or less frequently general anaesthetic. A single treatment for patients is usually offered and there is minimal pain associated with this technique. Complications of intratympanic injection of medication include a tympanic membrane perforation which may persist for more than six months (Shulman *et al*., 2000). Other limitations of intratympanic injections include the potential of ototoxicity which is seen

in up to 30% of patients (Jackson *et al*., 2002) due to the variable uptake to the inner ear. Factors influencing this include middle ear mucosal status, round window thickness and adhesions, patency of the eustachian tube and endolymphatic hydrops (fluctuations in the endolymphatic fluid) when gentamicin is applied to treat Ménière's disease (Berryhill *et al*., 2005). Serial doses maybe required as the eustachian tube rapidly clears the middle ear. Variations in the permeability of the round window have been identified through gadolinium contrast studies (Yoshioka *et al*., 2009) also contributing to variations in drug delivery to the middle ear through injections.

Local delivery of steroids to the middle ear is used as a treatment for sudden sensorineural hearing loss (Chen *et al*., 2010) and tinnitus (Cesarani *et al*., 2002) allowing medication to be transmitted to the inner ear via the round window. Topical steroid delivery is preferentially used in patients who have contraindications to systemic steroids such as during pregnancy or patients with active gastric ulceration (Chen *et al*., 2007). Increasing the dose of dexamethasone to the middle ear has been shown to increase the local concentration in the inner ear and the duration of action (Fu *et al*., 2011). A trial by Rauch *et al*., compared the administration of oral steroids in sudden SNHL with transtympanic injection and has shown no superior method (Rauch *et al*., 2011) therefore the transtympanic route would be preferable as systemic side effects are minimised.

1.5.8 Transtympanic administration of drugs with TM breech: incision (VT insertion)

Topical drug delivery to the middle ear can also be achieved through the application of drops through a perforation in the tympanic membrane. This may either be a perforation which has been created surgically via a myringotomy (incision in the tympanic membrane) and ventilation tube insertion, or it may occur naturally as a complication of chronic middle ear disease (CSOM). Patients can therefore self - administer for a prolonged treatment course which requires a degree of patient reliability, compliance and manual dexterity. Patency of the ventilation tube can also be influenced by wax and premature extrusion of the grommet renders them ineffective after the tympanic membrane seals over.

1.5.9 Transtympanic administration of drugs with TM elevation: tympanomeatal flap

Access to the middle ear can be achieved by raising the edge of the tympanic membrane surgically creating a tympanomeatal flap. This procedure is performed under local or general anaesthetic and allows the insertion of catheters, microwicks and sustained release treatments in the form of pellets or polymers. Considerable skill is required to insert the drug delivery device into the correct location and therefore this cannot be easily performed in the office setting. Catheters and microwicks aim to deliver drugs to the round window membrane at the interface of the middle and inner

ears. Transmission of drugs across the round window allows middle ear drug delivery to treat inner ear conditions. This can occur either intentionally or unintentionally as a side effect of middle ear drug delivery (Jackson *et al*., 2002). Studies using the ionic marker TMPA (trimethylphenylammonium) show that up to 65% of the marker crosses the round window membrane (Salt *et al*., 2012). Factors influencing the rate of drug delivery include middle ear mucosal status, round window thickness and the presence of adhesions (Berryhill *et al*., 2002). In a scenario of ME inflammation, there is the potential for increased transmission of drug to IE causing sesensorineural deafness (Münker, 1981). Transmission of drugs to the inner ear is an important factor to address when developing drug delivery systems for the middle ear in order to minimise potential ototoxicity with cochlear hair cell damage and vestibulotoxicity resulting in hearing loss and disequilibrium (Huth *et al*., 2011). Factors increasing the permeability of the round window to a substance have been found experimentally to include high osmolality, the presence of benzyl alcohol and suctioning near the round window membrane (Mikulec *et al*., 2008). Manufacturing drugs which are to be delivered to the middle ear with properties that reduce transmission to the inner ear are a future development that has potential to reduce vestibulotoxicity and ototoxicity.

Catheters have been used experimentally to deliver drugs accurately to the round window niche in the middle ear. This allows transmission of medication to the perilymph of the cochlea through the round window membrane. Animal models using this technique have shown that neuroprotective agents such as gacyclidine, a NMDA (N-Methyl-D-aspartate) receptor antagonist which maybe of clinical benefit in the

treatment of salicylate - induced tinnitus. Application to the round window niche in patients for 40-63 hours has shown a temporary relief of tinnitus in 67% (Wenzel *et al*., 2010). Catheters have also been utilised in the treatment of sudden sensorineural hearing loss allowing continuous application of dexamethasone to the round window (Plontke 2009) showing a mean improvement in the hearing of 8.5dB.

Techniques using a microwick have been developed to treat Ménière's disease, sensorineural hearing loss and autoimmune inner ear disease (Light *et al*., 2004) allowing for accurate delivery of drugs to the round window in a sustained fashion. This produces the best pharmacokinetic profile of the drug in the inner ear fluids and allows for patient self – administration after initial insertion. Ménière's disease is treated with the application of gentamicin to the inner ear via the round window (Suryanarayanan *et al*., 2009), showing a good symptomatic improvement with long term vertigo control shown in 76.8% of patients at 24 months (Hill *et al*., 2006). The Silverstein microwick has also been used in experiments with sudden sensorineural hearing loss (Van Wijck *et al*., 2007) allowing patients to self - administer steroids for three weeks showing a 67% improvement.

Drug - laden pellets can be inserted into the middle ear by tympanomeatal flap. This allows accurate placement of the pellets in the middle ear to treat conditions such as OME. Drugs are released in a sustained profile in high doses. Pellets, laden with antibiotics have the potential to eradicate biofilms in the middle ear. Studies *in vitro* have shown the potential efficacy of rifampicin and clindamycin for biofilm eradication

(Al-Zahid *et al*., 2011). This approach could show great promise as targeted drug delivery in the future as a superior way to treat biofilms in the middle ear in conditions such as OME.

Local application of polymers containing drugs can be performed by injection into the middle ear after a tympanomeatal flap is raised. This requires sufficiently low viscosity of the polymer to pass through a 19G needle. Examples include the administration of steroids to treat sensorineural hearing loss on a polymer vector such as OTO-104 (Piu *et al*., 2011) which is a poloxamer-based hydrogel containing micronized dexamethasone and lignocaine loaded on polylactic glycolic acid (PLGA) as a treatment for tinnitus (Horie *et al*., 2010). This technique can achieve up to three months of sustained release to the perilymph of the inner ear via diffusion across the round window without any middle ear inflammatory side effects observed (Piu *et al*., 2011, Horie *et al*., 2010) and it shows potential for the future of drug delivery to the middle ear.

1.5.10 Eustachian tube drug delivery

Delivery of drugs to the middle ear via the eustachian tube, located in the space at the back of the nose can be achieved using intranasal medication (Zou *et al*., 2008) with drops showing more efficacy than spray. The mechanism of action is via a reduction in tubal oedema and improved ventilation of the middle ear. Administration of metered dose surfactant with or without steroids (Tamura *et al*., 2005) has shown a reduction in opening pressure, but although this technique has interesting potential, it has not

gained favour clinically as it is technique – dependent and requires drug passage through the nasal vestibule. Additional variables including variations on nasal anatomy would therefore call into question the reliability and reproducibility of drug delivery to the ear via the nasal conduit.

The eustachian tube orifice can also be identified endoscopically and cannulated to facilitate drug delivery to the middle ear. This requires navigation using fibreoptic equipment through the nasal passage to access the Eustachian tube orifice. This procedure is typically performed under a general anaesthetic. The close anatomical proximity to the internal carotid artery and the possible elution of drug immediately back into the nasopharynx are also to be considered when selecting this possible route of drug delivery.

1.5.11 Other methods of drug delivery

Localised drug delivery to the middle ear can also be achieved through bone - anchored devices (McCall *et al*., 2010). A bone - anchored implantable system consisting of a subcutaneous micropump, drug reservoir and septum port has been developed in rat models and has been tested with bolus application of drugs to the round window. A future aim would be for long term implantation in humans delivering drugs continuously which would apply to the treatment of OME, but there are the risks of the implantation procedure, infection and long term safety (Gao *et al*., 2010) and hence overall acceptability.

1.5.12 Summary and future perspective

There are numerous methods of drug delivery to the middle ear which can be categorised as topical, systemic (intravenous), transtympanic and via the eustachian tube. Localised treatments have the advantages of directed drug delivery allowing higher therapeutic doses and minimising systemic side effects. Challenges are posed by the interventional techniques and the creation of modified release preparations. The advantages and disadvantages of each technique are summarised in Table 2.

Technology assisting drug delivery to the middle ear is likely to evolve in the next decade. There are exciting developments in the use of iontophoresis allowing charged ion particles to cross into the middle ear across an intact tympanic membrane when a magnetic field is applied. These drugs could then also be transmitted to the inner ear via the round window (Shapiro *et al*., 2014). As this would involve applying the drug topically into the external ear, this could be done as an office procedure with minimal intervention. The ideal future solution would be to have a carrier system which could cross the intact tympanic membrane which could be loaded with a choice of drugs or biochemical agents for the treatment of middle and inner ear and Eustachian tube pathologies. In context of OME, polymer pellet delivery to the middle ear facilitating sustained antibiotic release and biofilm disruption shows the most promise. Assessing this technique *in vivo* is an important next step.

	Condition	Advantages	Disadvantages
Topical	Inflammation of tympanic membrane	Low technology, inexpensive, outpatient delivery, single treatment	Limited applications, unsuitable if manual dexterity issues
Oral	AOM, SSNHL, Ménière's disease	Self-administered Short course No intravenous	Side effects of antibiotics, steroids and diuretics Antibiotics resistance Decreased efficacy of antibiotics with biofilms
Intravenous	Mastoiditis Necrotizing Otitis Externa	High dose	Inpatient delivery Local side effects – phlebitis Systemic side effects: nephrotoxicity, ototoxicity – level monitoring
Transtympanic delivery without breach	Iontophoresis Magnetic particles	Minimally invasive	Technology under development
Transtympanic injection	Middle ear: AOM Inner ear: Ménière's SSNHL, tinnitus	Biofilm treatment with pellets/ polymers Inner ear treatment via round window	Interventional Requires anaesthetic Perforation risk Ototoxicity potential Variable delivery RW thickness, adhesions, middle ear mucosal status
Transtympanic via ventilation tube	Middle ear: AOM, OME, CSOM	Sustained release, single treatment, Self-administered	Myringosclerosis Ototoxicity potential
Tymapnomeatal flap	Wide application, catheter, microwick,	Accurate delivery to round window	Potential ototoxicity

	pellet/ polymer insertion		Operation for placement and removal
Eustachian tube	AOM, CSOM	Self-administered	Dependent on nasal anatomy, technique
Implantable delivery systems	SSNHL, Ménière's tinnitus	Widespread conditions treated	Infection Long term safety Anaesthetic

Table 2: ***Summary of drug delivery to the ear***

1.6 Animal models for middle ear experimentation

1.6.1 History of animal models for experimentation

Animal experimentation dates back to the 4th century BC from the days of Greek philosopher Aristotle (384-322BC). He performed dissections on animals during the reign of Alexander the Great (Cohen *et al*., 1984). Erasistratus (304-258 BC) is believed to be the first to have experimented on live animals. In the 2nd century in Rome AD, Galen performed dissection on pigs and goats and was dubbed the "father of vivisection". Dissections continued, and in 12th century Spain AD an Arabic physician named Avenzoar rehearsed surgical procedures on animals before humans (Abdel-Halim *et al*., 2005).

1.6.2 Regulations of animal experimentation

As experimentation on animals grew, so did the controversy and ethical debate from society. Animal experimentation in the UK is stringently regulated by the Home Office and enforced by the Animals Scientific Procedures Act (ASPA 1986). The principles of

Replacement, Reduction and Refinement which are dubbed “Russell and Burch’s 3Rs” (Russell and Burch 1959) should be considered when planning animal experiments.

1.6.3 Otological research and animal experimentation

Otological research is commonly performed on animals. Von Békésy, who won a Noble prize for his cochlea recordings, initially used human temporal bones and later cats in his experiments (Békésy *et al*., 1974). Rodent groups have been popularized in recent years. Approximately 90% of animal experiments in the USA are on mice and rats (Trull *et al*., 1999). In the UK there is a trend for a reduction in primate experiments and hence rodents are the test group of choice for most experiments including those based on the auditory system. When considering replacement, there are currently no effective *in vitro* models or tissue substitutes to replace animal models for ototoxicity. This is because the cochlea is a complex sense organ with a very high metabolic rate in vivo and precisely regulated electrochemical environment that cannot be replicated *in vitro.* Therefore, when planning auditory experiments using animal models, rodents are frequently selected.

The guinea pig (*Cavia porcellus*) was first described as *Mus porcellus* by Linneus in 1758 and is a rodent animal model which is widely used in the UK for hearing and balance experiments. The guinea pig has a number of qualities which lends itself to being an experimental model including a large tympanic bulla volume (Wysocki *et al*., 2005). This feature allows potential drug delivery to the middle ear and also to the inner ear via transmission across the round window membrane (Hoskison *et al*., 2012). Access

to the middle ear is required for studies on middle ear mucosal disease including OME (Dai *et al*., 2008), inner ear access for cochlea recordings (Lavigne *et al*., 2016), perilymph sampling (Selvaduri *et al*., 2000) and models of ototoxicity (Xia *et al*., 2012 and 2014).

The rat model is also widely used in otological experiments because of the robust nature, cheaper cost and most importantly similar structural organisation to the human hearing apparatus (Judkins *et al*., 1997) with three separate ossicles.

1.6.4 Knowledge of anatomy of guinea pig and rat ear dimensions

It is known that the guinea pig EAC is narrow allowing a limited view of only the tympanic membrane and malleus handle (Albuquerque *et al*., 2009). Detailed measurements and surgical simulations however have not been made. There is little information in the literature of tympanic membrane dimensions surface area and also the accessible proportion of the tympanic membrane from the ear canal which is important for surgical access via the transtympanic route. No detailed dimensions of the middle ear relations have been published.

Studies on guinea pig models of OME have shown that volumes injected into the middle ear range up to 0.2mls (Guan *et al*., 2011) in a study using saline. Inducing OME by injecting lipopolysaccharide into the middle ear (Dai and Gan 2008) used up to 0.3mls of solution. Neither of these studies focused on inducing models of OME for

experimentation. No detailed measurements of the middle ear bulla volume of rats have been found for comparison.

Measurements of the rat incus and malleus masses have previously been recorded (Salih *et al*., 2001). However, measurements of guinea pig incudomalleal complex masses have not been made despite anatomical studies which have identified the union between the malleus and incus in the guinea pig (Wysocki *et al*., 2005).

Regarding the dimensions of the middle ear cavity for the rat and guinea pig, there is little comparative data. Similarly, when considering the surgical approaches to the middle ear for these animals there is limited information. When considering the use of an animal model for otological experimentations, guinea pig and rat models are both favourable. Detailed cadaveric studies of the rat and guinea pig middle ear and surgical access are required to select which animal model is most appropriate to study a potential new treatment for OME.

1.6.5 Selection of albino vs pigmented animals

Animal species selection is important, as is the selection of pigmented versus albino animals. The literature has a disparate view on this. Bock and Steel 1984 recommend that information on pigmentation should always be available as it could influence results. The Steel group states that pigmented animals are preferable, although this review is superseded by more contemporaneous work. However, studies on

ototoxicity using kanamycin in guinea pigs show that there is more hearing loss and hair cell degeneration in the pigmented variety compared to albino animals (Wästerström *et al*., 1986). However, in studies assessing noise exposure and oxidative stress levels in spiral ganglion cells, there appears to be more damage in albino guinea pigs (Xiong *et al*., 2011). The use of albino guinea pigs in experiments to assess the safety of a treatment and hence ototoxicity would therefore appear justified as hair cell damage would be easily detectable.

1.6.6 Physiological differences between animal species

The frequency of a sound wave is measured in Hertz (Hz) and represents how many cycles of the wave passes through a given point in space in one second. This frequency of a wave, correlates to the perceived pitch of the sound; higher frequencies are perceived as higher in pitch. Physiological differences between species result in ears which are adapted to hear different ranges of frequencies, with the range of rat and guinea pig hearing being comparable as seen in Figure 8 (Heffner *et al*., 2007).

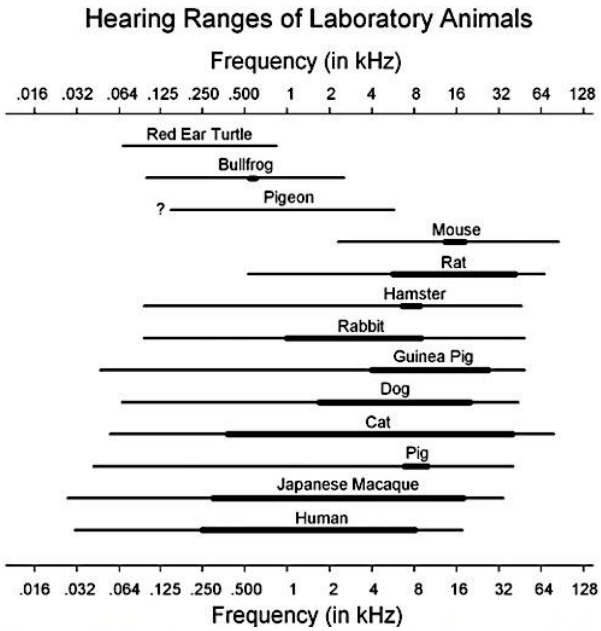


Figure 8: ***The hearing ranges of some common laboratory animals taken from Heffner et al., 2007.***

The thin lines represent frequencies perceived at 60 dB SPL and the thick lines represent frequencies perceived at 10 dB SPL. The symbol '?' denotes incomplete data

Therefore, anatomical differences should be the main deciding factor in determining whether rat or guinea pig models are used as *in vivo* models and not the physiological differences as they have similar hearing ranges. For experiments involving middle ear surgery, the spacious bulla of the guinea pig should be considered as a positive discriminator, but a detailed comparison between the rat and guinea pig middle ears and surgical approaches is required.

1.6.7 Animal models and OME

Laboratory animal models may develop OME over the course of experimentation as a side effect of intervention. Alternatively, OME can be created by a variety of means in laboratory animals to study the effects of OME treatments. The Eustachian tube can be blocked off experimentally using gutta perchate in mouse models creating TM thickening and OME seen at 4 weeks post operatively (Varsak et al., *2016*). Rat models have demonstrated ET blockage using gutta perchate blockage of the ET has an onset of OME at 1 week and at 1 year there are sterile effusions present in 80% of animals (Russell et al., *1998*).

Guinea pig animal models can develop OME experimentally by the injection of LPS into the ME (Dai *et al*., 2008). Measurements of otoscopy, tympanometry and histology show evidence of OME at 3, 4 and 14 days. Saline injection into the guinea pig bulla develops a MEE which is a simulation of OME (Guan et al., 2011). When ABR is tested at a range of frequencies (0.5-20kHz), OME has been shown to cause ABR threshold elevation by 23dB and latency elevation of 0.6msecs. The amount of saline injected is proportional to the degree of ABR threshold and latency elevation.

Other experimental models using guinea pigs have injected a nonviable heat killed pneumococci (HKP) into the ME to create an OME before testing potential new treatments such as pulmonary surfactant (Huang *et al*., 2005). ABR threshold elevations in OME for the guinea pig models were recorded as 45dB +/- 5.7dB which is elevated significantly from the baseline values of 14dB +/- 3 dB measured at 5 days.

These results demonstrate the potential to have a 40dB elevation in ABR threshold recordings with the presence of OME in guinea pig animal models and the onset of such an effusion can develop within a week of experimental insult.

OME causes an ABR threshold elevation of up to 40dB in animal models and this value is similar to the levels of hearing loss seen in children with OME who experience a 18-35dB conductive hearing loss measured on PTA and speech audiometry with a flat air conduction profile from 2-8kHz (Cai *et al*., 2017).

1.7 Ototoxicity

1.7.1 Definition of Ototoxicity

Ototoxicity is injury to the ear or more specifically the cochlea (cochleotoxicity) and / or the vestibular system (vestibulotoxicity). The source is usually chemical in the form of pharmacotherapy. As a result, hearing, balance or a combination of both may be affected. Some widely used drugs which cause irreversible ototoxicity include aminoglycosides and chemotherapeutic agents such as cisplatin. Other drugs may cause temporary ototoxicity including loop diuretics and salicylates. Aminoglycosides can enter the middle ear via a perforation or injection and then once in the middle ear,

transfer can occur across the round window membrane into the inner ear. Aminoglycosides can also cause ototoxicity from systemic administration.

1.7.2 Mechanism of ototoxicity of aminoglycosides

Aminoglycosides act via damaging the inner ear sensory neuroepithelium with the OHC being preferentially damaged by apoptosis. On a cellular level, the ototoxic action of aminoglycosides is believed to occur via disruption of the PIP_2 (phosphatidylinositol 4,5 bisphosphate) secondary messenger system which maintains the cell membrane (Schacht *et al*., 1986). The aminoglycosides bind with iron intracellularly which is a toxic metabolite and is involved in the generation of free radicals that cause oxidative stress to the cell and result in apoptosis (Song *et al*., 1997, Forge *et al*., 2000) taking approximately 5 days to kill the cell.

1.7.3 Mechanism of ototoxicity of cisplatin

Cisplatin ototoxicity has been shown on a cellular level to involve damage to the Organ of Corti predominantly affecting the basal region of the cochlea corresponding to high frequency sounds (Xia *et al*., 2014). Disorganisation of the spiral ganglion cells has also been seen alongside loss of the Organ of Corti architecture with cisplatin ototoxicity (Franceschi *et al*., 2011). In the guinea pig model, loss of OHC in the basal and middle turns of the cochlea have been seen after cisplatin administration (Cardinal *et al*., 2000). Hearing loss after cisplatin administration is also thought to occur via reactive oxygen species and cochlea inflammation (Sheth *et al*., 2017). Therapies have developed to scavenge reactive oxygen species and reduce inflammation for example

through transient receptor potential vanilloid channel inhibition in the cochlea (Mukherjea *et al*., 2008), preventing uptake of cisplatin into the cochlea. Inhibition of cisplatin induced DNA damage and subsequent apoptosis is also a potential therapeutic intervention to minimise cisplatin mediated ototoxicity (Sheth *et al*., 2017).

1.7.4 Mechanism of ototoxicity for noise induced hearing loss

Noise induced hearing loss in mice and guinea pigs has been shown to be due to spiral ganglion neuron degeneration in the cochlea (Lin *et al*., 2010). There is some recovery with repeated measurements at 2 years suggesting a potential synaptic repair mechanism.

1.7.5 Mechanism of ototoxicity without IHC and OHC loss

Damage to the mechanism of hearing may target the vulnerable synaptic connections between the cochlea hair cells and afferent neurons without hair cell loss. Sensorineural hearing loss which is associated with a loss synaptic connections between the cochlea hair cells and auditory nerves (Kujawa *et al*., 2015) is known as synaptopathy (Mehraei *et al*., 2016). This is associated with decreased ABR amplitude in wave I in animal models and increased latency in wave V. Experimentally, the mechanism of synaptopathy is gaining interest, but translating this to human cases is currently limited (Hickox *et al*., 2017) as there is no acceptable clinical test to

demonstrate the loss of synaptic connections from the cochlea to afferent nerves (Mehraei *et al*., 2016). The degree of loss of synaptic connections can vary and be considered as an occult damage to the hearing mechanism which may not be clinically detectable until a critical level of loss of synaptic connections is reached and hearing thresholds are affected (Liberman *et al*., 2017). Animal studies have shown that synaptopathy is able to account for hearing loss without corresponding IHC and OHC loss (Kujawa *et al*., 2009). Understanding the mechanisms of synaptopathy is important to allow for future therapeutic intervention (Kobel *et al*., 2017) preventing loss of synaptic connections and disruption of the auditory pathway.

1.7.6 Animal models used to assess for ototoxicity

Both *in vitro* and *in vivo* animal models are used to test for ototoxicity (Yorgason *et al*., 2011). Each has its merits and requires consideration when planning experiments. *In vivo* models allow a functional measurement of hearing and a biological comparison with humans. This is also important in the context of translational research. Animal models of choice are the guinea pig and chinchilla due to their larger size and hence ease of surgical manipulation in ototoxicity experiments. Guinea pigs have also been shown to be more sensitive to toxic medication than other rodents and hence is a preferred model (Poirrier *et al*., 2010). In contrast, mice models allow for genetic knock-out manipulations and have a short gestation of only 19 days and hence are less costly. Rat models are robust yet have a smaller middle ear for surgical manipulation

and their anatomy is comparable with humans with three separate ossicles and a single middle ear bulla chamber (Judkins *et al*., 1997).

1.7.7 Antibiotics and other drugs with known ototoxicity in rodents

Studies have shown that aminoglycoside antibiotics are ototoxic in mice models but at much higher concentrations than in humans. Guinea pigs have raised ABR thresholds after exposure to cisplatin (Blakley *et al*., 2008). This finding is supported by the systemic administration of gentamicin in mice and guinea pig models with elevation of ABR thresholds seen after two weeks in the latter group. Mice therefore are not considered a sensitive enough ototoxicity model (Poirrier *et al*., 2010). Experiments have also found that there is no evidence of ototoxicity in guinea pig models after prolonged exposure of ciprofloxacin hydrochloride 0.3% and dexamethasone 0.1% (Lemke *et al*., 2009). Other antibiotic groups are not known to be ototoxic in rodents.

1.7.8 Other adverse effects of antibiotics in rodents

Rat and guinea pig appear as the two realistic contenders for an animal model when considering surgical implantation of the middle ear. The table below gives an overview of the side effects of antibiotic in these two species (Table 3). The most serious side effects are related to the gastrointestinal tract causing haemorrhagic colitis and enterotoxaemia (Harkness *et al*., 1995). In relation to auditory experiments, aminoglycosides are ototoxic and hence should be avoided. This information on side effects is in the systemic form and hence any topical drug application would have

minimal systemic absorption. However, it is important when planning ototoxicity experiments even with localised drug delivery to the middle ear to understand that a small amount of drug may enter the circulation. In addition, topical treatments also have the potential to be slow release and hence there would be a lower total circulating concentration overall.

Antibiotic group	Examples	Side effect	Reference
Penicillins	Penicillin Ampicillin Penicillin G	Enterotoxaemia Haemorrhagic colitis	Harkness *et al*., 1995 Harkness *et al*., 1995 Botting *et al*., 1997
Lincosamides	Clindamycin	Clindamycin associated colitis with a heat labile toxin	Rehg *et al*., 1980
Fluoroquinones	Norfloxacin Enrofolxacin Ciprofloxacin Orbifloxacin	Articular degeneration in growing GPs – blisters and cartilage erosion Norflox – cholestasis	Bendele *et al*., 1980
Aminoglycosides	Vancomycin Gentamicin	Ascending flaccid paralysis and respiratory arrest (especially under general anaesthetic) Ototoxic Nephrotoxic	Harkness *et al*., 1995 Conlee *et al*., 1989 albino susceptible

			McClure *et al*., 1998 OD dosage best practice
Tetracyclines	Tetracycline Doxycycline	Nephrotoxic Phototoxicity Tetratogenic Hepatotoxicity	Deboyser *et al*., 1989
Rifampicin	Rifampicin Rifabutin Rifapentine	Hepatotoxicity Rash	Collins *et al*., 1985

Table 3: ***The known side effects of different antibiotic groups in rodents***

When considering an antibiotic carrier to deliver antibiotics to the middle ear in the form of a pellet, PLGA and pluronic are selected. As a delivery vehicle, any information on PLGA and pluronic's potential ototoxicity should be taken into account before pellet design.

1.7.9 Background of poly lactic-co-glycolic acid (PLGA) and pluronic use in rodents

In studies testing the safety of chemotherapy for glioblastoma using a mouse model and etoposide with PLGA as a delivery vehicle, there is no evidence of toxicity to the animals (Smith *et al*., 2014). The applications of PLGA in the fields of neuroscience include the potential treatment of cerebrovascular accidents (Bible *et al*., 2009) acting as a structural support for neural stem cells. Fibroblast growth factor has also been incorporated into PLGA fibrous membrane and implanted into *in vitro* and *in vivo* rat models of rotator cuff tear (Zhao *et al*., 2014). These studies have been without any reported toxicity. Studies using guinea pig models of tuberculosis have used PLGA nanoparticle technology to deliver isoniazid. This was done to improve bioavailability

and there have been no reports of toxicity (Horváti *et al*., 2014) after oral administration. It is important that even when delivering drugs directly to the middle ear using a PLGA vector, if there is any systemic absorption, this is non-toxic to the animal models. Guinea pig models have a propensity to gastrointestinal disturbances which is important as it can be potentially fatal. In addition, there have also been some experiments performed on drug delivery to the ear in guinea pig models. A PLGA-PEG-PLGA co-polymer was designed for sustained drug release into the middle ear (Feng *et al*., 2014) and ABR was used to assess for any evidence of ototoxicity with involvement of the inner ear. The PLGA-PEG-PLGA co-polymer was injected intra-tympanically at two concentrations: 0.05ml and 0.1ml. There was no evidence of ototoxicity in the lower dose. However, there was evidence of ototoxicity in the high dose with ABR elevation of thresholds seen especially at higher frequencies.

An *in vivo* study using PLGA as a drug delivery vehicle to the inner ear for lidocaine shows sustained release over three days after application to the round window membrane. However, there is a degree of temporary hearing loss seen in the guinea pig models (Horie *et al*., 2010).

A novel study by Zhang *et al*., 2013 used the concept of drug delivery to the middle ear and the transmission of drug to the inner ear via the round window to assess intracerebral delivery of therapies. The polymer drug vehicle used was PLGA and the drugs used were salvianolic acid B, transhinon IIA and panax notoginsenoside. There was no evidence of cochlea toxicity *in vivo* when using guinea pig animal models,

reinforcing the otological safety of PLGA nanoparticles as a potential drug delivery system to the middle ear.

1.7.10 *In vitro* studies testing for ototoxicity

In vitro studies have been developed to reduce the use of animal experimentation and to test concepts prior to moving to *in vivo* models. Neonatal mouse cochlea culture was first undertaken in 1991 (Richardson *et al*., 1991) with morphological changes seen on electron microscopy after adding ototoxic antibiotics. Murine culture models *in vitro* allow studies of the underlying cellular mechanisms involved and a high throughput of tests. *In vitro* tests however require skill and the observed response may not correlate to cellular responses as predicted. Neonatal cultures may also not correlate to mature findings of adult mice (Yorgason *et al*., 2011). *In vitro* results must be correlated with more time consuming and expensive animal studies before any consideration of translation of a treatment into a human.

Studies *in vitro* have also attempted to simulate the dimensions of the middle ear and hence drug delivery to the inner ear via diffusion across the round window membrane (Liu *et al*., 2014). Methods are aimed at developing a sustained release drug delivery system *in vitro* and results have shown the longest sustained delivery using the PLGA-PEG-PGLA co-polymer. However, when testing for ototoxicity, there is no adequate *in vitro* model at present.

1.7.11 *In vivo* studies test for ototoxicity

Hearing tests including Auditory Brainstem Evoked Response (ABR) measurements are widely used in testing for ototoxicity (Murillo-Cuesta *et al*., 2009). Brain stem auditory evoked potentials were first recorded in neurosurgical patients from surface electrodes on the nerves VIII, medulla, pons, midbrain and the cortex and from a removable electrode in the IIIrd, IVth and lateral ventricles (Hashimoto *et al*., 1981). Two potentials were recorded within 10ms after click stimulation with a slow positive wave (5-6ms) and a negative wave 8-10ms with 7 smaller waveforms in-between. These waves correspond to different components of the auditory pathway from the distal VIII nerve to the medial geniculate body (see section 1.9).

In addition, cochlear histology studies can be performed to assess for hair cell damage (Furness *et al*., 1986). The cochlea is highly organised across mammalian species with three rows of OHC and one row of IHC. The IHC bundles face the modiolus and any displacement in this orientation is thought to contribute to disorders in mechanoelectrical transduction (Hudspeth *et al*., 1983). Both acoustic trauma (Spoendlin *et al*., 1971; Liberman *et al*., 1979) and aminoglycoside antibiotic kanamycin (Ylikoski *et al*., 1974; Furness *et al*., 1986) have been shown to cause a number of cochlea changes including hair cell loss, stereocilia disorganisation and fusion (Kiang *et al*., 1986). Murine models of hair cell loss show a pattern of basal loss prior to apical (Mahendrasingham *et al*., 2011). Quantitative analysis of the IHC and OHC in guinea pig models can be used to assess ototoxicity after application of drugs such as azithromycin (Pawlowski *et al*., 2010).

Immunohistochemistry provides information of any damage to other aspects of the inner ear including spiral ligament and stria vascularis. The stria vascularis is known to be the histological changes associated with age related hearing loss (Kusunoki *et al*., 2004). Damage to the spiral ganglion cells is also associated with presbyacusis (Schuknecht *et al*., 1993). The ototoxic effects of chemotherapy drugs such as cisplatin have been shown to cause IHC and OHC loss, degeneration of the stria vascularis and a decrease in spiral ganglion cells (Rybak *et al*., 1995). It is possible to study the histological slices of inner ears after drug delivery to the middle ear to attempt to elucidate any damage to these structures which would suggest potential ototoxicity.

1.8 Novel treatment strategies for OME:

1.8.1 Pellets

The current treatment strategy for OME is ventilation tube insertion and drainage of the effusion (NICE Guidelines 2008). This does not include treatment of any persistent infection and biofilm eradication which is believed to be the basis for recurrence of OME. To achieve biofilm eradication in the middle ear and hence treat OME and prevent recurrence (Gates *et al*., 1987, Daniel *et al*., 2006), direct drug delivery to the middle ear is an attractive solution. The treatment would be optimal over several weeks in the form of a bio-degradable, modified-release antibiotic formulation. Research has already been undertaken in this field developing pellets for middle ear insertion with a modified release antibiotic.

The use of poly lactic-co-glycolic acid (PLGA) has been combined with a carrier gel pluronic F127 to create a pellet which has the potential to deliver drugs to the middle ear in a modified release formula. Two antibiotics have been tested *in vitro* for this purpose: rifampicin and clindamycin. The results have shown that *in vitro* the pellet releases antibiotics for up to three weeks and is capable of eradication of a *Staphylococcus Aureus* biofilm in an *in vitro* model of OME (Daniel *et al*., 2010). PLGA is one of the most effective bio-degradable polymeric nanoparticles already in widespread clinical use. It has been approved for clinical use due to its properties of being low toxicity and biocompatibility with tissues. To date, there have been no reports of adverse effects of PLGA and pluronic (Horváti *et al*., 2014).

The antibiotic combination of rifampicin and clindamycin was carefully selected due to their broad spectrum cover and without evidence of ototoxicity. Rifampicin is a member of the ansamycin antibiotic group (Sensi 1983). It is a heterocyclic structure and is used to treat tuberculosis (WHO 2010), leprosy and other Mycobacterial infections. Rifampicin is a powerful inducer of the hepatic cytochrome P450 and has side effects including nausea, vomiting, orange discolouration of urine and drug interaction with other medications metabolised by the liver. There is no evidence of any ototoxicity caused by rifampicin.

Clindamycin is a licosamide and is a semi-synthetic derivative of lincomycin which is a natural antibiotic produced by actinobacterium *Streptomyces lincolnensis* (Birkenmeyer et al., 1970). Clindamycin is used to treat middle ear infections, bone

and joint infections and pneumonia (Smieja 1998). Side effects include rash, diarrhoea, vomiting and a metallic taste. Similarly to rifampicin, there are no reports of ototoxicity. The combination of clindamycin and rifampicin antibiotics loaded onto PLGA and Pluronic pellets as a potential treatment for OME is therefore considered safe from an ototoxicity perspective.

Another research group has also studied a slow release antibiotic middle ear implant using ampicillin in an animal model (Goycoolea *et al*., 1991, Goycoolea *et al*., 1994). These studies were performed using a drug delivery device consisting of PLGA loaded with ampicillin which was inserted into the middle ear of cats and chinchillas with OME. Histopathology showed no adverse reaction to the implantation device and there was no evidence of ototoxicity on hair cell studies of the cochlea. However, these models show no assessment of biofilms. *In vitro* experiments have used biodegradable, modified release antibiotic pellets and studied their action on *Staphylococcus Aureus* biofilms (Daniel *et al*., 2012). PLGA pellets containing rifampicin and clindamycin were tested. The results showed that drug release was continuous for up to 21 days and that biofilms were eradicated with pellets containing 7% or 28% of antibiotic. This *in vitro* work requires translation into *in vivo* models.

1.8.2 Hydrogel

Other novel methods of drug delivery to the middle ear which aim at sustained release include intra-tympanic injection of hydrogel with ciprofloxacin (Wang *et al*., 2014) into guinea pig and chinchilla models of otitis media. No evidence of middle or inner ear

ototoxicity has been reported and sustained release was achieved for up to two weeks. With such sustained release of antibiotics, there is the potential for biofilm disruption *in vivo* and also the potential for a single treatment strategy for OME. It is however, undetermined in this study how long the hydrogel is present in the middle ear and whether there is any dissipation down the Eustachian tube.

1.8.3 Biodegradable ventilation tubes

A new, novel treatment for OME is the insertion of biodegradable ventilation tubes which are impregnated with antibiotic ciprofloxacin (Gan *et al*., 2013). Over a period of three months the antibiotic was released and less bacterial adherence to the ventilation tube was seen. Insertion of foreign bodies into the middle ear such as ventilation tubes is known to be a potential problem in the development of novel drug delivery systems to the middle ear (Belfield *et al*., 2015) and can create a chronic inflammatory state and act as a substrate for bacterial colonisation. This would potentially contribute to biofilm formation instead of potential eradication. Importantly, there was no evidence of ototoxicity in the middle or inner ear using biodegradable ventilation tubes as a method of drug delivery to the middle ear.

1.8.4 Magnetic nanoparticles

Using magnetic nanoparticles and applying an external magnetic field has the future possibility of delivering drugs in a non-invasive manner to localised targets around the

body. Such technology would allow precise delivery of drugs to the middle ear to treat conditions such as OME (Shapiro *et al*., 2014). Such technology however, is under development and there are potential limitations including the complex technology of multiple high powered magnets which would allow accessibility to the relatively small and shallow target of the middle ear. Preliminary animal models of nanoparticle technology used to deliver prednisolone to the middle ear has shown increased inflammatory changes in rats after 30 days (Lafond *et al*., 2018) and therefore more studies are required before consideration of translating this technology to humans.

Magnetic manipulation of nanoparticles, however has the exciting possibility of being a therapy free from surgery and hopefully devoid of any side effects due to the localised delivery mechanism.

Delivery of PLGA and pluronic pellets laden with rifampicin and clindamycin into guinea pig middle ears is an important step into developing new therapies for OME which treat the biofilm in a sustained manner. Testing the safety of this potential new treatment *in vivo* is essential and requires several different techniques: ABR, cytocochleograms and middle ear histology to assess the effects of the pellet and antibiotics on the middle, inner ear and auditory pathway.

1.9 Auditory Brainstem Response

The auditory brainstem response (ABR) test is electroencephalograph (EEG) recording which measures the neural activity of the animal while different sounds are presented. In the ABR recording, both a click stimulus and single tone stimulus are presented to determine both the general thresholds of hearing (click) and the animal's sensitivity to various frequencies. The click stimulus is a square wave stimulus which consists of a wide range of frequencies presented simultaneously. The frequency "range" (f) of the click stimulus can be calculated as:

$$f = \frac{1}{t}$$

where *t* is the duration of the stimulus in seconds. For the click ABR recordings, the duration of the stimulus is 0.01ms hence,

$f = \frac{1}{1\times10^{-5}} = 100000Hz = 100kHz.$

As the initial frequency of the click stimulus was 100Hz, this means that the click ABR recording tests across the range of 0.1kHz – 100.1kHz.

Single tone frequency ABR recordings are tested at 6, 12, 18, 24, and 30kHz for laboratory mice as this represents the most sensitive regions in the hearing ranges (Turner *et al.*, 2005). The hearing for the guinea pig is shown to be most sensitive in the 16kHz-24kHz range (Figure 9).

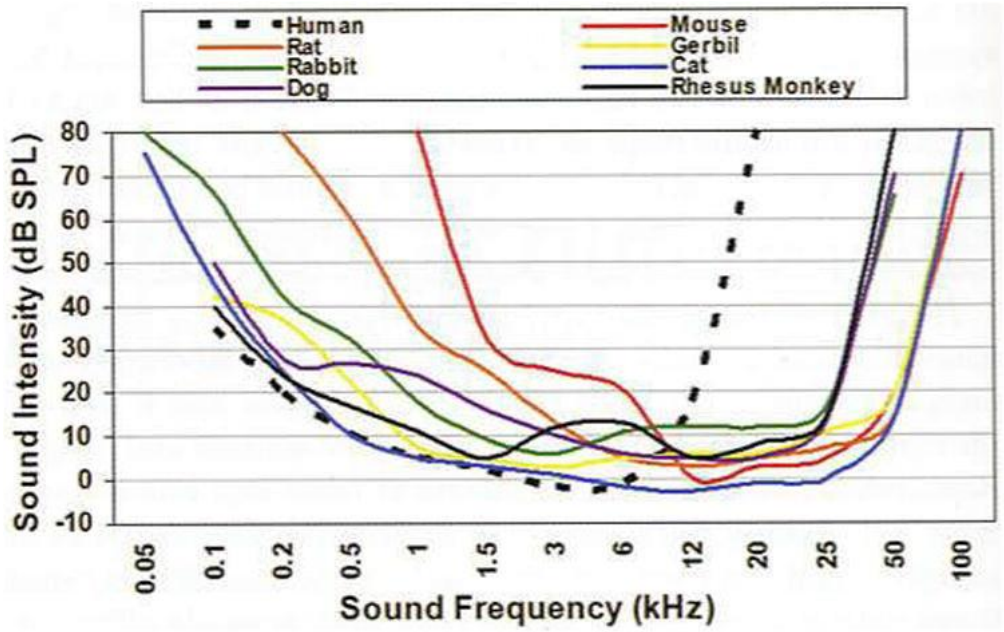


Figure 9 *Graph showing the sensitivity to various frequencies of eight different species including commonly used laboratory animals and humans (Turner* ***et al.****, 2005). The data has been adapted from Fay* ***et al.****, 1988*

For both the click and single tone ABR, measurements are taken by presenting the stimulus 256-512 times at a single intensity, and an average waveform is produced. This is repeated between 0dB SPL and 95dB SPL with 5 dB increments.

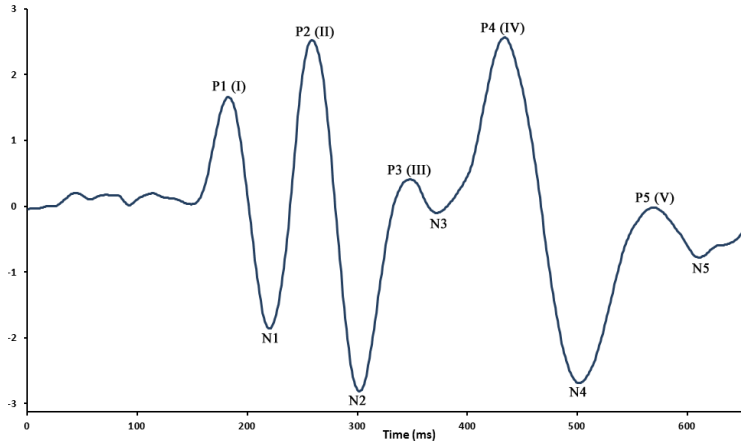
The guinea pig ABR consists of five waves (I-V) which present within 8ms of the stimulus being received. These five waves represent distinct regions of the auditory pathway. Of particular interest in this study are waves I and II, which represent the SGNs (spiral ganglion neurons) /auditory nerve, and the cochlear nucleus respectively, with waves III-V representing higher levels of the auditory brainstem (Melcher *et al*., 1996; Henry *et al*., 1979). In addition to this, the ABR can also consist of other, peripheral evoked potentials such as cochlear microphones which originate from the hair cells and can therefore provide insight into cochlea function (Eggermont *et al*.,

1976). The summation potential also originates form the cochlea hair cells and can be detected during ABR recordings (Honrubia *et al*., 1969).

1.9.1 Auditory Brainstem Response Threshold

Analysis of the ABR waveform can take into account threshold. This is the intensity of sound where the waveform is first distinguishable from noise. The amplitude of the peaks and troughs of each wave can also be measured over a range of intensities; and the latency of the peaks and troughs measured over a range of intensities. By using this analysis, and the knowledge that each wave corresponds to a specific region of the auditory pathway, the ABR measurement can be used to build a picture of how the animal processes sound before and after presentation of a noise stimulus.

Studies have shown that ABR threshold elevation occurs after insults such as amikacin (Nekrassov *et al*., 2000) in guinea pigs at 4kHz and 8kHz. Cisplatin is also known to cause ABR threshold elevation (Cheng *et al*., 2005) in experimental guinea pig animal models and the condition of kernicterus, with an elevated levels of unconjugated bilirubin in a newborn baby has been shown to cause threshold elevation (Kaga *et al*., 1979).



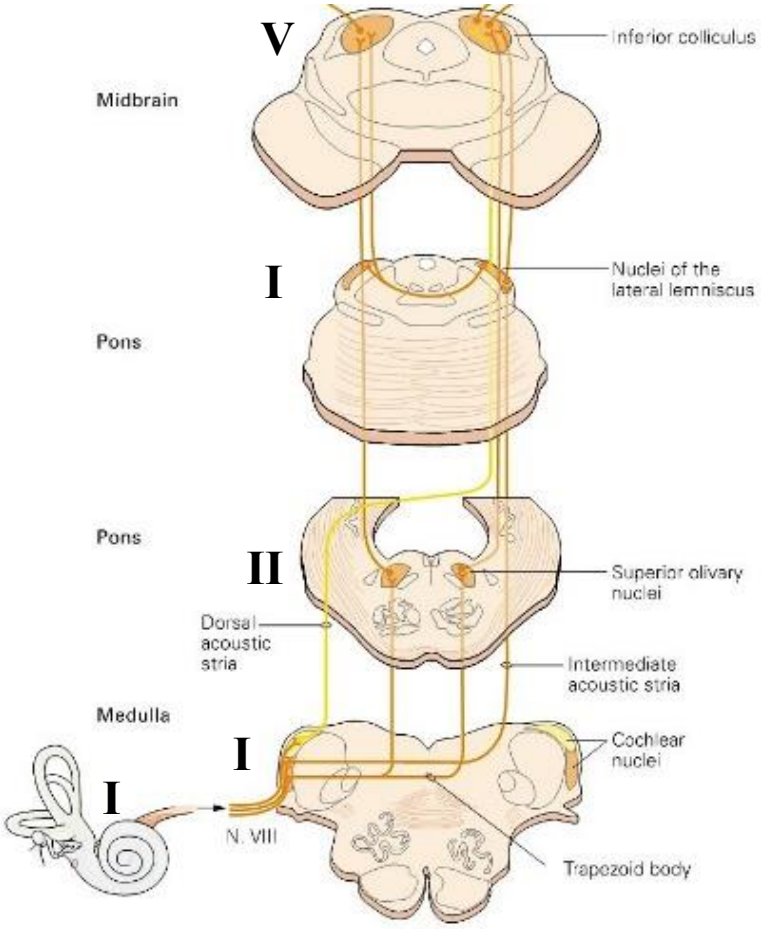


Figure 10: *An example of a "clean" ABR waveform showing the peaks (P1-P5) and troughs (N1-N5) of the five waves (I-V)*

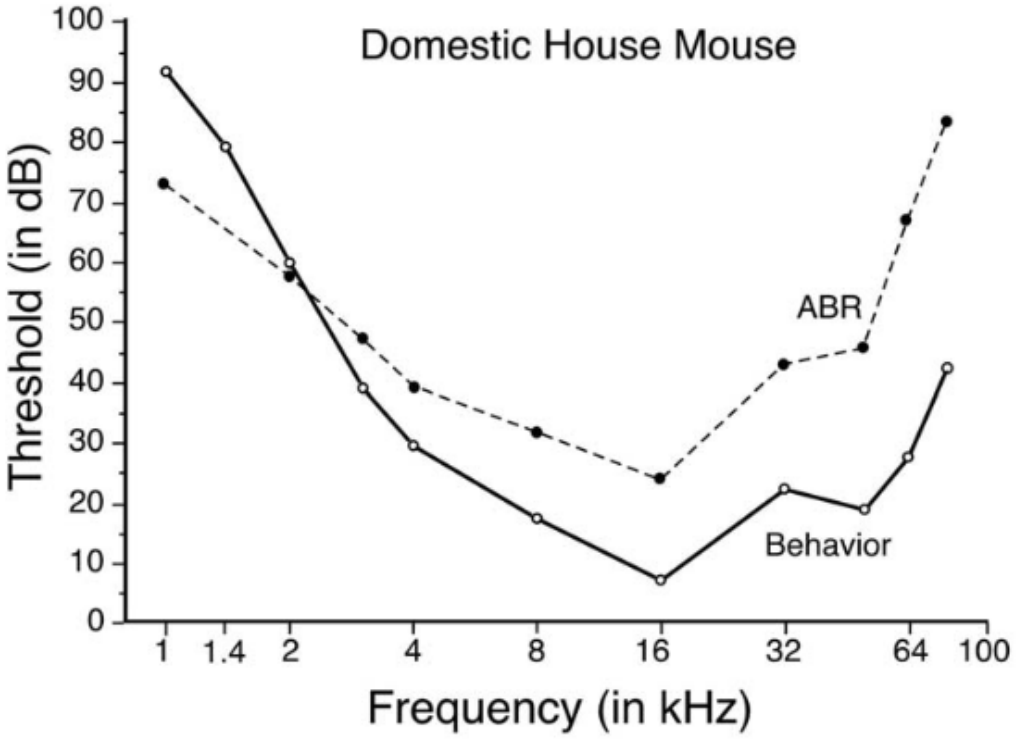


Figure 11. *ABR recordings may misrepresent the behavioural thresholds of hearing in animals (Heffner et al., 2003)*

Behavioural hearing tests, although they can be difficult and time consuming, have been shown to produce better estimates of hearing across a range of species (Szymanski *et al*., 1999; Heffner and Heffner, 2003). **Error! Reference source not found.**11 shows the measured threshold across a range of frequencies of the domestic house mouse; here you can see that there is a distinct difference of average threshold measured at >2kHz. One theory is these differences are thought to arise from the relatively "impure" tones presented in ABR analyses, caused by the rapid onset and offset of the tones used for ABR analysis, compared to the longer, more "pure" 400ms tones presented in behavioural studies; however it is also possible that the use of anaesthetics and the inherent electrical background noise could also interfere with the estimation of threshold in ABR analysis.

Despite this discrepancy between ABR thresholds and behaviour thresholds, ABRs are widely used as a simple and non-invasive test of threshold shifts in laboratory animals after noise insult, and have been shown to be particularly effective in estimating shifts of threshold in response to broadband noise and high frequency tones.

1.9.2 Auditory Brainstem Response Latency

Measurements in the latency of ABR traces and changes over time also provides information regarding the transmission of sound from the cochlea to the brain (Figure 10). Therefore a latency shift provides complementary information about the neural transmission and hence the possibility of neurotoxicity. This has been demonstrated with an increase in latency seen after acoustic trauma (Gourévitch *et al*., 2009) and is seen in aging guinea pigs (Ingham *et al*., 1998; Nozawa *et al*., 1998). This correlates with the finding of increased latency seen in elderly patients in waves I and III (Konrad-Martin *et al*., 2012). The underlying pathogenesis is believed to be related to reduction in auditory nerve units and their synchrony of firing. Aminoglycoside treatment has been shown to cause increase in ABR latencies of waves I and V in human subjects after netilmicin and tobramycin administration (Hotz *et al*., 1990).

Studies have shown that increases in latency of P1 precede P3 and P5 and correspond to ototoxicity of the basal cochlea (Jacobson *et al*., 1985). This initial effect is thought to be due to compromise of the vascular supply of the basal cochlea.

Aspirin toxicity in rats causes an increase latency of P1 and P2 and P4 at 1kHz and 2kHz but was preserved at 4 and 8kHz suggesting that low frequency hair cells of the rat's cochlea are susceptible to aspirin ototoxicity (Kurata *et al*., 1997). Cisplatin, which is frequently used as a chemotherapeutic agent and has known ototoxic effects has been

shown to cause an increase in wave V latency (De Lauretis *et al*., 1999) This has been postulated to be an early sign of hearing deterioration which may have some clinical applications in attempting to calibrate the dose tolerated by individual patients receiving cisplatin in order to avoid the ototoxic side effects. The patients with increases in latency also have hearing loss detected by audiograms.

1.9.3 Auditory Brainstem Response Amplitude

Aspirin studies on rats have shown that the P2 and P4 amplitude was reduced at 2kHz but this was not seen at higher frequencies of 4 and 8kHz (Kurata *et al*., 1997). Aminoglycoside antibiotic testing of rats in the form of amikacin has been shown to decrease amplitude of ABR recordings for each wave (Yamamoto *et al*., 1992).

Studies on patients have shown that with age, the amplitudes of all the ABR peaks were reduced suggesting a reduction in the number of nerve conducting units (Konrad-Martin *et al*., 2012). Similarly, noise exposure in rats has been shown to cause a decrease in amplitude proportionally to the level of noise exposure and the basal region of the cochlea was most affected (Chen *et al*., 2014) with hair loss noted. Noise exposure experiments using guinea pigs has also shown that the amplitudes of ABR wave I was consistently decreased, yet wave IV which was also assessed recovered a week after the noise exposure period (Heeringa *et al*., 2014). The mechanism is postulated to be related to a disturbance of the auditory inputs to the inferior colliculus with an imbalance between inhibitory and excitatory responses which may result in hyperacusis after noise exposure in the acute setting.

Table 4 summarises the ABR latency and amplitude changes with different aetiologies.

Stimulus	Latency	Amplitude
Acoustic trauma	Increase (Gourévitch *et al*., 2009)	Proportional decrease with noise exposure (Chen *et al*., 2014)
Presbyacusis	Increase guinea pig (Ingam *et al*., 1998; Nozawa *et al*., 1996) Human – increase wave I and III (Konrad-Martin *et al*., 2012)	All waves reduced (Konrad-Martin *et al*., 2012)
Salicylate	Increase P1,2 and 4 at 2kHz (Kurata *et al*., 1997)	Reduced P2 and P4 at 2kHz (Kurata *et al*., 1997)
Cisplatin	Increase wave V (De Lauretis *et al*.,1999)	Reduced P1 and P3 (Otto *et al*., 1988)
Aminoglycosides	Increase I and V (Hotz *et al*., 1990)	All waves reduced (Yamamoto *et al*., 1992)

Table 4: ***Summary of ABR latency and amplitude changes with different stimuli presented to the cochlea***

1.10 Cytocochleograms

Creating cytocochleograms is a method used to count hair cells and to ascertain and quantify any loss of both IHC and OHC. For details on preparation please refer to section 3.11. This method has been widely used before (Mahendrasingham *et al*., 2011). Studies using mouse models CD/1 for presbyacusis have shown that OHC are damaged initially in the basal cochlea and with associated IHC degeneration (Mahendrasingham *et al*., 2011).

It is already known from studying cytocochleograms and hair cell counts that chemotherapy agents such as cisplatin cause OHC loss from base to apex and from outer most row of hair cells to the inner hair cells (Tropitzsch 2014). Increasing the concentration of cisplatin also resulted in progression of hair cell loss.

Aminoglycoside antibiotics are also known to cause hair cell loss of both the IHC and OHC as seen after administration of gentamicin (Forge *et al*., 2000) and kanamycin to rats (Matsuda *et al*., 1999). The rapid accumulation of aminoglycoside gentamicin in the hair cells is thought to be the basis of this toxicity (De Groot *et al*., 1990) resulting in apoptosis.

1.11 Histology

Looking at the ultrastructure of the middle ear and inner ear is important in assessing any morphological changes. Such structural alterations may contribute towards ototoxicity and hence impact the safety of compounds introduced into the middle ear. Cisplatin ototoxicity is known to cause such changes including degeneration of epithelial cells in the stria vascularis (Meech *et al*., 1998; Ravi *et al*., 1995) and the neurones of the spiral ganglion (Van Ruijven *et al*., 2005, Zheng *et al*., 1995, Zheng *et al*., 1996). The cisplatin induced degeneration of the Organ of Corti (Zheng *et al*., 1996; Van Ruijven *et al*., 2005) is better appreciated using cytocochleograms to identify IHC or OHC loss than using histology.

It is also important to assess the impact of any surgical intervention on the middle ear on the mucosa and if there is any evidence of fibrosis or scarring. This can be seen in histology cross sections looking at inflammatory cells and the presence of fibrin. When using carrier molecules such as PLGA and pluronic in the form of pellets, histology allows for an assessment of the degree of residual foreign body after a designated time and any potential inflammatory response associated with this.

Noise exposure in the acute setting results in stria vascularis swelling and in the chronic setting over two weeks results in degeneration (Hirose 2003). The stria vascularis is also known to be damaged in noise induced hearing loss (Gratton 1996; Spicer 1997; Ichimaya 2000).

Chapter 2: Project Aims

2.1 Overall aims

Delivering rifampicin and clindamycin laden PLGA and Pluronic pellets into an animal model middle ear and assessing for safety is the primary aim. There is no prior evidence of ototoxicity from the antibiotics or components of the middle ear pellet and therefore the hypothesis is that there will be no evidence of ototoxicity after insertion. There is also the hypothesis of no evidence of inflammation or disruption of function of the middle ear after pellet insertion.

2.1.1 Selection of animal model

Selecting the correct animal model for implantation of middle ear pellets is important for reduction and refinement of the experiments (Russell and Burch 1959). A comparison of the anatomy and dimensions of the auditory system in cadaveric rats and guinea pigs will be made. Studies will be focused on middle ear dimensions to differentiate between these two animal models especially in relation to ME volume.

2.1.2 Development of surgical delivery to the middle ear

Surgical approaches to the middle ear will be compared using cadaveric animals to determine the best route for delivery of middle ear pellets which have fixed dimensions. The transtympanic route, posterobulla and anterobulla approaches will be assessed for their merits and feasibility of insertion of a ME pellet with set dimensions.

2.2.3 Testing the safety of middle ear surgery

Surgical controls will be undertaken to determine if implantation of middle ear pellets is ototoxic and traumatic in any way.

2.2.4 Testing middle ear pellets made of PLGA and pluronic for safety including ototoxicity

Pellets made of poly lactic-co-glycolic acid (PLGA) and pluronic will be inserted into the middle ears of animal models and safety tested in the form of ABRs over a period of 16 weeks. After culling humanely, histology sections and cytocochleograms will be prepared and analysed to assess for evidence of ototoxicity. In addition, immunohistochemistry will be performed on cochlear sections; using DAPI and Phalloidin staining to assess for morphology and presence of IHC and OHC.

2.2.5 Testing middle ear pellets made of PLGA and pluronic loaded with rifampicin and clindamycin for safety including ototoxicity

Poly lactic-co-glycolic acid (PLGA) and pluronic pellets laden with antibiotics rifampicin and clindamycin will be inserted into the middle ears of animal models and safety tested in the form of ABRs over a period of 16 weeks. After culling humanely, histology sections and cytocochleograms will be prepared and analysed to assess for evidence of ototoxicity. In addition, immunohistochemistry will be performed on cochlear sections; using DAPI and Phalloidin staining to assess for morphology and presence of IHC and OHC.

2.2.6 Testing middle ear pellets made of PLGA and pluronic loaded with rifampicin and clindamycin individually for safety including ototoxicity

PLGA and pluronic pellets laden with either rifampicin or clindamycin will be inserted into the middle ears of animal models and safety tested in the form of ABRs over a period of up to 16 weeks. After culling humanely, histology sections and cytocochleograms will be prepared and analysed for evidence of ototoxicity assessing the IHC and OHC and evidence of inflammation. In addition, immunostaining will be performed on cochlear sections; using DAPI and Phalloidin staining to assess for the presence or absence of both IHC and OHC and their morphology.

Chapter 3: Experimental Methods

3.1 Principal Experimental Groups

The main experimental groups were carried out using albino Dunkin Hartley guinea pigs as the test species. Each set of experiments had specific technical variation to evaluate the following:

1. Biological control group of animals to assess the changes in ABR over time
2. Surgical control group to assess the effects of opening the middle ear bulla without pellet insertion into the male albino guinea pig
3. Treatment control group to assess the effects of PLGA and pluronic pellet inserted into the middle ear of guinea pigs
4. The effects of PLGA and pluronic pellet loaded with rifampicin inserted into the middle ear of male albino guinea pigs
5. The effects of PLGA and pluronic pellet loaded with clindamycin inserted into the middle ear of male albino guinea pigs
6. The effects of PLGA and pluronic pellet loaded with both rifampicin and clindamycin inserted into the middle ear of male albino guinea pigs

3.2 Animal Procurement and Husbandry

A total of 48 healthy Dunkin Hartley adult albino male guinea pigs (Harlan UK, Limited) weighing between 350g and 450g were used experimentally. Animals were all given a minimum of 72 hours of acclimatisation prior to experimental use. All experiments were carried out in accordance with Home Office Regulations in accordance with The Animals Act (Scientific Procedures) 1986 and covered by the appropriate Personal (60/13670) and Project (60/4436) Home Office Licences with assistance from the technical support staff at the Clinical Research Facility in Leicester which has a license covering guinea pig procedures. Advice was taken from the Home Office vet regarding anaesthesia and analgesia.

Animals were randomly allocated to cage and housed in groups of up to four in open cages (Scanbur). Identification marks were as follows: head, back, rump and no mark. Fresh sawdust and hay were supplied every 3 days. Water was changed daily and a guinea pig pellet diet was administered daily. Water and solid food was supplied *ad libitum*. The water was from the domestic supply and replaced daily and guinea pig pellet diet, FD1 SQC supplied by Special Diet Services Limited, UK.

Temperature was maintained between 16-20 ^{o}c and humidity between 45-70%. Lighting was on a 12 hour light/dark cycle (commencing at 7am). There was minimal natural sunlight. The animal house staff fed and watered the animals daily and monitored their general wellbeing including inspection of fur, teeth and any surgical scars.

Any animal showing signs of general illness was excluded from the study. Furthermore, any animal with signs of middle ear infection at surgery was excluded.

3.3 Monitoring and maintenance of physiological function during experiments

After the induction of anaesthesia, ABR electrodes were attached and the guinea pig was placed on a heated mat with the left ear facing up. Core body temperature was maintained between 37 +/- 1^{o}c using a Harvard homeothermic control unit and blanket placed under the guinea pig with a silicone sealed rectal temperature probe inserted (calibrated using a water bath and thermometer). A non-invasive pulse oximeter (Nonin 8500AV, Nonin Medical inc., Plymouth, USA) was placed on the left hind paw to continuously monitor arterial blood oxygen saturation. This was maintained above 97%. Supplementary oxygen was delivered if required via a facemask. The pulse oximeter also gave a pulse reading and this was kept in the normal range for guinea pigs: 180-350 beats per minute. Respiration rate was also noted throughout the experiments.

Lacrilube ointment consisting of liquid paraffin, was used to protect the corneas bilaterally during the ABR recordings and operative procedures.

3.4 Surgical procedure

Prior to sedation or surgery, the guinea pigs were weighed and the experimental drug doses were calculated accordingly (Table 6).

After an initial ABR recording, the recording electrodes and monitoring equipment were removed and the guinea pig transferred to the adjacent surgical suite whilst under sedation. The animal was then attached via a face mask (Blease Boyles

Apparatus) to isofluorane (1%) in the induction room and the skin prepared with shaving of fur in the left submandibular region and chlorhexidine antiseptic to the skin. The guinea pig was transferred to the operating table and positioned using a beanbag cradle with a mouthpiece connection to isoflurane 1% for the duration of the procedure. Intraoperative monitoring was performed using pulse oximetry and rectal temperature probe. The skin was draped and instruments cleaned using an autoclave (121 degrees centigrade). Using a sterile technique, a 2cm incision was made over the mandible using a scalpel. The platysma was divided and the masseter muscle exposed (Figure 12). The posterior belly of digastric runs underneath the masseter and was followed to the bulla of the middle ear. This approach to the middle ear bulla has previously been described by Gil-Carcedo *et al*., (1991). The anterior and undersurface of the middle ear bulla was exposed gently and a round fenestration, approximately 2.5mm in diameter, was made in the bone. This was achieved using a Schucknecht pick and joining small perforations together.

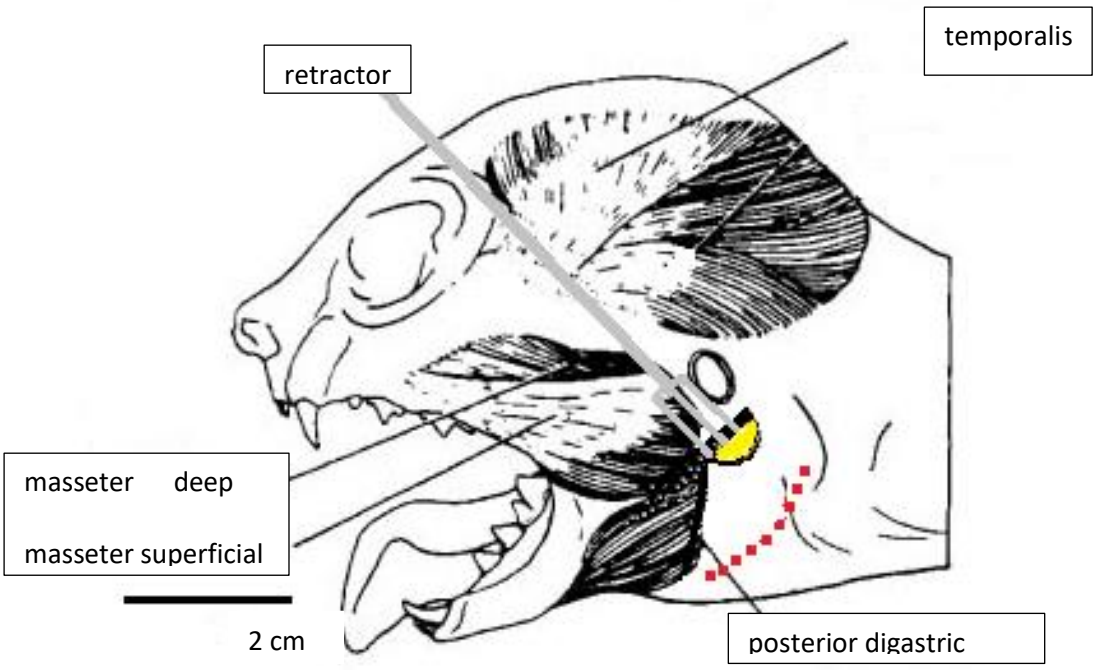


Figure 12. ***Diagram of surgical approach to guinea pig middle ear bulla (highlighted yellow) with retraction of the posterior digastric. Level of cervical skin incision indicated (red dotted line)***

For the surgical control animals, a piece of bone wax (70% beeswax, 30% Vaseline) was placed over the bulla hole. For the guinea pigs which have pellets inserted, this was done prior to the bone wax application using McIndoe non-toothed forceps. The pellets were stored in a fridge at 4 degrees centigrade in separate sterile packages prior to their insertion into the middle ear bulla. The skin was closed using a subcuticular 5/0 vicryl suture and glue. Please refer to section 3.12 for manufacture and preparation of the pellets.

Analgesia was given to the guinea pigs in the form of metacam (1mg/kg) initially subcutaneously and then orally in the initial post-operative period and buprenorphine (0.05mg/kg) was administered to counteract the hypnorm and to provide opiate based pain relief.

In the initial post-operative period, the guinea pigs were monitored carefully in the recovery area with gel based water, bottled water, carrot, hay and pellet supplements to eat. The cages were kept on a heated mat. The following day, the guinea pigs were transferred into their open cages. The guinea pigs were weighed daily for the initial post-operative period and were given 72 hours of metacam.

3.5 The use of sedation/anaesthesia in the experimental design

Surgical anaesthesia had to meet the criteria of achieving analgesia, muscle relaxation and loss of reflexes in order to optimise recordings. Minimal physiological and metabolic disturbance to each guinea pig was achieved. The mode of administration of drugs aimed to minimise stress and discomfort to the animal. Historically, guinea pigs are one of the most difficult animals to anaesthetise with injectable or inhalational

anaesthetics due to the problems with compromising respiratory or cardiac function with bradycardia (Cannell *et al*., 1972).

The overall aim was to develop a regimen allowing surgical intervention and repeatable auditory recordings. The loss of the guinea pig pedal reflex was used as a guide to depth of anaesthesia. Parenteral agents were preferred as they did not require a facemask as this had the potential to interfere with the experimental set up.

3.6 Experimental regimens

3.6.1 Regimen 1: ABR Recording

A subcutaneous injection of 0.6ml/kg of fentanyl/fluanisone (Hypnorm) was administered subcutaneously into the neck. In addition, subcutaneous administration of midazolam (Hypnovel) was also given. Together, this created a moderately deep anaesthetic allowing electrode placement and ABR recording.

A second regimen was developed for a small subset of additional experiments which were carried out in 2014 because Hypnorm was discontinued by the manufacturer. This was an unavoidable alteration in the drug regimen. Please refer for Regimen 4 section 3.6.4 for details of this change.

3.6.2 Regimen 2: ABR Recording and surgery

A subcutaneous injection of 0.6ml/kg of fentanyl/fluanisone (Hypnorm) was administered subcutaneously to the neck. An addition subcutaneous administration of midazolam (Hypnovel) was also given. Together, this created a moderately deep anaesthetic allowing electrode placement and ABR recording. After ABR recording, Isoflurane was administered using a facemask and surgery was undertaken to insert the pellet into the middle ear.

3.6.3 Regimen 3: ABR Recording and terminal anaesthesia

A subcutaneous injection of 0.6ml/kg of fentanyl/fluanisone (Hypnorm) was administered subcutaneously to the neck. An addition subcutaneous administration of midazolam (Hypnovel) was also given. Together, this created a moderately deep

anaesthetic allowing electrode placement and ABR recording. Intraperitoneal injection of barbiturate Medetomidine was then performed and death certified from clinical examination before perfusion-fixation.

3.6.4 Regimen 4: Hypnorm substitution

A small cohort of animals (8) underwent anaesthesia without the availability of Hypnorm as this was discontinued by the manufacturer. As a substitute, a combination of midazolam (4mg/kg), fentanyl (0.04mg/kg) and medetomidine (0.4mg/kg) was developed as a regimen. This was administered subcutaneously and reversed using atipamezole (1mg/kg) at the end of the experimental recording.

Drug	Dose
Midazolam	4.0mg/kg
Fentanyl	0.04mg/kg
Medetomidine	0.4mg/kg
Atipamezole	1.0mg/kg
Hypnorm (fentanyl/fluanisone)	0.6mg/kg
Buprenorphine	0.5mg/kg
Atropine	0.5mg/kg

Table 5: ***Drug doses used in experimental regimens according to animal weight***

3.7 Pharmacology of anaesthetic agents

3.7.1 Isofluorane

Isoflurane is a halogenated methyl-ethyl-ether. This is an established anaesthetic agent for small animals and is ideal for short procedures as there is limited central nervous system depression. Studies on isoflurane in guinea pigs have shown that there is a dose dependent reduction in the amplitude and increase in the latency of the ABR (Stronks *et al*., 2010). It is therefore important that the isoflurane is used after the ABR recording is completed for the surgical experimental component.

3.7.2 Midazolam (Hypnovel)

Midazolam is a water soluble benzodiazepine and acts to potentiate fentanyl (Pieri *et al*., 1981). Previous studies show that fentanyl and midazolam in combination produce good skeletal muscle relaxation in small rodents and guinea pigs (Flecknall and Mitchell 1984). Fentanyl used in combination with diazepam in guinea pigs has been shown to provide a safe effective anaesthetic regimen with reduced respiratory depression and no alteration of ABR thresholds.

3.7.3 Fentanyl/Fluanisone (Hypnorm)

Administration of Fentanyl and Fluanisone is used to initiate neuroleptanalgesia in small laboratory animals including guinea pigs.

Fentanyl is a potent and effective opioid agonist active against μ receptors. It is up to 100 times more effective than morphine regarding analgesia (Green *et al*., 1975). Fentanyl has a rapid onset but short duration of action.

Fluanisone is a tranquiliser which potentiates the analgesic action of fentanyl and antagonises any respiratory depression (Inoue *et al*., 1994).

3.7.4 Medetomidine

Medetomidine is a synthetic barbiturate used as an anaesthetic or an analgesic acting as an alpha two adrenergic receptor agonist. It is often used in combination with opioids as premedication. Side effects include peripheral vasoconstriction and bradycardia (Sinclair *et al*., 2003). It is frequently used in euthanasia with intraperitoneal or intracardiac injection and is injected once deep anaesthesia is established.

3.7.5 Atipamezole

Atipamezole is a synthetic alpha-adrenergic receptor antagonist (Pertovaara *et al*., 2005). It is administered subcutaneously and is rapidly absorbed from the periphery to the central nervous system. It is used as a reversal agent for medetomidine.

3.7.6 Atropine

Atropine is an anticholinergic drug and its actions are on the parasympathetic nervous system to inhibit salivary gland and mucous secretions, aiming to reduce guinea pig secretions during the experiments. It is administered subcutaneously and side effects include ventricular tachycardia, nausea and blurred vision.

3.8 Auditory Brainstem Response

3.8.1 ABR analysis

In order to generate a short, shaped tone pip suitable for eliciting a frequency specific response, a computer controlled wave form generator was used. This system was designed and built to order by Dr. Patrick Jones of Applied Technology at Glaxo Smith Kline. A schematized diagram of its components is shown in Figure 13.

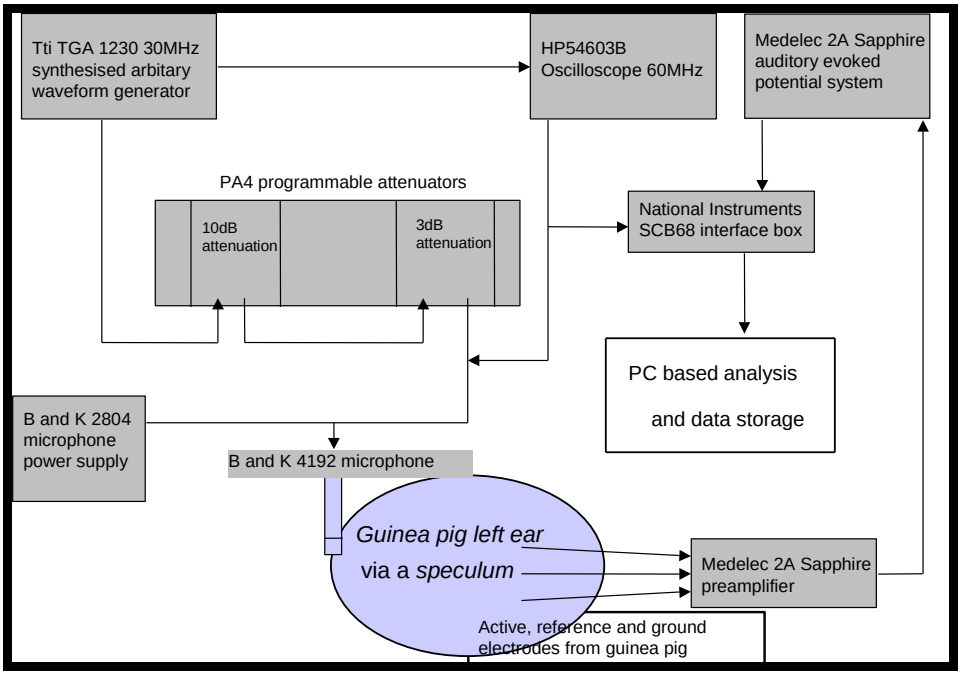


Figure 13: *Schematic diagram of signal generator and recording system*

Cosine enveloped wave forms of the desired frequency (8,12,16,24,30) KHz with a total length of 5 milliseconds including a 1 millisecond rise and fall time were generated using a Thurlby Thandar Arbitary Wave Form Generator (TGA 1230, 30MHz, Tucker Davis, US). The maximum amplitude of the signal from the TGA 1230 was 20V peak to peak.

The signal from this device was fed into paired Tucker Davis DA-4 Signal attenuators. This allowed 99dB attenuation of the maximal output of the signal generator in 1 dB increments. For increased speed of use one attenuator was set to 10 dB steps and the other to 1 to 3 dB steps. This signal was fed to an ultra high performance Bruel and Kjaer reverse driven microphone (Model 4192) for transduction. The microphone was fed by a 200 V bias current to ensure reliable and flat frequency response (B&K battery operated microphone power supply 2804 coupled to the signal line by a 0.01μF capacitor). The signal was concurrently fed to a Hewlett Packard 54600 oscilloscope for real time signal monitoring throughout the experiment.

The signal generator was electronically switched by the master PC (Kayak XA, Hewlett Packard running Microsoft Windows NT4.0). Thus the onset of signal generation triggered the onset of compound action potential recording. The signal was repeated and recording averaged from up to 400 times whilst being continuously displayed on a PC screen oscilloscope. This repetition was user determined according to the clarity of the signal displayed. At high intensities, 20 to 50 cycles would be adequate.

The CAP signal was pre-amplified using a Medelec Sapphire 4a x 10 000 and filtered between 5Hz –5 kHz then fed through to the PC. Within the PC, the real time signal was digitally sampled using a National Instruments sampler at 16kHz. This sampled signal was then averaged for CAP display with sensitivity (Volts/division) and time base (ms/division) set manually by the user at each recording. For each recording, captured data was saved by the computer in a user defined file. This allowed offline analysis using Microsoft Excel for organisation of the data and statistical analysis. Analysis was carried out using MINITAB software (Minitab Inc).

Hearing thresholds were evaluated using ABR auditory brainstem responses because auditory nerve fibre thresholds maintain a systemic relationship across different degrees of hearing loss (Ngan 2001). After recording of the ABRs by subcutaneous electrodes, the waveforms were averaged and stored for offline analysis using GSK analysis programme and TDT. On analysis of the waves, threshold was defined as the lowest level in dB at which a clear waveform could be observed. Wave 1 was the focus for analysis with a particular emphasis on P1-N1. When wave 1 was unclear, other peaks were analysed with P2-N2 and subsequently P3-N3.

Amplitude was measured as the difference between P1 and N1 and between P2 and N2 and P3 to N3. Latencies were measured from the tip of the first deflection to the bottom of the first, second and third peaks (N1, N2 and N3). We included the first three waves because N3 is known to have the best signal to noise ratio and hence can be easily identified (Gourévitch 2009). The latencies and amplitudes were measured at 16kHz and 24kHz because these frequencies are thought to be most representative of clear traces in the guinea pig animal model.

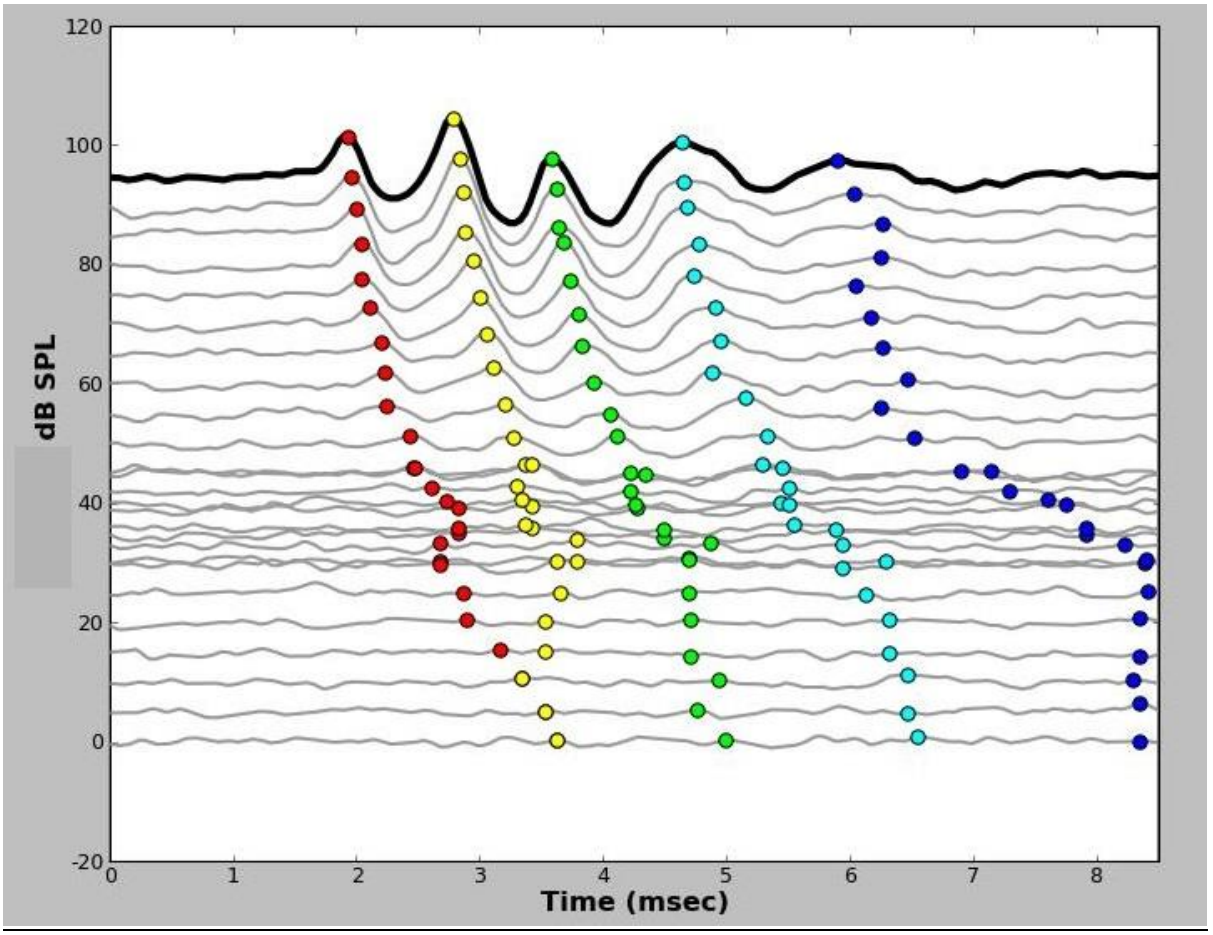


Figure 14: ***Example of cumulative views of ABR recording showing peaks P1 (red), P2 (yellow), P3 (green), P4 (turquoise) and P5 (blue).***

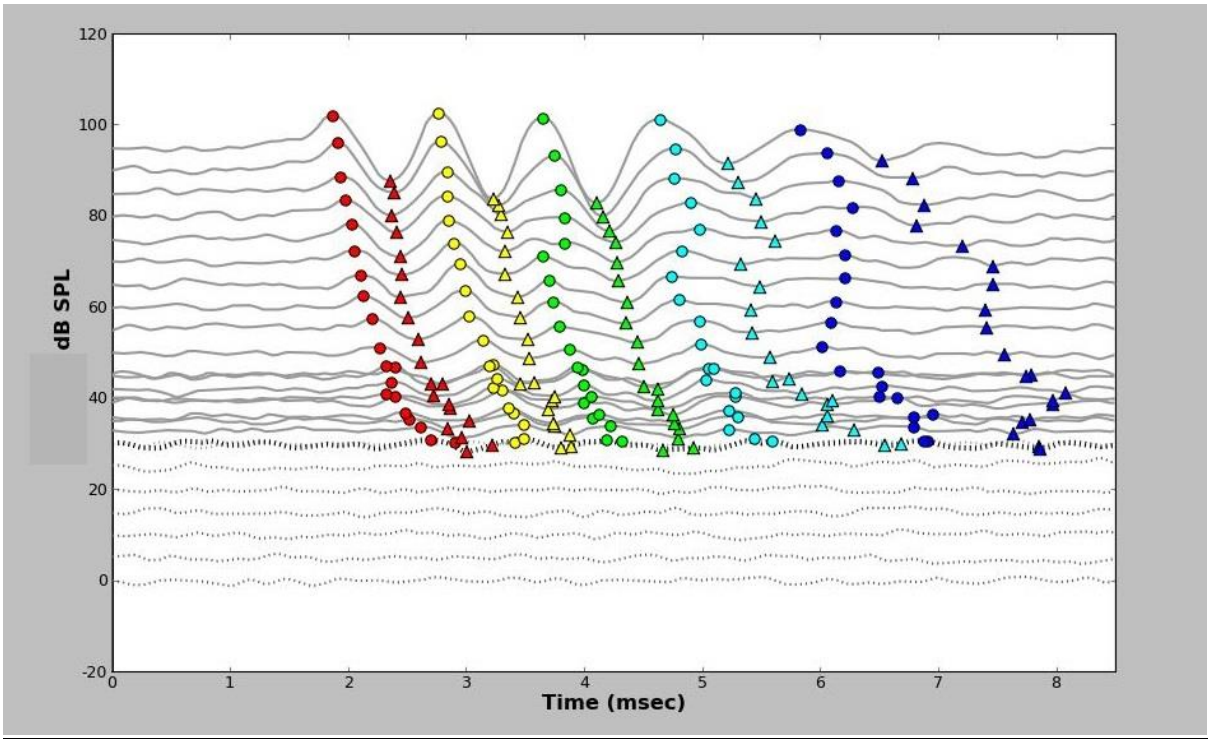


Figure 15: ***Example of selection of peaks P1-P5 with circles and troughs N1-N5 (triangles). Threshold for this ABR recording would be at 30dB***



Please note amplitude measurements were as follows: P1-N1, P2-N2 and P3-N3 in µVolts

Please note latency measurements were as follows: P1 – N1, P2-N2, P3-N3 in msecs

After measurements of the amplitude and latency are made, information regarding the transduction of the electrical signal down the auditory pathway can be deduced. Both increases and decreases in latency and amplitude can be scientifically important. The amplitude and latency results for each animal in an experimental group were pooled and mean values and standard errors calculated for each value for 94, 84 and 74dB. Paired t-tests were done to assess for significance with $p<0.05$ taken as the level of significance.

3.8.2 Acoustic Calibration

The ABR machine was set up and calibrated monthly and also in a shorter fashion at the beginning of each experimental session. The short calibration involved connecting output 2 to the oscilloscope and holding the calibration microphone connected to the driver output x. The calibration microphone was held next to the recording microphone of 4192 and the oscilloscope recording at 20mv/div.

With a calibration stimulus of 1kHz at 94dB SPL the 4192 modified microphone using a 20V signal (peak to peak) at 1kHz was used. When coupled with the 4134 calibration microphone this would produce a reference voltage of 38mV peak to peak or 13.8mVrms. This was monitored on an oscilloscope and used as a quick check to ensure the 4192 driver was generating a calibrated acoustic signal referenced at 94dB SPL which was referenced as the 0dB system output. This was concluded that the system was operating as required to drive a guinea pig cochlea.

The settings of the equipment should read as follows – increment 1:10db, increment 2:3db SPL. The Thurlby Thandar machine was turned to the Patrick test and the power supply charged with three 1.5V batteries was turned on.

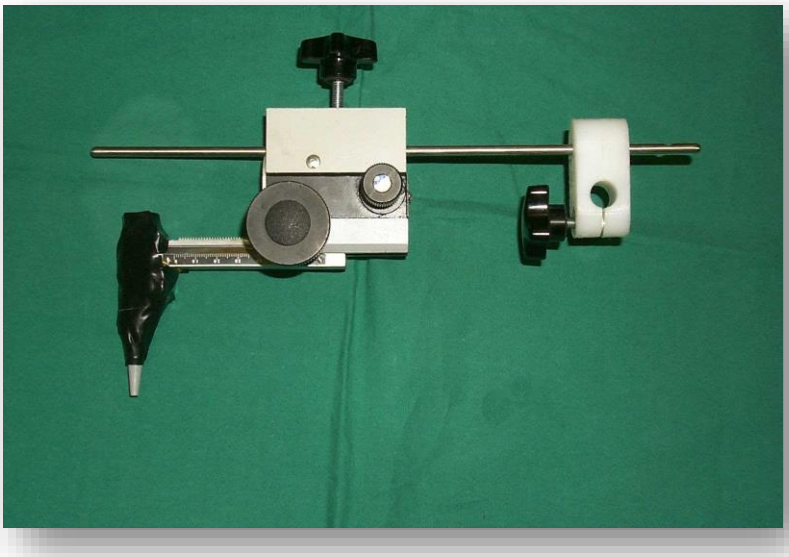


Figure 16*: The acoustic coupler set up.*

The computer programme CAP allowed measurements of click33, 30kHz, 24kHz, 16kHz, 12kHz and 8kHz. Attenuation was used from 94dB in increments of combinations of 10dB and 3dB. Recordings were saved onto the computer for joint

analysis; the threshold was found and measurements peri threshold taken in increments of 3dB. The stimulus used to determine CAP responses was carefully calibrated prior to experimentation as outlined below. It is notable that the results presented in the thesis generally refer to the stimulus level as dB attenuation, thus the reader is directed to Figure 2.6 for the dB SPL equivalent.

The B&K 4134/4192 driver was coupled via a reciprocity closed calibration chamber B&K Type 4142 to a B&K 4134 microphone acting as the reciprocal calibrator. The B&K 4134 driver was then continuously driven by the TGA1230 at 20 volts peak to peak with the 200V bias voltage provided by the B&K 2804 power supply which also powered the 4134 microphone. A secondary output from the B&K 2804 was fed to the Hewlett Packard 35665A signal analyser, which gave a graphic display of signal intensity in dB SPL. The driver was calibrated for frequencies between 1 to 30 kHz and found to operate within the B&K specification. The maximal output values, in dB SPL, obtained at 8, 16, 24 and 30 kHz are shown in Figure 17.

The acoustic calibration was provided by a 1 kHz tone generator that delivered a 112 dB SPL tone (this device was calibrated by the National Physics Laboratory, Teddington, UK). The output of the B&K 2804 was also visually checked on an oscilloscope, which was used to inspect shaping, and symmetry of the stimulus waveforms.

Frequency (kHz)	Voltage (peak to peak) mV	dB SPL
8	35	92
16	36	92
24	10	83
30	10	84

Figure 17: ***Maximal driver output (dB SPL) after closed field stimulus at 8,16,24 and 30kHz***

3.8.3 Regimen for Auditory Brainstem Response recordings

Guinea pigs had an initial ABR recording before any surgery which was either a surgical control procedure, PLGA pellet insertion or PLGA with antibiotic insertion. ABR recordings were then repeated at 1, 2, 4 and 16 weeks for the following groups: biological control, surgical control, pellet control without antibiotics, pellet loaded with rifampicin and clindamycin. The guinea pigs tested with pellets loaded with either rifampicin or clindamycin separately were tested at 0, 2, 4 and 9-12 weeks. After the final ABR recording, the guinea pigs were killed by a Schedule one procedure of the Animals and Scientific Procedures Act (ASPA) 1986.

3.8.4 Auditory Brainstem Response recording

Weight was measured prior to each recording and anaesthetic calculations were made (see Table 6). Guinea pigs were anaesthetised subcutaneously and after 5 minutes was placed next to the recording apparatus. The animals were carefully positioned on a heated mat and a rectal thermometer recorded the core body temperature to ensure it remained between 37-38 degrees centigrade. This is important given that ABR measurements can be affected by core body temperature (Murakami *et al*., 1992). Three recording electrodes were positioned subcutaneously as indicated in Figure 14. Is was important to ensure that the electrodes were placed subcutaneously and not in the muscle layer as this increased the resistance and hence background noise of the signal and reduced clarity of the recording. A pair of curved forceps were used to assist this placement to pick up the skin and avoid placement in the muscular layer. The black preauricular reference electrode was carefully positioned anterior to the pinna as this was a hairless field and therefore relatively easy to achieve a good position.

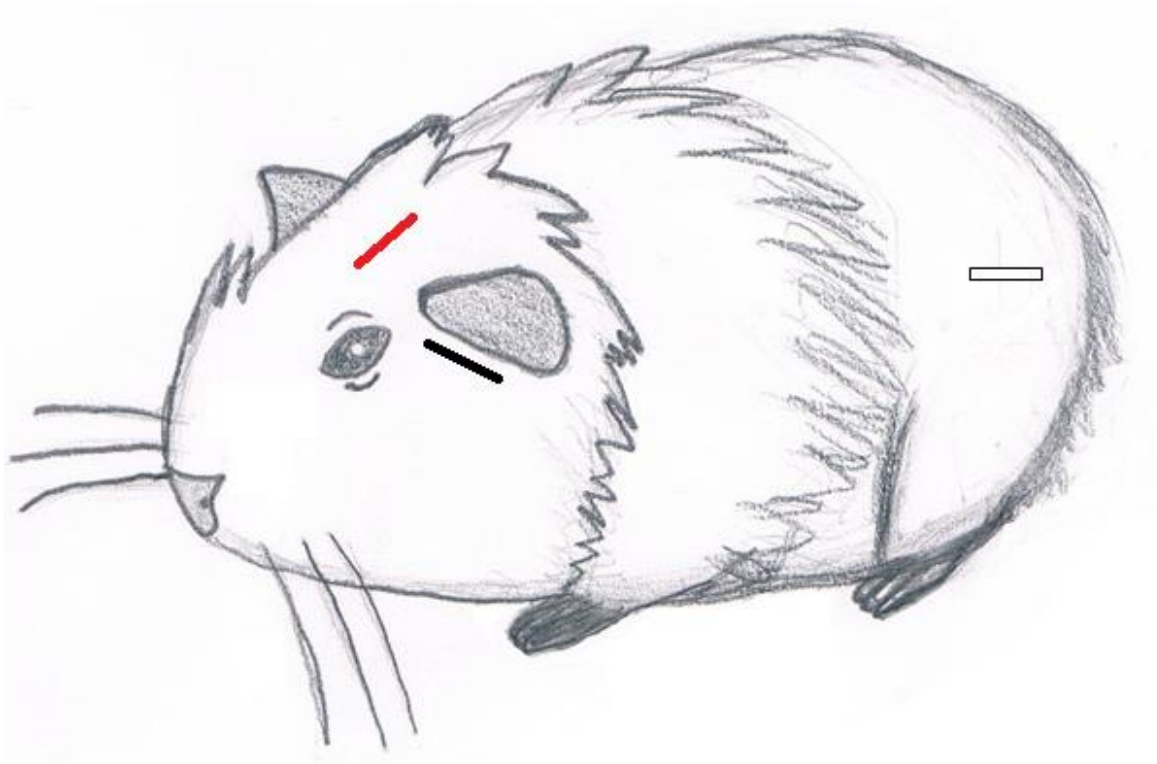


Figure 18: ***Image of three electrodes positioned on guinea pig (red: midline live electrode, black: pre-auricular reference electrode, white: rump ground electrode)***

To ensure that the electrodes were positioned correctly in the subcutaneous tissue, a resistance reading was made to ensure recordings were <4 kOhms. The microphone and its speculum attachment was then carefully placed into the left external auditory meatus of the animal to create a closed system and tight seal. Occasionally, a small amount of debris was required to be removed from the external auditory canal to minimal conductive losses. Whilst ABR recordings were being taken, the guinea pig was given oxygen via a face mask of 1litre/min and a pulse oximeter attached to the front left leg to monitor saturations of oxygen and heart rate during the recording. Oxygen levels are known to affect the accuracy of ABR recordings with hypoxia causing threshold elevation and increase in latency (Attias 1990).

3.9 Terminal anaesthesia and preparation of specimens

3.9.1 Schedule 1 Animal Scientific Procedures Act euthanasia

In accordance with Home Office Guidelines, guinea pigs were euthanized by decapitation after terminal anaesthetic administration. This was given in the form of intraperitoneal barbiturate called pentobarbitone at a dose of 5mls and was performed under NACWO supervision (see acknowledgements). The animals were monitored for signs of death including loss of respiration, loss of femoral pulses and rigor mortis. Half of the animals were then decapitated immediately and the middle ear bulla harvested and preserved by freezing for histology studies at a later date. The other half underwent perfusion-fixation.

3.9.2 Perfusion and fixation

Perfusion-fixation was performed on a downflow bench. As soon as death was established by palpating for asystole, the animal was pinned onto a cork mat and the abdominal skin incised. The peritoneal cavity was opened and the sternum identified. The sternum was quickly removed using dissection scissors and the immobile heart identified. The inferior vena cava was then divided and a perfusion catheter inserted into the left ventricle. A three way stop tap was then started and fluid for irrigation and then for fixation entered the circulation to perfuse and fix the animal's brain and surrounding tissues including the cochlea. The fluid consists of 4% paraformaldehyde in 0.1M PBS with a pH 7.2-7.4 and approximately 500 mls was run through over a period of 30 minutes for each animal. Signs of fixation which were observed included rigidity and extension of the limbs. Once the procedure has been completed, the head was decapitated and the middle ear bulla dissected out and stored in formalin for immunostaining and analysis at a later date.

3.10 Middle Ear Histology

After the animals were euthanized, the animals were perfused with fixative and the temporal bones stored in EDTA (Ethylenediaminetetra-acetic acid) for decalcification. Fixation can be influenced by autolysis of the tissues from intracellular enzymes and bacterial decomposition. The temporal bones were carefully labelled and were stored in a freezer at minus 18 degrees celsius.

For preparation of the histological slides, credit is given to Dr Jennifer Edwards (see acknowledgements). The stages involved in preparation of the slides and the steps are described below and were observed. This work was carried out in the MRC (Medical Research Council) Building at Leicester University.

Three of the temporal bones were embedded in wax and sliced using a microtome to create slides to visualise and study the middle ear histology. Details of the slide preparation are given in sections 3.10.1- 3.10.7. One in twenty slices were taken every five microns. The slides were then studied and analysed for evidence of middle ear chronic inflammation and the pellet remnants were also assessed.

3.10.1 Dehydration

After fixation, temporal bones were dehydrated to allow for paraffin wax penetration. Immersion in 70% ethyl alcohol prior to dehydration, assists the process.

3.10.2 Clearing

This stage treats the specimens with an agent, xylene, to allow the tissue blocks to be mixed with both alcohol and paraffin wax. This step alters the refractive index of the tissues rendering it almost transparent.

3.10.3 Wax Impregnation

The paraffin wax used had a melting point of 57 ^{o}C (TCS Biosciences LTD). The temporal bones were carefully orientated during immersion allowing blocks to form on solidification at room temperature.

3.10.4 Slicing

The specimen blocks were carefully sliced in 1: 20 with 5 µm between each slice.

3.10.5 Removal of paraffin

The paraffin was removed using xylene solvent and then washed away with 90% alcohol as xylene is immiscible with aqueous solutions. A wash with distilled water was then required for each slice.

3.10.6 Staining

Haematoxylin and Eosin (H and E) staining was selected for the specimens. Haematoxylin is a basic dye which stains the nucleic acids in the specimens and Eosin is and acidic dye which stains the cytoplasm. This combination is the most commonly used staining method allowing for the histology of the tissues to be studied using conventional light microscopy.

3.10.7 Mounting

A coverslip was carefully placed over the specimens to preserve and protect the tissue sections with a small quantity of mounting medium DPX distrene – tri cresyl phosphate made up in xylene.

3.11 Cytocochleograms

After the temporal bones in the guinea pigs were isolated post perfusion-fixation, they were treated with 10% EDTA decalcifying agent (made in 0.1M PBS pH 7.2-7.4) with storage at 4^{o}c and rotation over four weeks.

Once decalcified, the temporal bones were kept in PBS at 4 ^{o}c and after an interval, were dissected to isolate the cochleas. Dissection was supervised by Professor Furness using micro instrumentation and the use of micro blades. This work was undertaken at Keele University (please see acknowledgements). These were made using slices of razor blades mounted on cocktail sticks using superglue adhesive (cyanoacrylate). The technique of en-bloc cochlea dissection and then isolation of the cochlea turns separately was found to create the greatest yield in terms of hair cell preservation. Once the turns had been dissected and the excess tissue trimmed away, the specimens were mounted on a slide under a coverslip. Care was taken to ensure that the specimens were prevented from drying out and that Reissner's membrane was upright to ensure correct orientation of the specimens.

Once the slides were mounted, using a Nomarski microscope, the hair cells both outer and inner were counted in rows. The presence of a cell was determined by viewing an intact apical plate and stereocilia (Mahendrasingham *et al*., 2011). A template was used to mark off the absent hair cells. This was provided by Professor Furness and all analysis took place under his supervision at Keele University. The cochlea were examined quantitatively allowing a comparison between OHC and IHC in the apex, middle and basal turns of the cochlea (Furness *et al*., 1990). This was done sequentially, starting at the apex and moving in a clockwise manner to the base.

Cytocochleograms were constructed by plotting the percentage of missing IHC or OHC as a function of percentage distance from the apex of the cochlea. When hair cells could not be counted, the size of the gaps were estimated and recorded.

In addition, immunofluorescence was performed in the University of Leicester to demonstrate the hair cells. After specimen dissection of the individual cochlea turns, samples were treated with 0.25% Triton dissolved in PBS for 30 minutes and repeated twice. A mixture of PBS and Triton 0.25%, Phalloidin 2.5% and DAPI (4', 6-diamidino-2-phenylindole) 4 micrograms (with a concentration of 5mg/ml). Specimens were left shielded from the ambient light with a foil cover for over 2 hours. After this exposure, washing the specimens in PBS for 10 minutes was required before mounting on a coverslip. The specimens were visualised under an immunofluorescence microscope and images were captured.

3.12 Pellet manufacture and preparation

Pellet design, manufacture and preparation has been undertaken at the University of Nottingham Department of Trauma and Orthopaedics under the supervision of Professor R Bayston and Professor K Shakesheff. This is recognised in my acknowledgements. The details of the pellet manufacture are also published (Daniel *et al*., 2012).

Pellets are made with PLGA 50:50 56kDa micro particles with pluronic F127 (20%) solution. The ratio of the PLGA to the gel is 1 to 0.8. The oil/water emulsion method was used to prepare micro particles with 1g of PLGA was dissolved in 6.7 mL of dichloromethane (DCM) (Sigma-Aldrich, Gillingham, UK) in a glass container, and added to 200 mL of 0.3% polyvinyl alcohol (PVA) (Sigma-Aldrich, Gillingham, UK). The mix was homogenised using a Silverson L5M mixer for 2 minutes at 9000RPM (Silverson Machines, Chesham, UK) (Silverson 2010).

The emulsion, at room temperature, was then left stirring overnight (16 hours) with a 50 mm glass flea on Variomag Poly magnetic stirrer (Variomag, Daytona Beach, USA) set at 300rpm, to allow DCM to evaporate. The following day, the PVA / PLGA emulsion was aliquotted into 50 mL containers, and centrifuged at 3000 rpm for 5 minutes (MSE Mistral 1000, London, UK). The supernatant was discarded, and the particles re-suspended in de-ionised water and centrifuged again.

The step was repeated until the samples had been centrifuged three times in water. The resulting PLGA suspension was filtered through a 40µm filter to remove any large clumps, frozen in liquid nitrogen and then freeze dried (ModulyoD, Thermo Electron

Corporation, Waltham, MA USA) prior to storage at minus 20°C. The size of the particles was determined by laser diffraction with Coulter LS230 particle size analyser (Beckman Coulter, High Wycombe, UK, solid state 780nm laser) using the Garnett optical formula. Using this method, the mean particle diameter size obtained was 12.31 μm, median 11.70 μm and mode 15.37 μm.

The pellets were produced by mixing UV-sterilised PLGA micro particles with a carrier gel and antibiotics, placing the mix into a Polytetrafluoroethylene mould designed to produce pellets 3mm long and 2.5 mm diameter, with a central 1mm diameter hole (the result of a stainless steel pin); the pellets thus had the appearance of a small tube, with the central hole designed to prevent airtight obstruction of the Eustachian tube should the pellet move in the middle ear following placement. The pellets were sintered at 60°C for 16 hours, taken out of the mould, and sterilised again with UV (ultraviolet) light.

The pellets were composed of PLGA (Lakeshore Biomaterials, Birmingham, USA) with 2% high viscosity sodium CMC (Blanose®, Aqualon / Hercules, Widnes, UK) or 20% Poloxamer pluronic F127 (Sigma-Aldrich, Gillingham, UK) (the PLGA to gel ratio was 1:0.8) and antibiotics rifampicin (Codman, Wokingham, UK) and clindamycin (Sigma-Aldrich, Gillingham, UK) at a high concentration of 4% (rifampicin) and 24% (clindamycin) of the PLGA weight.

The antibiotics added to the pellets are rifampicin from Sigma and clindamycin from Fluka. The doses of rifampicin and clindamycin used are equivalent to 10^6 MIC (minimum inhibitory concentration) and are sufficient to achieve eradication of biofilms of Staphylococcus Aureus. These are clindamycin 2.10^{-4}g; rifampicin 2.10^{-5}g.

The pellets underwent E-beam sterilisation and were vacuum packed prior to transfer on ice to the University of Leicester where the *in vivo* work was carried out. The pellets were stored in a fridge at 4°c and individually labelled until implantation in the animal models.

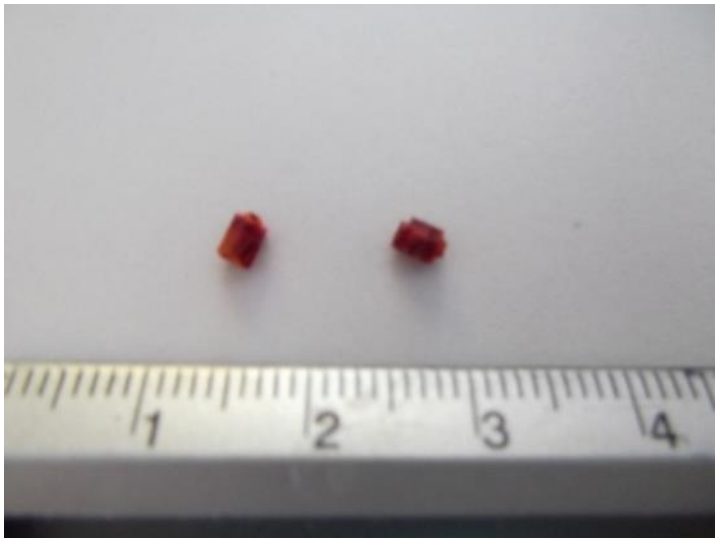


Figure 19: ***Image of two pellets laden with rifampicin with cm scale***

The concentrations of the pellets can be calculated with the assumption that the volume of each pellet is cylindrical and is calculated as therefore 14microlitres.

In this volume there is a molar concentration of rifampicin and clindamycin as follows:

Rifampicin 823 g/mol

823 g in 1M in 1litre

1152g is 1.4M in 1 litres

1152g is 1M in 1.4 litres

1152g is 1M in 1400 000 000 microlitres

There is 2 x 10^{-7} g in 14microlitres

So divide 1152g by 10-9 to get how many grams for 1M in 14microlitres

=1.15 x 10-6g for 1M in 14microlitres

The concentration is 1.8mM for 2.1 x 10^{-5}g

Clindamycin 425g/mol

425g in 1M in 1litre

595g is 1.4M in 1 litre

There is 2 x 10^{-4}g in 14 microlitres

So divide 595g by 10-9 to get how many grams for 1M in 14 microlitres

=5.95 x 10-7g for 1M in 14 microlitres

The concentration is 35.3mM for 2.1 x 10^{-4}g

The doses of rifampicin and clindamycin used in combination are the same as when the antibiotics are individually loaded onto the pellets.

Summary

Rifampicin concentration is 1.8mM for 2.1 x 10^{-5}g

Clindamycin concentration is 35.3mM for 2.1 x 10^{-4}g

3.13 Cadaveric experiments

Ten temporal bones were collected from five adult male guinea pigs of Dunkin-Hartley strain. Their weight ranged from 470 - 558g with a mean of 524g. The guinea pigs were being used for cardiology research carried out at the University of Leicester. After they were killed by a schedule one procedure, guinea pig heads were collected. No ethical approval was required for this study. Guinea pig cadavers were studied and dissected under the microscope (KAPS DP Medical) and anatomical measurements were made using a specially designed sliced transparent ruler in millimetres.

Simulation of surgical access to the middle ear was performed assessing the transtympanic access and bulla approaches (both anterior and posterior). Volume measurements were undertaken using micro-syringe to inject IMS (Industrial Methylated Spirit) via the ventral bulla and then the fluid level was seen at the tympanic membrane where a myringotomy had been made. IMS was chosen to eliminate air bubbles in the bulla. This was repeated in triplicate and averaged. The ossicles were identified and also weighed.

Ten temporal bones were also collected from five adult male Wistar rats. They were also being used for cardiology experiments at the same site. Again, no ethical approval was required for this anatomical comparison study using cadaveric specimens. Measurements were again made under the microscope, volume measurements using the same technique and the ossicles were weighed.

Photograph of cadaveric images were taken using Image J computer programme.

3.14 Statistical analysis

Data was arranged in Excel spreadsheets for analysis. Data was analysed by one tailed paired t-tests with a *priori* assumption of threshold increase. Significance was set at $p<0.05$ (Bonferroni correction). This was used to analyse ABR threshold elevation.

Repeated measures ANOVA on all data sets was not justified due to changes in variance post week 0 (week 0 starting on the day of initial ABR recording). Holm-Bonferroni correction was made to minimise a Type 1 error given the multiple comparisons made using t-tests (Holm, 1979).

Friedman's two way analysis of variance was undertaken using software programme Minitab 17. This was selected as the most appropriate test for analysis over time of the median values and was selected for amplitude and latency analysis of ABR due to the variability seen.

Chapter 4: Development of the animal model: results of cadaveric work comparing the middle ear of the guinea pig and rat

4.1 Anatomical comparison

4.1.1 External relations of the temporal bone

The guinea pig temporal bone is located at the posterior-inferior aspect of the skull and is composed of the four main components: squamous, tympanic, zygomatic and mastoid. The zygomatic arch articulates with the temporomandibular joint.

The tympanic section is composed of the tympanic ring, ventral and dorsal tympanic bulla. The ventral bulla is the dominant air space in the guinea pig middle ear and articulates with the smaller dorsal bulla via the incudomalleal complex. The smaller dorsal bulla is analogous to the epitympanum in the human.

The rat temporal bone has a similar basic structure and is also found in the posterior inferior part of the skull. There is only one middle ear bulla compartment in the rat, unlike the guinea pig which has both the dorsal and ventral bulla.

4.1.2 Outer ear:

The guinea pig pinna has a characteristic round shape with a consistent tragal/anti-tragal to widest diameter of 29mm. The range of this measurement was 26–30mm (Table 6). The outer ear canal is cartilaginous with a curvature which could be straightened by pulling the pinna in a posterior dorsal direction to visualise the tympanic membrane under the microscope.

The ear canal narrows to its smallest diameter of 3mm measured obliquely at the bony canal opening. After this point, it widens again to reach the tympanic membrane. The mean total length of the ear canal is 10.2mm (range 10-11mm) and the bony length is 3mm. The view of the guinea pig tympanic membrane from the ear canal and hence a transtympanic approach is limited to the malleus handle and the superior part of the annulus only (Table 6).

In contrast, the rat's outer ear has a smaller pinna with a mean diameter of 20.2mm (range 20-21mm). Again this was measured from the tragal/antitragal junction to the point of greatest distance on the pinna. The rat's ear canal has a more consistent diameter in comparison with the guinea pig ear canal as it does not have the fluting aspect getting narrower and then widening again before reaching the tympanic membrane. The narrowest point of the rat EAC, however, is at the bony canal rim measuring 2mm in diameter. The view of the tympanic membrane under the microscope is greater than that of the guinea pig allowing a greater view of the tympanic membrane due to the consistent diameter and lack of fluting.

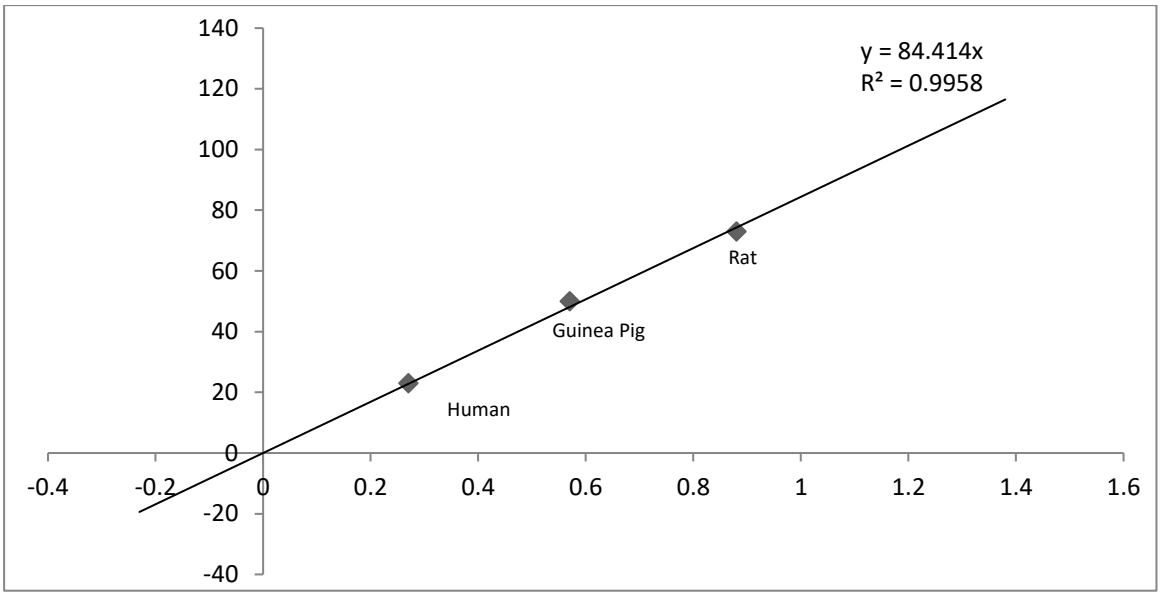
Animal	Mean pinna diameter /mm	Mean external auditory canal length/mm	Mean bony canal diameter/mm	Mean bony canal length/mm	Area of tympanic membrane /mm^2
Guinea pig n=10	29.0	10.2	2.9	3.0	35.2
Rat n=10	20.2	8.2	2.0	1.0	10.7

Table 6: ***Measurements of the external auditory canal and tympanic membrane in the guinea pig and rat***

Animal	Anterior-posterior distance of bulla/mm	Malleus handle to hypotympanum /mm	Malleus handle to epitympanum/mm	Malleus handle to round window/mm	Malleus handle to Eustachian tube/mm
Guinea pig n=10	10.0	7.0	3.0	1.8	7.0
Rat n=10	6.9	4.0	1.35	1.3	2.75

Table 7: ***Measurements of the ventral bulla of the guinea pig and middle ear of the rat.***

Measurements of the mass of the guinea pig malleus and incus in combination can be plotted as a function of the inverse root to the power 3 against the highest frequency in kHz guinea pigs species can hear (Figure 20). There is a linear correlation seen when other malleus and incus measurements are made and plotted against highest frequency of hearing in kHz for rat (Salih et al., 2001) and human species (Hemilä et al., 1995).



X axis: $1/\sqrt[3]{}$malleus and incus mass (mg) Y axis: highest frequency of hearing /kHz

Figure 20: ***Graph to show the relationship between the highest frequency of hearing (Hz) and mass of malleus and incus (mg) for different species: human, guinea pig and rat***

4.1.3 Middle ear:

The tympanic membrane of the guinea pig has a diameter of 6.9mm (range 6.5-7mm) which was measured using a millimetre gauge ruler from the inner mucosal surface after opening up the ventral bulla.

The ventral bulla is the main air space of the middle ear and has a mean volume of 119 microlitres. The dimensions of the ventral bulla are shown in Table 7. The anterior posterior diameter is 13mm and the distance from the malleus neck to the floor of the hypotympanum 7mm. The width is variable along the length with the cochlear positioned posteriorly and the ossicular chain on the medial wall.

The ossicular chain in the guinea pig unusually has a fused malleus and incus and a separate stapes. The mass of the incudomalleal complex is 5.4 mg (range 5.0mg-5.9mg).

The cochlear impression is clearly seen in the ventral bulla with the round window and oval window via the stapes footplate clearly identifiable. This is the anatomical connection from the middle to the inner ear and hence can be accessed to facilitate recording or drug delivery to the inner ear.

In contrast, the rat tympanic membrane has an oval shape with a diameter of 4mm. Again this was measured from the inner mucosal surface after opening up the ventral bulla. The rat middle ear has one main compartment, unlike the guinea pig which has both the ventral and dorsal bulla. The rat middle ear has a volume of 40 microliters. The anterior – posterior diameter is 6.9mm and the distance from the malleus neck to

the hypotympanum 4mm. The promontory is less defined. The dimensions of the rat middle ear bulla are shown in Table 7.

4.2 Surgical approaches to the middle ear

4.2.1 Transtympanic

Transtympanic access to the middle ear in the guinea pig is possible for surgical implementation down the External Auditory Canal (EAC) but is limited by 3mm diameter at its narrowest point. This constriction makes manipulation of instruments and hence surgery difficult or impossible. The tympanic membrane area accessible down the transtympanic approach is limited to the superior quadrant. With the benefit of cadaveric work, transtympanic injections and myringotomy are possible although technically challenging. Insertion of a mini Shah grommet (Adept medical) with a diameter of 1.5mm would be feasible (Adept medical) but not a regular size Shah grommet with a diameter of 2.5mm.

Instrumentation down the EAC of the guinea pig and surgical manipulation of the ossicles would be very difficult. Due to the narrowing and then funnelling out of the EAC, raising a transtympanic flap would also not be possible to allow access to the middle ear for ossiculoplasty, myringoplasty or drug delivery routes to the middle ear.

The rat EAC does not narrow in the same manner as the guinea pig, but it has an overall narrower diameter of 2mm. A relatively larger area of the tympanic membrane is accessible in comparison with the guinea pig, but restricted access is again problematic. Instrumentation and insertion of ventilation tubes down the EAC would be technically challenging in the rat due to the narrow dimensions.

4.2.2 Retrobulla

In the guinea pig, a post auricular incision and removing post auricular muscle attachments would expose the ventral bulla posteriorly. This would allow a hole to be made in the bulla wall and visualise the cochlea and access the round window. Catheter insertion and sampling of the perilymph could be done via this route (Selvadurai *et al*., 2000). The distance from the posterior ventral bulla to the anterior becomes constricted between the cochlea and the tympanic membrane and hence access to the anterior aspect of the ventral bulla from this posterior approach is limited.

In the rat model, the retrobulla approach also allows exposure to the cochlea and round window. However, there is less constriction between the cochlea and tympanic membrane at its narrowest point allowing a conduit from posterior to anterior bulla.

4.2.3 Anterobulla

This approach to the middle ear would be challenging due to the proximity of the temporomandibular joint to the anterior aspect of the ventral bulla. Disruption of this joint would prove to be disabling to the animal post operatively especially regarding feeding. Access can be achieved via an incision in the neck and dissection. By following the posterior belly of digastric superiorly to its insertion at the styloid process, the adjacent middle ear bulla can be identified (Pinilla *et al*., 2001). The anterior bulla wall can be breeched and access to the ventral bulla gained. Other important structures which should be recognised and preserved include the facial nerve, facial vein and branches of the internal carotid artery.

The antero-bulla approach in the guinea pig is more technically difficult than the rat model because of the larger mandible and the thicker anterior bulla wall. In both the rat and guinea pig animal models this approach is possible allowing access to the Eustachian tube and ventral bulla.

Access to the ME bulla via the anterobulla approach allows careful placement of pellets away from the ossicular chain. This situation differs from transtympanic access where the pellet is “posted” through a myringotomy. This can results in increased variation in the pellet’s resting position in the ME.

4.2.4 Discussion of cadaveric work

With the fixed pellet dimensions, both the guinea pig and rat models are unsuitable for transtympanic insertion of the pellet via a myringotomy into the middle ear as would be the future potential clinical scenario in patients. This is precluded in the rodent animal models due to the diameter of the pellet at 2.5mm and the relative diameters of the bony ear canals of the rat and guinea pig at 2.0mm and 2.9mm respectively.

The guinea pig model is the preferred to the rat model because of the larger bulla volume of 119 microlitres compared to 40 microlitres. Insertion of the pellets into the ventral bulla via a fenestration of the anterior wall allows careful placement away from the ossicular chain and in a consistent location of the ventral bulla which is important for experimental ototoxicity testing. Minimising variables between experiments including the position of the pellet is important to standardise testing. This can be more readily achieved through the surgical anterobulla approach.

The anterobulla approach has technical challenges due to the access via a cervical incision and careful dissection and avoidance of structures including the facial nerve, vein and branches of the carotid artery. The temporomandibular joint is also at risk of potential damage and should be carefully preserved. The surgical approach and its success can be reviewed from the post-operative complication rate and the response of the surgical control groups to surgery.

The guinea pig model is suitable when considering its similarities with the human temporal bone. There is a ME compartment – the bulla which contains the ossicles and communicates with the IE. The guinea pig ossicular chain is fused with the incudo-malleal complex, whereas the human has three separate ossicles. This is an anatomical difference but is not considered to impact on the guinea pig use as an animal model. The human ME communicates with the mastoid air cell complex for aeration in a similar manner to the guinea pig tympanic bulla connecting to the mastoid air cell system (Goksu *et al*., 1992). These anatomical similarities between the human and guinea pig temporal bones emphasise the suitability of using guinea pigs as an animal model in experiments assessing ME pellet insertion.

Chapter 5: Results of Auditory Brainstem Responses

5.1.1 ABR threshold results analysis

Data was analysed by one tailed paired t-tests with a *priori* assumption of threshold increase. Significance was set at $p<0.05$ (Bonferroni correction). Repeated measures ANOVA analysis on all data sets was not justified due to changes in variance post week 0 which is defined as the initial ABR recording. The Holm-Bonferroni correction was also applied to the data.

For these three treatment groups, biological control, surgical control and PLGA pellets (see Figures 21, 22 and 23), the mean ABR thresholds at week 0 were directly comparable falling between 35-52 dB SPL.

5.1.2 Changes in ABR threshold over 8-30 kHz over weeks 0-16: biological control group

Figure 21 shows the changes in threshold for the Biological, or time Control Group. In this non-intervention group without surgery, mean ABR thresholds over 8-30 kHz remained stable with relatively low variability. Mean thresholds from week 0 which is the day of initial ABR recording varied from -1 to 6 dB. Only one excursion of 6dB at 30 kHz reached significance at week 16 and was not considered to be of marked biological significance.

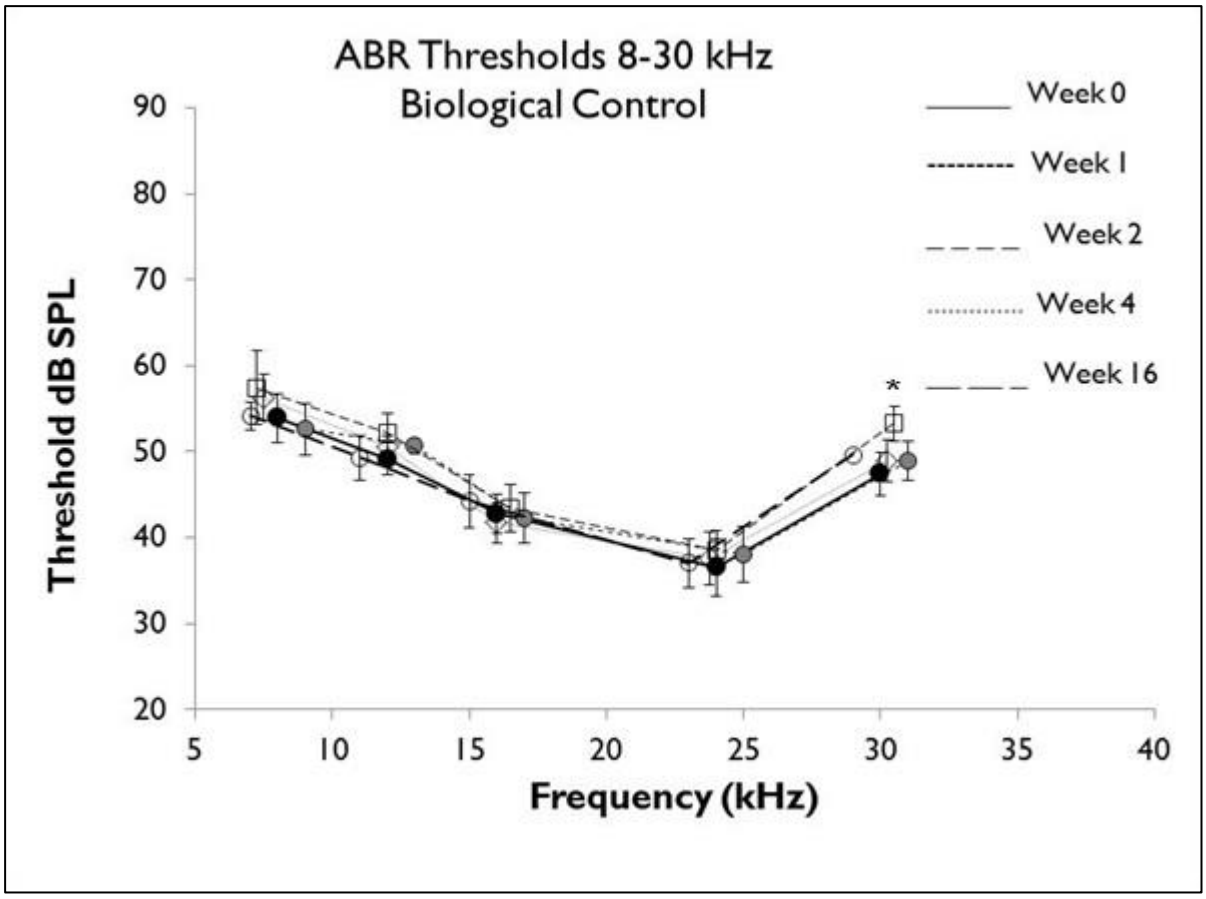


Figure 21: ***Biological Control showing no significant changes in mean ABR thresholds over 0-16 weeks***

5.1.3 Changes in ABR threshold over 8-30 kHz over weeks 0-16: surgical control group

Figure 22 shows the changes in threshold for the surgical control group. ABR thresholds over 8-30 kHz showed greater variance post week 0 at the onset of ABR recording. Mean ABR thresholds from week 0 varied from 1 to about 10 dB. Only one excursion of 10dB at 16 kHz reached significance which would be considered of biological significance. By week 16 mean thresholds were within 1 to 4dB of those at week 0 when ABR recording commenced.

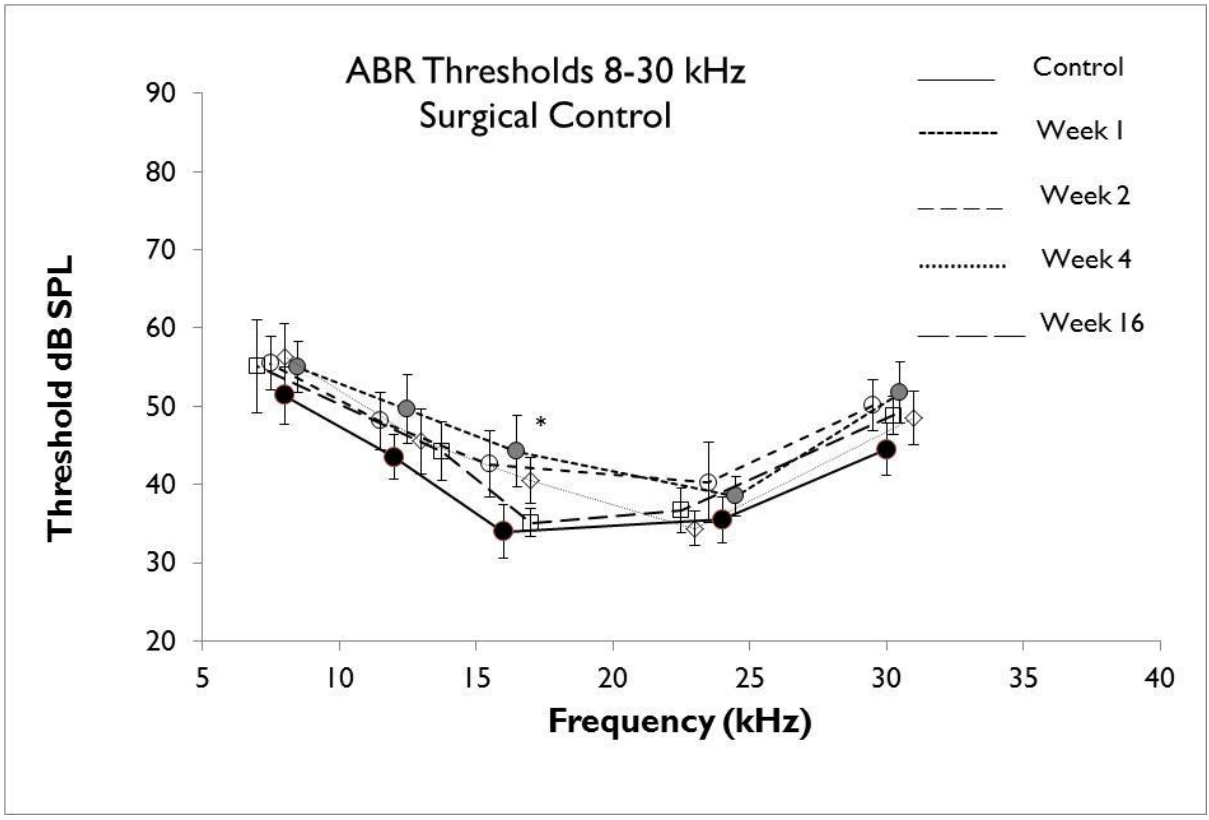


Figure 22: ***Surgical Control group showing only one significant change in ABR threshold at 16 kHz at week 1 (marked with a *).***

5.1.4 Changes in ABR threshold over 8-30 kHz over weeks 0-16: PLGA and pluronic pellet control group

Figure 23 summarises threshold changes for the PLGA pellet Group. Mean ABR threshold shifts over 8-30 kHz fell between -1 to about 12 dB. Whilst some elevations at 24-30 kHz were significant, only one was above 10 dB (12.3 dB) at 30 kHz for week 16 (p=0.016).

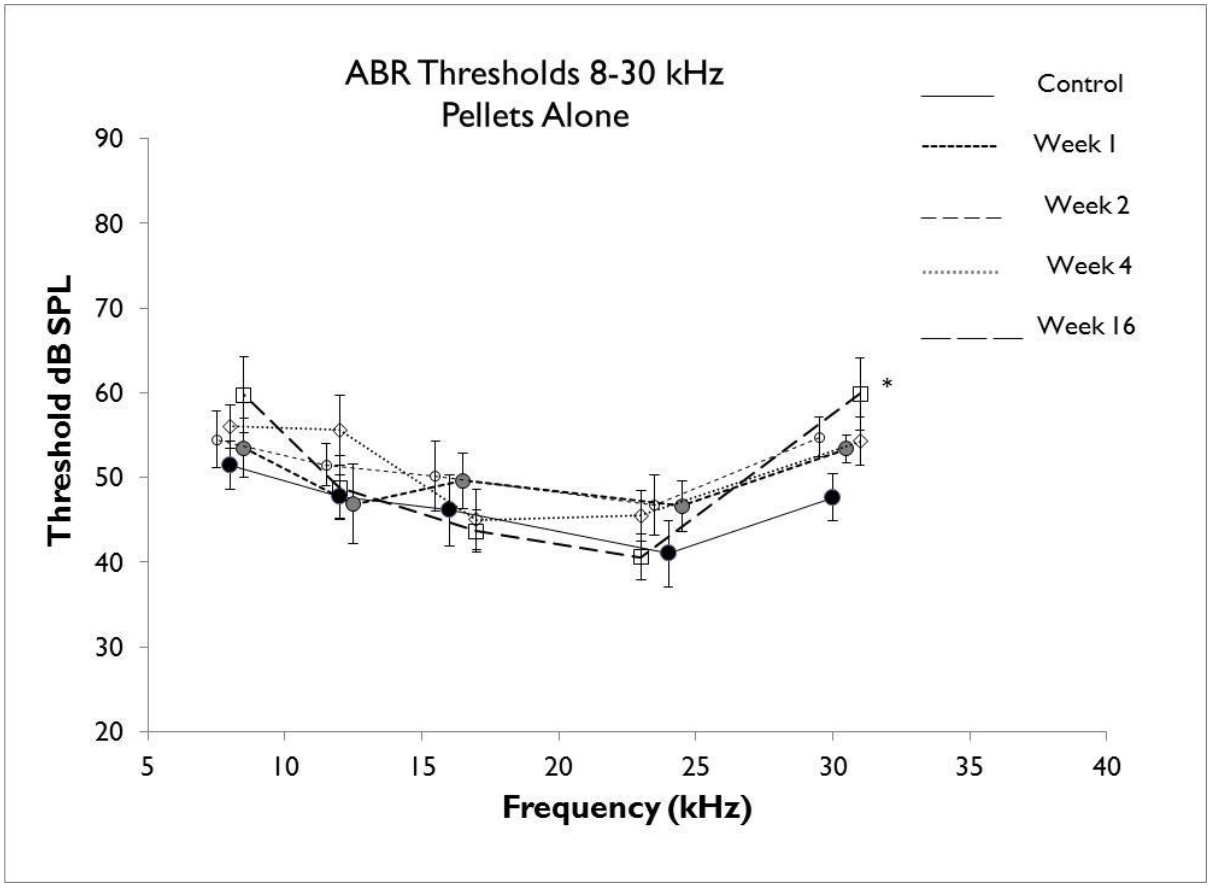


Figure 23: ***PLGA and pluronic Pellet alone showing one significant change in threshold of 10 dB at 30 kHz at week 16 (marked with a *)***

5.1.5 Changes in ABR threshold over 8-30 kHz over weeks 0-16: Pellets with rifampicin and clindamycin in combination

Figure 24 shows the highly significant changes in mean ABR threshold across virtually all frequencies over weeks 1-16. A number of unusual features are present in these threshold elevations which are discussed at the different time points.

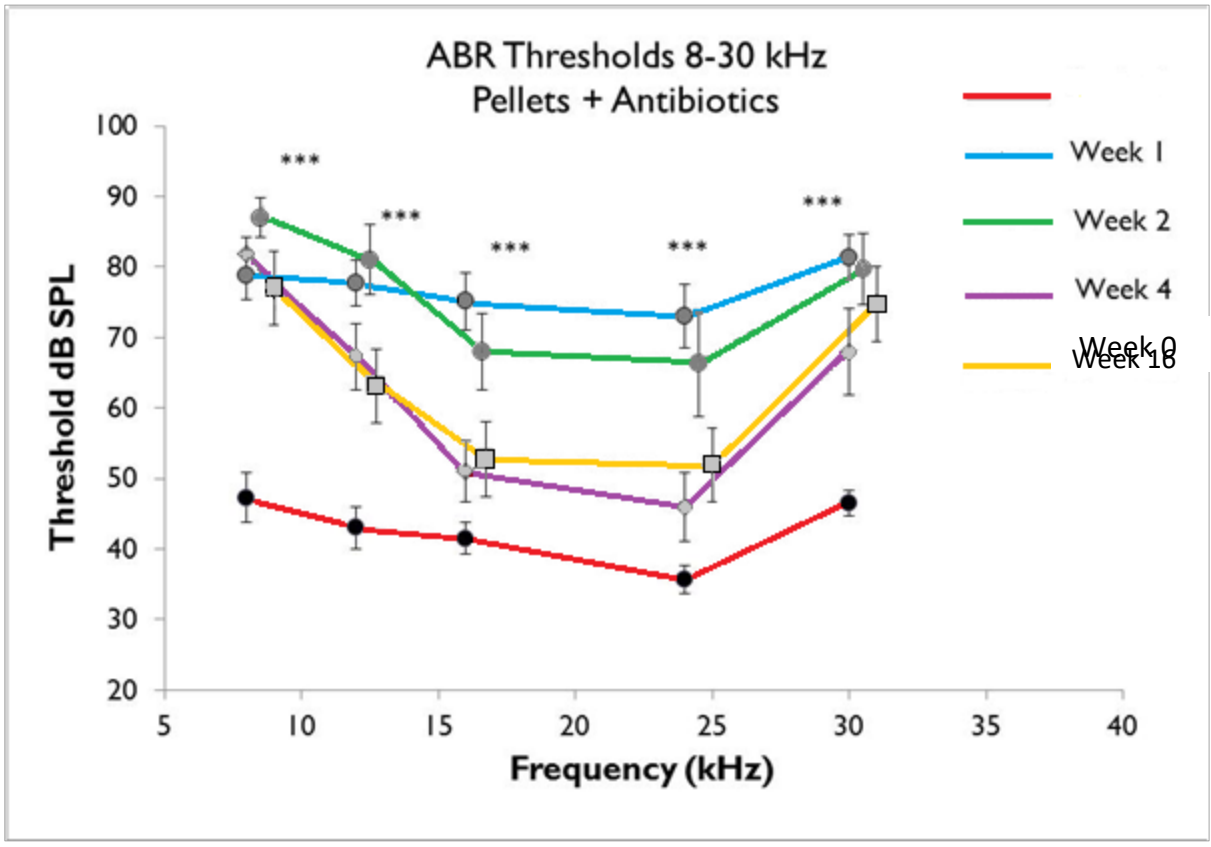


Figure 24: ***Rifampicin and clindamycin loaded PLGA and pluronic pellets. Highly significant changes at virtually all frequencies over weeks 1-16. Not all significance levels indicated.***

Week 1

Highly significant (P< 0.002 – 0.0001) threshold elevations of between 30-40 dB are seen at all frequencies at 1 week post pellet implantation which occurred initially at week 0. The pattern of elevation is unusual as it affects all frequencies. This would be

considered an atypical pattern of loss for ototoxicity as higher frequencies are typically affected more than lower frequencies.

Week 2

Mean threshold elevations remain highly significant across all frequencies of between 25-40dB at week 2 post pellet implantation. There is some evidence of slight recovery at 16-24 kHz.

Week 4

In Figure 24 at week 4 there appears more marked recovery over 12 -24 kHz with mean threshold elevations of between 10-25 dB. The mean elevations of about 10 dB at 16 and 24 kHz are statistically significant (p=0.05 and 0.07). However, mean ABR thresholds at 8, 12 and 30 kHz remain clearly elevated between 20-35 dB.

Week 16

Significant threshold elevation ranges between 11-30 dB over 8-30 kHz at week 16. Elevation at 16-24 kHz was significant (p=0.019 – 0.005). The largest elevations of nearly 30 dB were seen at 8 and 30 kHz. The unusual pattern of threshold elevation affecting low and high frequencies is maintained.

5.1.6 Changes in ABR threshold over 8-30 kHz over weeks 0-16: pellets with rifampicin tested separately

Following the findings with the antibiotics in combination, the effect of the PLGA and pluronic pellets loaded separately with either rifampicin or clindamycin was examined. This was performed in two separate experimental sittings: 2012 and 2013. There was

an altered anaesthetic regimen for experiments performed in 2013 due to the lack of availability of Hypnorm (see section 3.6.4 anaesthetic regimen 4: Hypnorm substitution).

Figure 25 shows the results for rifampicin alone at weeks 0, 2, 4 and 12. At week 2, thresholds were elevated by 20-30 dB across all frequencies. Notwithstanding these elevations the variability means that post Bonferroni correction, significance was marginal (p=0.031 to 0.083) apart from at 8 kHz where the 28 dB elevation was highly significant at p =0.006. Over experimental weeks 2-12, mean thresholds gradually show recovery finally falling to within 6-15 dB of initial values at week 0. These did not reach significance, but are considered likely to be biologically real. Again, the pattern of threshold elevation is of interest as it involves all frequencies.

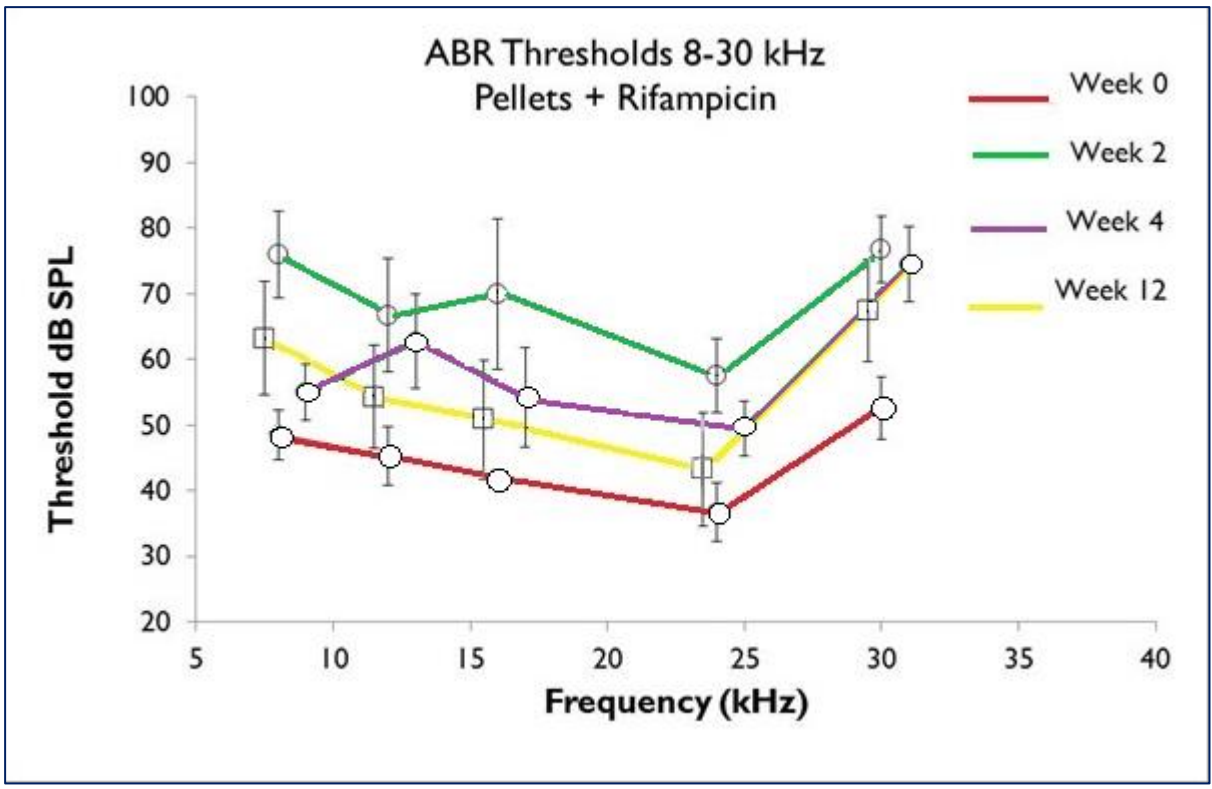


Figure 25: ***PLGA and pluronic pellets loaded with rifampicin alone (n=8).***

5.1.7 Changes in ABR Threshold over 8-30 kHz over Weeks 0-16: pellets with clindamycin tested separately

Figure 26 shows the results for clindamycin alone (n=8). Mean elevations at week 2 were between 15-30 dB. Only one value reached significance at week 2, 30kHz with a mean threshold elevation of 32dB.

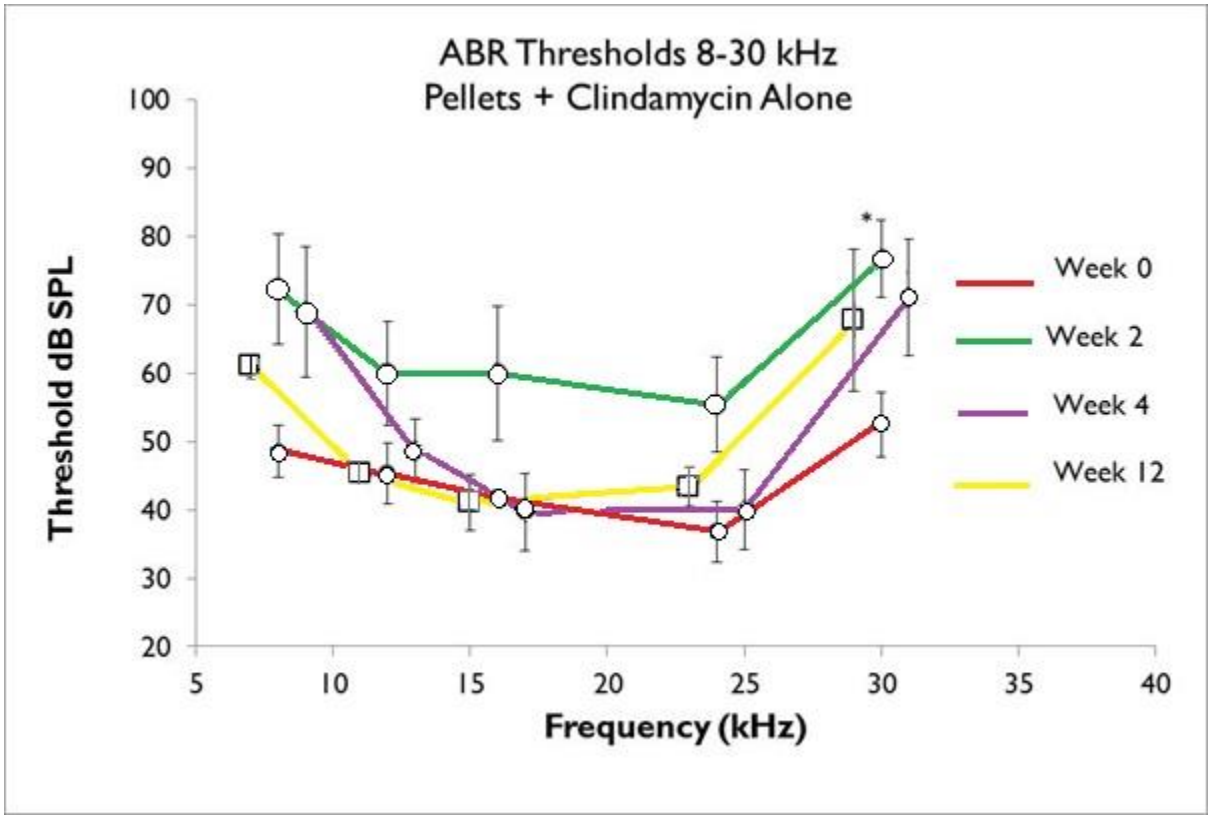


Figure 26: ***PLGA and pluronic pellets loaded with clindamycin alone (n=8).***

Over weeks 2-12, mean thresholds again gradually demonstrated recovery reaching within approximately 0-25 dB of initial week 0 values. These again were not significant. The 'U' shaped elevation pattern of thresholds is also apparent with clindamycin with relative sparing of mid frequency values seen.

5.1.8 Holm-Bonferroni correction for the ABR threshold data

Multiple comparisons were performed on the ABR threshold data and therefore the Holm-Bonferroni correction was applied to the p values. This was done to minimise the risk of a Type I error.

Tables 8-13 show the Holm Bonferroni corrections applied to the ABR threshold data. There is only sporadic rejection of the null hypothesis which is highlighted red except for Table 11 which shows the null hypothesis rejected for most of the p values. Overall, this statistical correction therefore confirms the significance of the results from the t tests with no significant threshold elevation seen in the control groups and pellet with either rifampicin or clindamycin separately. There is significant threshold elevation seen in the pellet loaded with both rifampicin and clindamycin across all thresholds at weeks 1 and 2 with some low frequency recovery at week 16.

BC	Frequency				
Week	8kHz	12kHz	16kHz	24kHz	30kHz
1	0.040 2	0.070 1 >0.0125	0.950 4	0.534 3	0.070 1 >0.0125
2	0.088 3	0.070 1 >0.0125	0.350 3	0.090 2 >0.167	0.150 2
4	0.030 1 >0.0125	0.550 3	0.169 2 > 0.167	0.686 4	0.250 4
16	0.579 4	0.870 4	0.002 1 <0.0125	<0.001 1 <0.0125	0.210 3

Table 8: ***Biological control threshold p values and the Holm Bonferroni correction. Values where the null hypothesis is rejected are highlighted red.***

SC	Frequency				
Week	8kHz	12kHz	16kHz	24kHz	30kHz
1	0.084 2	0.227 3	0.677 3	0.036 1 >0.0125	0.233 3
2	0.864 4	0.908 4	0.365 1 >0.0125	0.732 4	0.115 2 >0.0167
4	0.052 1 >0.0125	0.164 1 >0.0125	0.553 2	0.138 2	0.233 3
16	0.334 3	0.225 2	0.702 4	0.398 3	<0.001 1 >0.0125

Table 9: ***Surgical control threshold p values and the Holm Bonferroni correction. Values where the null hypothesis is rejected are highlighted red.***

P	Frequency				
Week	8kHz	12kHz	16kHz	24kHz	30kHz
1	0.603 4	0.842 4	0.129 1 >0.0125	0.177 3	0.131 4
2	0.277 3	0.273 2	0.365 2	0.029 1 >0.0125	0.023 1 >0.0125
4	0.137 1 >0.0125	0.111 1 >0.0125	0.656 4	0.070 2	0.028 2
16	0.142 2	0.814 3	0.605 3	0.941 4	0.033 3

Table 10: ***Pellet control threshold p values and the Holm Bonferroni correction. Values where the null hypothesis is rejected are highlighted red.***

PA	Frequency				
Week	8kHz	12kHz	16kHz	24kHz	30kHz
1	0.00004 1 <0.0125	0.000012 1 <0.0125	0.0011 1 <0.0125	0.0009 1 <0.0125	0.00008 1 <0.0125
2	0.0003 3<0.025	0.001 2<0.0167	0.005 2<0.0167	0.005 2<0.0167	0.0009 3<0.025
4	0.00015 2<0.0167	0.007 3<0.025	0.101 4	0.136 4	0.0136 4
16	0.001 4	0.009 4	0.037 3>0.025	0.010 3<0.025	0.0008 2<0.0167

Table 11: ***Pellet with rifampicin and clindamycin threshold p values and the Holm Bonferroni correction. Values where the null hypothesis is rejected are highlighted red.***

PRif	Frequency				
Week	8kHz	12kHz	16kHz	24kHz	30kHz
1	0.012 1<0.0125	0.166 1>0.0125	0.106 1>0.0125	0.062 1 >0.0125	0.090 1>0.0125
4	0.441 3	0.202 2	0.178 2	0.146 2	0.125 2
12	0.251 2>0.0167	0.499 3	0.427 3	0.620 3	0.199 3

Table 12: ***Pellet with rifampicin threshold p values and the Holm Bonferroni correction. Values where the null hypothesis is rejected are highlighted red.***

PClind	Frequency				
Week	8kHz	12kHz	16kHz	24kHz	30kHz
1	0.225 2	0.201 1>0.0125	0.197 2	0.074 1>0.0125	0.049 1>0.0125
4	0.318 3	0.618 2	0.432 3	0.570 3	0.124 2
12	0.051 1>0.0125	0.966 3	0.192 1>0.0125	0.120 2	0.188 3

Table 13: ***Pellet with clindamycin threshold p values and the Holm Bonferroni correction. Values where the null hypothesis is rejected are highlighted red.***

5.1.9 Summary and discussion of ABR threshold results

The ABR threshold results do not show any significant excursions from initial week 0 values when initial ABR testing occurred for the biological control, surgical control and PLGA and pluronic pellet groups. As ABR threshold elevation is used as a measure of safety of ME pellets, it can be concluded that the surgical access to the middle ear bulla and insertion of the PLGA and Pluronic pellet did not affect the hearing mechanism. These results support the guinea pig animal model for middle ear experimentation and was an interesting finding for model development because of the significant surgical and experimental intervention in a small middle ear space. The anterobulla access to the middle ear in the guinea pig has also been shown to be reproducible and safe method without damaging to the hearing mechanism.

The ABR threshold elevation seen at all frequencies after PLGA and pluronic pellet loaded with rifampicin and clindamycin in combination persists at the high and low frequencies at week 16 however, there was some recovery in the mid frequency range. This ABR threshold elevation suggests that the antibiotics in the pellets may affect the ME hearing mechanism.

The significant and sustained elevation of threshold seen with the antibiotic combination of rifampicin and clindamycin was unexpected and unusual in appearance. The partial mid frequency recovery and persistent elevation at 8 and 30 kHz seen at week 16 does not appear to have been reported elsewhere. This first reporting would suggest that the drugs in combination at these levels in the pellet may not be suited for use in humans.

The ABR threshold results for pellets loaded with either rifampicin or clindamycin tested separately also resulted in unusual patterns of threshold elevation. These results are not as pronounced as the drugs used in combination, suggesting a synergistic effect between the two antibiotics when used together.

Analysis of the amplitude and latency changes of the ABR waveforms from initial readings at week 0 to week 16 would show if there is any evidence of neurotoxicity with waves P2 and P3 indicating an effect on the central processes in the auditory pathway.

5.2 ABR amplitude results analysis

5.2.1 Changes in ABR amplitude of biological control group over 74-94dB at 16kHz

The amplitude of each of the waveforms P1,P2 and P3 was analysed in turn at 94dB, 84dB and 74dB. The amplitude of wave P1 did not show any significant changes over 16 weeks.

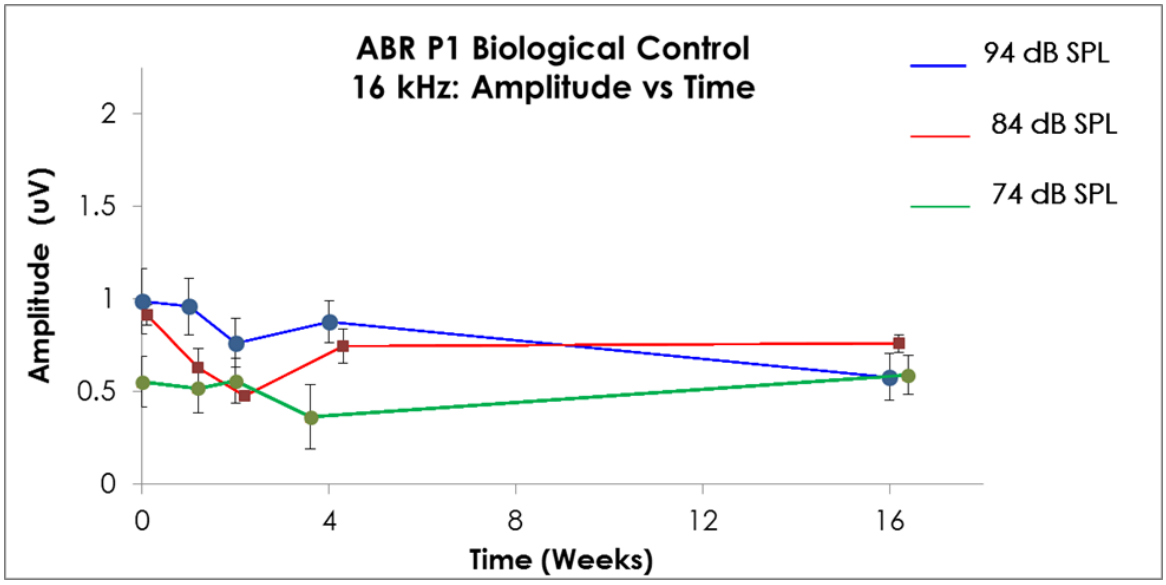


Figure 27: ***Changes in amplitude over time for biological control group at 16kHz analysing the P1 wave. Significance is denoted by a *.***

Wave P2 showed one significant decrease in amplitude for week 1 at 94dB from 1.594 uV to 0.976 uV (see Figure 28).

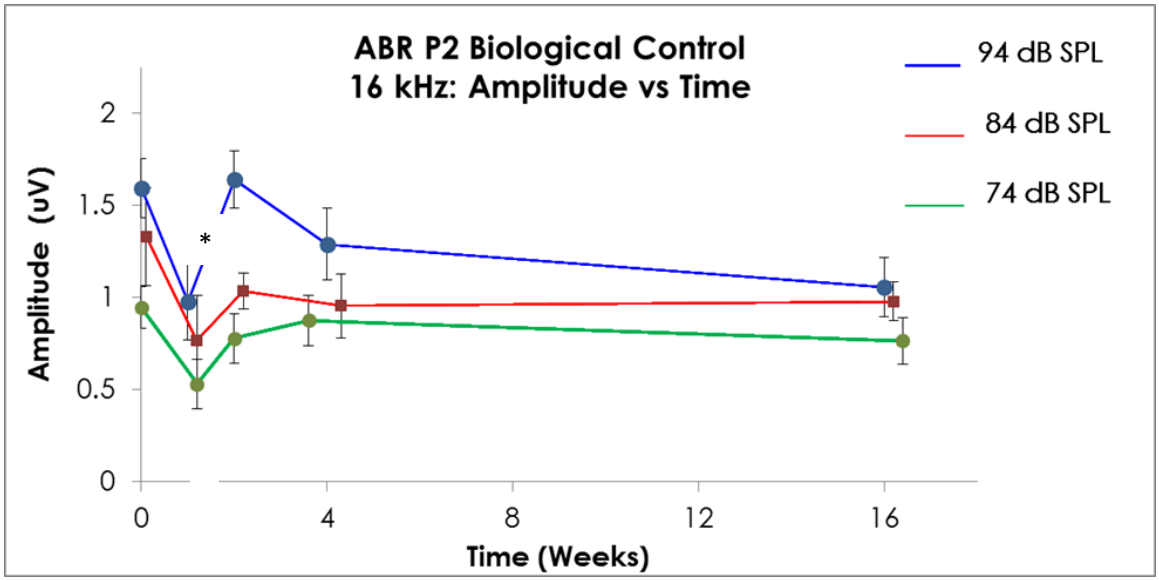


Figure 28: ***Changes in amplitude against time biological control group at 16kHz analysing the P2 wave. Significance is denoted by a *.***

Analysis of wave P3 at 16kHz shows a significant reduction in amplitude at week 1 from 2.02 uV to 1.029 uV (p 0.037) at 94dB. See Figure 29.

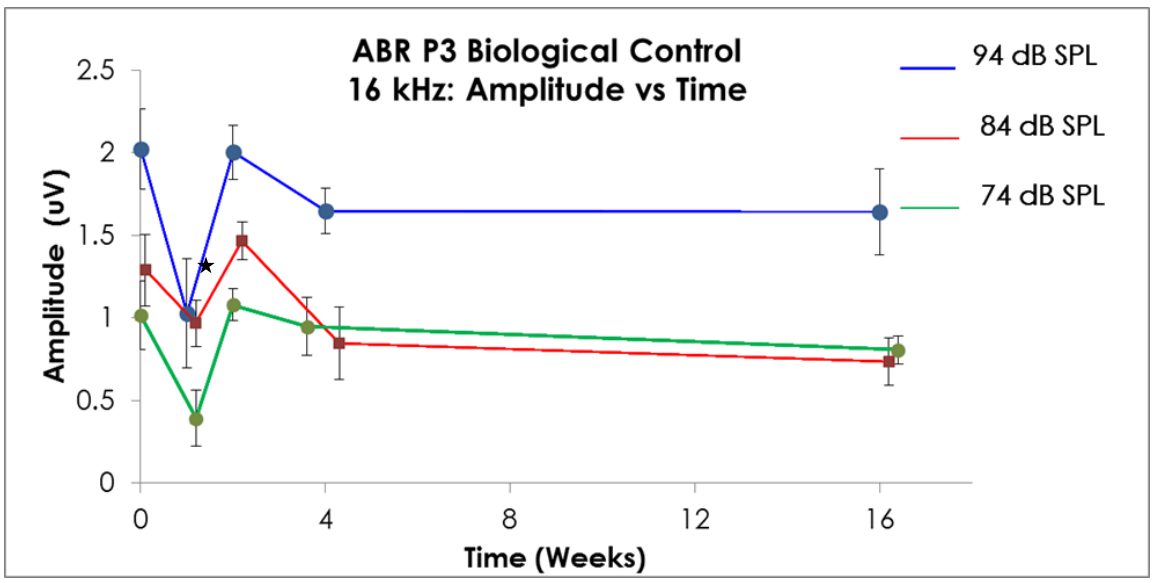


Figure 29: ***Changes in amplitude against time biological control group at 16kHz analysing the P3 wave. Significance is denoted by a *.***

Overall, there are some excursions seen in the amplitude for the biological control group from initial ABR readings at week 0 at all three levels of hearing (74, 84 and 94kHz) when analysing at 16kHz. The most significant results however seem to be at week 1 with resolution at weeks 2, 4 and 16. The most pronounced results also appear to be seen in waves P2 and P3.

5.2.2 Changes in ABR amplitude of biological control group over 74-94dB at 24kHz

Biological control group at 24kHz shows no significant excursions from the initial week 0 ABR values on analysis of P1 for amplitude. See Figure 30.

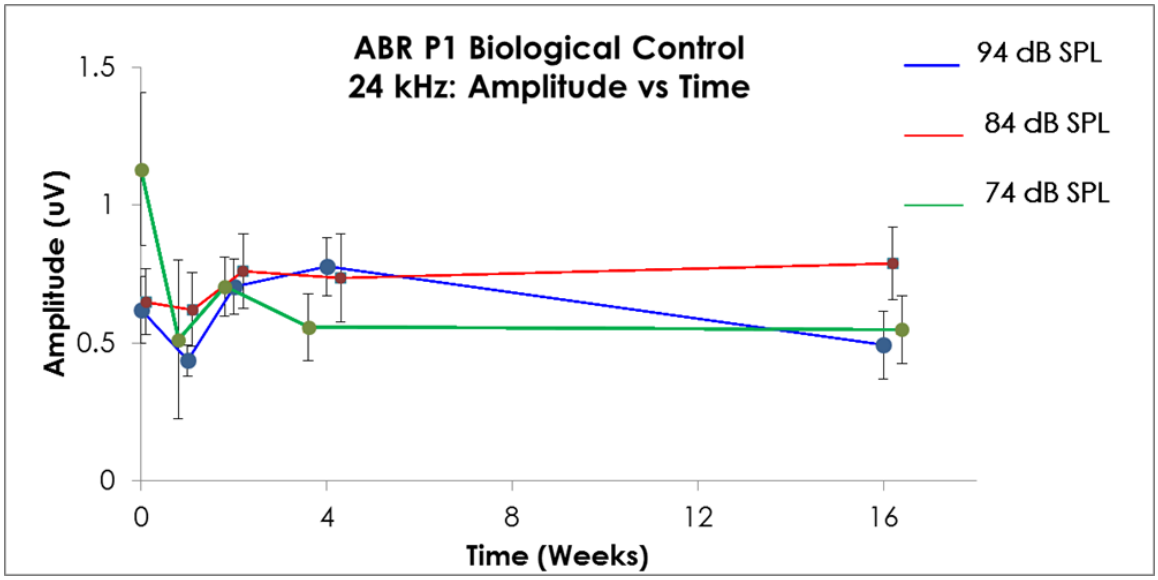


Figure 30: ***Changes in amplitude against time biological control group at 24kHz analysing the P1 wave. Significance is denoted by a *.***

Analysis of wave P2 at 24kHz showed that there was one significant reduction in amplitude at 94kHz from 1.348uV from initial ABR recordings at week 0 to 0.722 uV at week 1 (p=0.0438). See Figure 31.

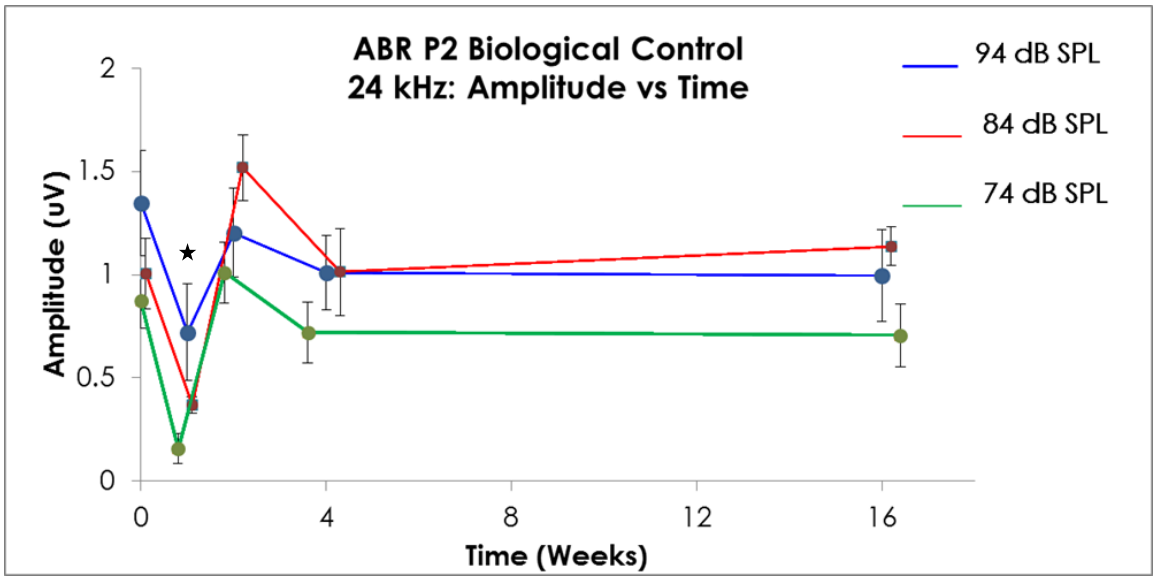


Figure 31: ***Changes in amplitude against time biological control group at 24kHz analysing the P2 wave. Significance is denoted by a *.***

Wave P3 for biological control group at 24kHz also shows a significant decrease in amplitude at week 1 for both 94dB (p=0.029) and 84dB (p <0.01). See Figure 32.

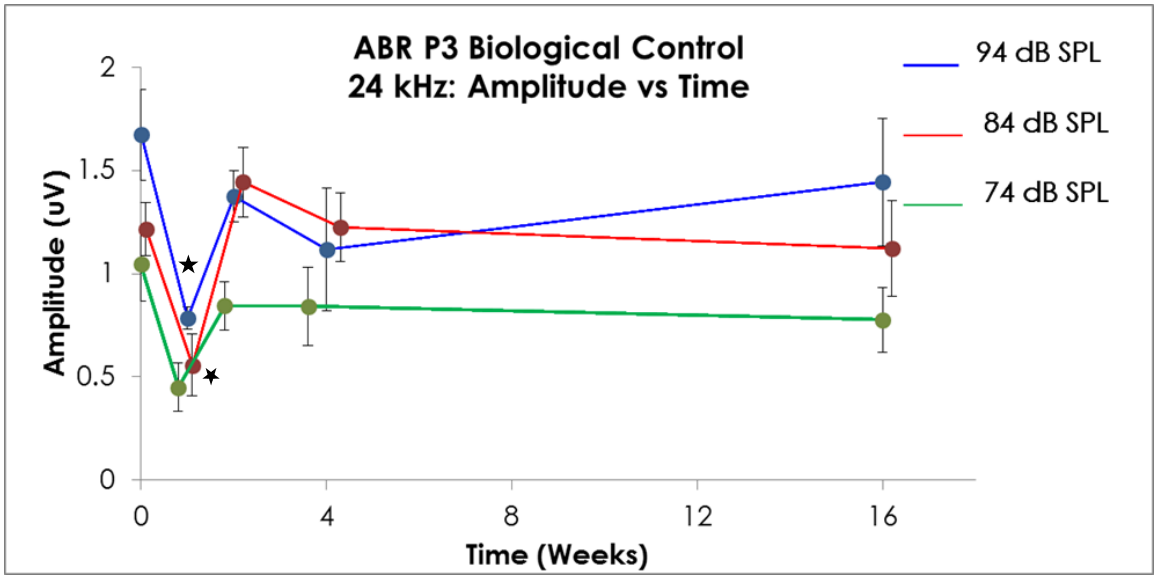


Figure 32: ***Changes in amplitude against time for biological control group at 24kHz analysing the P3 wave. Significance is denoted by a *.***

Overall, the amplitude results for the biological control group show decreased values at both 16kHz and 24kHz in waves P2 and P3 at week 1. 94dB showed significant decreases in waves P2 and P3 for both 16kHz and 24kHz and for wave P3 was also a significant amplitude reduction for 84dB at week 1.

5.2.3 Summary of changes in ABR amplitude of biological control groups at 16kHz and 24kHz

There are no changes in the P1 wave amplitude seen at both 16kHz and 24kHz. For wave P2 there is a decrease in amplitude at week 1 only seen at 94dB for both 16kHz and 24kHz. There is also a decrease in amplitude for wave P3 at week one in both 16kHz and 24kHz at 94dB and also 84dB at week one for 24kHz (Table 14).

	P1	P2	P3
BC 16kHz	-	↓ week 1 94dB	↓ week 1 94dB
BC 24kHz	-	↓ week 1 94dB	↓ week 1 94dB,84dB

Table 14: ***Changes in amplitude for waves P1-P3 measured at 16kHz and 24kHz for the biological control group.***

5.2.4 Changes in ABR amplitude of surgical control group over 74-94dB at 16kHz

There are no significant excursions from initial ABR recordings at week 0 on analysis of wave P1 in the surgical control group for 16kHz (Figure 33).

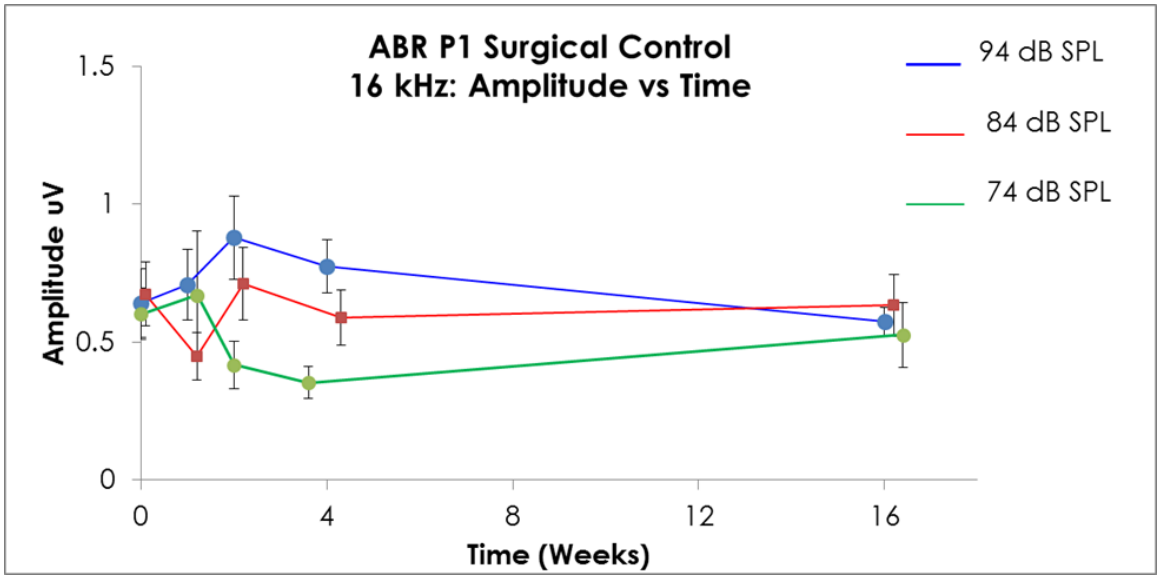


Figure 33: ***Changes in amplitude against time for surgical control group at 16kHz analysing the P1 wave. Significance is denoted by a *.***

Wave P2 shows one significant decrease in amplitude at week 1 for 94dB in the surgical control group at 16kHz. There is a decrease from 1.503 uV to 0.771 uV (p =0.01) using a two tailed test. Figure 34 demonstrates this.

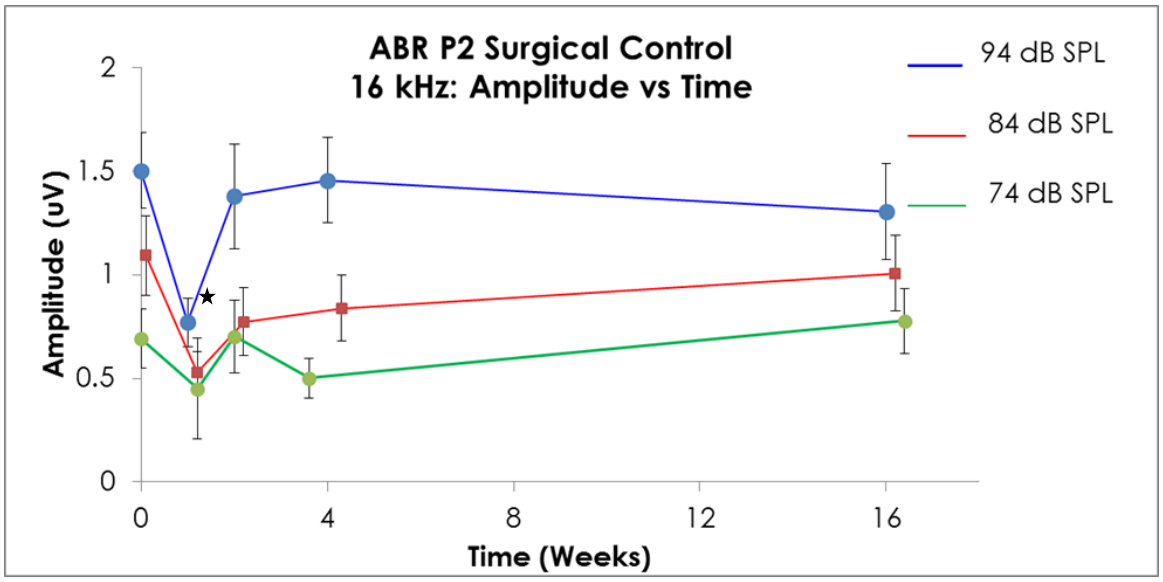


Figure 34: ***Changes in amplitude against time for surgical control group at 16kHz analysing the P2 wave. Significance is denoted by a *.***

Wave P3 shows significant decreases in amplitude at weeks 1 for 94dB with a reduction form 2.54uV to 1.584 µV ($p < 0.01$) and also at week 1 at 74dB with a reduction from 1.091uV to 0.653uV ($p = 0.02$). This is shown in Figure 35.

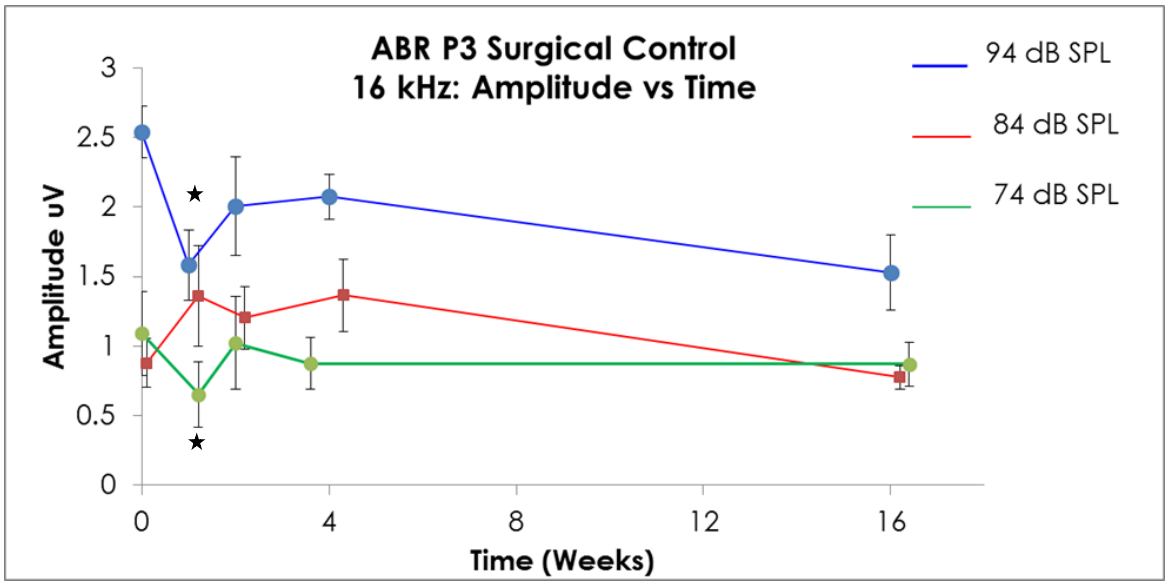


Figure 35: ***Changes in amplitude against time for surgical control group at 16kHz analysing the P3 wave. Significance is denoted by a *.***

5.2.5 Changes in ABR amplitude of surgical control group over 74-94dB at 24kHz

There were no significant excursions from initial ABR recordings at week 0 seen on analysis of wave P1 at 24kHz (see Figure 36).

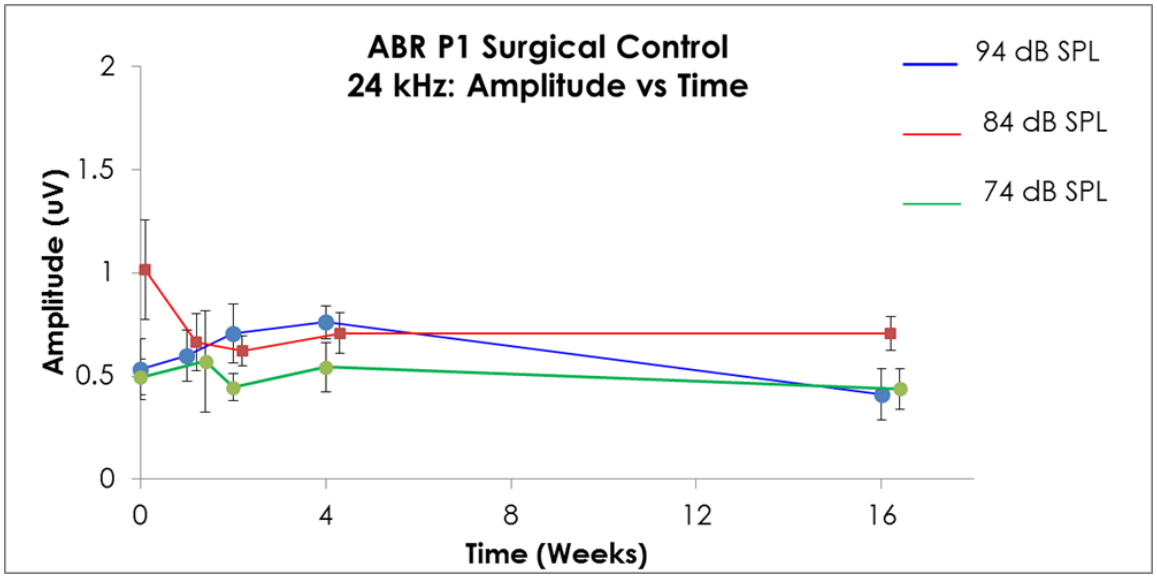


Figure 36: ***Changes in amplitude against time for surgical control group at 24kHz analysing the P1 wave. Significance is denoted by a *.***

For wave P2 there was one significant reduction in amplitude seen at 94dB. At week 1 the amplitude was 1.396 uV and this changed to 0.664uV (p=0.049). At week 1 there was also a reduction in amplitude for 84dB from 1.321 to 0.6 uV and this did not reach statistical significance but was close with a p value of 0.054 (Figure 37).

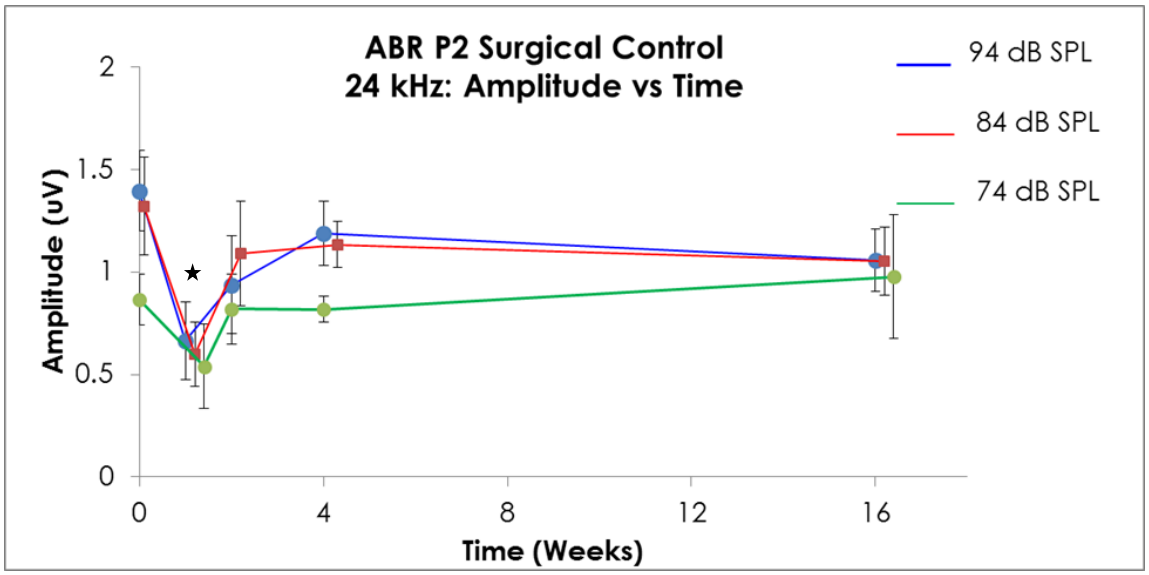


Figure 37: ***Changes in amplitude against time for surgical control group at 24kHz analysing the P2 wave. Significance is denoted by a *.***

Wave P3 shows a significant reduction in amplitude at week 1 for 94dB (p=0.05) and 74dB (p=0.012). Please refer to Figure 38.

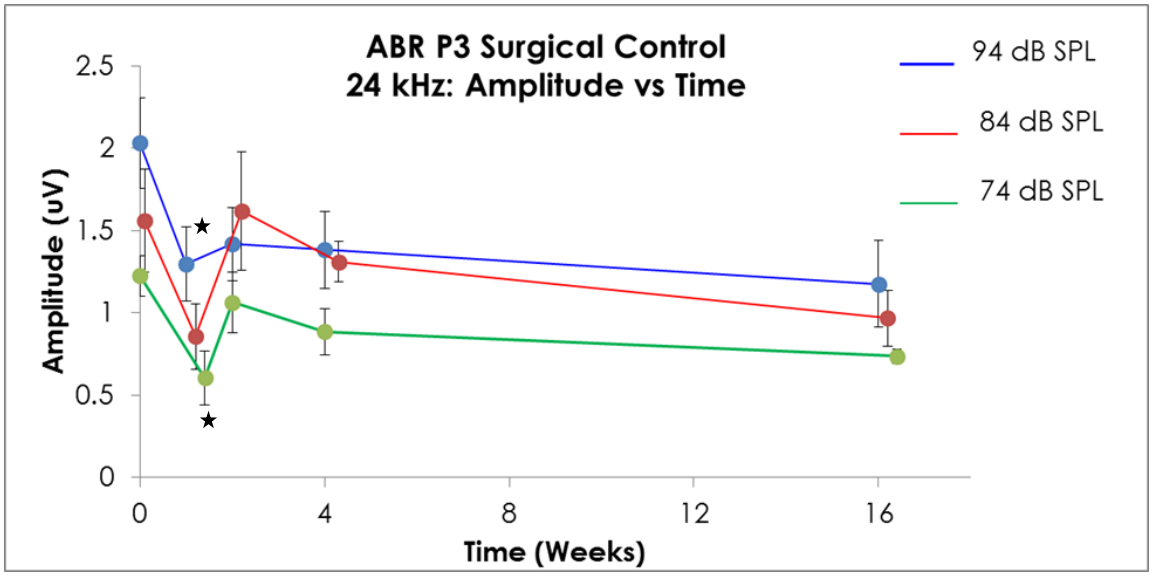


Figure 38: Changes in amplitude against time for surgical control group at 24kHz analysing the P3 wave. Significance is denoted by a *.

5.2.6 Summary of changes in ABR amplitude of surgical control group at 16kHz and 24kHz

	P1	P2	P3
SC 16kHz	-	↓ week 1 94dB	↓ week 1 94dB,74dB
SC 24kHz	-	↓ week 1 94dB	↓ week 1 94dB, 74dB

Table 15: ***Changes in amplitude for waves P1-P3 measured at 16kHz and 24kHz for the surgical control group*.**

Overall, there are no changes in amplitude for wave P1 in the surgical control group at 16kHz and 24kHz. For wave P2 there is a significant decrease in amplitude seen in wave P2 at 94dB week 1 at both 16kHz and 24kHz (Table 15). There is a decrease in amplitude seen in wave P3 at both 16kHz and 24kHz for 94dB and 74dB.

5.2.7 Changes in ABR amplitude of PLGA and pluronic pellet control group over 74-94dB at 16kHz

There were no significant excursions from weeks 0-16 for the pellet control group at 16kHz on analysis of the amplitude of waves P1,P2 and P3 (Figures 39,40,41).

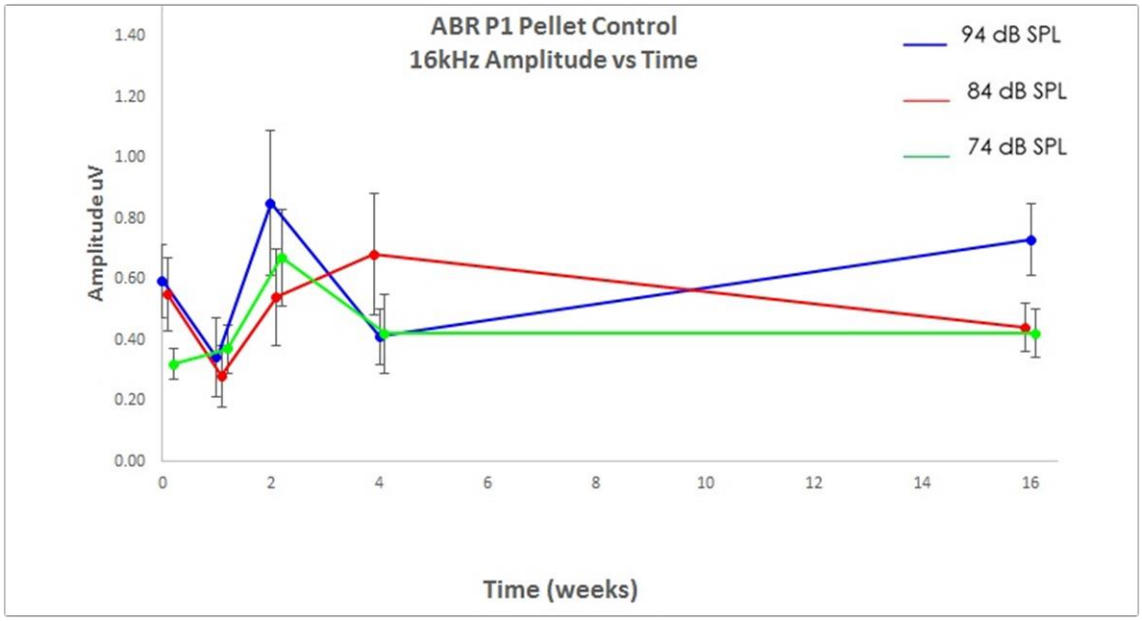


Figure 39: ***Changes in amplitude against time PLGA and pluronic pellet control group at 16kHz analysing the P1 wave. Significance is denoted by a *.***

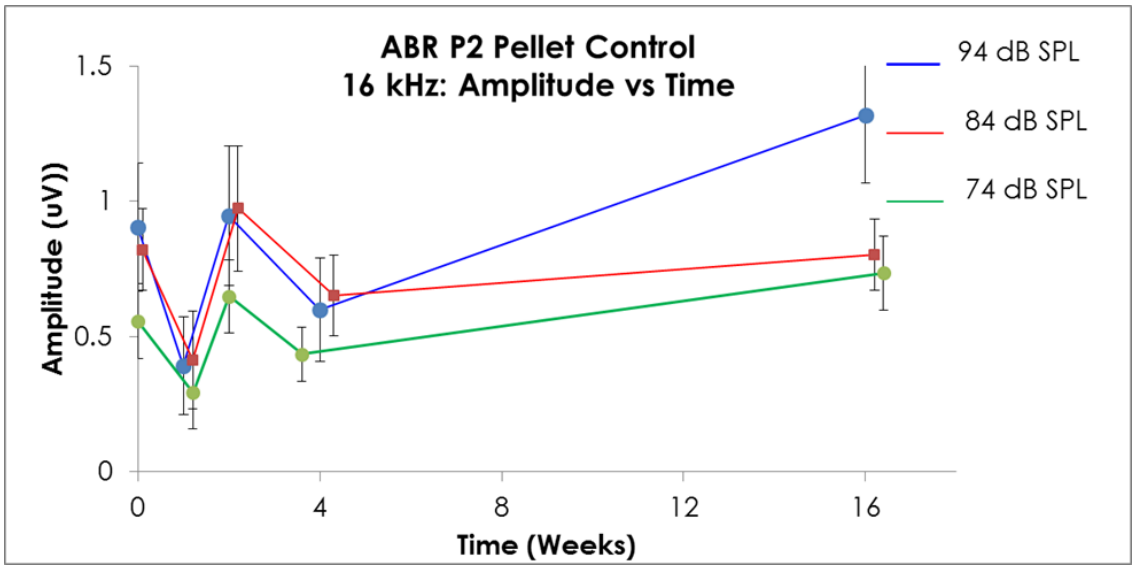


Figure 40: ***Changes in amplitude against time PLGA and pluronic pellet control group at 16kHz analysing the P2 wave. Significance is denoted by a *.***

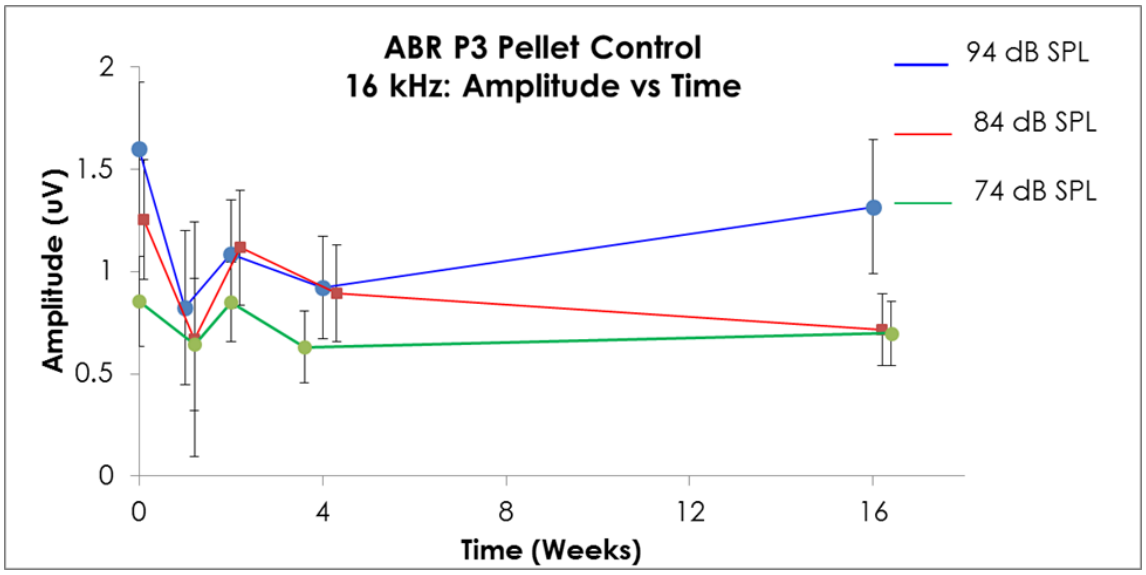


Figure 41: ***Changes in amplitude against time PLGA and pluronic pellet control group at 16kHz analysing the P3 wave. Significance is denoted by a *.***

5.2.8 Changes in amplitude of PLGA and pluronic pellet over 74-94dB at 24kHz

There were no significant excursions from weeks 0-16 for the pellet control group at 24kHz when analysing amplitude of waves P1,2 and 3 (Figures 42,43,44).

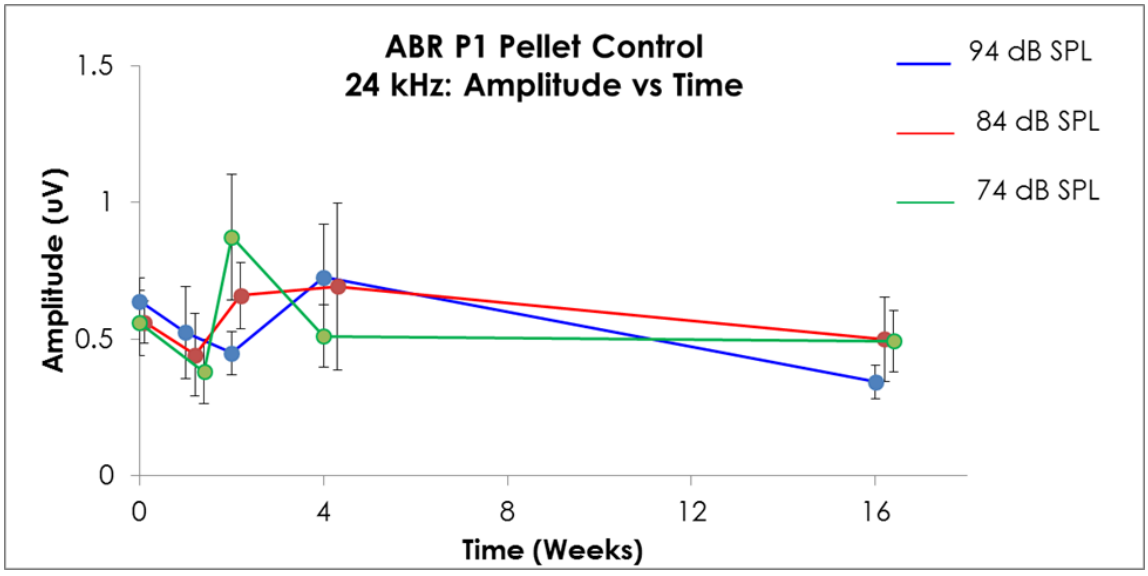


Figure 42: ***Changes in amplitude against time PLGA and pluronic pellet control group at 24kHz analysing the P1 wave. Significance is denoted by a *.***

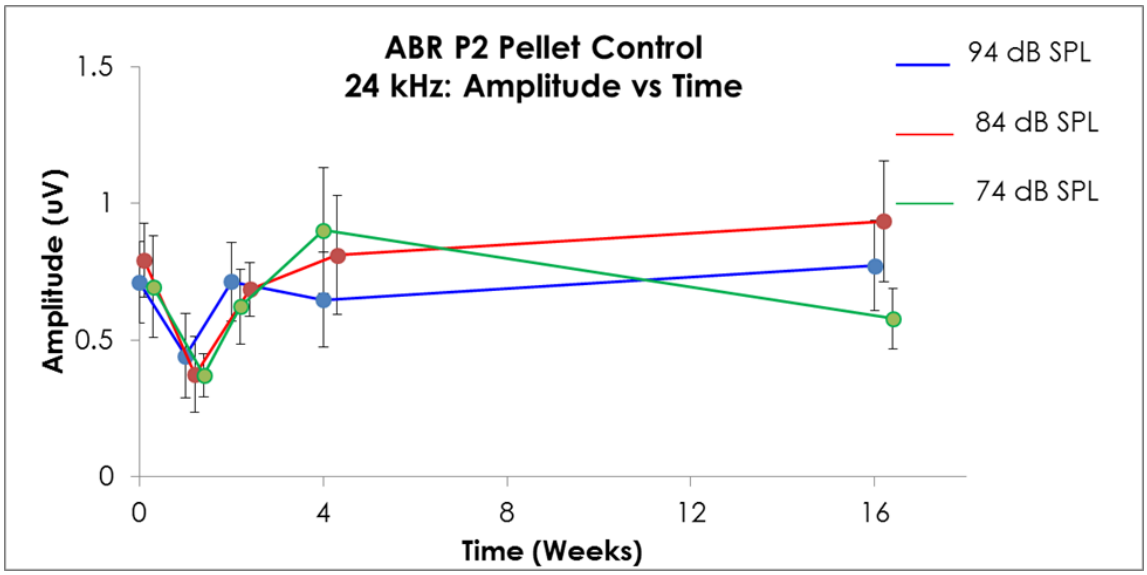


Figure 43: ***Changes in amplitude against time PLGA and pluronic pellet control group at 24kHz analysing the P1 wave. Significance is denoted by a *.***

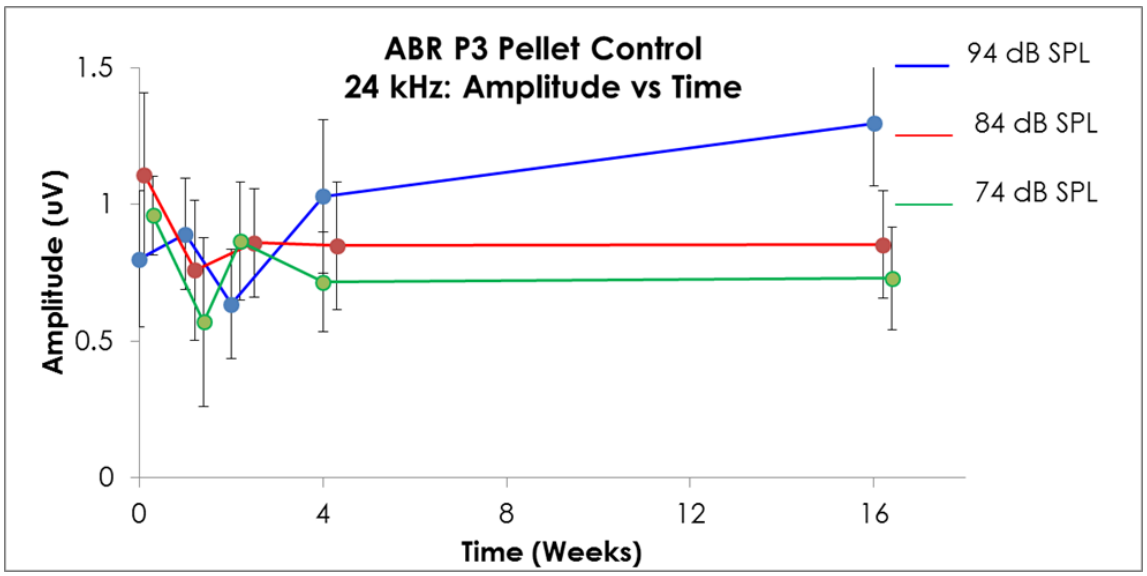


Figure 44: ***Changes in amplitude against time PLGA and pluronic pellet control group at 24kHz analysing the P1 wave. Significance is denoted by a *.***

5.2.9 Summary of changes in amplitude of PLGA and pluronic pellet at 16kHz and 24kHz

Overall, there was no significant consistent changes seen in the amplitude of the pellet control groups on analysis of waves P1, 2, and 3 at 16kHz and 24kHz (Table 16).

	P1	P2	P3
PLGA + pluronic 16kHz	-	-	-
PLGA + pluronic 24kHz	-	-	-

Table 16: ***Changes in amplitude for waves P1-P3 measured at 16kHz and 24kHz for the PLGA and pluronic pellet control group.***

5.2.10 Changes in amplitude of pellets loaded with rifampicin and clindamycin in combination over 74-94dB at 16kHz

For wave P1 there were no significant excursions in amplitude between initial ABR recordings at week 0 and week 16 for the pellet group loaded with both rifampicin and clindamycin tested at 16kHz (Figure 45).

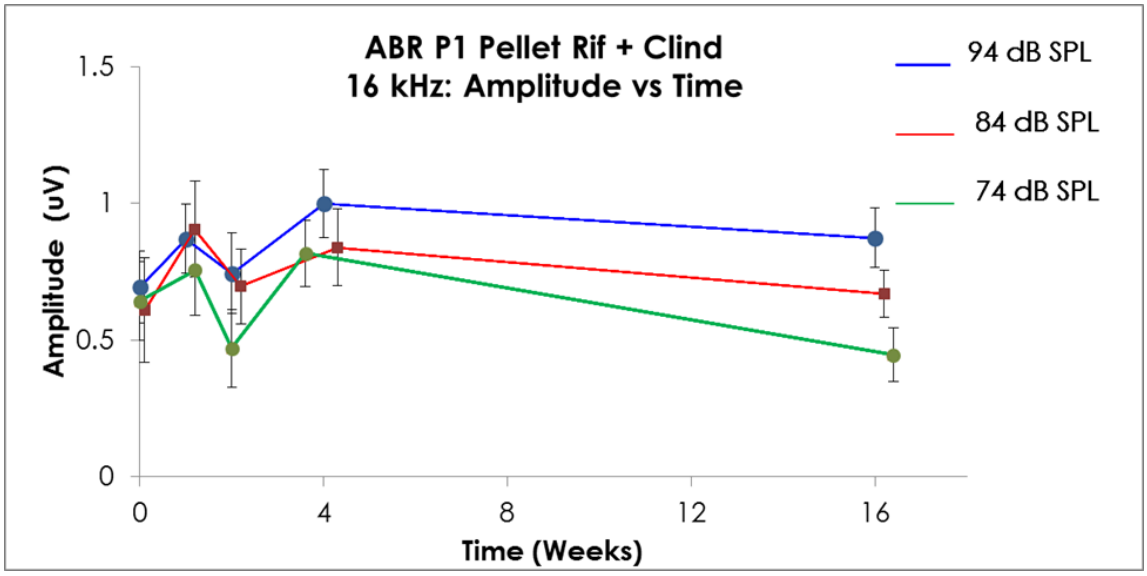


Figure 45: ***Changes in amplitude against time PLGA and pluronic pellet with rifampicin and clindamycin at 16kHz analysing the P1 wave. Significance is denoted by a *.***

For wave P2 there were no significant excursions in amplitude between initial ABR recordings at week 0 and week 16 for the pellet group loaded with both rifampicin and clindamycin tested at 16kHz.

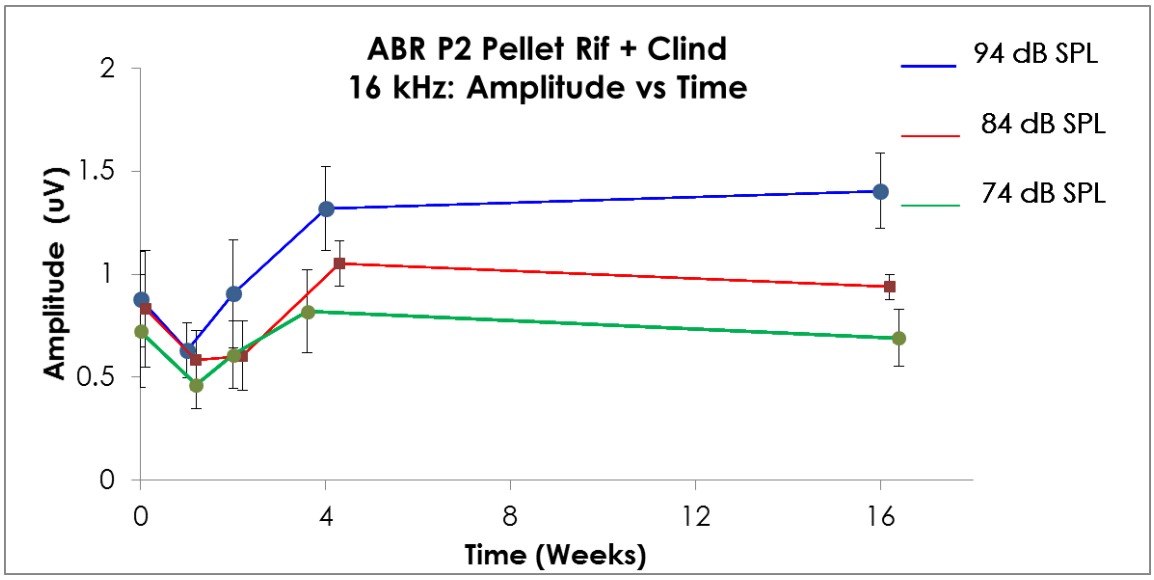


Figure 46: ***Changes in amplitude against time PLGA and pluronic pellet with rifampicin and clindamycin at 16kHz analysing the P2 wave. Significance is denoted by a *.***

On analysis of wave P3 there was a significant decrease in amplitude at week 2 for 94dB from 1.901 initially recorded at week 0 to 1.199 at week 2 (p=0.0465). There was also a significant reduction in amplitude at 74dB at week 2 (p=0.0365) and week 16 (p=0.029).

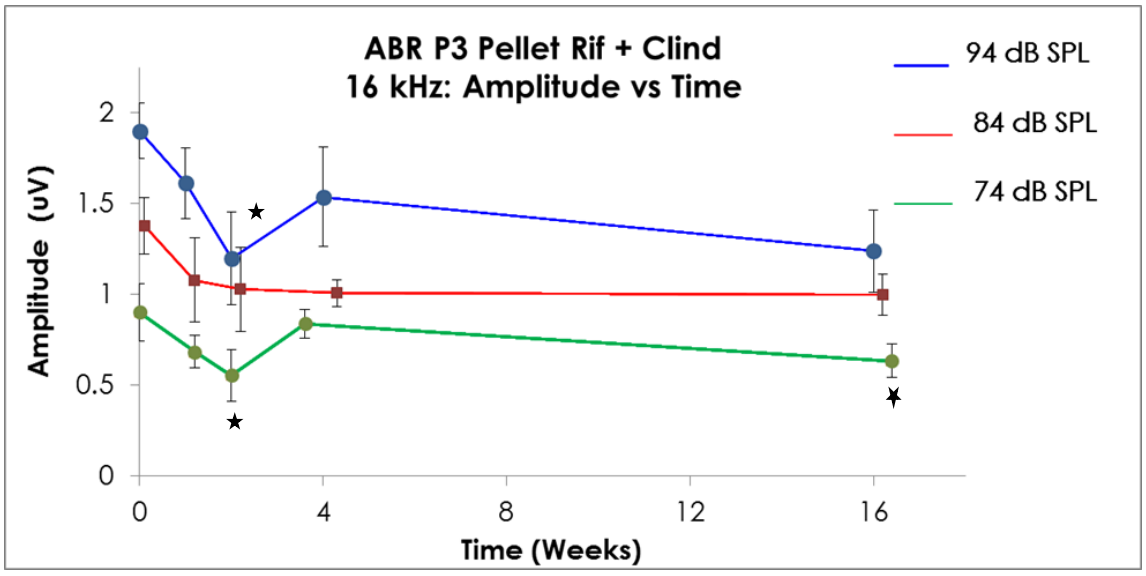


Figure 47: ***Changes in amplitude against time PLGA and pluronic pellet with rifampicin and clindamycin at 16kHz analysing the P3 wave. Significance is denoted by a *.***

5.2.11 Changes in ABR amplitude of pellets loaded with rifampicin and clindamycin over 74-94dB at 24kHz

For wave P1 there were no significant excursions in amplitude between initial recordings at week 0 and week 16 for the pellet group loaded with both rifampicin and clindamycin tested at 24kHz.

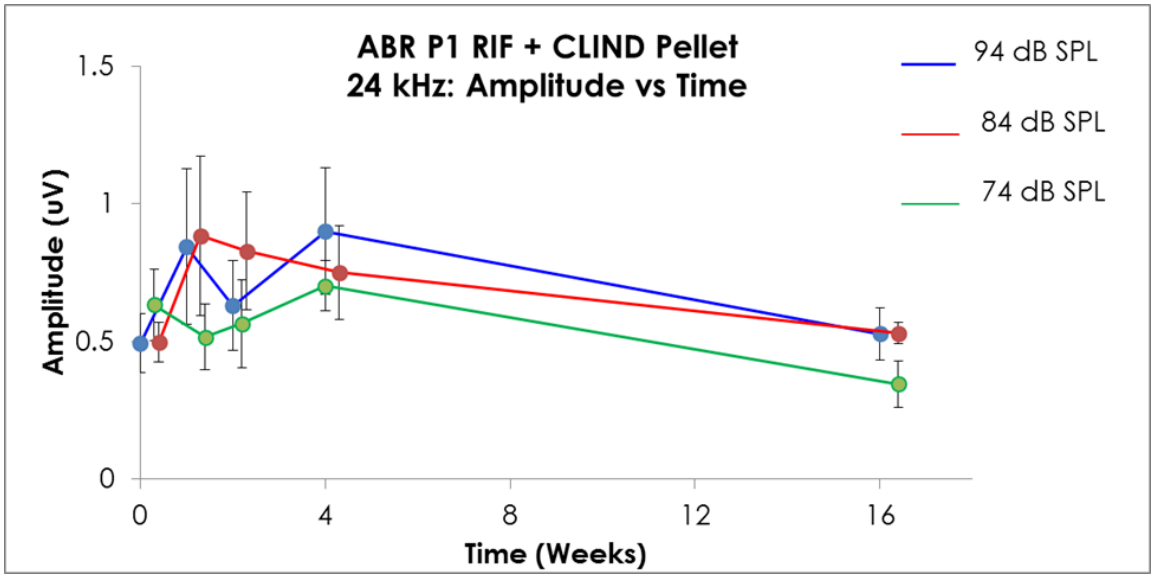


Figure 48: ***Changes in amplitude against time PLGA and pluronic pellet with rifampicin and clindamycin at 24kHz analysing the P1 wave. Significance is denoted by a *.***

For wave P2 there were a significant increase in amplitude seen at week 16 at 84dB from 0.6 uV initially at week 0 to 0.829uV at week 16 ($p<0.01$).

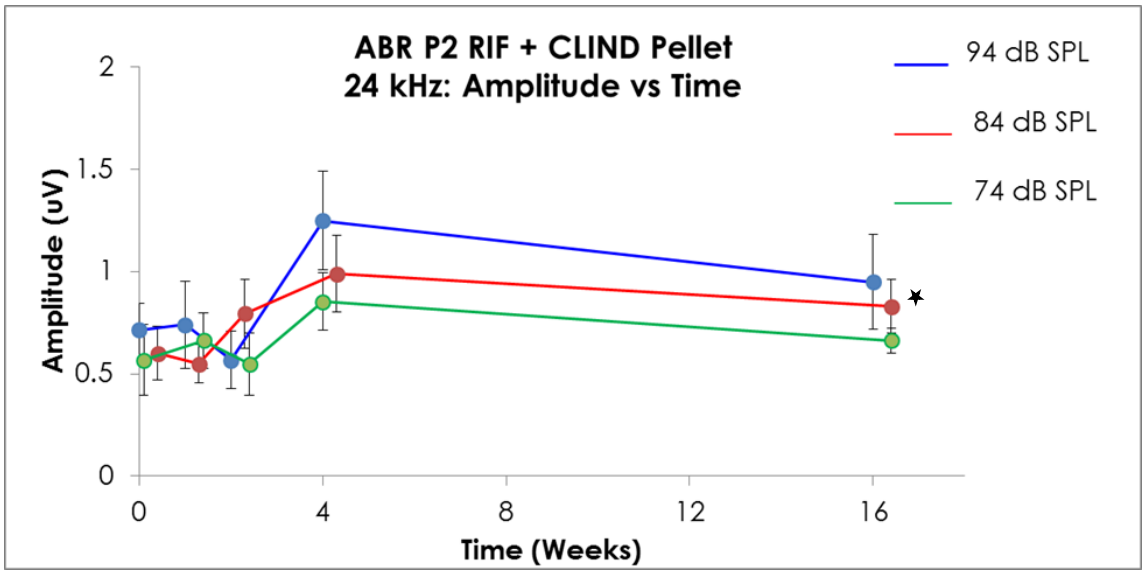


Figure 49: ***Changes in amplitude against time PLGA and pluronic pellet with rifampicin and clindamycin at 24kHz analysing the P2 wave. Significance is denoted by a *.***

For wave P3 there were no significant excursions in amplitude between initial recordings at week 0 and week 16 for the pellet group loaded with both rifampicin and clindamycin tested at 24kHz (Figure 50).

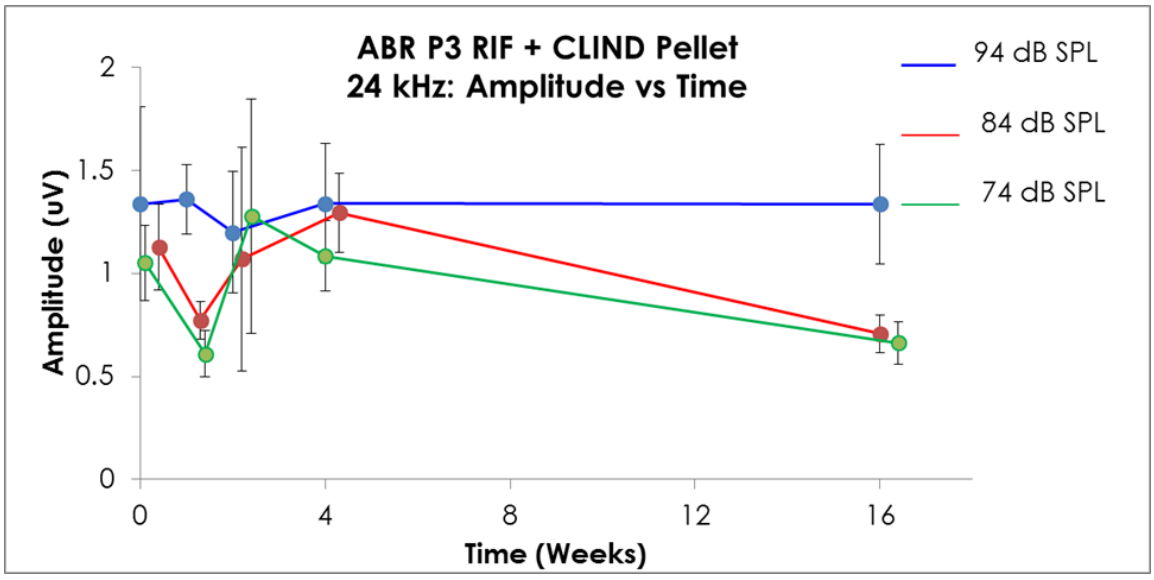


Figure 50: ***Changes in amplitude against time PLGA and pluronic pellet with rifampicin and clindamycin at 24kHz analysing the P3 wave. Significance is denoted by a *.***

5.2.12 Summary of changes in PLGA and pluronic pellet loaded with rifampicin and clindamycin in combination over 74-94dB at 16kHz and 24kHz

	P1	P2	P3
Pellet + rifampicin and clindamycin 16kHz	-	-	↓ week 2 94dB,74dB ↓ week 16 74dB
Pellet + rifampicin and clindamycin 24kHz	-	↑week 16 84dB	-

Table 17*: Changes in amplitude for waves P1-P3 measured at 16kHz and 24kHz for the PLGA and pluronic loaded with rifampicin and clindamycin in combination*

Overall the amplitude results for pellet loaded with rifampicin and clindamycin show no significant excursions from initial recordings at week 0 for P1 at both 16kHz and 24kHz. An increase in amplitude at 84dB at week 16 for P2 is seen in 24kHz, but with no associated changes in 16kHz. For wave P3 at 16kHz there is a significant reduction in amplitude at week 2 compared to week 0 for 94dB and 74dB. There was also a reduction in amplitude at week 16 for 74dB (Table 17).

5.2.13 Changes in ABR amplitude of pellet loaded with rifampicin over 74-94dB at 16kHz

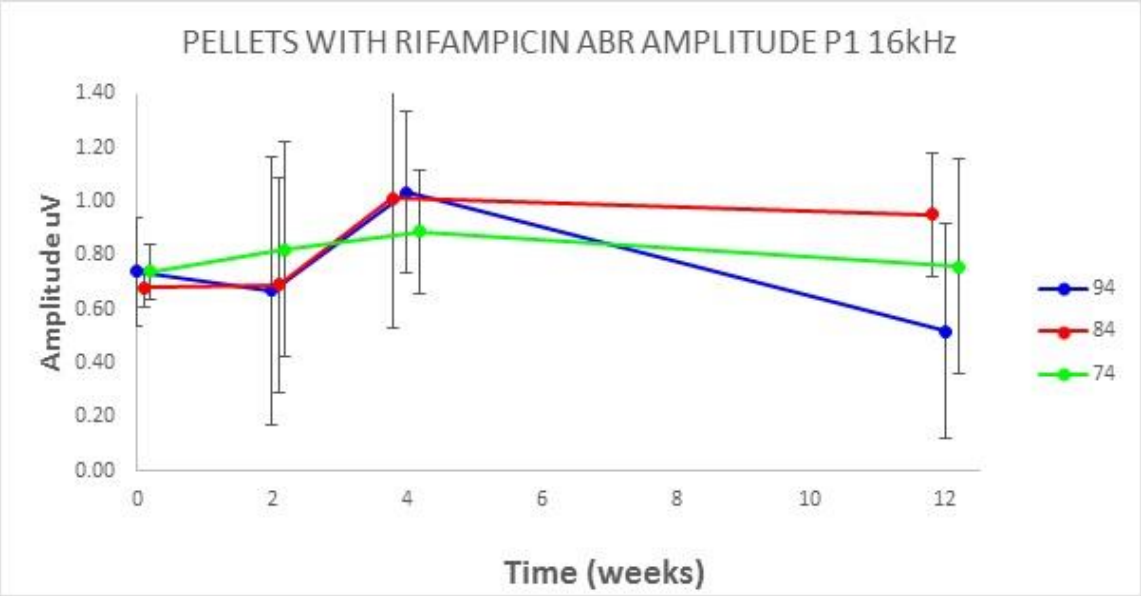


Figure 51: ***Changes in amplitude against time PLGA and pluronic pellet with rifampicin at 16kHz analysing the P1 wave. Significance is denoted by a *.***

For wave P1 there were no significant excursions in amplitude between initial recordings at week 0 and week 12 for the pellet group loaded with both rifampicin at 16kHz (Figure 51).

For wave P2 there were no significant excursions in amplitude between initial recordings at week 0 and week 16 for the pellet group loaded with both rifampicin and clindamycin tested at 16kHz (Figure 52).

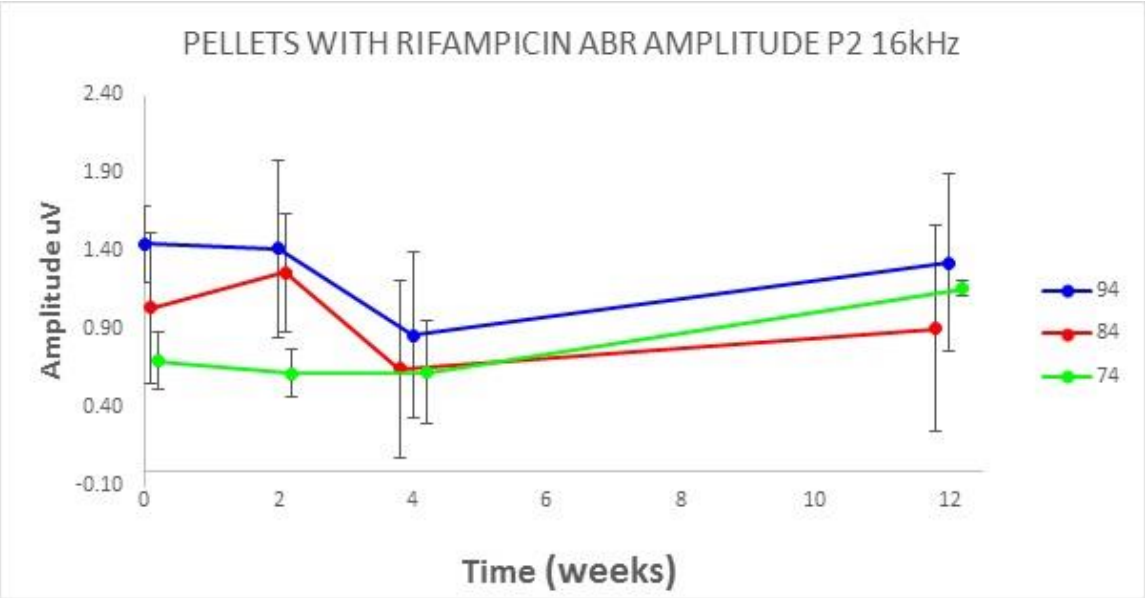


Figure 52*: Changes in amplitude against time PLGA and pluronic pellet with rifampicin at 16kHz analysing the P2 wave. Significance is denoted by a **.*

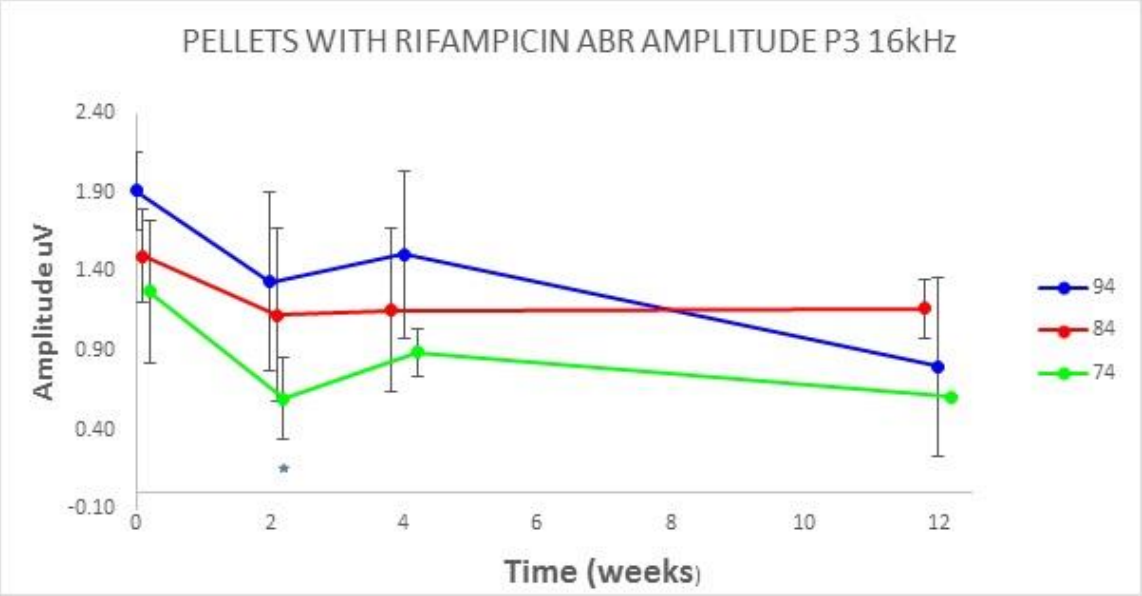


Figure 53: ***Changes in amplitude against time PLGA and pluronic pellet with rifampicin at 16kHz analysing the P3 wave. Significance is denoted by a **.***

On analysis of wave P3 there was a significant decrease in mean amplitude at week 2 for 74dB from 1.273 at week 0 to 0.597 at week 2 (p=0.045).

5.2.14 Changes in ABR amplitude of pellet loaded with rifampicin over 74-94dB at 24kHz

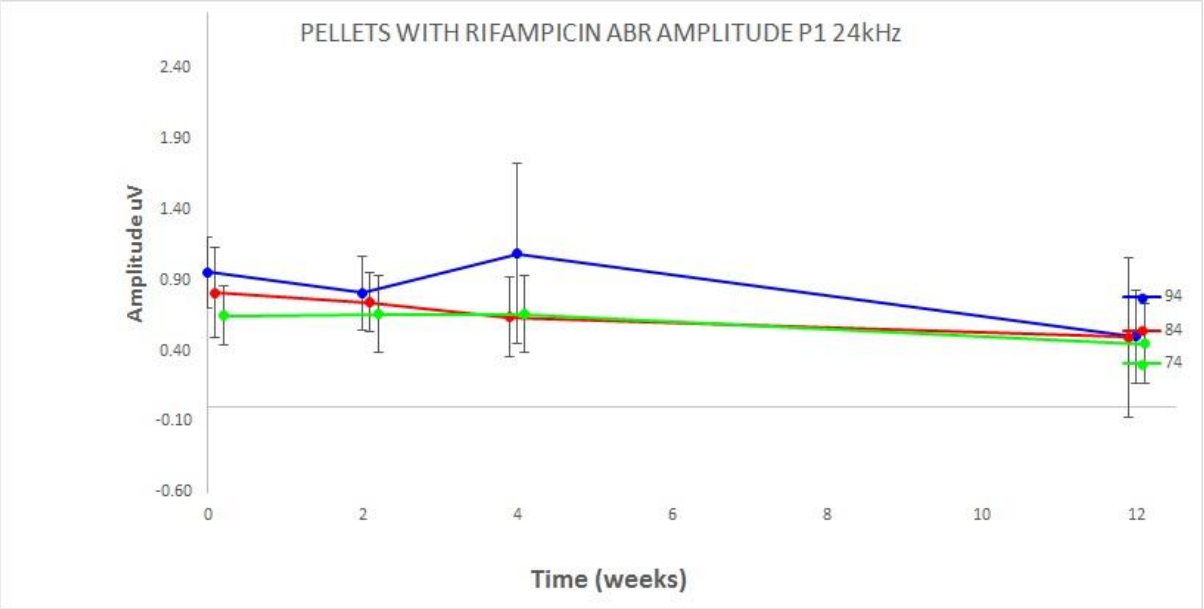


Figure 54: ***Changes in amplitude against time PLGA and pluronic pellet with rifampicin at 24kHz analysing the P1 wave. Significance is denoted by a *.***

For waves P1, P2 and P3 there were no significant excursions in amplitude between initial recordings at week 0 and week 12 for the pellet group loaded with both rifampicin at 16kHz (Figures 54,55,56).

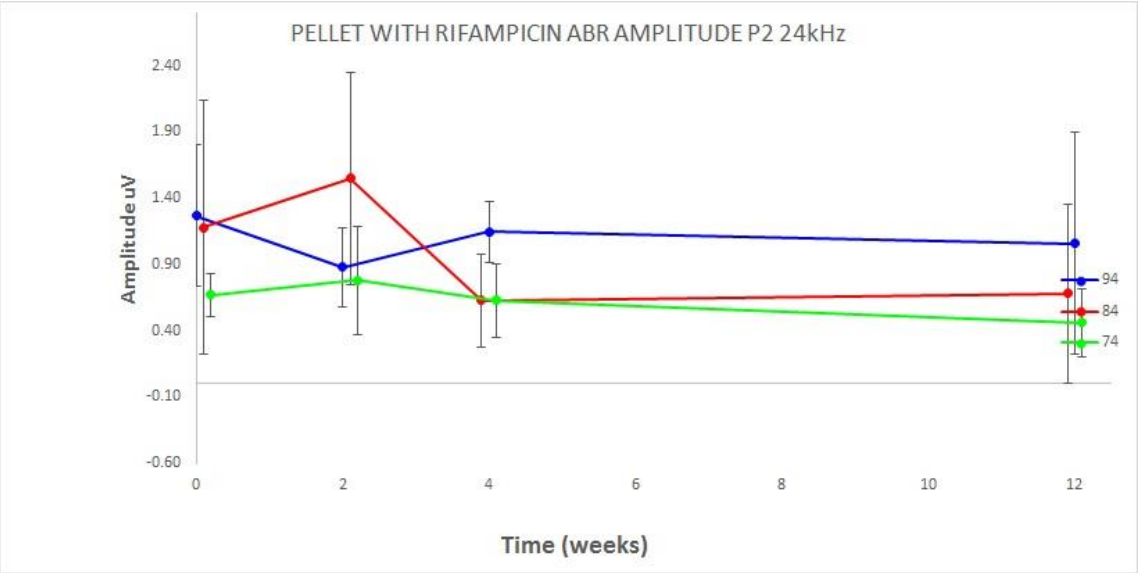


Figure 55*: Changes in amplitude against time PLGA and pluronic pellet with rifampicin at 24kHz analysing the P2 wave. Significance is denoted by a **.*

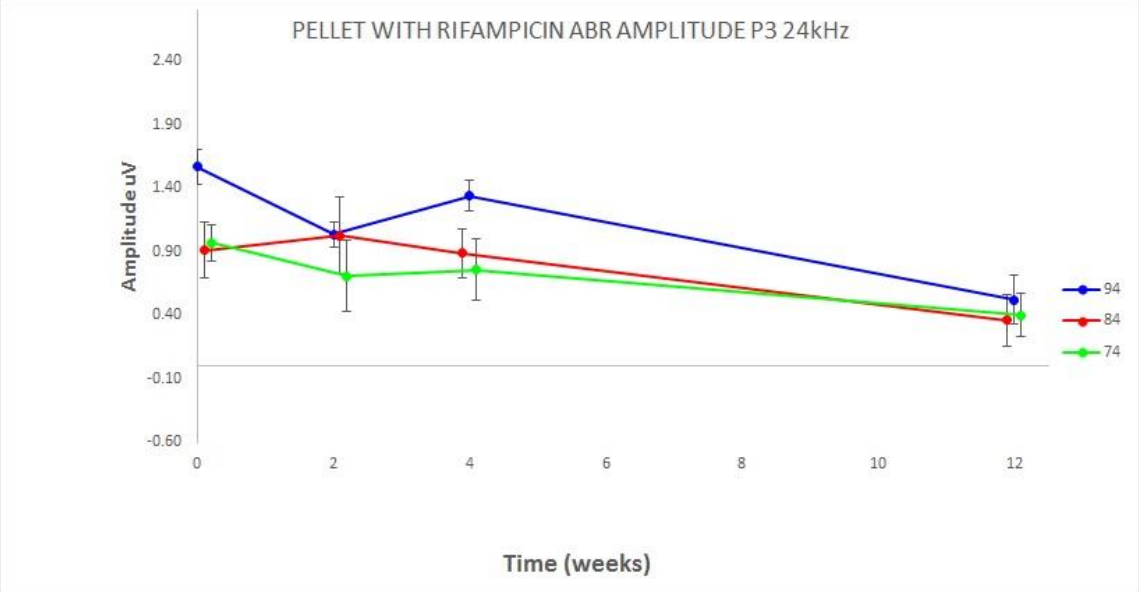


Figure 56: ***Changes in amplitude against time PLGA and pluronic pellet with rifampicin at 24kHz analysing the P3 wave. Significance is denoted by a **.***

5.2.15 Summary of changes in amplitude of Pellet loaded with Rifampicin at 16kHz and 24kHz

	P1	P2	P3
Pellet + Rifampicin 16kHz	-	-	↓ week 2 74dB
Pellet + Rifampicin 24kHz	-	-	-

Table 18: ***Changes in amplitude for waves P1-P3 measured at 16kHz and 24kHz for the PLGA and pluronic loaded with rifampicin group.***

For wave P3 there is one significant decrease in amplitude seen at week 2 and 74dB on analysis of ABR for guinea pigs loaded with pellets and rifampicin and tested at 16kHz (Table 18).

5.2.16 Changes in ABR amplitude of pellet loaded with clindamycin over 74-94dB at 16kHz

On analysis of wave P1 there was a significant decrease in mean amplitude at week 2 for 74dB from 0.953 at week 0 to 0.79 at week 2 (p=0.03).

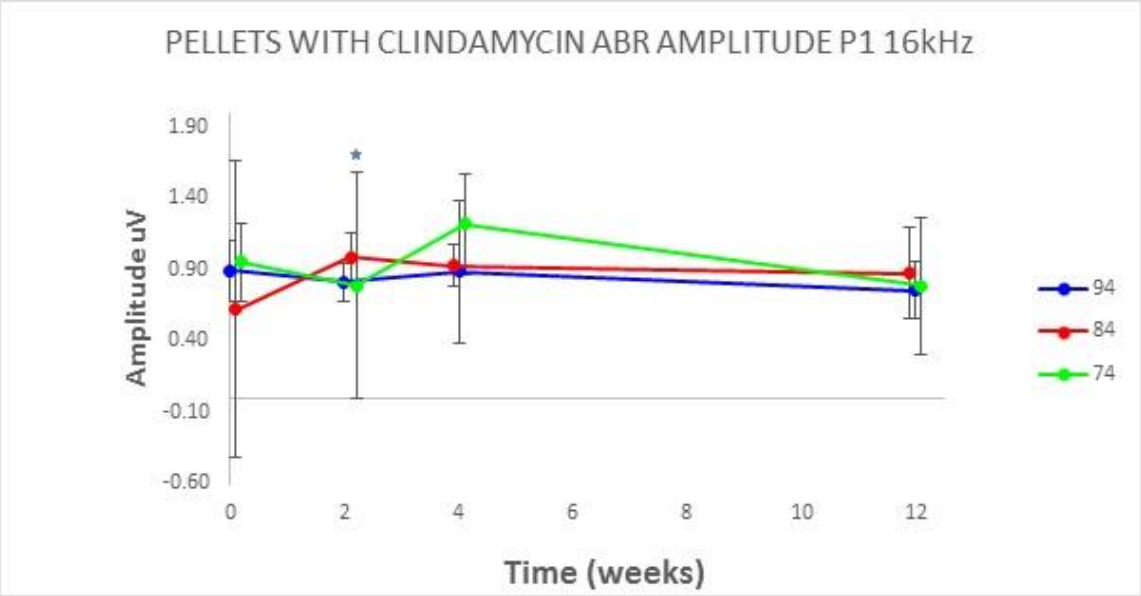


Figure 57: **Changes in amplitude against time PLGA and pluronic pellet with clindamycin at 16kHz analysing the P1 wave. Significance is denoted by a *.**

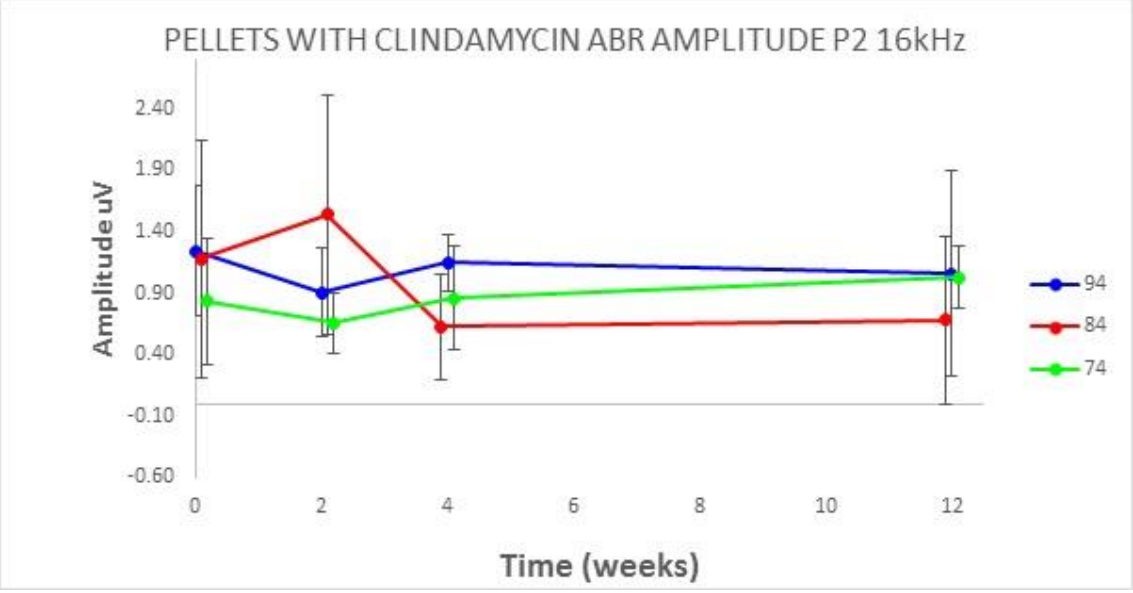


Figure 58: ***Changes in amplitude against time PLGA and pluronic pellet with clindamycin at 16kHz analysing the P2 wave. Significance is denoted by a *.***

For wave P2 there were no significant excursions in amplitude between initial recordings at week 0 and week 12 for the pellet group loaded with clindamycin at 16kHz.

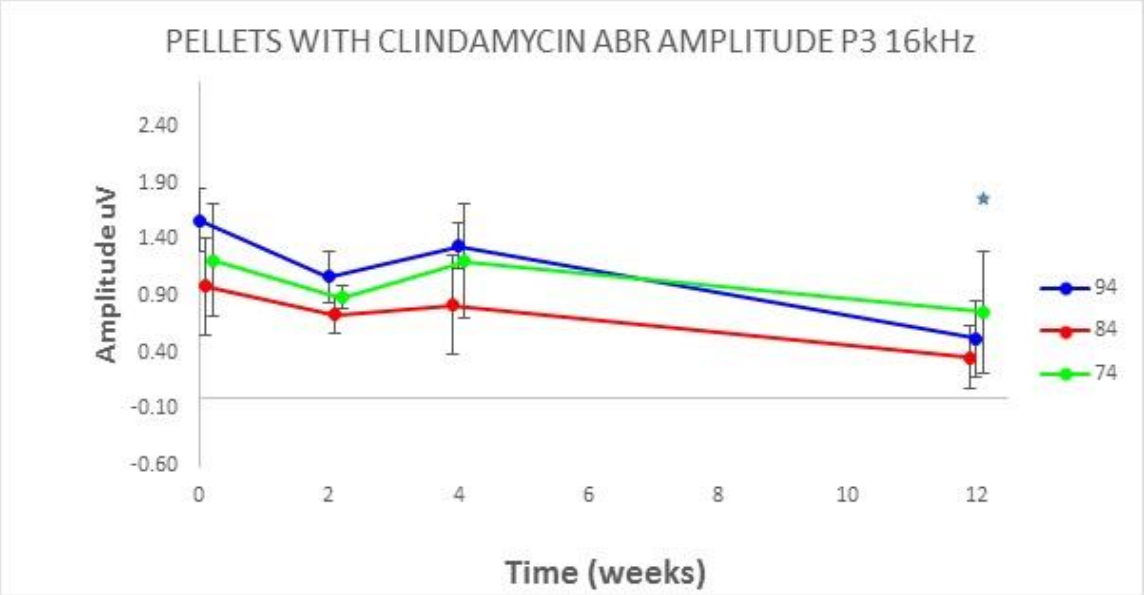


Figure 59: Changes in amplitude against time PLGA and pluronic pellet with clindamycin at 16kHz analysing the P3 wave. Significance is denoted by a *.

On analysis of wave P3 there was a significant decrease in mean amplitude at week 12 for 74dB from 1.217 at week 0 to 0.76 at week 12 (p=0.03).

5.2.17 Changes in ABR amplitude of pellet loaded with clindamycin over 74-94dB at 24kHz

On analysis of wave P1 there was a significant decrease in mean amplitude at week 12 for 74dB from 0.757 at week 0 to 0.59 at week 12 (p=0.04) (Figure 60).

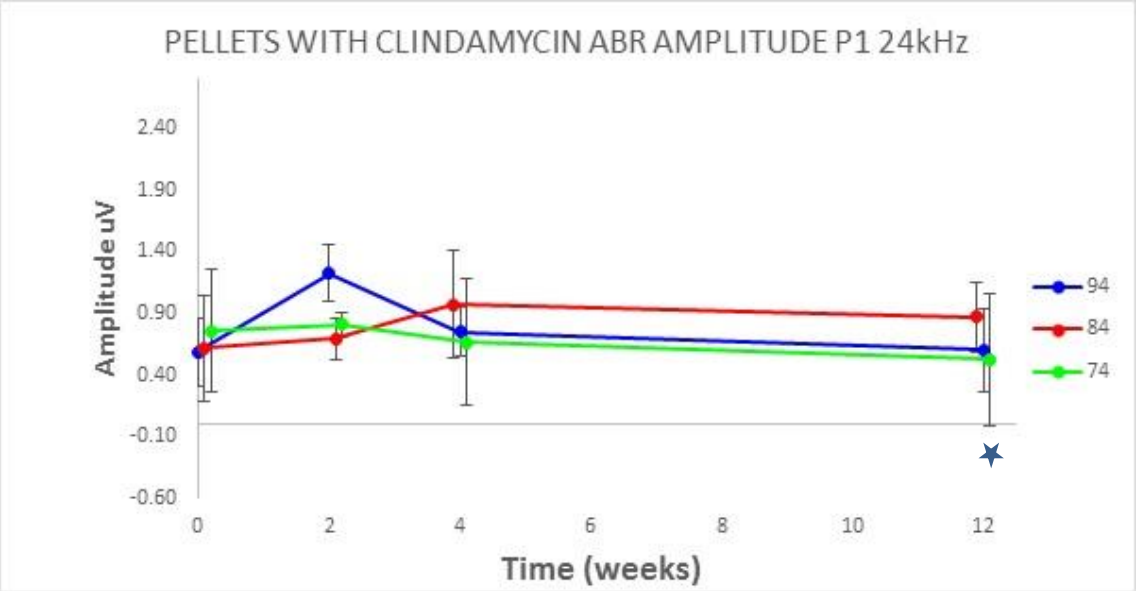


Figure 60: ***Changes in amplitude against time PLGA and pluronic pellet with clindamycin at 24kHz analysing the P1 wave. Significance is denoted by a *.***

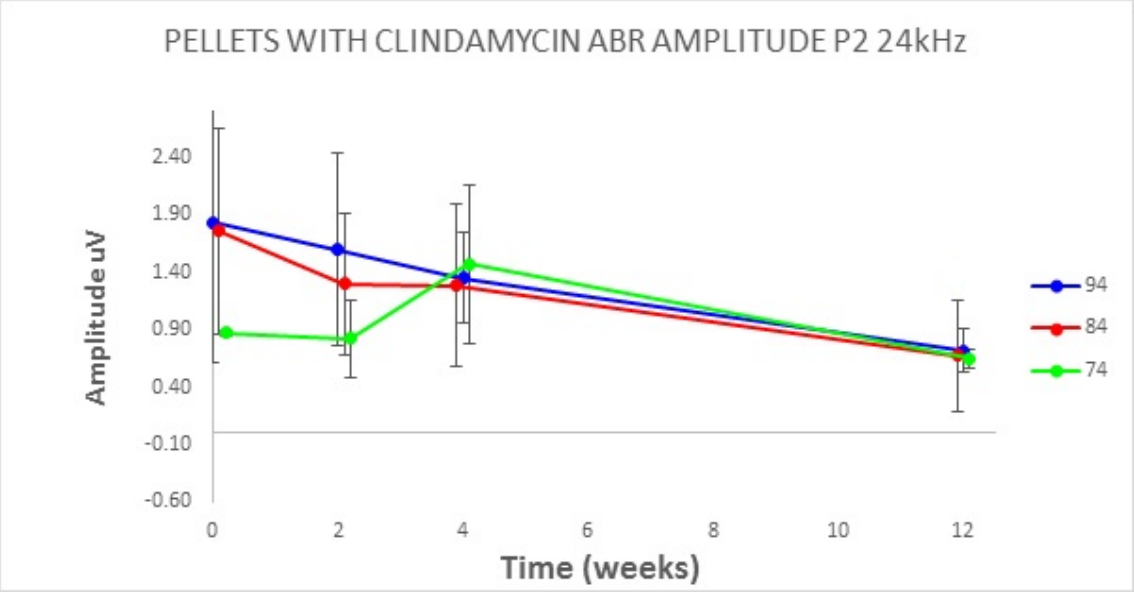


Figure 61: ***Changes in amplitude against time PLGA and pluronic pellet with clindamycin at 24kHz analysing the P2 wave. Significance is denoted by a *.***

For wave P2 there were no significant excursions in amplitude between initial recordings at week 0 and week 12 for the pellet group loaded with clindamycin at 24kHz (Figure 61).

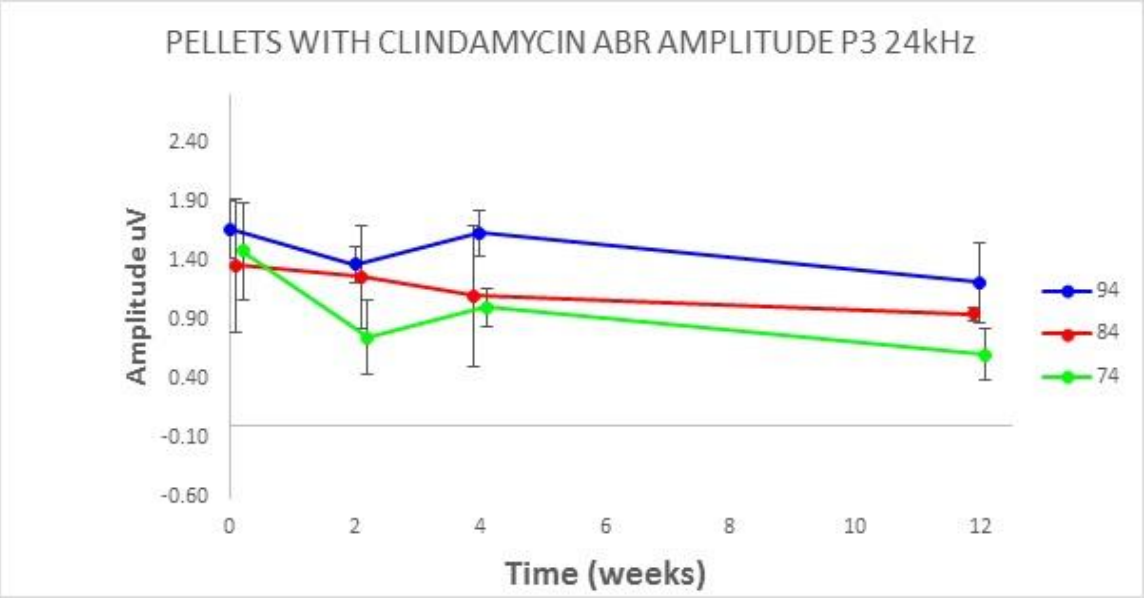


Figure 62*: Changes in amplitude against time PLGA and pluronic pellet with clindamycin at 24kHz analysing the P3 wave. Significance is denoted by a **.*

For wave P3 there were no significant excursions in amplitude between initial recordings at week 0 and week 12 for the pellet group loaded with clindamycin at 24kHz (Figure 62).

5.2.18 Summary of changes in amplitude of pellet loaded with clindamycin at 16kHz and 24kHz

	P1	P2	P3
Pellet + Clindamycin 16kHz	↓ week 2 74dB	-	↓ week 12 74dB
Pellet + Clindamycin 24kHz	↓ week 12 74dB	-	-

Table 19*: Changes in amplitude for waves P1-P3 measured at 16kHz and 24kHz for the PLGA and pluronic loaded with clindamycin group.*

For wave P1 there is a significant decrease in amplitude seen at 74dB week 2 for 16kHz and week 12 for 24kHz. There are no changes in ABR amplitude for waves P2 in the group at 16kHz and 24kHz and P3 for 24kHz. For wave P3 there is a significant decrease in amplitude seen for 16kHz at 74dB (Table 19).

5.2.19 Summary of amplitude results

	P1	P2	P3
BC 16kHz	-	↓ week 1 94dB	↓ week 1 94dB
BC 24kHz	-	↓ week 1 94dB	↓ week 1 94dB,84dB
SC 16kHz	-	↓ week 1 94dB	↓ week 1 94dB,74dB
SC 24kHz	-	↓ week 1 94dB	↓ week 1 94dB, 74dB
P 16kHz	-	-	-
P 24kHz	-	-	-
PA 16kHz	-	-	↓ week 2 94dB ↓ week 2,16 74dB
PA24kHz	-	↑ week 16 84dB	-
PRif 16kHz	-	-	↓ week 2 74dB
PRif 24Hz	-	-	-
PClind 16kHz	↓ week 2 74dB	-	↓ week 12 74dB
PClind 24kHx	↓ week 12 74dB	-	-

Table 20: ***Summary of the changes in amplitude for waves P1-P3 measured at 16kHz and 24kHz for all experimental groups.***

All of the changes in amplitude seen in the control groups: biological control and surgical control are in P2 and P3 and all measured at week 1 and showed decreases. This is unexpected as the control groups ideally would not show any amplitude changes. This may be due to background electromagnetic noise and difficulties with interpretation of traces. Figure 63 is an example of a poor ABR trace and shows the difficulties in determining the waveform peaks. In contrast, Figure 64 is an example of a good quality ABR trace with clear waveforms easily identifiable.

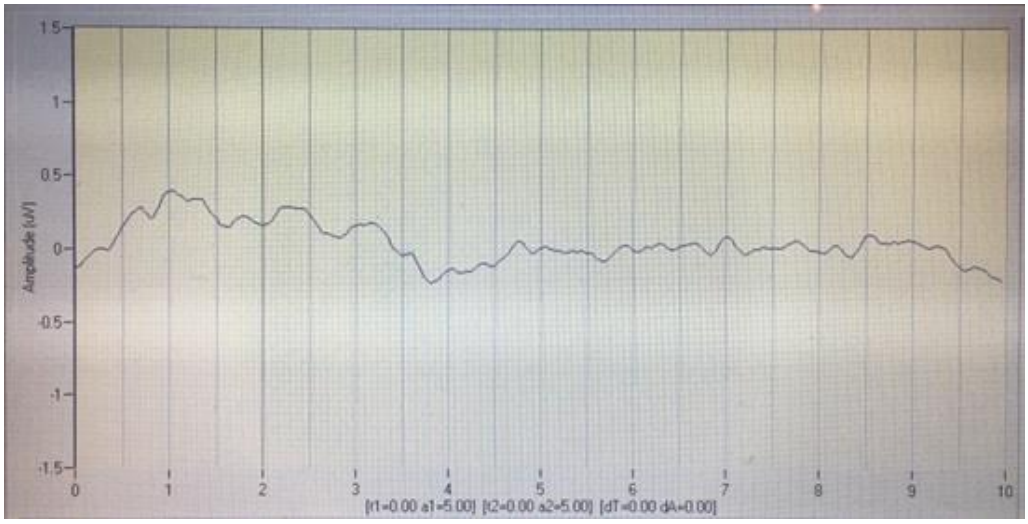


Figure 63: Example of ABR trace with poor definition of waveforms. Y axis: amplitude/mV, X axis time/msecs

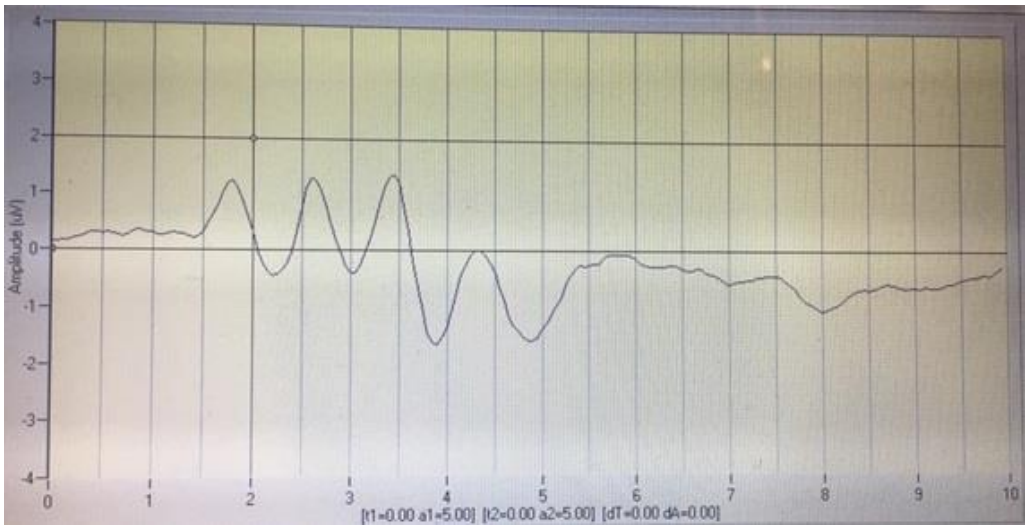


Figure 64: Example of ABR trace with good definition of waveforms. Y axis: amplitude/mV, X axis time/msecs

The significant changes identified with pellets loaded with both rifampicin and clindamycin were seen in P3 at weeks 2 and 16 at 74dB. This is the same finding with rifampicin pellets tested at 2 weeks and clindamycin pellets tested at 12 weeks suggesting that both rifampicin and clindamycin are contributing to this decrease in amplitude seen. Otherwise, the elevation seen from pellets loaded with antibiotics rifampicin and clindamycin at week 16 measured at 84dB cannot be attributed to any results seen from rifampicin and clindamycin studied separately. This is also the only significant result which is elevated, all other significant changes measured in amplitude are decreases.

The decreased mean amplitude in P1 measured at both 16kHz and 24kHz for ABR measured in guinea pigs laden with clindamycin pellets at weeks 2 and 12 without any changes seen in P1 values with pellets loaded with rifampicin and clindamycin together cannot be clearly explained. This inconsistency could potentially be attributable to noise and difficulties with interpretation of poor quality traces. This can be seen with some of the graphs having large error bars.

5.2.20 Amplitude results using Friedman's two way analysis of variance

Due to the variability of results around the mean values which is seen with the error bars, Friedman's two way analysis was used to identify significant excursions from the value at week 0. The results are shown for 16kHz and 24kHz analysing ABR waveform P1 (Table 21), for P2 (Table 22) and for P3 (Table 23).

	P1	94	84	74
16kHz	**BC**	0.49	0.31	0.32
16kHz	**SC**	0.386	0.23	0.153
16kHz	**P**	0.131	0.525	0.267
16kHz	**PA Rif + Clind**	0.576	0.55	0.149
24kHz	**BC**	0.298	0.876	0.515
24kHz	**SC**	0.166	0.674	0.768
24kHz	**P**	0.058	0.714	0.532
24kHz	**PA Rif + Clind**	0.478	0.802	0.766

Table 21: ***Results of Friedman's two way analysis of amplitude of wave P1. Significance denoted as p<0.05 marked with *.***

None of the Friedman's two way analysis of the amplitude results for ABR waveform P1 reached significance. Therefore there are no significant excursions from initial week 0 for the amplitude results on analysis of P1.

	P2	94	84	74
16kHz	**BC**	0.04*	0.663	0.252
16kHz	**SC**	0.064	0.386	0.166
16kHz	**P**	0.136	0.055	0.258
16kHz	**PA Rif + Clind**	0.277	0.043*	0.71
24kHz	**BC**	0.509	0.019*	0.021*
24kHz	**SC**	0.367	0.17	0.534
24kHz	**P**	0.949	0.385	0.421
24kHz	**PA Rif + Clind**	0.478	0.234	0.283

Table 22: ***Results of Friedman's two way analysis of amplitude wave P2. Significance denoted as p<0.05 marked with *.***

The amplitudes of ABR waveform P2 using Friedman's two way analysis show significant excursions from initial recordings at week 0 at 16kHz in the biological control group at 94dB and the group of guinea pigs laden with pellet containing rifampicin and clindamycin at 84dB. At 24kHz, significant excursions from initial recordings at week 0 were seen in the biological control group at 84dB and 74dB.

	P3	94	84	74
16kHz	**BC**	0.574	0.48	0.627
16kHz	**SC**	0.057	0.42	0.219
16kHz	**P**	0.214	0.296	0.701
16kHz	**PA Rif + Clind**	0.076	0.226	0.115
24kHz	**BC**	0.153	0.195	0.155
24kHz	**SC**	0.155	0.347	0.069
24kHz	**P**	0.053	0.946	0.461
24kHz	**PA Rif + Clind**	0.925	0.081	0.104

Table 23: ***Results of Friedman's two way analysis of amplitude of wave P3. Significance denoted as p<0.05 marked with *.***

Using Friedman's two way analysis, there are no significant excursions from initial recordings at week 0 at 16kHz and 24kHz for ABR waveform P3.

5.2.21 Summary of Friedman's two way analysis of amplitude

Overall, there are no consistent excursions from initial recordings at week 0 values for the amplitude results for ABR waveforms P1, P2 and P3. There are occasional excursions seen on analysis of the P2 waveform, but no pattern can be identified and three out of four involve the biological control group.

5.2.22 Holm- Bonferroni correction for the ABR amplitude data

Multiple comparisons were performed on the ABR amplitude data and therefore the Holm-Bonferroni correction was applied to the p values. This was done to minimise the risk of a Type I error.

Tables 24-35 show the Holm Bonferroni correction applied to the ABR amplitude data. There is only sporadic rejection of the null hypothesis which is highlighted red. Overall, this statistical correction therefore confirms the significance of the results from the t tests with no significant amplitude changes seen in the experimental groups in waves P1, P2 and P3 when analysed at 16kHz and 24 kHz.

BC 16kHz	P1	P2	P3
94dB	H1: 0.783 4	H1: 0.014 1 <0.0125	H1: 0.037 1>0.0125
	H2: 0.479 3	H2: 0.912 4	H2: 0.732 3
	H3: 0.460 2	H3: 0.052 2	H3: 0.981 4
	H4: 0.143 1>0.0125	H4: 0.071 3	H4: 0.467 2
84dB	H1: 0.169 2	H1: 0.513 4	H1: 0.082 1>0.0125
	H2: 0.069 1 >0.0125	H2: 0.304 3	H2: 0.532 4
	H3: 0.539 4	H3: 0.184 1>0.0125	H3: 0.278 3
	H4: 0.439 3	H4: 0.258 2	H4: 0.097 2
74dB	H1: 0.427 2	H1: 0.119 2	H1: 0.191 1>0.0125
	H2: 0.982 4	H2: 0.488 3	H2: 0.874 4
	H3: 0.262 1>0.0125	H3: 0.861 4	H3: 0.845 3
	H4: 0.805 3	H4: 0.115 1>0.0125	H4: 0.448 2

Table 24: ***Biological control amplitude p values at 16kHz and the Holm Bonferroni correction. Values where the null hypothesis is rejected are highlighted red.***

BC 24kHz	P1	P2	P3
94dB	H1: 0.238 1>0.0125	H1: 0.044 1 >0.0125	H1: 0.029 1>0.0125
	H2: 0.346 3	H2: 0.612 3	H2: 0.296 3
	H3: 0.300 2	H3: 0.379 2	H3: 0.161 2
	H4: 0.591 4	H4: 0.614 4	H4: 0.713 4
84dB	H1: 0.960 4	H1: 0.092 2	H1: 0.0001 1<0.0125
	H2: 0.600 2	H2: 0.068 1>0.0125	H2: 0.480 2>0.0167
	H3: 0.678 3	H3: 0.976 4	H3: 0.964 4
	H4: 0.462 1>0.0125	H4: 0.556 3	H4: 0.802 3
74dB	H1: 0.367 4	H1: 0.102 2	H1: 0.106 1>0.0125
	H2: 0.278 3	H2: 0.515 3	H2: 0.269 3
	H3: 0.091 1>0.0125	H3: 0.583 4	H3: 0.639 4
	H4: 0.115 2	H4: 0.093 1>0.0125	H4: 0.107 2

Table 25: ***Biological control amplitude p values at 24kHz and the Holm Bonferroni correction. Values where the null hypothesis is rejected are highlighted red.***

SC 16kHz	P1	P2	P3
94dB	H1: 0.484 3	H1: 0.009 1 <0.0125	H1: 0.005 1<0.0125
	H2: 0.103 1>0.0125	H2: 0.747 2	H2: 0.262 4
	H3: 0.464 2	H3: 0.847 4	H3: 0.151 3
	H4: 0.558 4	H4: 0.699 3	H4: 0.072 2>0.0167
84dB	H1: 0.200 1 >0.0125	H1: 0.017 1>0.0125	H1: 0.215 2
	H2: 0.899 3	H2: 0.324 2	H2: 0.535 4
	H3: 0.561 2	H3: 0.334 3	H3: 0.074 1>0.0125
	H4: 0.965 4	H4: 0.871 4	H4: 0.372 3
74dB	H1: 0.804 4	H1: 0.727 4	H1: 0.022 1>0.0125
	H2: 0.157 2	H2: 0.529 2	H2: 0.809 4
	H3: 0.065 1>0.0125	H3: 0.393 1>0.0125	H3: 0.502 2
	H4: 0.541 3	H4: 0.565 3	H4: 0.505 3

Table 26: ***Surgical control amplitude p values at 16kHz and the Holm Bonferroni correction. Values where the null hypothesis is rejected are highlighted red.***

SC 24kHz	P1	P2	P3
94dB	H1: 0.975 4	H1: 0.049 1<0.0125	H1: 0.030 2
	H2: 0.603 2	H2: 0.160 2	H2: 0.015 1>0.0125
	H3: 0.367 1>0.0125	H3: 0.617 4	H3: 0.216 4
	H4: 0.750 3	H4: 0.346 3	H4: 0.118 3
84dB	H1: 0.253 2	H1: 0.054 1>0.0125	H1: 0.092 1>0.0125
	H2: 0.215 1 >0.0125	H2: 0.566 3	H2: 0.885 4
	H3: 0.351 3	H3: 0.739 4	H3: 0.317 3
	H4: 0.374 4	H4: 0.494 2	H4: 0.140 2
74dB	H1: 0.995 4	H1: 0.167 1>0.0125	H1: 0.012 1>0.0125
	H2: 0.556 1>0.0125	H2: 0.555 3	H2: 0.449 4
	H3: 0.573 2	H3: 0.460 2	H3: 0.408 3
	H4: 0.691 3	H4: 0.799 4	H4: 0.024 2

Table 27: ***Surgical control amplitude p values at 24kHz and the Holm Bonferroni correction. Values where the null hypothesis is rejected are highlighted red.***

P 16kHz	P1	P2	P3
94dB	H1: 0.152 2	H1: 0.059 2	H1: 0.195 2
	H2: 0.049 1>0.0125	H2: 0.016 1<0.0125	H2: 0.060 1>0.0125
	H3: 0.470 4	H3: 0.115 4	H3: 0.504 4
	H4: 0.402 3	H4: 0.063 3	H4: 0.430 3
84dB	H1: 0.178 1>0.0125	H1: 0.106 1>0.0125	H1: 0.144 1>0.0125
	H2: 0.842 3	H2: 0.470 3	H2: 0.824 4
	H3: -	H3: 0.331 2	H3: 0.437 3
	H4: 0.545 2	H4: 0.934 4	H4: 0.271 2
74dB	H1: 0.518 4	H1: 0.129 1>0.0125	H1: 0.551 1>0.0125
	H2: 0.056 1>0.0125	H2: 0.559 3	H2: 0.930 3
	H3: 0.424 2	H3: 0.590 4	H3: 0.930 4
	H4: 0.428 3	H4: 0.484 2	H4: 0.921 2

Table 28: ***Pellet control amplitude p values at 16kHz and the Holm Bonferroni correction. Values where the null hypothesis is rejected are highlighted red.***

P 24kHz	P1	P2	P3
94dB	H1: 0.827 4	H1: 0.438 2	H1: 0.195 2
	H2: 0.241 2	H2: 0.388 1>0.0125	H2: 0.060 1>0.0125
	H3: 0.739 3	H3: 0.728 3	H3: 0.504 4
	H4: 0.069 1>0.0125	H4: 0.857 4	H4: 0.430 3
84dB	H1: 0.592 2	H1: 0.214 1>0.0125	H1: 0.144 1>0.0125
	H2: 0.512 1 >0.0125	H2: 0.982 4	H2: 0.824 4
	H3: 0.680 3	H3: 0.702 2	H3: 0.437 3
	H4: 0.813 4	H4: 0.783 3	H4: 0.271 2
74dB	H1: 0.320 1>0.0125	H1: 0.352 1>0.0125	H1: 0.551 1>0.0125
	H2: 0.350 2	H2: 0.884 4	H2: 0.930 3
	H3: 0.750 3	H3: 0.775 3	H3: 0.930 3
	H4: 0.933 4	H4: 0.556 2	H4: 0.921 2

Table 29: ***Pellet control amplitude p values at 24kHz and the Holm Bonferroni correction. Values where the null hypothesis is rejected are highlighted red.***

PA 16kHz	P1	P2	P3
94dB	H1: 0.431 3	H1: 0.191 1 >0.0125	H1: 0.001 1>0.0125
	H2: 0.811 4	H2: 0.464 3	H2: 0.047 2
	H3: 0.233 2	H3: 0.619 4	H3: 0.332 4
	H4: 0.142 1>0.0125	H4: 0.273 2	H4: 0.060 3
84dB	H1: 0.467 2	H1: 0.475 3	H1: 0.396 4
	H2: 0.528 3	H2: 0.207 1>0.0125	H2: 0.123 3
	H3: 0.418 1>0.0125	H3: 0.470 2	H3: 0.116 2
	H4: 0.759 4	H4: 0.731 4	H4: 0.097 1>0.0125
74dB	H1: 0.756 4	H1: 0.430 1>0.0125	H1: 0.474 3
	H2: 0.072 1>0.0125	H2: 0.530 2	H2: 0.037 2
	H3: 0.454 3	H3: 0.819 4	H3: 0.816 4
	H4: 0.345 2	H4: 0.542 3	H4: 0.030 1>0.0125

Table 30: ***Pellet with rifampicin and clindamycin amplitude p values at 16kHz and the Holm Bonferroni correction. Values where the null hypothesis is rejected are highlighted red.***

PA 24kHz	P1	P2	P3
94dB	H1: 0.220 2	H1: 0.880 4	H1: 0.830 1>0.0125
	H2: 0.580 3	H2: 0.520 3	H2: 0.980 3
	H3: 0.150 1>0.0125	H3: 0.110 1>0.0125	H3: 0.990 4
	H4: 0.810 4	H4: 0.350 2	H4: 0.850 2
84dB	H1: 0.320 2	H1: 0.770 3	H1: 0.300 2
	H2: 0.170 1 >0.0125	H2: 0.160 2	H2: 0.850 4
	H3: 0.390 3	H3: 0.070 1>0.0125	H3: 0.370 3
	H4: 0.590 4	H4: -	H4: 0.140 1>0.0125
74dB	H1: 0.710 4	H1: 0.850 4	H1: 0.070 1>0.0125
	H2: 0.580 2	H2: 0.600 3	H2: 0.070 1>0.0125
	H3: 0.670 3	H3: 0.160 1>0.0125	H3: 0.440 4
	H4: 0.170 1>0.0125	H4: 0.590 2	H4: 0.120 3

Table 31: ***Pellet with rifampicin and clindamycin amplitude p values at 24kHz and the Holm Bonferroni correction. Values where the null hypothesis is rejected are highlighted red.***

PRif 16kHz	P1	P2	P3
94dB	H1: -	H1: -	H1: -
	H2: 0.800 3	H2: 0.890 2	H2: 0.200 1
	H3: 0.260 1>0.0125	H3: 0.280 1>0.0125	H3: 0.330 2
	H4: 0.520 2	H4: 0.970 3	H4: 0.400 3
84dB	H1: 0.370 2	H1: -	H1: -
	H2: 0.310 1 >0.0125	H2: 0.810 3	H2: 0.120 1>0.0125
	H3: 0.580 4	H3: 0.130 1>0.0125	H3: 0.500 2
	H4: 0.520 3	H4: 0.700 2	H4: 0.570 3
74dB	H1: -	H1: -	H1: -
	H2: 0.740 1>0.0125	H2: 0.650 3	H2: 0.040 1>0.0125
	H3: 0.800 2	H3: 0.260 1	H3: 0.150 2
	H4: 0.800 2	H4: 0.260 1>0.0125	H4: 0.150 2

Table 32: ***Pellet with rifampicin amplitude p values at 16kHz and the Holm Bonferroni correction. Values where the null hypothesis is rejected are highlighted red.***

PRif 24kHz	P1	P2	P3
94dB	H1: -	H1: -	H1: -
	H2: 0.430 2	H2: 0.680 1>0.0125	H2: 0.087 1>0.0125
	H3: 0.477 3	H3: 0.705 2	H3: 0.781 3
	H4: 0.196 1>0.0125	H4: 0.947 3	H4: 0.217 2
84dB	H1: -	H1: -	H1: -
	H2: 0.560 3	H2: 0.182 1>0.0125	H2: 0.912 3
	H3: 0.142 1>0.0125	H3: 0.420 2	H3: 0.281 1>0.0125
	H4: 0.227 2	H4: 0.459 3	H4: 0.759 2
74dB	H1: -	H1: -	H1: -
	H2: 0.991 3	H2: 0.587 2	H2: 0.483 3
	H3: 0.162 1>0.0125	H3: 0.825 3	H3: 0.481 2
	H4: 0.260 2	H4: 0.346 1>0.0125	H4: 0.140 1>0.0125

Table 33: ***Pellet with rifampicin amplitude p values at 24kHz and the Holm Bonferroni correction. Values where the null hypothesis is rejected are highlighted red.***

PClind 16kHz	P1	P2	P3
94dB	H1: 0.370 1>0.0125	H1: 0.154 1	H1: 0.614 3
	H2: 0.970 3	H2: 0.630 2>0.0125	H2: 0.070 1>0.0125
	H3: 0.452 2	H3: 0.690 3	H3: 0.158 2
84dB	H1: 0.410 1>0.0125	H1: 0.420	H1: 0.423 2
	H2: 0.580 2	H2: 0.510 1>0.0125	H2: 0.156 1>0.0125
	H3: 0.940 3	H3: 0.540 2	H3: 0.633 3
74dB	H1: 0.030 1>0.0125	H1: 0.510 1>0.0125	H1: 0.320 2
	H2: 0.540 3	H2: 0.940 3	H2: 0.977 3
	H3: 0.529 2	H3: 0.560 2	H3: 0.030 1>0.0125

Table 34: ***Pellet with clindamycin amplitude p values at 16kHz and the Holm Bonferroni correction. Values where the null hypothesis is rejected are highlighted red.***

PClind 24kHz	P1	P2	P3
94dB	H1: 0.260 1>0.0125	H1: 0.663 3	H1: 0.305 3
	H2: 0.540 2	H2: 0.540 2	H2: 0.890 2
	H3: 0.970 3	H3: 0.218 1>0.0125	H3: 0.080 1>0.0125
84dB	H1: 0.980 3	H1: 0.186 2	H1: 0.640 3
	H2: 0.530 1 >0.0125	H2: 0.210 3	H2: 0.617 2
	H3: 0.770 2	H3: 0.040 1>0.0125	H3: 0.300 1>0.0125
74dB	H1: 0.890 3	H1: 0.840 3	H1: 0.220 3
	H2: 0.780 2	H2: 0.280 2	H2: 0.145 2
	H3: 0.040 1>0.0125	H3: 0.060 1>0.0125	H3: 0.052 1>0.0125

Table 35: ***Pellet with rifampicin clindamycin amplitude p values at 24kHz and the Holm Bonferroni correction. Values where the null hypothesis is rejected are highlighted red.***

5.2.23 Discussion of ABR amplitude results

The results of ABR amplitude measurement show that there is no consistent alteration in ABR amplitude across the groups. This is seen on analysis of ABR amplitude using the t-test analysis and Friedman's two way analysis of variance and applying the Holm Bonferroni correction. The ABR amplitude reduction of waves P1, P2 and P3 would indicate potential neurotoxicity to the auditory pathway as a sound wave is propagated from the cochlea to the cortex. Both amplitude decrease and increase may indicate damage to the auditory pathway.

ABR amplitude can be reduced, as seen with noise exposure (Kujawa *et al*., 2009), amikacin antibiotics (Nekrassov *et al*., 2000) and hyperthermia (Gold *et al*., 1985, Takahashi *et al*., 1991). These associations are frequently seen in conjunction with ABR threshold elevation, but not always.

ABR amplitude can also be increased as measured in the administration of sildenafil, a type-5 phosphodiesterase inhibitor (Hong 2008). Other studies using kanamycin in rats have shown an increase in ABR amplitude to precede ABR threshold elevation (Kuse *et al*., 2011). Both of these elevations indicate decreased auditory function.

No consistent changes in amplitude does not support any damage to the auditory pathway from the control groups and pellets loaded with rifampicin and clindamycin.

Another important measure for potential neurotoxicity is changes in the ABR latency. Both ABR amplitude and latency changes can be associated with threshold elevation.

Therefore, this was assessed for waves P1, P2 and P3 for each of the experimental groups. Analysis of waves P2 and P3 assessed the transmission of the auditory signal from the periphery to centrally and hence is another assessment for evidence of neurotoxicity.

5.3 ABR latency results analysis

5.3.1 Changes in latency of biological control group over 74-94dB at 16kHz

On analysis of wave P1, there was one significant increase in latency at 84dB at week 1 from 1.825 msecs to 2.1 msecs (p=0.012) (Figure 65).

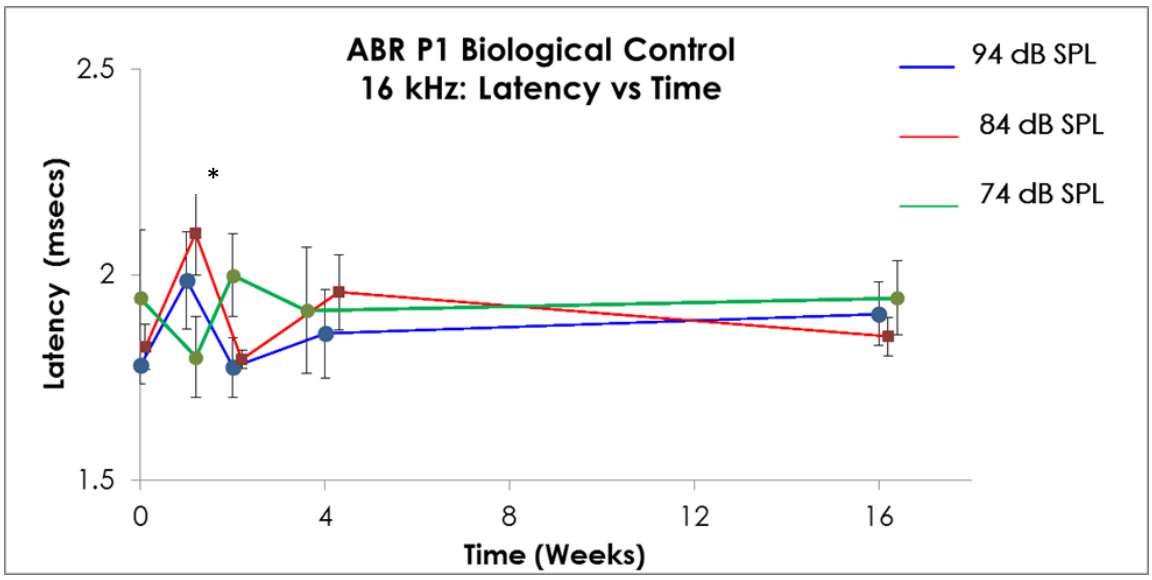


Figure 65: ***Changes in latency over time for biological control group at 16kHz analysing the P1 wave. Significance is denoted by a *.***

Wave P2 showed two latency values that were significantly elevated at week 1 for 94dB and 74dB (see Figure 66). The standard errors for this cohort of results however is high due to the variation in values.

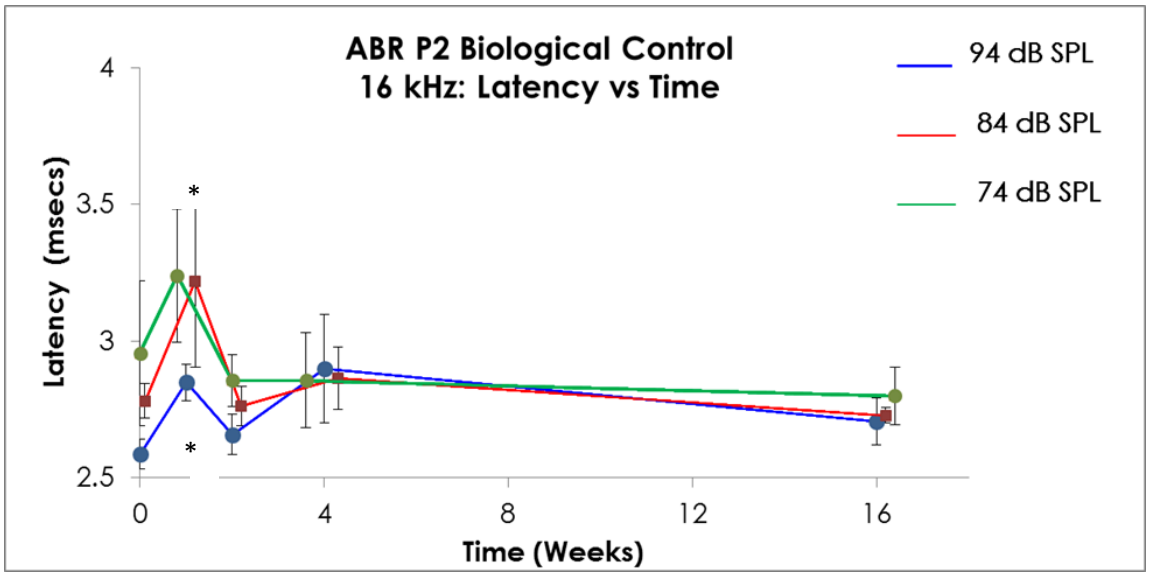


Figure 66: ***Changes in latency over time for biological control group at 16kHz analysing the P2 wave. Significance is denoted by a *.***

Analysis of wave P3 at 16kHz shows one significant elevation of latency at week 1 at 84kHz (p 0.043) (Figure 67).

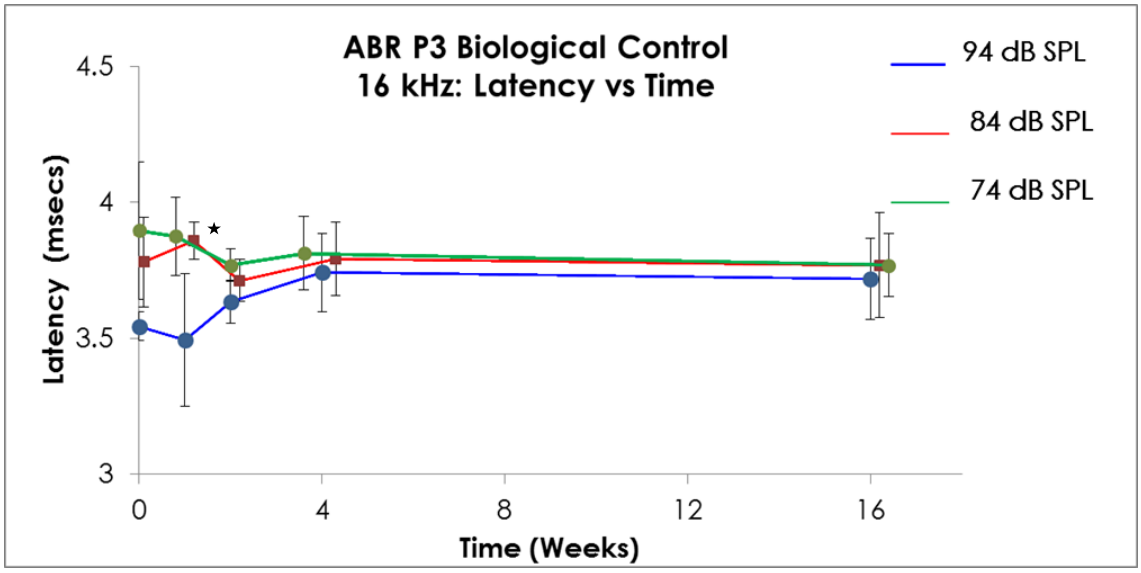


Figure 65: ***Changes in latency over time for biological control group at 16kHz analysing the P3 wave. Significance is denoted by a *.***

5.3.2 Changes in latency of biological control group over 74-94kHz at 24kHz

The biological control group at 24kHz shows no significant excursions from initial recordings at week 0 values on analysis of P1 for latency (Figure 68).

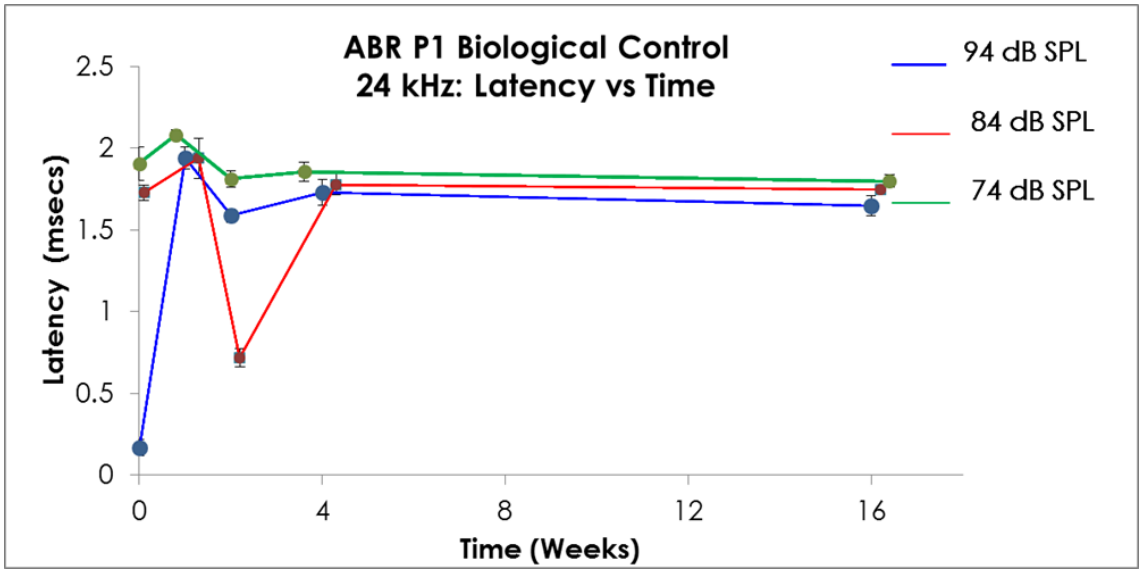


Figure 66: ***Changes in latency over time for biological control group at 24kHz analysing the P1 wave. Significance is denoted by a *.***

The biological control group at 24kHz shows no significant excursions from initial recordings at week 0 values on analysis of P2 for latency (Figure 69).

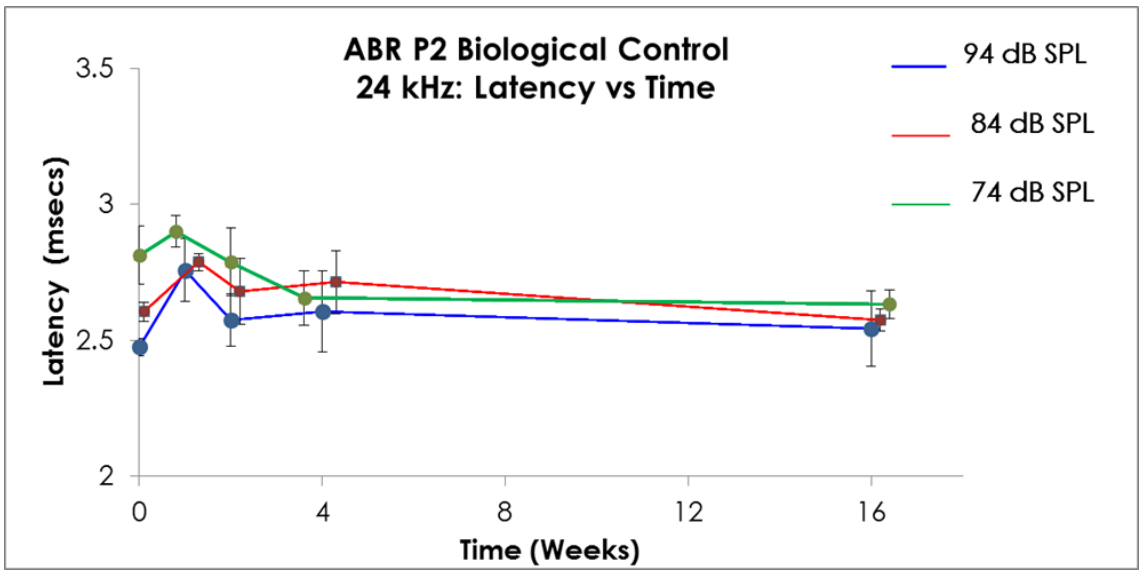


Figure 67: ***Changes in latency over time for biological control group at 24kHz analysing the P2 wave. Significance is denoted by a *.***

Analysing the latency of the biological control group at 24kHz for P3, there is one significant excursion from initial recordings at week 0 which is elevation at week 16 at 94dB (Figure 70).

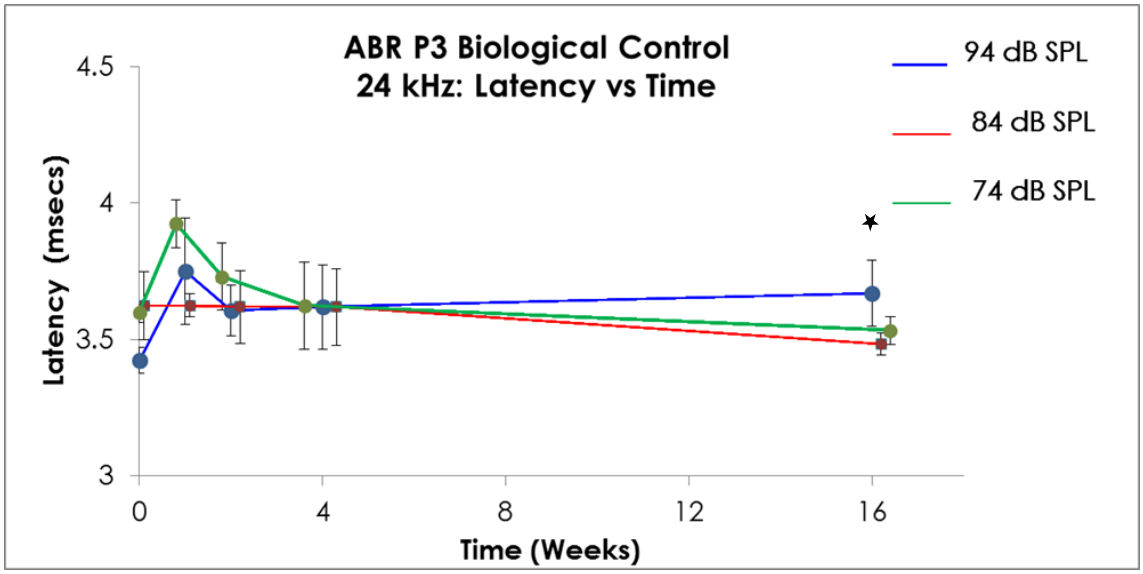


Figure 68: ***Changes in latency over time for biological control group at 16kHz analysing the P3 wave. Significance is denoted by a *.***

5.3.3 Summary of latency results of biological control group at 16kHz and 24kHz

	P1	P2	P3
Biological control 16kHz	↑week 1 84dB	↑week 1 74dB,94dB	↑week 1 84dB
Biological control 24kHz	-	-	↑week 16 94dB

Table 36: ***The changes in latency for waves P1-P3 measured at 16kHz and 24kHz for the biological control group.***

5.3.4 Surgical control group latency over time at 16kHz

On analysis of wave P1 there are significant increases in latency over time at week 1 and week 16 for 94dB at 16kHz (Figure 71). There is an increase from initial latency value of 1.656 msecs at week 0 to 1.95msecs at week 1 (p=0.01). There is also an increase to 1.836 msecs at week 16 (p=0.05).

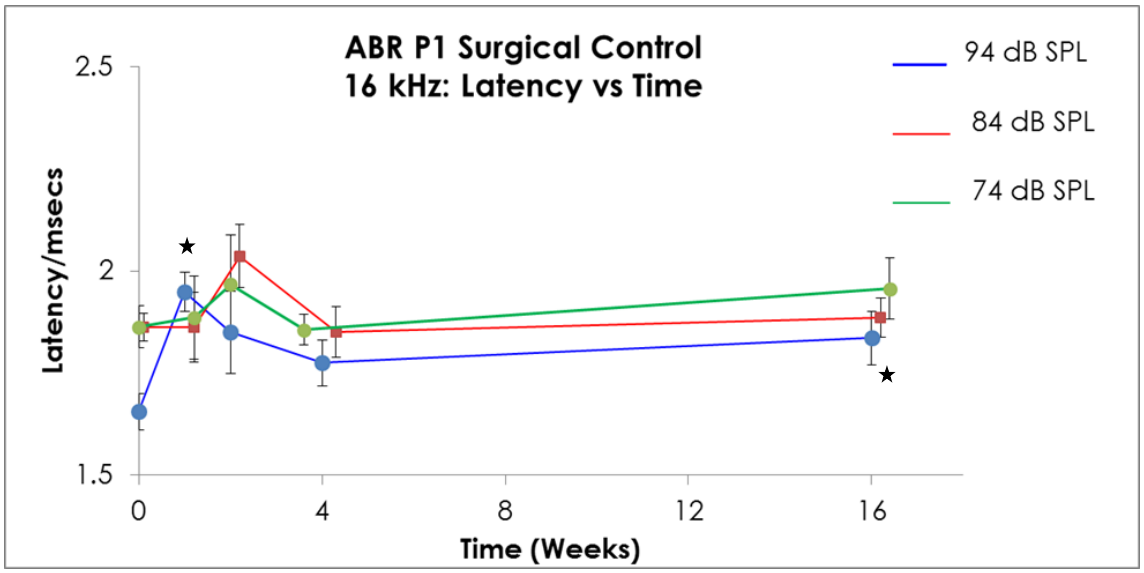


Figure 69: ***Changes in latency over time for surgical control group at 16kHz analysing the P1 wave. Significance is denoted by a *.***

Wave P2 shows a significant increase in latency from initial recordings of 2.55 msecs week 0 to 2.819 msecs at week 1 (p=0.03) at 94dB (Figure 72). At 84dB there is a significant increase from 2.638 msecs at week 0 to 2.788 msecs at week 4 (p=0.04). At 74dB there is also an increase in latency from initial recordings of 2.725msecs at week 0 to 2.917 msecs at week 1 (p=0.02).

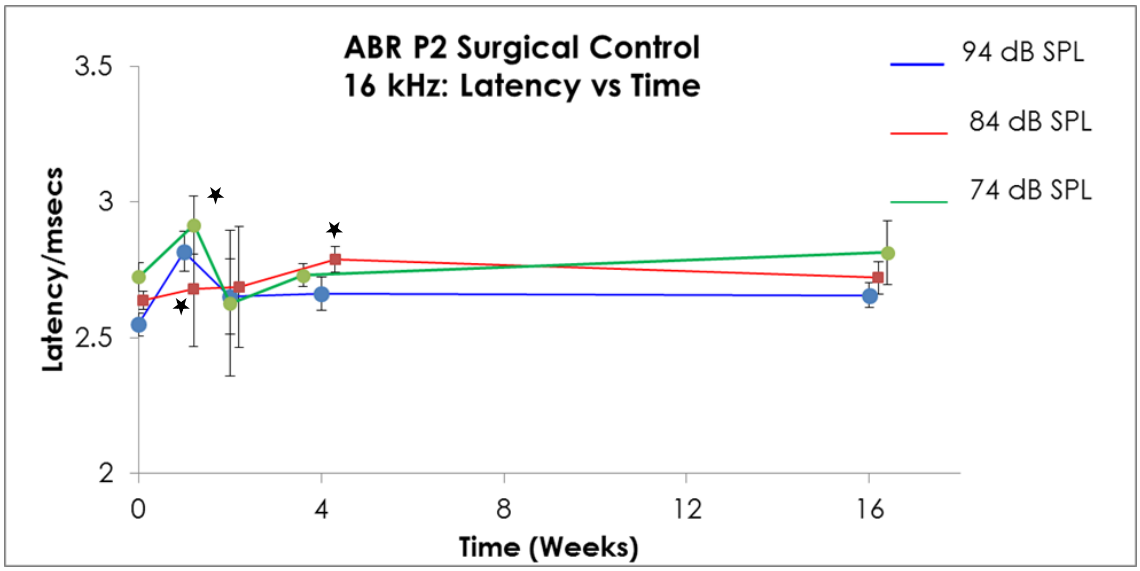


Figure 70: Changes in latency over time for surgical control group at 16kHz analysing the P2 wave. Significance is denoted by a *.

Analysis of wave P3 at 94dB shows a significant increase from initial recordings of 3.463 msecs at week 0 to 3.813 msecs at week 1 ($p<0.01$) and again 3.729 msecs at week 2 ($p =0.04$) (Figure 73). At 84 dB there is an increase in latency from initial recordings at week 0 of 3.52 msecs to 3.83 msecs at week 2 which reaches significance ($p=0.05$) and also at week 1 ($p=0.02$) for 74dB from 3.59mscesc to 3.8 msecs.

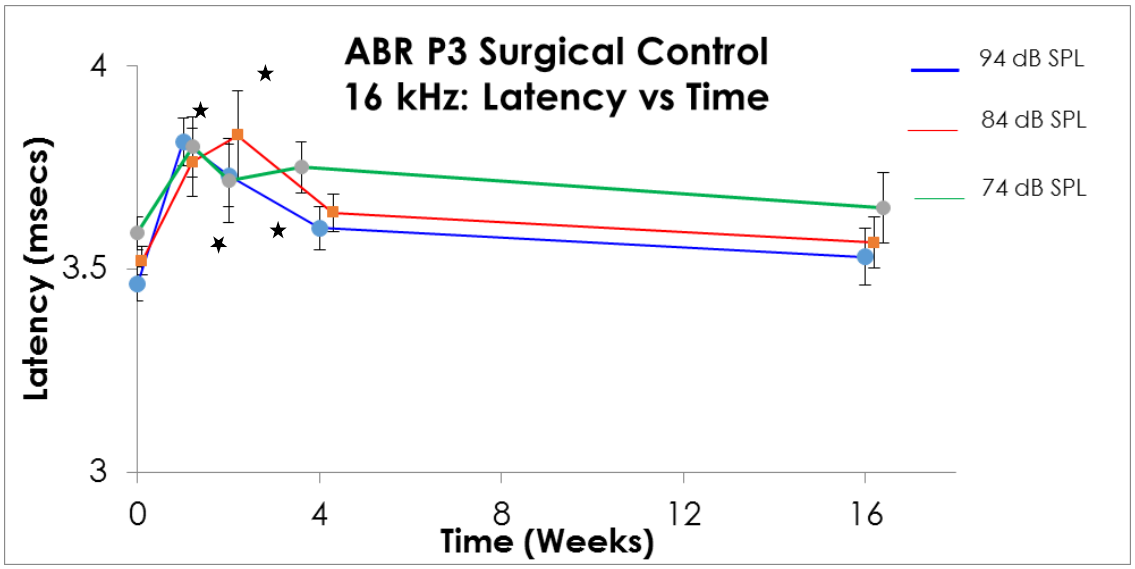


Figure 71: Changes in latency over time for surgical control group at 16kHz analysing the P3 wave. Significance is denoted by a *.

5.3.5 Surgical control group latency over time at 24kHz

On analysis of wave P1 there was a significant increase in latency from 1.538 msecs initially at week 0 to 1.857 msecs at week 1 ($p<0.01$) at 94dB (Figure 74).

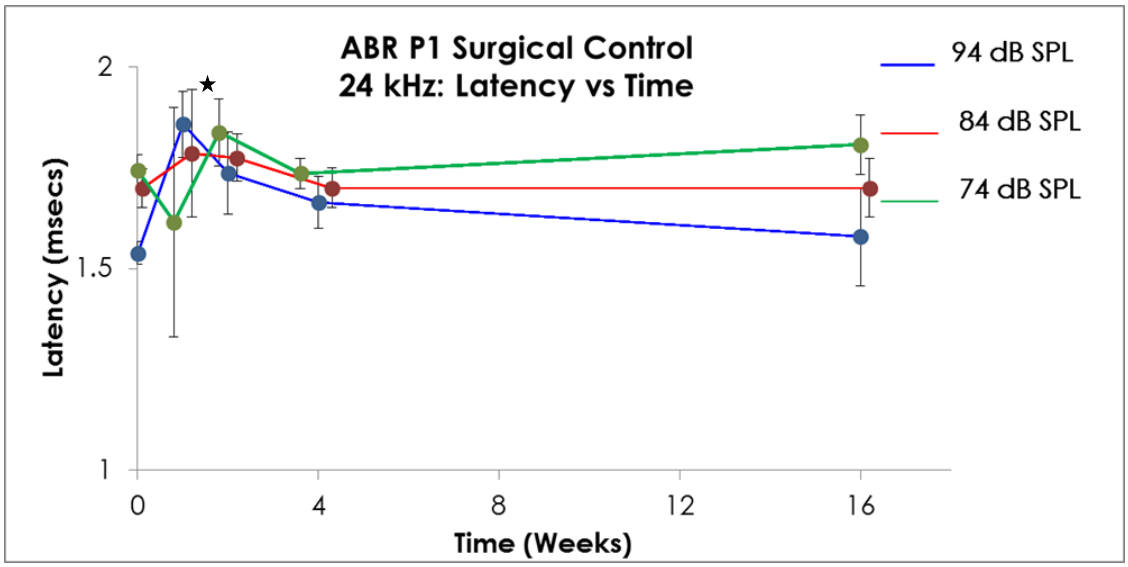


Figure 72: ***Changes in latency over time for surgical control group at 24kHz analysing the P1 wave. Significance is denoted by a *.***

For waves P2 and P3 there were no significant excursions from the mean latency at the onset of recording (week 0) seen over the experimental period of 16 weeks (Figures 75 and 76).

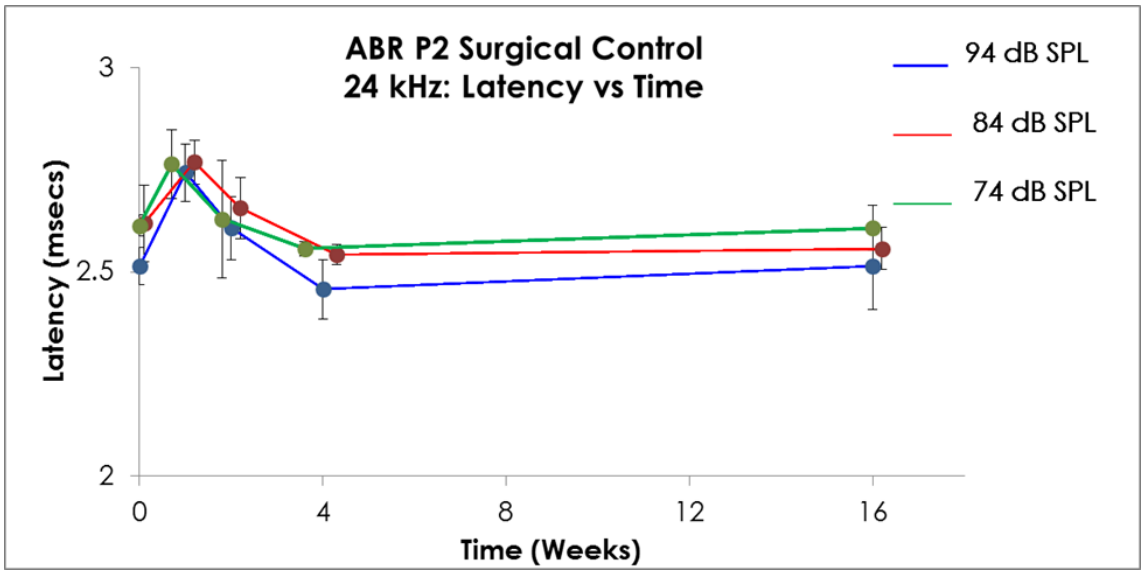


Figure 73: ***Changes in latency over time for surgical control group at 24kHz analysing the P2 wave. Significance is denoted by a *.***

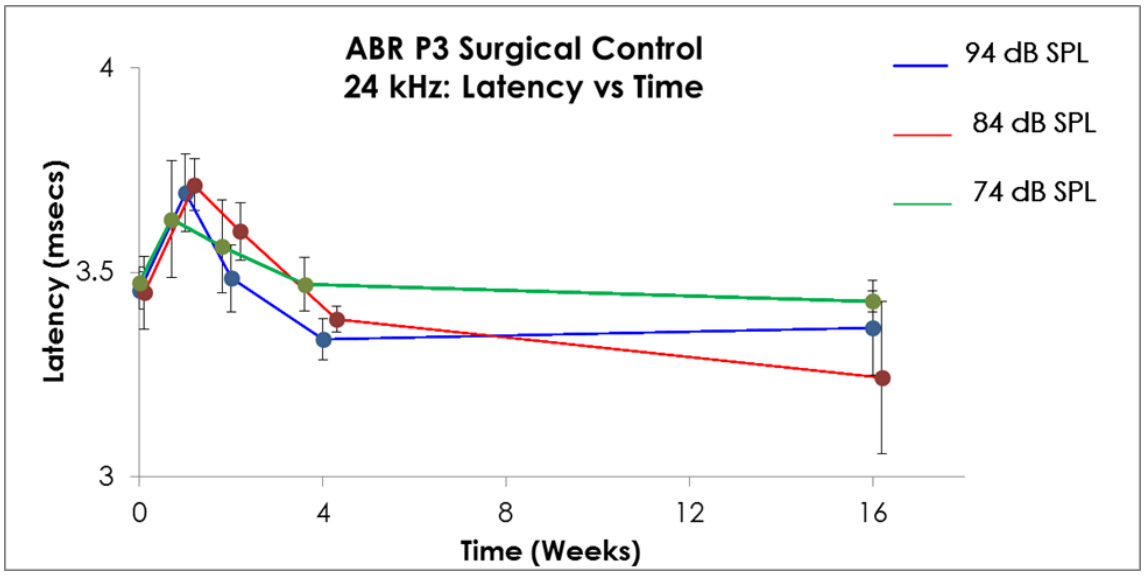


Figure 74: ***Changes in latency over time for surgical control group at 24kHz analysing the P3 wave. Significance is denoted by a *.***

5.3.6 Summary of latency results of surgical control group at 16kHz and 24kHz

	P1	P2	P3
surgical control 16kHz	↑week 1 94dB ↑week 16 94dB	↑week 1 74dB, 94dB ↑week 4 84dB	↑week 1, 2 94dB ↑week 1, 2 84dB
surgical control 24kHz	↑week 1 94dB	-	-

Table 37: ***Changes in latency for waves P1-P3 measured at 16kHz and 24kHz for the surgical control group.***

Overall, the latency results for the SC group show changes in P1 at week 1 for 94dB at 16kHz and 24kHz (Table 37). There was also an increase in latency for week 16 at 16kHz. Waves had increase at week 1 for 94dB and 74dB for 16kHz and week 4 increase at 84dB. Wave P3 had increased latency seen in week 1 for 84 and 94dB. There were no significant excursions from week 0 values for P2 and P3 over 16 weeks.

5.3.7 Pellet control group latency over time at 16kHz

There was a significant increase in latency for wave P1 at 94dB from 1.71 msecs at initial week 0 readings to 1.89 msecs at week 1 (p=0.05) (Figure 75).

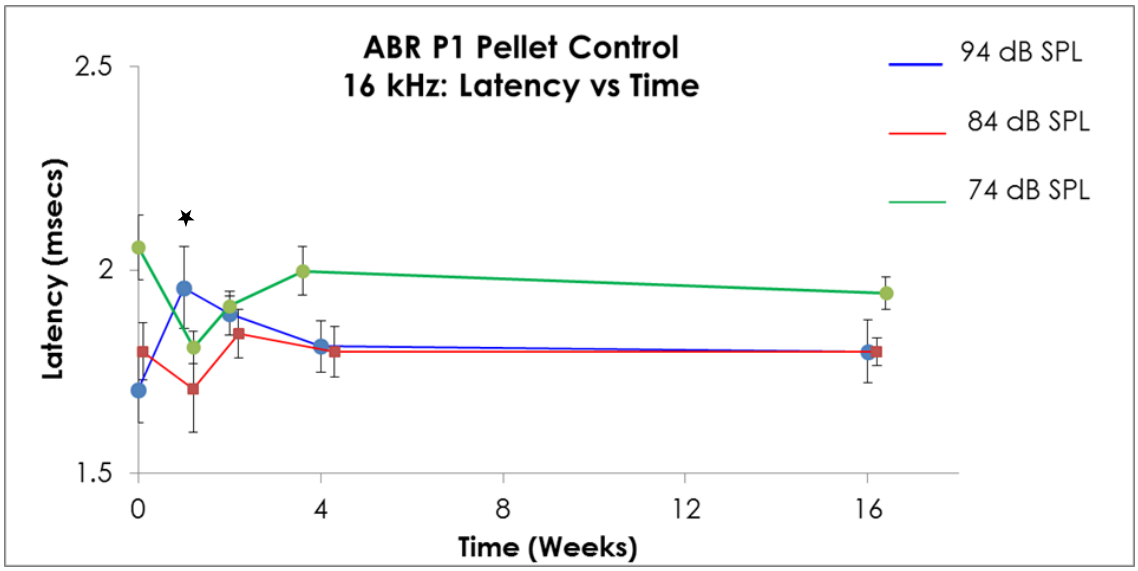


Figure 75: ***Changes in latency over time for PLGA and pluronic control group at 16kHz analysing the P1 wave. Significance is denoted by a *.***

At 16kHz there are was one significant increase in latency from 2.57 msecs initially at week 0 to 2.89msces at week 2 (p=0.02) at 94dB (Figure 78).

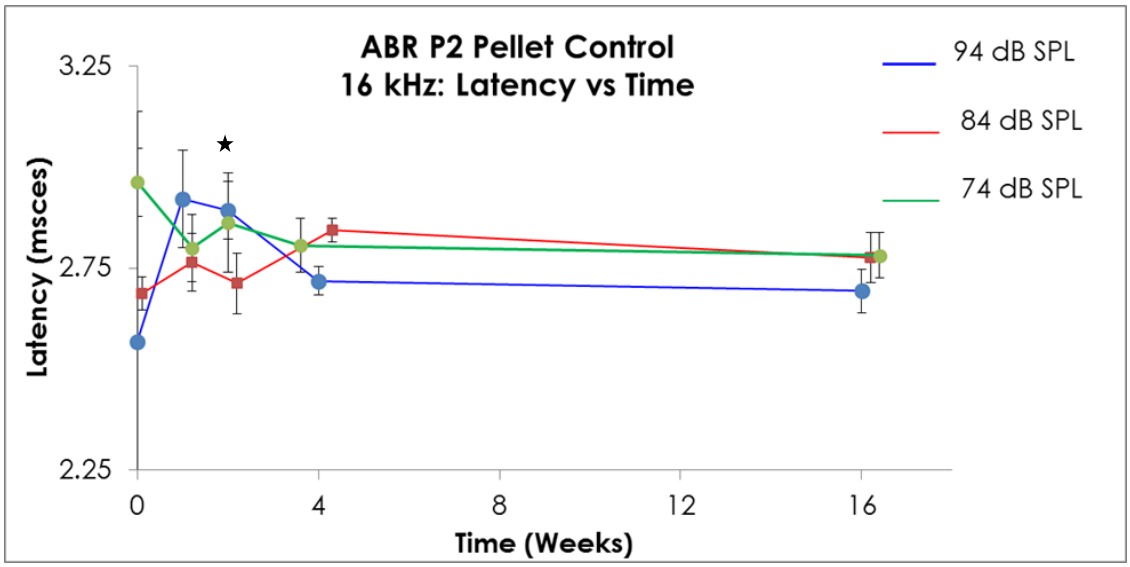


Figure 76: ***Changes in latency over time for PLGA and pluronic control group at 16kHz analysing the P2 wave. Significance is denoted by a *.***

There is one significant decrease in latency at 74dB on analysis of wave P3 from 3.92 msecs measured initially at week 0 to 3.62 msecs at week 16 (Figure 79).

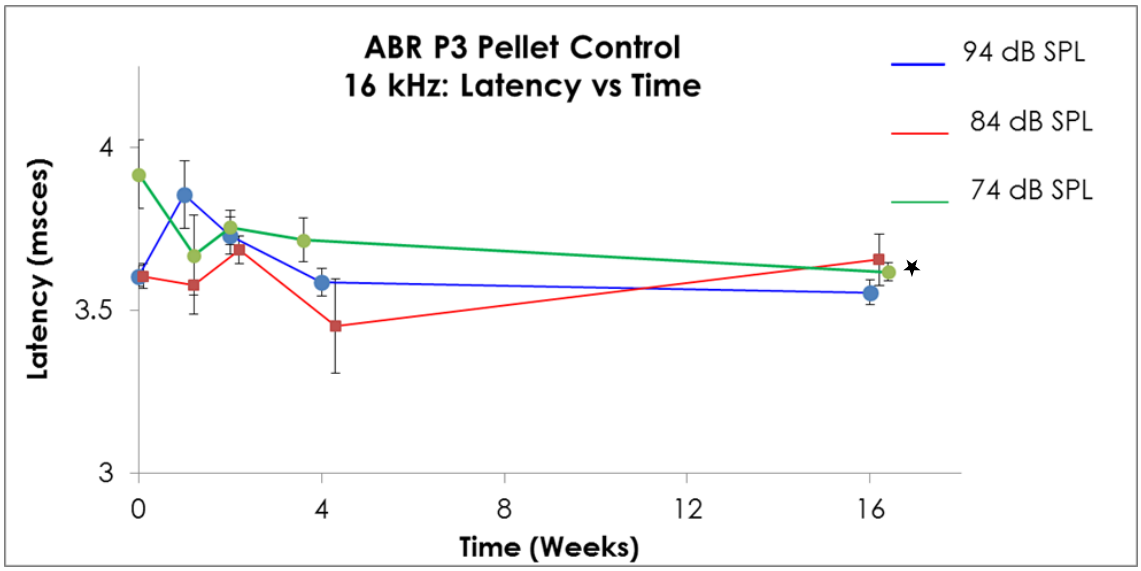


Figure 77: ***Changes in latency over time for PLGA and pluronic control group at 16kHz analysing the P3 wave. Significance is denoted by a *.***

5.3.8 Pellet control group latency over time 24kHz

There were no significant excursions from initial readings at week 0 for latency values on analysis of waves P1 or P2 for the pellet control group at 24kHz (Figures 78 and 79).

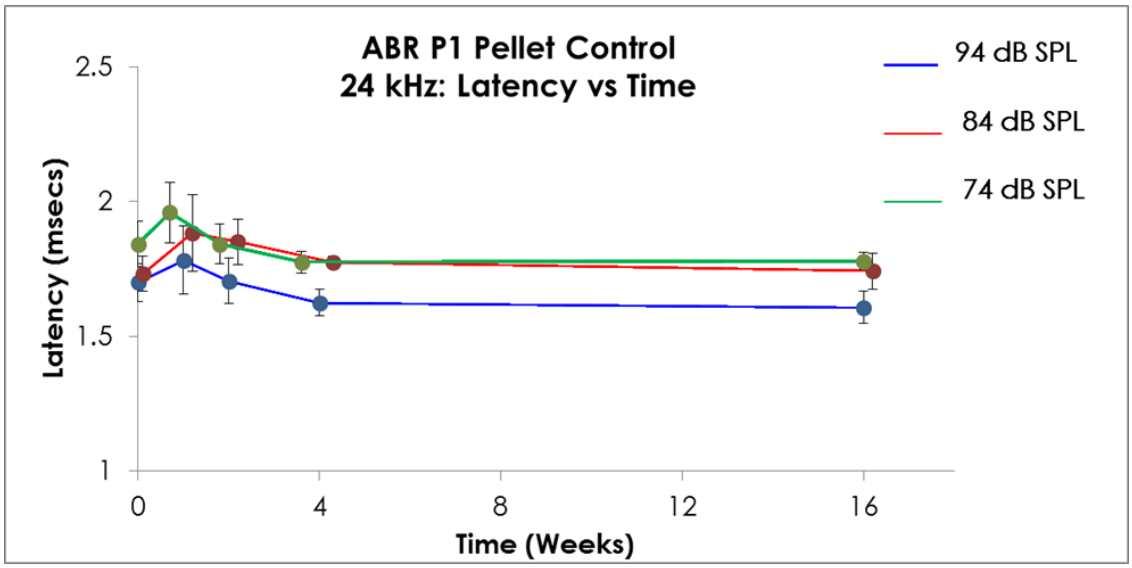


Figure 78: ***Changes in latency over time for PLGA and pluronic control group at 16kHz analysing the P1 wave. Significance is denoted by a *.***

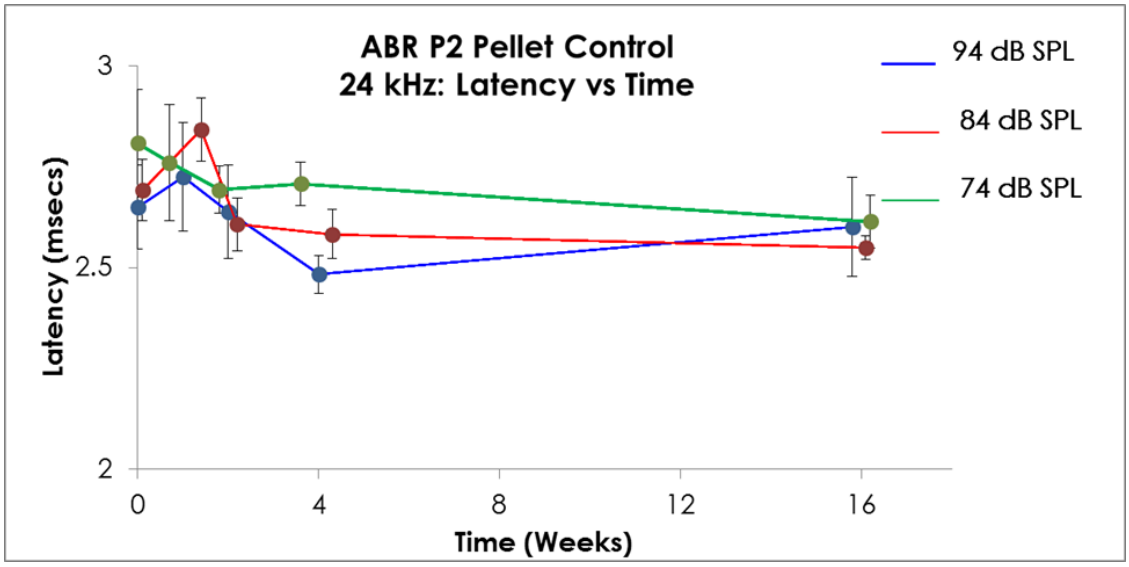


Figure 79: ***Changes in latency over time for PLGA and pluronic control group at 24kHz analysing the P2 wave. Significance is denoted by a *.***

For wave P3 there was a significant decrease in latency from 3.61msecs recorded initially at week 0 to 3.47 msecs at week 4 (p=0.067) at 94dB.

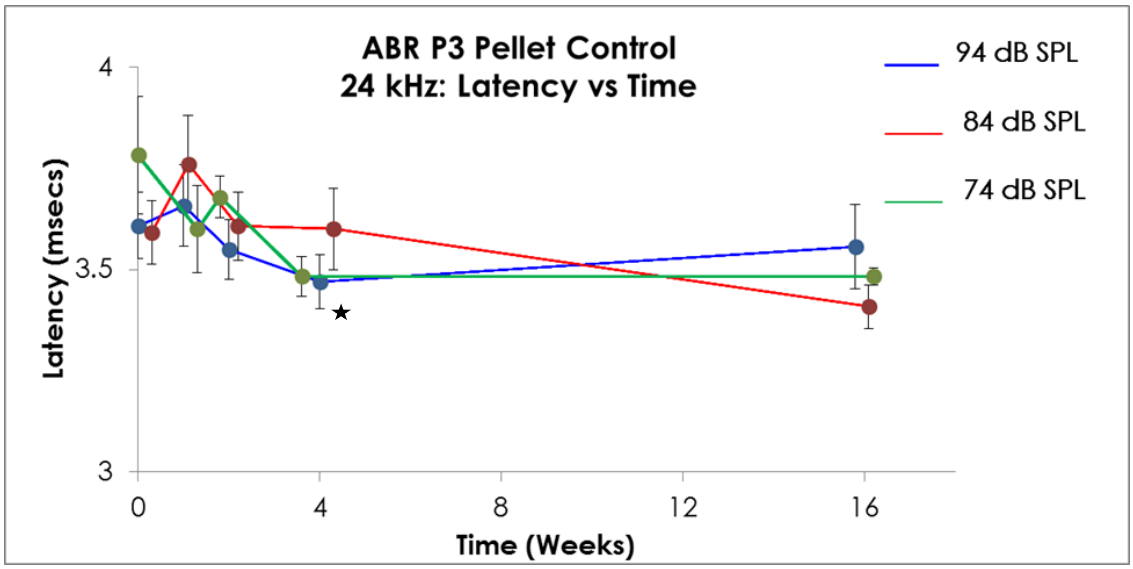


Figure 80: ***Changes in latency over time for PLGA and pluronic control group at 24kHz analysing the P3 wave. Significance is denoted by a *.***

5.3.9 Summary of changes in latency results of PLGA and pluronic pellet control group at 16kHz and 24kHz

	P1	P2	P3
pellet control 16kHz	↑ week 2 94dB	↑ week 2 94dB	↓week 16 94dB
pellet control 24kHz	-	-	↓week 4 94dB

Table 38: ***Changes in latency for waves P1-P3 measured at 16kHz and 24kHz for the PLGA and pluronic pellet control group.***

Overall, the latency results for the pellet control group show increase in P1 and P2 at week 2 and 94dB. There is a decrease in latency seen on analysis of P3 at 94dB at week 16 for 16kHz and week 4 94dB at 24kHz (Table 38).

5.3.10 Changes in ABR latency of PLGA and pluronic pellet with rifampicin and clindamycin in combination over 74-94dB at 16kHz

On analysis of the waves P1, P2 and P3 there were no significant excursions from the values at week 0 for latency at 74-94dB (Figures 83,84 and 85).

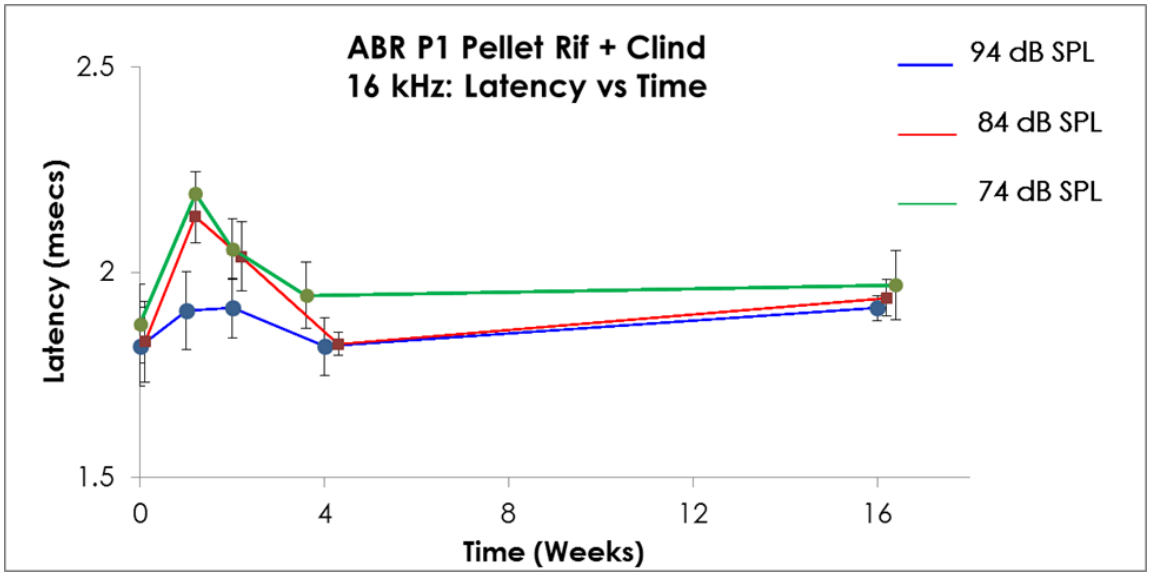


Figure 81: ***Changes in latency over time for PLGA and pluronic pellet with rifampicin and clindamycin in combination at 16kHz analysing the P1 wave. Significance is denoted by a *.***

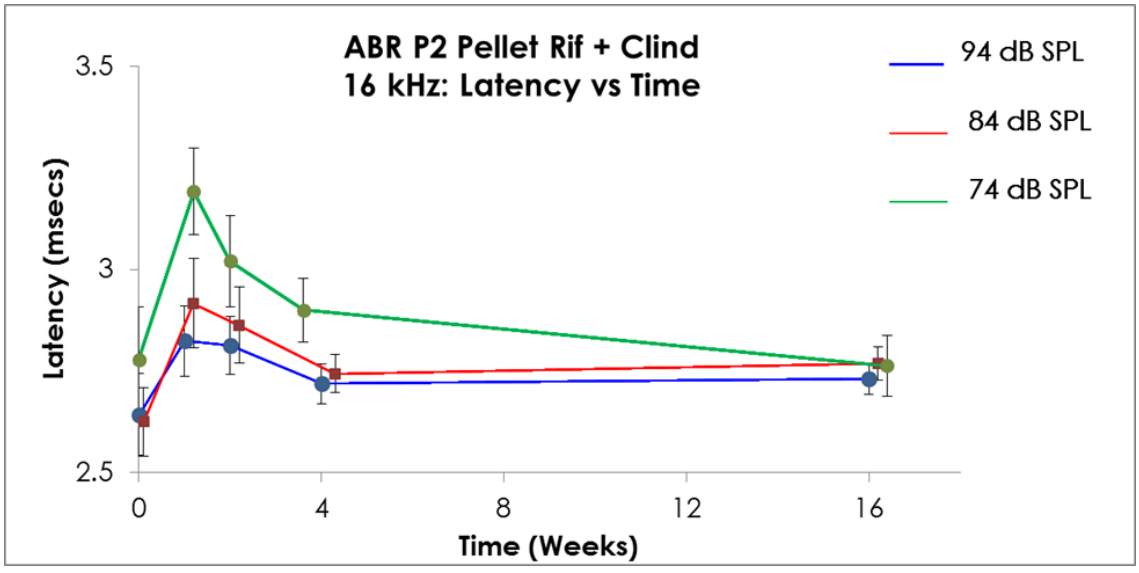


Figure 82: ***Changes in latency over time for PLGA and pluronic pellet with rifampicin and clindamycin in combination at 16kHz analysing the P2 wave. Significance is denoted by a *.***

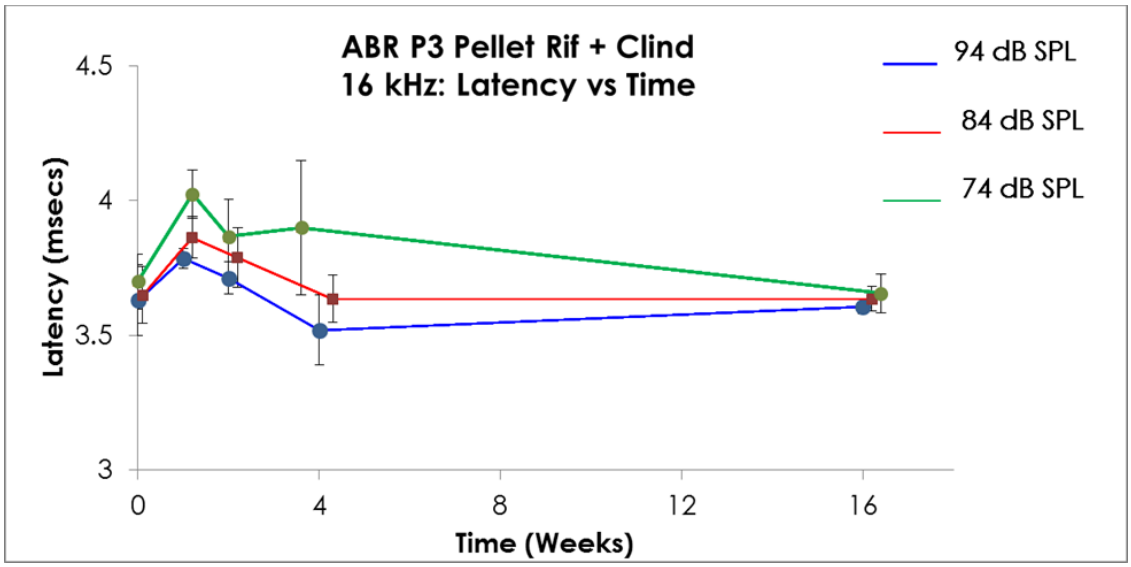


Figure 83: ***Changes in latency over time for PLGA and pluronic pellet with rifampicin and clindamycin in combination at 16kHz analysing the P3 wave. Significance is denoted by a *.***

5.3.11 Changes in ABR latency of PLGA and pluronic pellet with rifampicin and clindamycin in combination over 74-94dB at 24kHz

On analysis of wave P1 there are no significant excursions from the latency values between initial recordings at week 0 and week 16 (Figure 86).

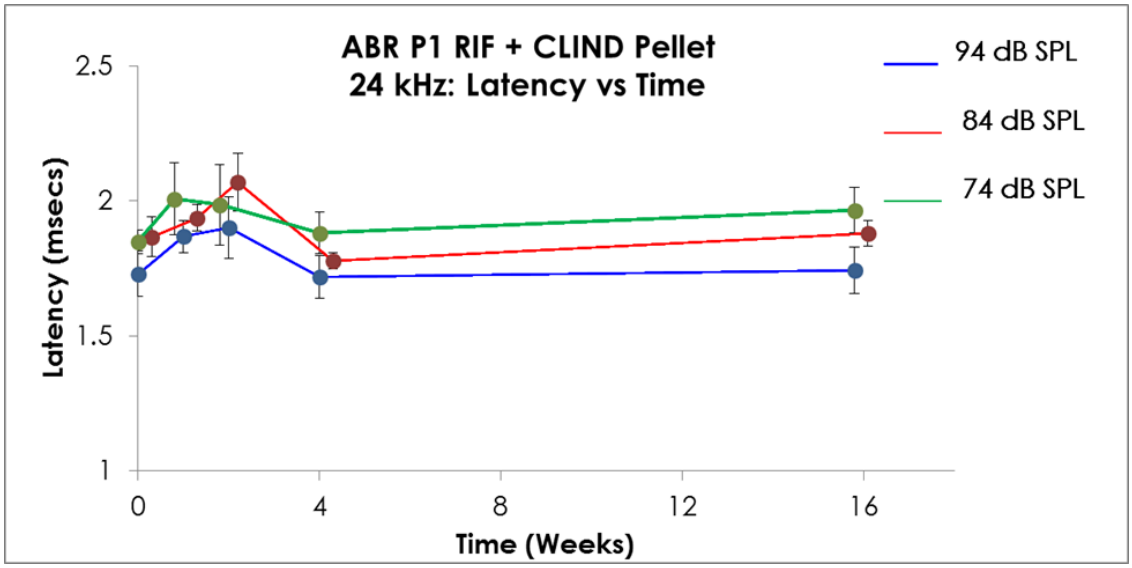


Figure 84: ***Changes in latency over time for PLGA and pluronic control with rifampicin and clindamycin in combination at 24kHz analysing the P1 wave. Significance is denoted by a *.***

For wave P2 there was one significant increase in latency from 2.65msecs initially at week 0 to 3.006 msecs at week 2 ($p<0.01$) at 84dB (Figure 87).

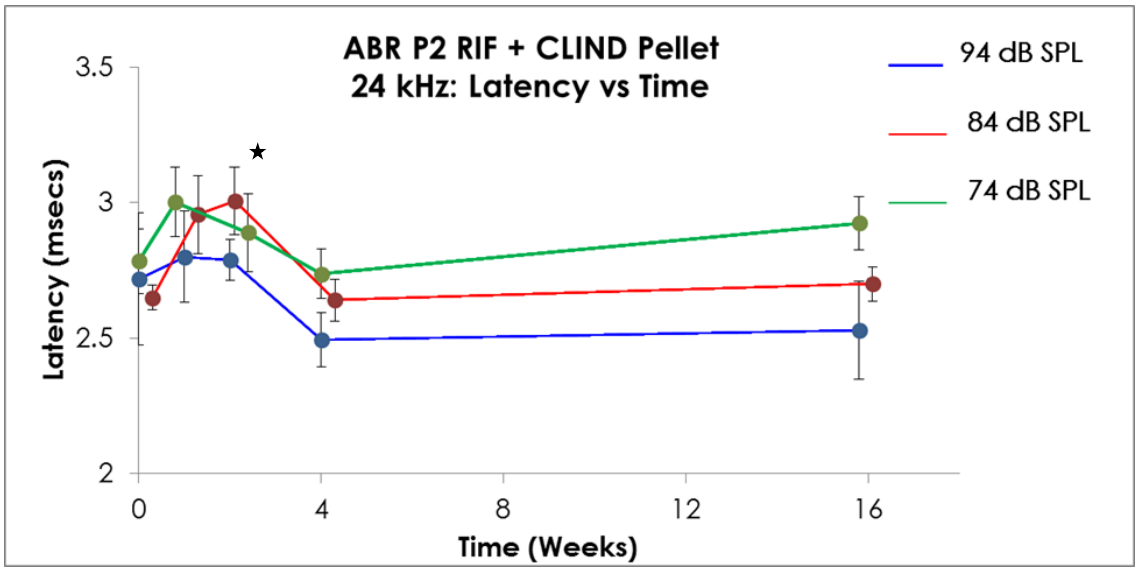


Figure 85: ***Changes in latency over time for PLGA and pluronic pellet with rifampicin and clindamycin in combination at 24kHz analysing the P2 wave. Significance is denoted by a *.***

On analysis of wave P3 there are no significant excursions from the latency values between initial recordings at week 0 and week 16 (Figure 88).

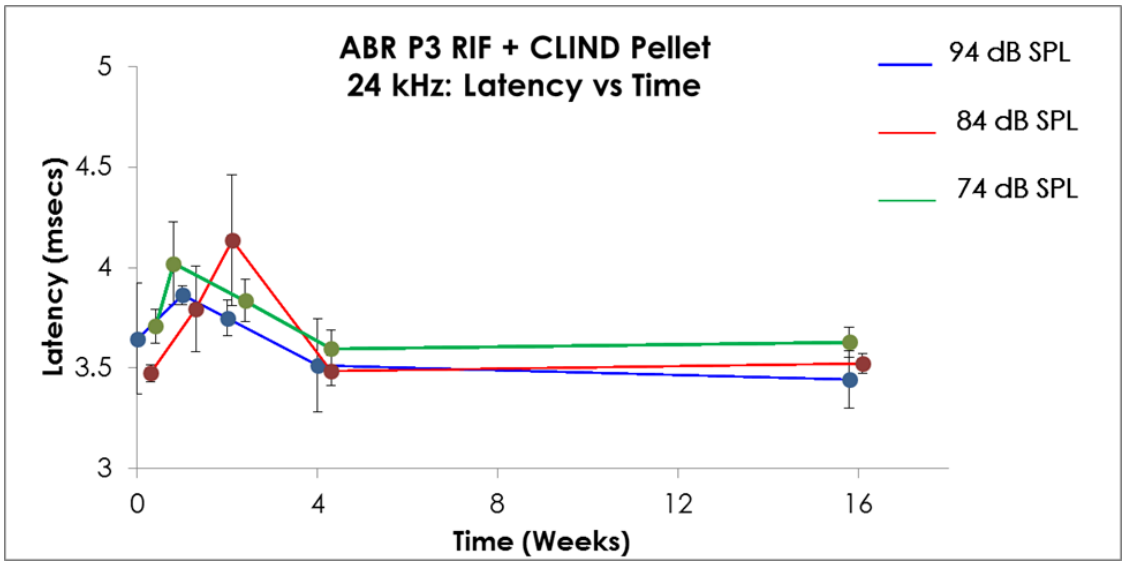


Figure 86: ***Changes in latency over time for PLGA and pluronic pellet with rifampicin and clindamycin in combination at 24kHz analysing the P3 wave. Significance is denoted by a *.***

5.3.12 Summary of changes in latency results of pellet with rifampicin and clindamycin pellets at 16kHz and 24kHz

	P1	P2	P3
Pellet rifampicin + clindamycin 16kHz	-	-	-
Pellet rifampicin + clindamycin 24kHz	-	↑ week 2 84dB	-

Table 39: ***The changes in latency for waves P1-P3 measured at 16kHz and 24kHz for the PLGA and pluronic loaded with rifampicin and clindamycin group.***

Overall, the latency results for the pellet loaded with rifampicin and clindamycin show no significant excursions from week 0 for 16kHz at P1, P2 and P3 and also P1 and P3 for 24kHz (Table 39). A significant increase in latency for P2 seem at week 2 for 84dB at 24kHz.

5.3.13 Changes in ABR latency of PLGA and pluronic pellet with rifampicin over 74-94dB at 16kHz

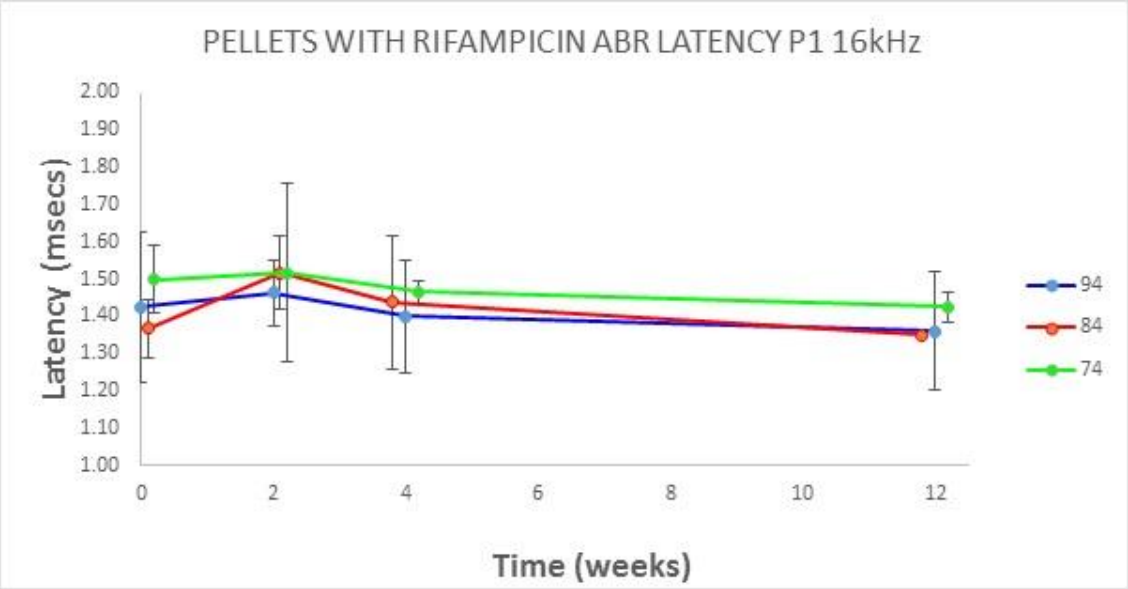


Figure 87: ***Changes in amplitude over time for PLGA and pluronic control with rifampicin and clindamycin in combination at 16kHz analysing the P1 wave. Significance is denoted by a *.***

On analysis of the waves P1, P2 and P3 there is no significant excursions from the initial values at week 0 for latency at 74dB, 84dB and 94dB for 16kHz (Figures 89, 90 and 91).

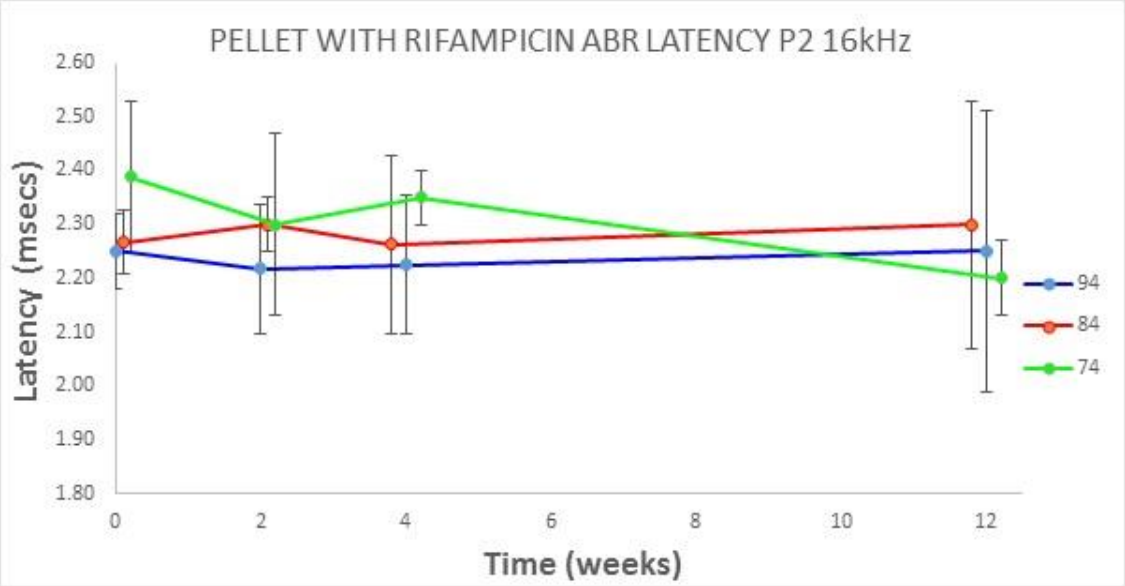


Figure 88*: Changes in amplitude over time for PLGA and pluronic pellet with rifampicin at 16kHz analysing the P2 wave. Significance is denoted by a **.*

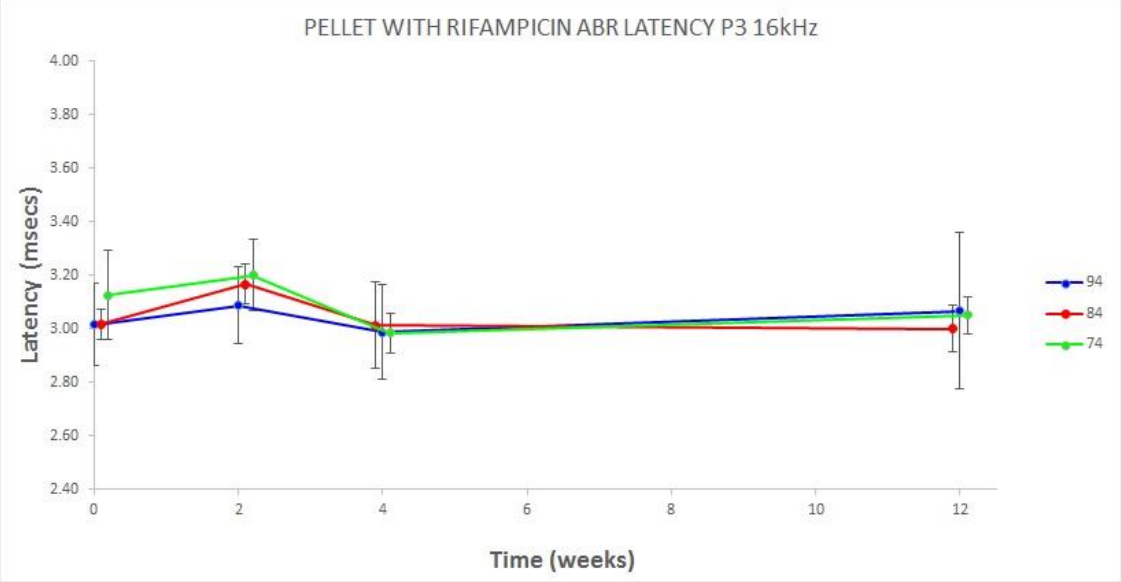


Figure 89: ***Changes in amplitude over time for PLGA and pluronic pellet with rifampicin at 16kHz analysing the P3 wave. Significance is denoted by a **.***

5.3.14 Changes in ABR latency of PLGA and pluronic pellet with rifampicin over 74-94dB at 24kHz

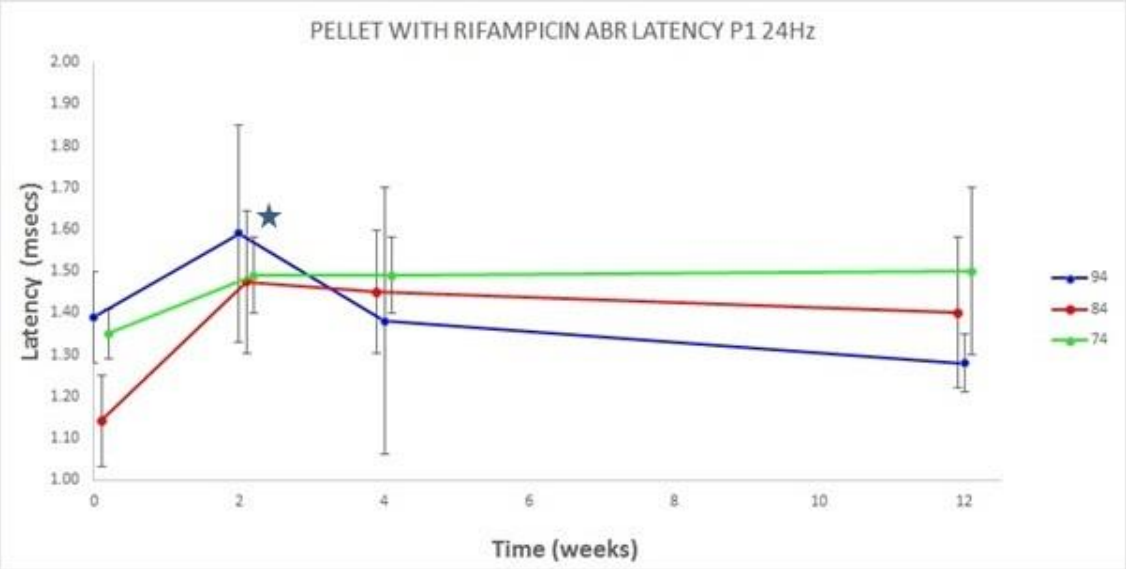


Figure 90: ***Changes in amplitude over time for PLGA and pluronic pellet with rifampicin at 24kHz analysing the P1 wave. Significance is denoted by a *.***

On analysis of wave P1 there was one significant increase in mean latency at week 2 for 74dB from 1.35 initially at week 0 to 1.49 at week 2 (p=0.04) (Figure 90).

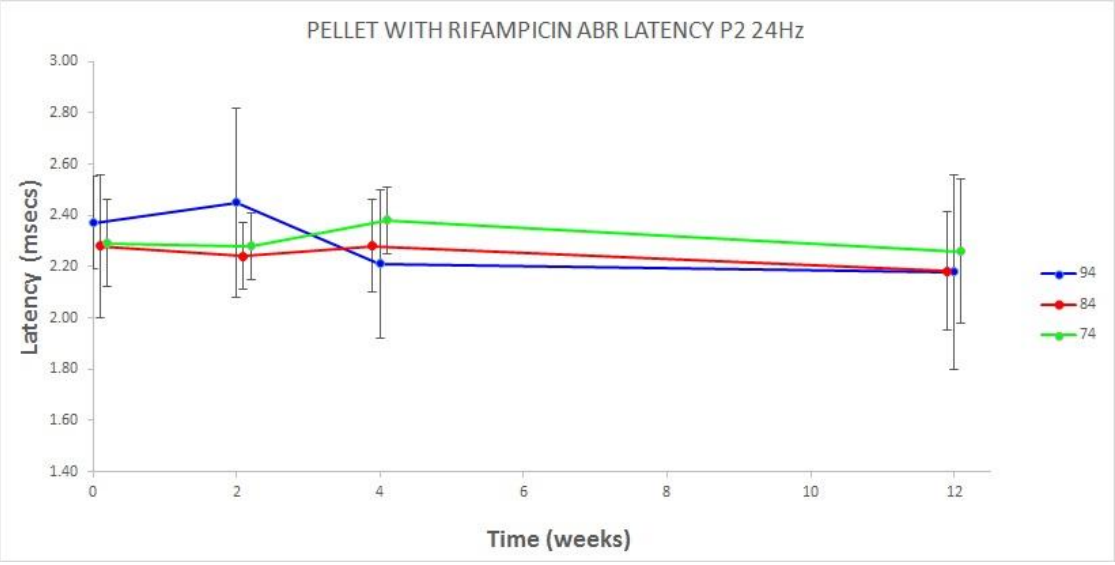


Figure 91: ***Changes in amplitude over time for PLGA and pluronic pellet with rifampicin at 24kHz analysing the P2 wave. Significance is denoted by a *.***

On analysis of the waves P2 and P3 there are no significant excursions from the values at week 0 for latency at 74dB, 84dB and 94dB (Figures 93 and 94).

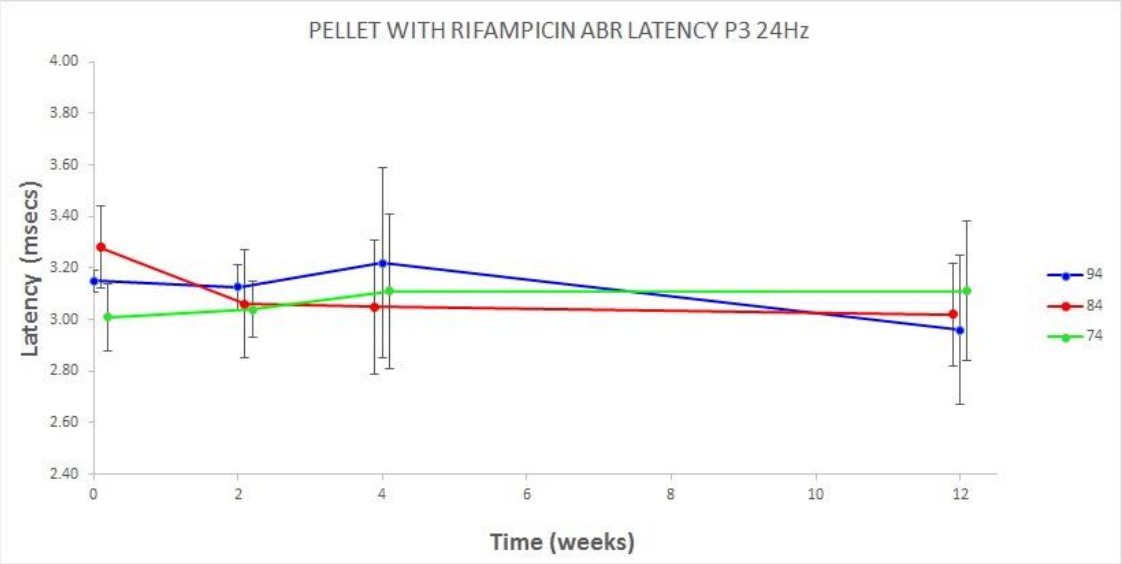


Figure 92: ***Changes in amplitude over time for PLGA and pluronic pellet with rifampicin at 24kHz analysing the P3 wave. Significance is denoted by a *.***

5.3.15 Summary of latency results pellet loaded with rifampicin 16kHz and 24kHz

	P1	P2	P3
Pellet + Rifampicin 16kHz	-	-	-
Pellet + Rifampicin 24kHz	↑week 2 74dB	-	-

Table 40: ***Changes in latency for waves P1-P3 measured at 16kHz and 24kHz for the PLGA and pluronic loaded with rifampicin group.***

For wave P1 there is a significant increase in amplitude seen at 74dB week 2 for 24kHz. There are no other changes in ABR latency for waves P2 and P3 in the group at 16kHz and 24kHz (Table 40).

5.3.16 Changes in ABR latency of PLGA and pluronic pellet with clindamycin pellet over 74-94dB at 16kHz

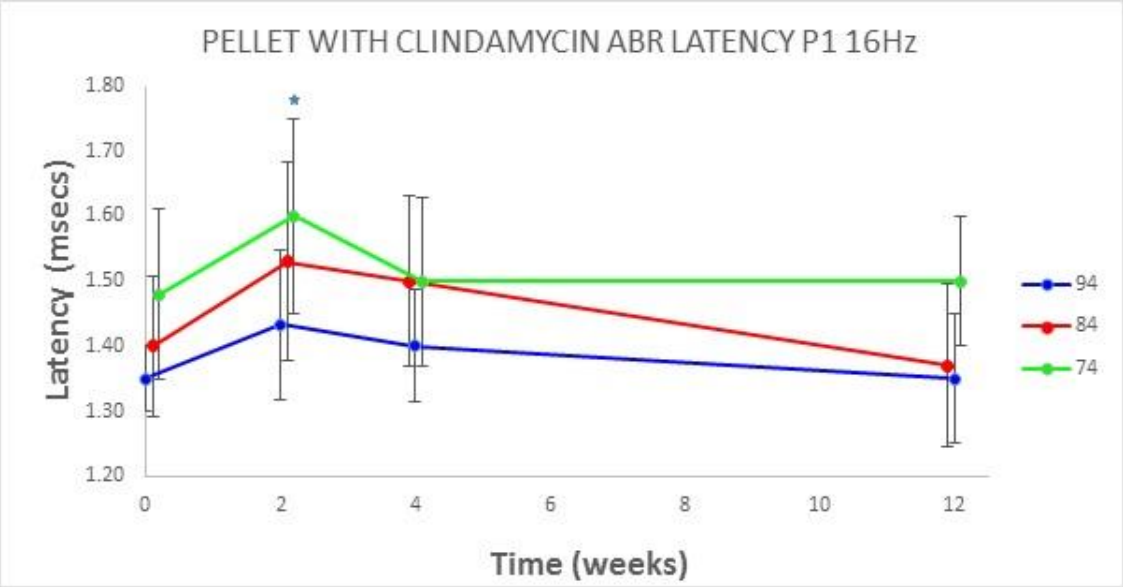


Figure 93: ***Changes in latency over time for PLGA and pluronic pellet with rifampicin at 16kHz analysing the P1 wave. Significance is denoted by a *.***

On analysis of wave P1 there was a significant increase in mean latency at week 2 for 74dB from 1.48 msecs initially at week 0 to 1.6 msecs at week 2 (p=0.02) (Figure 95).

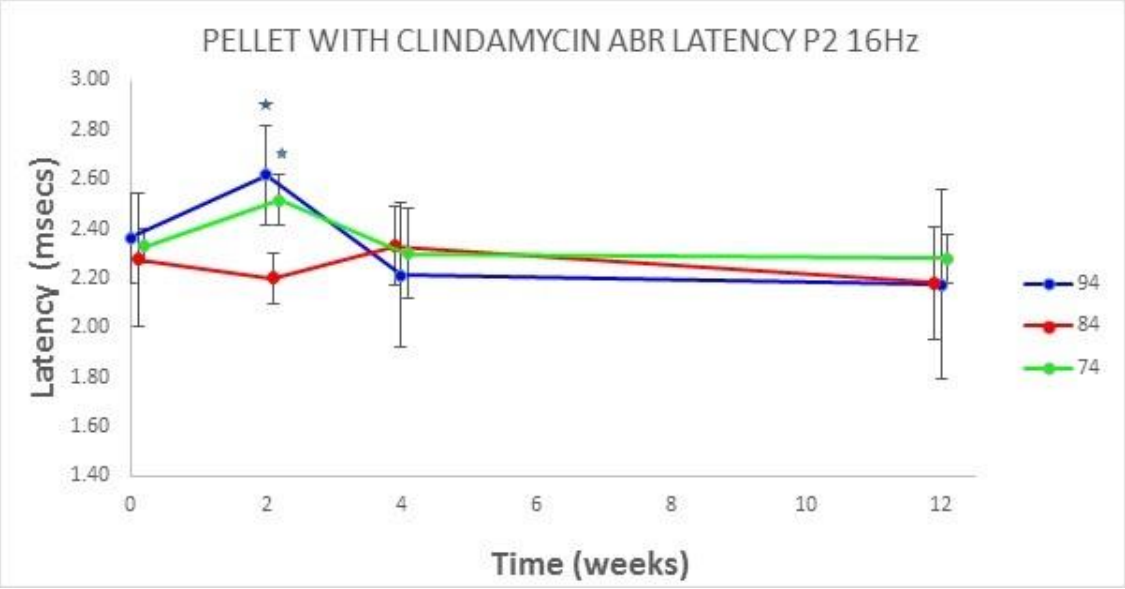


Figure 94: ***Changes in amplitude over time for PLGA and pluronic pellet with clindamycin at 16kHz analysing the P2 wave. Significance is denoted by a *.***

On analysis of wave P2 there was a significant increase in mean latency at 94dB from 2.63 msecs initially at week 0 to 2.62 msecs at week 2 (p=0.004). There is also a significant increase in mean latency at 74dB from 2.33 msecs initially at week 0 to 2.52 msecs at week 2 (p=0.03) (Figure 96).

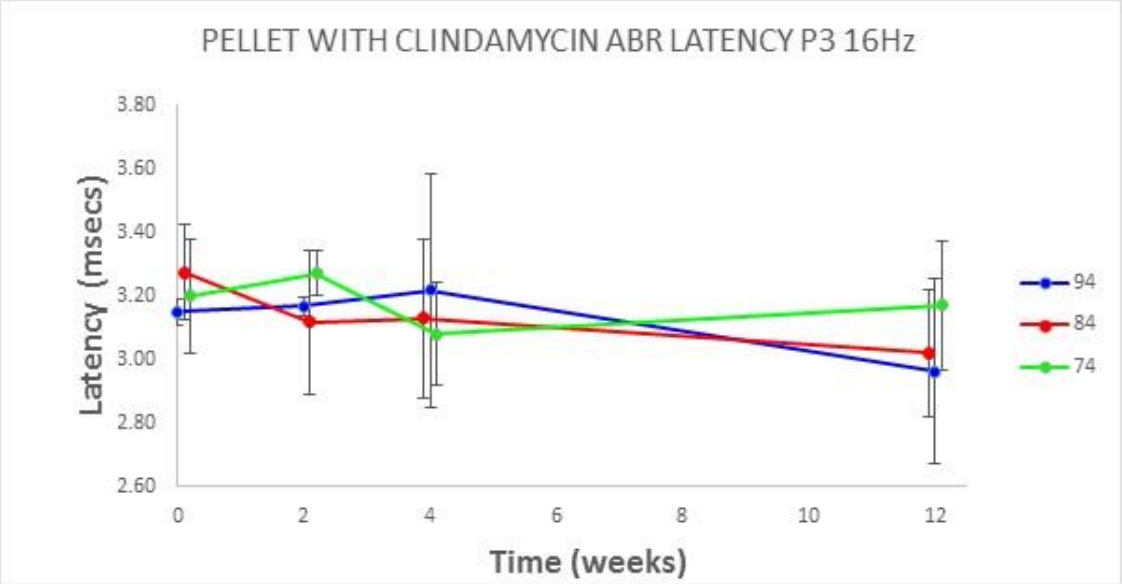


Figure 95: ***Changes in latency over time for PLGA and pluronic pellet with clindamycin at 16kHz analysing the P3 wave. Significance is denoted by a *.***

On analysis of the wave P3 there are no significant excursions from the initial values at week 0 for latency at 74dB, 84dB and 94dB (Figure 97).

5.3.17 Changes in ABR latency of PLGA and pluronic pellet over 74-94dB at 24kHz

On analysis of the waves P1, P2 and P3 there are no significant excursions from the initial values at week 0 for latency at 74dB, 84dB and 94dB (Figures 98,99 and 100).

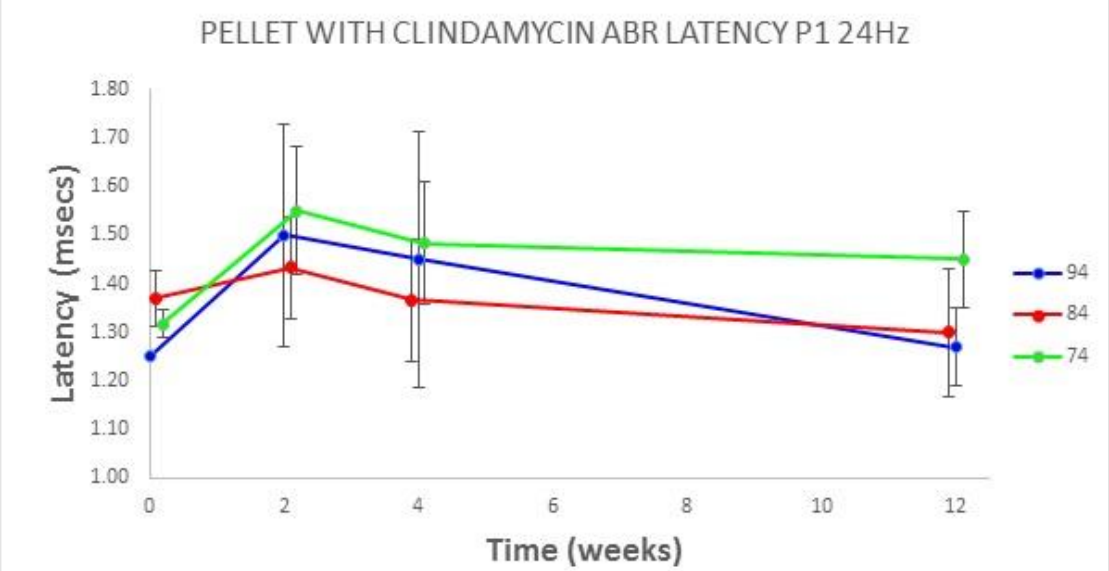


Figure 96: ***Changes in latency over time for PLGA and pluronic pellet with clindamycin at 24kHz analysing the P1 wave. Significance is denoted by a *.***

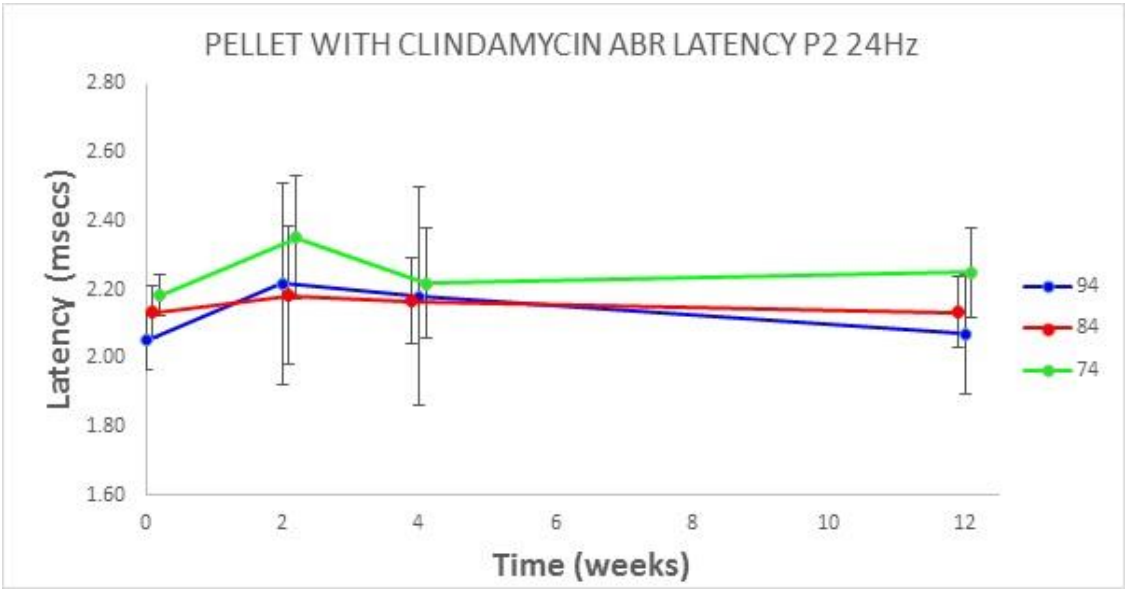


Figure 97: ***Changes in clindamycin over time for PLGA and pluronic pellet with rifampicin at 24kHz analysing the P2 wave. Significance is denoted by a *.***

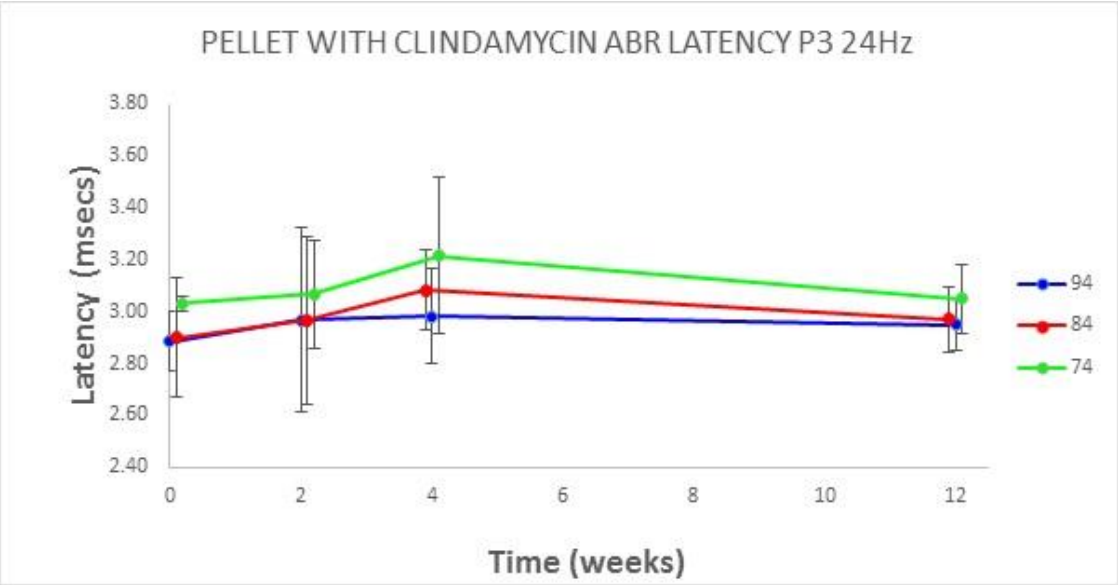


Figure 98: ***Changes in latency over time for PLGA and pluronic pellet with clindamycin at 24kHz analysing the P3 wave. Significance is denoted by a *.***

5.3.18 Summary of changes in latency results of PLGA and pluronic pellet loaded with clindamycin over 16kHz and 24kHz

	P1	P2	P3
Pellet + Clindamycin 16kHz	↑ week 2 74dB	↑ week 2 74dB,94dB	-
Pellet + Clindamycin 24kHz	-	-	-

Table 41: ***Changes in latency for waves P1-P3 measured at 16kHz and 24kHz for the PLGA and pluronic loaded with clindamycin group.***

Overall there are increases in latency seen for P1 at week 2 at 74dB and P2 at 74 and 94dB on analysis of pellet and clindamycin group. There are no significant changes in latency for P3 at 16kHz or waves P1, P2 and P3 at 24kHz (Table 41).

5.3.19 Summary of overall ABR latency results

	P1	P2	P3
BC 16kHz	↑week 1 84dB	↑week 1 74dB,94dB	↑week 1 84dB
BC 24kHz	-	-	↑week 12 94dB
SC 16kHz	↑week 1 94dB ↑week 16 94dB	↑week 1 74dB, 94dB ↑week 4 84dB	↑week 1, 2 94dB ↑week1,2 84dB
SC 16kHz	↑week 1 94dB	-	-
P 16kHz	↑ week 2 94dB	↑ week 2 94dB	↓week 16 94dB
P 24kHz	-	-	↓week 4 94dB
PA 16kHz	-	-	-
PA 24kHz	-	↑ week 2 84dB	-
PRif 16kHz	-	-	-
PRif 24kHz	↑week 2 74dB	-	-
PClind 16kHz	↑week 2 74dB	↑ week 2 74dB, 94dB	-
PClind 24kHx	-	-	-

Table 42: ***Summary of the changes in latency for waves P1-P3 measured at 16kHz and 24kHz for all experimental groups.***

Significant changes in latency seen in the control groups: biological control, surgical control and pellet without antibiotics are in waves P1, P2 and P3 and demonstrated latency increases from week 0 – week 16 (Table 42). These were predominantly seen at 16kHz. It is also interesting to note that changes in latency are pre dominantly elevations. However, when testing the pellet without antibiotics, at 94dB there were latency decreases seen at weeks 4 and 16. Significant changes in ABR latency are unexpected in the control groups. This may be due to background noise and difficulties with measurement with traces.

The significant changes identified with pellets loaded with both rifampicin and clindamycin were seen only in wave P2 at week 2 at 84dB and 24kHz. When pellets are separately loaded with rifampicin or clindamycin, there is ABR latency elevation at week 2 in P1 at 74dB at both 16kHz and 24kHz and P2 waves at 16kHz at both 74dB and 94dB.

Inconsistencies in results could potentially be attributable to noise and difficulties with measurements using poor quality traces. This can be seen with some of the graphs having large error bars.

5.3.20 Latency results using Friedman's two way analysis

Due to the variability of results around the mean values which is seen with the error bars, Friedman's two way analysis was used to identify significant excursions from the initial values at week 0. The results are shown for 16kHz and 24kHz analysing ABR waveform P1 (Table 26), P2 (Table 27) and P3 (Table 43).

	P1	94	84	74
16kHz	**BC**	0.392	0.053	0.971
16kHz	**SC**	0.015*	0.413	0.74
16kHz	**P**	0.269	0.56	0.262
16kHz	**PA Rif + Clind**	0.858	0.015*	0.484
24kHz	**BC**	0.05	0.219	0.365
24kHz	**SC**	0.009*	0.107	0.891
24kHz	**P**	0.835	0.843	0.836
24kHz	**PA Rif + Clind**	0.578	0.078	0.674

Table 43: ***Results of Friedman's two way analysis of latency of wave P1. Significance is denoted by a *.***

The latency of ABR waveform P1 using Friedman's two way analysis shows significant excursions from initial week 0 values at 16kHz in the surgical control group at 94dB and the group of guinea pigs laden with pellet containing rifampicin and clindamycin at 84dB. At 24kHz, significant excursions from initial recordings at week 0 were seen in the surgical control group at 94dB (Table 43).

	P2	94	84	74
16kHz	**BC**	0.032*	0.406	0.102
16kHz	**SC**	0.013*	0.385	0.57
16kHz	**P**	0.073	0.186	0.57
16kHz	**PA Rif + Clind**	0.629	0.562	0.019*
24kHz	**BC**	0.513	0.681	0.117
24kHz	**SC**	0.011*	0.157	0.07
24kHz	**P**	0.725	0.135	0.838
24kHz	**PA Rif + Clind**	0.382	0.046*	0.335

Table 44: ***Results of Friedman's two way analysis of latency of wave P2. Significance is denoted by a *.***

The latency of ABR waveform P2 using Friedman's two way analysis shows significant excursions from initial week 0 recordings at 16kHz in the biological control group and surgical control group at 94dB and the group of guinea pigs laden with pellet containing rifampicin and clindamycin at 74dB. At 24kHz, significant excursions from initial values at week 0 were seen in the surgical control group at 94dB and the group of guinea pigs laden with pellet containing rifampicin and clindamycin at 84dB (Table 44).

	P3	94	84	74
16kHz	**BC**	0.504	0.35	0.814
16kHz	**SC**	0.001*	0.117	0.124
16kHz	**P**	0.37	0.185	0.103
16kHz	**PA Rif + Clind**	0.046*	0.268	0.207
24kHz	**BC**	0.117	0.876	0.267
24kHz	**SC**	0.139	0.674	0.638
24kHz	**P**	0.507	0.714	0.037*
24kHz	**PA Rif + Clind**	0.053	0.802	0.059

Table 45: ***Results of Friedman's two way analysis of latency of wave P3. Significance is denoted by a *.***

The latency of ABR waveform P3 using Friedman's two way analysis shows significant excursions from initial week 0 values at 16kHz in the surgical control group and the group of guinea pigs laden with pellet containing rifampicin and clindamycin at 94dB. At 24kHz, significant excursions from initial week 0 recordings were seen in the PLGA and Pluronic pellet control group at 74dB (Table 45).

5.3.21 Summary of Friedman's two way analysis of latency

Overall, there are no consistent excursions from initial week 0 values for latency results for ABR waveforms P1, P2 and P3. There are excursions seen in every group including the control groups biological, surgical and pellet. There is no clear pattern of change identified.

5.3.22 Holm- Bonferroni correction for the ABR latency data

Multiple comparisons were performed on the ABR latency data and therefore the Holm-Bonferroni correction was applied to the p values. This was done to minimise the risk of a Type I error.

Tables 46-57 show the Holm Bonferroni correction applied to the ABR latency data. There is only sporadic rejection of the null hypothesis which is highlighted red. Overall, this statistical correction therefore confirms the significance of the results from the t tests with no significant latency changes seen in the experimental groups in waves P1, P2 and P3 when analysed at 16kHz and 24 kHz.

BC 16kHz	**P1**	**P2**	**P3**
94dB	H1: 0.067 1 >0.0125	H1: 0.0001 1 <0.0125	H1: 0.826 4
	H2: 0.615 4	H2: 0.33 4	H2: 0.414 3
	H3: 0.548 3	H3: 0.167 3	H3: 0.175 1 >0.0125
	H4: 0.229 2	H4: 0.122 2>0.0167	H4: 0.289 2
84dB	H1: 0.0117 1 >0.0125	H1: 0.21 1 <0.0125	H1: 0.043 1>0.0125
	H2: 0.6293 3	H2: 0.863 4	H2: 0.751 3
	H3: 0.2667 2>0.0167	H3: 0.323 2	H3: 0.225 2
	H4: 0.7949 4	H4: 0.415 3	H4: 0.962 4
74dB	H1: 0.614 1>0.0125	H1: 0.017 1>0.0125	H1: 0.183 1>0.0125
	H2: 0.694 2	H2: 0.495 3	H2: 0.647 2
	H3: 0.820 3	H3: 0.635 4	H3: 0.766 4
	H4: 1 4	H4: 0.389 2	H4: 0.66 3

Table 46: ***Biological control latency p values at 16kHz and the Holm Bonferroni correction. Values where the null hypothesis is rejected are highlighted red.***

BC 24kHz	P1	P2	P3
94dB	H1: 0.0615 1>0.0125	H1: 0.0635 1>0.0125	H1: 0.083 2
	H2: 0.105 2	H2: 0.3445 2	H2: 0.121 3
	H3: 0.6036 3	H3: 0.4681 3	H3: 0.312 4
	H4: 0.6132 4	H4: 0.6555 4	H4: 0.033 1>0.0125
84dB	H1: 0.082 1>0.0125	H1: 0.172 1>0.0125	H1: 0.163 1>0.0125
	H2: 0.664 4	H2: 0.593 4	H2: 0.977 4
	H3: 0.338 2	H3: 0.426 3	H3: 0.976 3
	H4: 0.581 3	H4: 0.239 2	H4: 0.224 2
74dB	H1: 0.1869 1>0.0125	H1: 0.192 1>0.0125	H1: 0.084 1>0.0125
	H2: 0.4422 3	H2: 0.898 4	H2: 0.394 2
	H3: 0.338 2	H3: 0.830 3	H3: 0.612 4
	H4: 0.581 4	H4: 0.266 2	H4: 0.447 3

Table 47: ***Biological control latency p values at 24kHz and the Holm Bonferroni correction. Values where the null hypothesis is rejected are highlighted red.***

SC 16kHz	P1	P2	P3
94dB	H1: 0.006 1 <0.0125	H1: 0.026 1 >0.0125	H1: 0.001 1<0.0125
	H2: 0.075 3	H2: 0.438 4	H2: 0.039 2>0.0167
	H3: 0.187 4	H3: 0.211 3	H3: 0.118 3
	H4: 0.048 2>0.0167	H4: 0.239 2	H4: 0.533 4
84dB	H1: 1.000 4	H1: 0.841 3	H1: 0.033 1>0.0125
	H2: 0.161 1>0.0125	H2: 0.883 4	H2: 0.051 2
	H3: 0.889 3	H3: 0.044 1>0.0125	H3: 0.131 3
	H4: 0.824 2	H4: 0.300 2	H4: 0.659 4
74dB	H1: 0.953 4	H1: 0.016 1>0.0125	H1: 0.018 1>0.0125
	H2: 0.271 1>0.0125	H2: 0.714 3	H2: 0.269 3
	H3: 0.901 3	H3: 0.921 4	H3: 0.099 2
	H4: 0.419 2	H4: 0.621 2	H4: 0.707 4

Table 48: ***Surgical control latency p values at 16kHz and the Holm Bonferroni correction. Values where the null hypothesis is rejected are highlighted red.***

SC 24kHz	P1	P2	P3
94dB	H1: 0.006 1<0.0125	H1: 0.004 1 <0.0125	H1: 0.050 2
	H2: 0.039 2>0.0167	H2: 0.235 4	H2: 0.753 4
	H3: 0.047 3	H3: 0.368 3	H3: 0.042 1 >0.0125
	H4: 0.799 4	H4: 0.323 2>0.0167	H4: 0.323 3
84dB	H1: 0.642 3	H1: 0.103 1 >0.0125	H1: 0.103 1>0.0125
	H2: 0.142 1>0.0125	H2: 0.107 4	H2: 0.107 2
	H3: 0.485 2	H3: 0.542 2	H3: 0.542 4
	H4: 0.932 4	H4: 0.276 3	H4: 0.276 3
74dB	H1: 0.771 4	H1: 0.304 2	H1: 0.304 2
	H2: 0.329 1>0.0125	H2: 0.493 3	H2: 0.493 3
	H3: 0.394 2	H3: 0.830 4	H3: 0.830 4
	H4: 0.552 3	H4: 0.070 1>0.0125	H4: 0.070 1>0.0125

Table 49: ***Surgical control latency p values at 24kHz and the Holm Bonferroni correction. Values where the null hypothesis is rejected are highlighted red.***

P 16kHz	P1	P2	P3
94dB	H1: 0.307 3	H1: 0.321 2	H1: 0.050 2
	H2: 0.339 4	H2: 0.901 4	H2: 0.753 4
	H3: 0.305 2	H3: 0.426 3	H3: 0.042 1 >0.0125
	H4: 0.280 1>0.0125	H4: 0.237 1>0.0125	H4: 0.323 3
84dB	H1: 0.178 1>0.0125	H1: 0.200 3	H1: 0.103 1>0.0125
	H2: 0.422 2	H2: 0.766 4	H2: 0.107 2
	H3: 1.000 3	H3: 0.021 1>0.0125	H3: 0.542 4
	H4: 1.000 3	H4: 0.128 2	H4: 0.276 3
74dB	H1: 0.053 1>0.0125	H1: 0.161 2	H1: 0.304 2
	H2: 0.165 2	H2: 0.309 4	H2: 0.493 3
	H3: 0.620 4	H3: 0.102 1>0.0125	H3: 0.830 4
	H4: 0.299 3	H4: 0.217 3	H4: 0.070 1>0.0125

Table 50: ***Pellet control latency p values at 16kHz and the Holm Bonferroni correction. Values where the null hypothesis is rejected are highlighted red.***

P 24kHz	P1	P2	P3
94dB	H1: 0.572 4	H1: 0.622 3	H1: 0.852 4
	H2: 0.279 1>0.0125	H2: 0.538 2	H2: 0.791 2
	H3: 0.523 2	H3: 0.516 1>0.0125	H3: 0.014 1 >0.0125
	H4: 0.553 3	H4: 1.000 4	H4: 0.832 3
84dB	H1: 0.486 2	H1: 0.254 2	H1: 0.371 2
	H2: 0.284 1>0.0125	H2: 0.438 4	H2: 0.864 3
	H3: 0.594 3	H3: 0.435 3	H3: 0.958 4
	H4: 0.775 4	H4: 0.174 1 >0.0125	H4: 0.100 1 >0.0125
74dB	H1: 0.698 3	H1: 0.775 4	H1: 0.147 1 >0.0125
	H2: 0.216 2	H2: 0.275 1>0.0125	H2: 0.254 3
	H3: 0.207 1>0.0125	H3: 0.289 2	H3: 0.424 4
	H4: 0.710 4	H4: 0.365 3	H4: 0.154 2

Table 51: ***Pellet control latency p values at 24kHz and the Holm Bonferroni correction. Values where the null hypothesis is rejected are highlighted red.***

PA 16kHz	P1	P2	P3
94dB	H1: 0.589 3	H1: 0.622 3	H1: 0.852 4
	H2: 0.502 2	H2: 0.538 2	H2: 0.791 2
	H3: 1.000 4	H3: 0.516 1>0.0125	H3: 0.014 1 >0.0125
	H4: 0.388 1>0.0125	H4: 1.000 4	H4: 0.832 3
84dB	H1: 0.112 1>0.0125	H1: 0.254 2	H1: 0.371 2
	H2: 0.183 2	H2: 0.438 4	H2: 0.864 3
	H3: 0.953 4	H3: 0.435 3	H3: 0.958 4
	H4: 0.390 3	H4: 0.174 1 >0.0125	H4: 0.100 1 >0.0125
74dB	H1: 0.144 1>0.0125	H1: 0.775 4	H1: 0.147 1 >0.0125
	H2: 0.194 2	H2: 0.275 1>0.0125	H2: 0.254 3
	H3: 0.245 3	H3: 0.289 2	H3: 0.424 4
	H4: 0.527 4	H4: 0.365 3	H4: 0.154 2

Table 52: ***Pellet with rifampicin and clindamycin latency p values at 16kHz and the Holm Bonferroni correction. Values where the null hypothesis is rejected are highlighted red.***

PA 24kHz	P1	P2	P3
94dB	H1: 0.097 4	H1: 0.800 4	H1: 0.852 4
	H2: 0.296 1>0.0125	H2: 0.780 3	H2: 0.791 2
	H3: 0.920 2	H3: 0.410 1>0.0125	H3: 0.014 1 >0.0125
	H4: 0.937 3	H4: 0.580 2	H4: 0.832 3
84dB	H1: 0.660 2	H1: 0.140 1 >0.0125	H1: 0.371 1
	H2: 0.369 1>0.0125	H2: 1.000 3	H2: 0.864 2
	H3: 0.271 3	H3: 0.970 2	H3: 0.958 3
	H4: 0.868 4	H4: 1.000 4	H4: 0.100 4 >0.0125
74dB	H1: 0.443 3	H1: 0.410 1>0.0125	H1: 0.147 1 >0.0125
	H2: 0.400 2	H2: 0.760 3	H2: 0.254 3
	H3: 0.736 1>0.0125	H3: 0.800 4	H3: 0.424 4
	H4: 0.172 4	H4: 0.460 2	H4: 0.154 2

Table 53: ***Pellet with rifampicin and clindamycin latency p values at 24kHz and the Holm Bonferroni correction. Values where the null hypothesis is rejected are highlighted red.***

PRif 16kHz	P1	P2	P3
94dB	H1: -	H1: -	H1: -
	H2: 0.724 3	H2: 0.770 3	H2: 0.920 2
	H3: 0.854 4	H3: 0.820 1>0.0125	H3: 0.560 1 >0.0125
	H4: 0.716 2	H4: 1.000 2	H4: 0.850 3
84dB	H1: -	H1: -	H1: -
	H2: 0.126 1>0.0125	H2: 0.500 3	H2: 0.390 2
	H3: 0.514 3	H3: 0.830 2	H3: 0.920 3
	H4: 0.500 4	H4: 0.370 4	H4: 0.500 4 >0.0125
74dB	H1: -	H1: -	H1: -
	H2: 0.881 2	H2: 0.620 3	H2: 0.710 3
	H3: 0.655 1>0.0125	H3: 0.590 4	H3: 0.680 4
	H4: 0.656 4	H4: 0.590 2	H4: 0.680 2

Table 54: ***Pellet with rifampicin latency p values at 16kHz and the Holm Bonferroni correction. Values where the null hypothesis is rejected are highlighted red.***

PRif 24kHz	P1	P2	P3
94dB	H1: -	H1: -	H1: -
	H2: 0.399 2	H2: 0.785 3	H2: 0.074 1>0.0125
	H3: 0.777 3	H3: 0.155 1>0.0125	H3: 0.928 3
	H4: 0.141 1>0.0125	H4: 0.405 2	H4: 0.385 2
84dB	H1: -	H1 -	H1: -
	H2: 0.658 1>0.0125	H2: 0.835 2	H2: 0.439 3
	H3: 0.783 2	H3: 1.000 3	H3: 0.375 2
	H4: 0.669 3	H4: 0.604 1 >0.0125	H4: 0.251 1 >0.0125
74dB	H1: -	H1 -	H1: -
	H2: 0.063 1>0.0125	H2: 0.903 3	H2: 0.844 3
	H3: 0.249 2	H3: 0.375 1>0.0125	H3: 0.676 2
	H4: 0.650 3	H4: 0.781 2	H4: 0.575 1>0.0125

Table 55: ***Pellet with rifampicin latency p values at 24kHz and the Holm Bonferroni correction. Values where the null hypothesis is rejected are highlighted red.***

PClind 16kHz	P1	P2	P3
94dB	H1: 0.190 1>0.0125	H1: 0.004 1<0.0125	H1: 1.000 3
	H2: 0.230 2	H2: 0.210 2>0.0167	H2: 0.830 2
	H3: 1.000 3	H3: 0.500 3	H3: 0.290 1 >0.0125
84dB	H1: 0.490 1>0.0125	H1 0.950 3	H1: 0.225 3
	H2: 0.530 2	H2: 0.890 2	H2: 0.057 1>0.0125
	H3: 0.840 3	H3: 0.740 1>0.0125	H3: 0.185 2
74dB	H1: 0.020 1>0.0125	H1: 0.030 1>0.0125	H1: 0.460 2
	H2: 0.810 2	H2: 0.760 3	H2: 0.192 1>0.0125
	H3: 0.840 3	H3: 0.420 2	H3: 0.480 3

Table 56: ***Pellet with clindamycin latency p values at 16kHz and the Holm Bonferroni correction. Values where the null hypothesis is rejected are highlighted red.***

PClind 24kHz	P1	P2	P3
94dB	H1: 0.200 1>0.0125	H1: 0.580 2	H1: 0.652 3
	H2: 0.320 2	H2: 0.400 1	H2: 0.370 1>0.0125
	H3: 0.740 3	H3: 1.000 3>0.0125	H3: 0.530 2
84dB	H1: 0.190 1>0.0125	H1: 0.580 2	H1: 0.423 2
	H2: 0.420 2	H2: 0.400 1>0.0125	H2: 0.260 1>0.0125
	H3: 0.830 3	H3: 1.000 3	H3: 0.640 3
74dB	H1: 0.120 1>0.0125	H1: 0.150 1>0.0125	H1: 0.800 2
	H2: 0.150 2	H2: 0.640 3	H2: 0.370 1>0.0125
	H3: 0.157 3	H3: 0.270 2	H3: 0.830 3

Table 57: ***Pellet with clindamycin latency p values at 24kHz and the Holm Bonferroni correction. Values where the null hypothesis is rejected are highlighted red.***

5.3.23 Discussion of ABR latency results

The results of ABR latency measurement show that there is no consistent alteration in ABR latency across the groups to account for the ABR threshold elevations. This is seen on analysis of ABR latency using the t-test analysis and Friedman's two way analysis of variance and Holm-Bonferroni correction. The ABR latency changes would indicate potential neurotoxicity to the auditory pathway as sound waves are propagated from the cochlea to the cortex.

Studies have shown latency increases in hyperbilirubinaemia in waves P1 and P5 (Kaga *et al*., 1979), noise exposure (Gourévitch *et al*., 2009), aminoglycosides in waves P1 and P5 (Hotz *et al*., 1990, Nekrassov *et al*., 2000) and cisplatin (De Lauretis *et al*., 1999). ABR latency decreases are also seen in hyperthermia experimentally (Takahashi *et al*., 1991, Gold *et al*., 1985) with reversibility on cooling to normal body temperature.

Without consistent changes in the latency values identified, there is no evidence of neurotoxicity on analysis of waves P1, P2 and P3. This indicates that the ABR threshold

elevation recorded is attributable to a peripheral effect on the auditory conduction pathway as opposed to central. In order to assess this further, a detailed analysis of the cochlea is required. The technique of cytocochleograms can be used to assess for inner or outer hair cell presence or loss in the different experimental groups. Cytocochleograms carefully assess the entire length of the cochlea from the apex to the base. In addition, immunofluorescence allows a detailed analysis of the morphology and presence of the inner and outer hair cells in sample sections of the cochlea. The hypothesis of ABR threshold elevation in the pellet group with rifampicin and clindamycin in combination being attributable to outer and/or inner hair cell loss can therefore be tested (Chapter 6).

Before the onset of each ABR experiment, the weights of the guinea pigs were recorded. This allowed for accurate anaesthetic drug calculation and as a measure of each animal's individual welfare. Overall, markers of the animals' general wellbeing including weight gain over time is important to ensure a high standard of animal husbandry (section 5.4).

5.4.0 Weight changes seen during ABR testing

5.4.1 Guinea pig weight change with treatment

The initial mean values of weight for treatment groups show variation as they were of different ages when experimentation started. This was due to procurement of a subset of animals for the testing the pellet loaded with either rifampicin or clindamycin at an interval from another source. This subset of animals was older (at 8 weeks) when the ABR tested was performed. Standard errors are not shown as they are relatively small. Changes in weight were expected over time. All groups were n=8. There were two experimental cohorts; 1) Biological control, surgical control, pellet control and pellet laden with rifampicin and clindamycin tested up to 16 weeks and 2) pellets loaded with rifampicin and clindamycin separately tested up to 12 weeks.

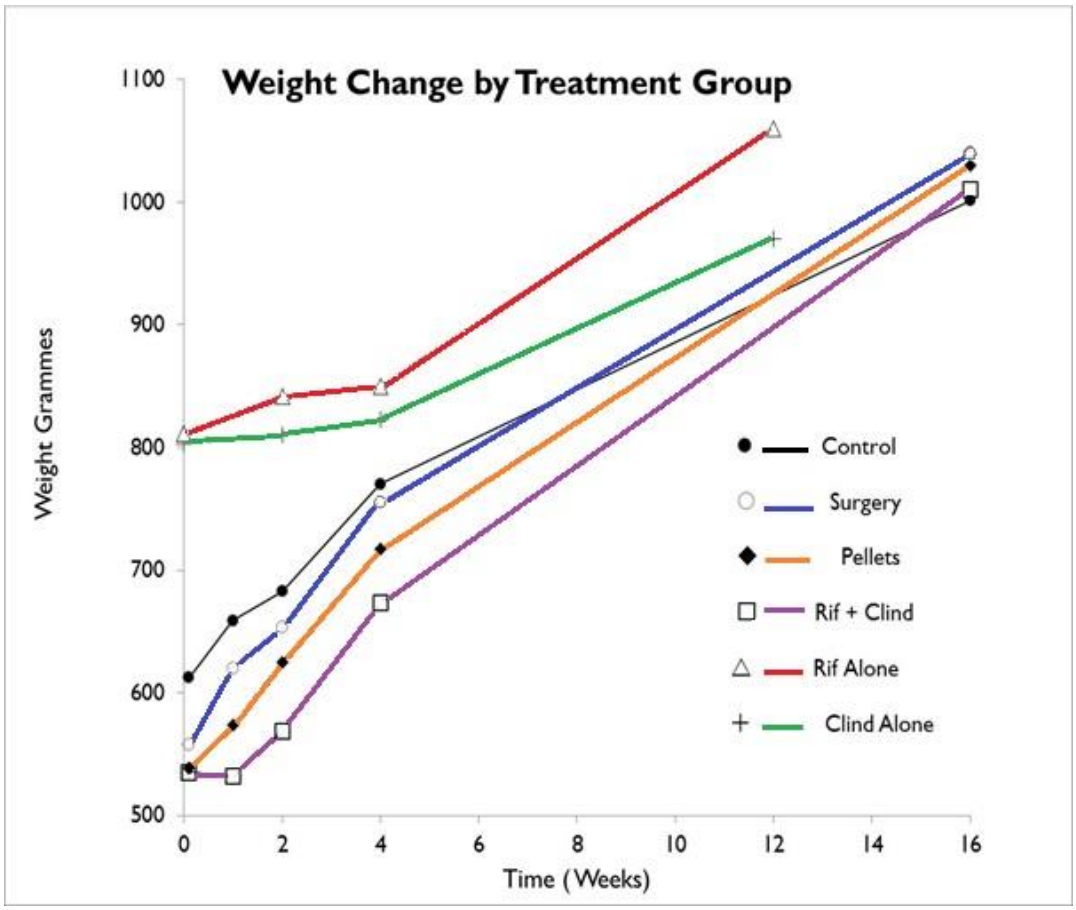


Figure 99: ***Weight change (grams) over time (weeks) for different treatment groups.***

5.4.2 Biological control, surgical control and pellet control groups.

The mean starting values of 540-610g are accompanied by largely comparable gradients over weeks 0-16 finishing at around 1000g with a slower growth rate over weeks 4-16 (Figure 99).

5.4.3 Pellets loaded with Rifampicin and Clindamycin in combination

Figure 99 shows the growth rate is clearly affected over weeks 0-2 but then appears to recover over weeks 2-16. This clearly indicates that the antibiotics in combination delivered via the middle ear affected acute weight gain. There is evidence of slower

acute growth in drug animals treated with drug laden pellets. This recovers in weeks 12-16 with the final recorded weight comparable with the first cohort.

5.4.4 Pellets loaded with Rifampicin or Clindamycin separately

The animals in these groups were utilised at a later date and were significantly older and heavier as shown on the graph at week 0 when ABR recordings commenced. They were subject to fewer time points following pellet placement. Compared to the other groups and their extrapolated growth rates, there appears to be a slowing over weeks 0-4 which then recovers over weeks 4-12. At the end of the experimental time course, their weight is comparable to the other treatment groups at about 950 -1050g.

5.4.5 Dominant boars

Several of the guinea pigs showed aggressive dominant behaviour. This was noticed and monitored by animal house staff and the Home Office Vet. These boars dominated the other three in the cage with biting, scratching and general aggression. Section 8.2 discusses the animal husbandry issues with the aggressive boars and animals which were victimised. It was noted in the animals which had scratches and bites, there was less weight gain. This correlated with a high proportion of guinea pigs who had undergone pellet placement with rifampicin and clindamycin in combination. This indicates that the pellet may result in a systemic disturbance that the other animals exploited or there is a decrease in appetite following pellet placement. This is discussed further alongside animal husbandry (section 8.2).

Chapter 6: Cytocochleograms and IHC and OHC morphology studies

6.1.1 Cytocochleogram of the biological control group

One full cochlea from a guinea pig in the biological control group was prepared, dissected and a cytocochleogram was made. Hair cells were counted systematically from base to apex and marked off on a template (Figure 106). Hair cell counts from the cytocochleograms show very few missing inner or outer hair cells for the biological control group analysed. There were only two areas of the cochlea that were difficult to visualise; rows 16 and 20. The greatest loss of inner hair cells was seen in the middle section of the cochlea with approximately 12% in row 19 (Figure 102).

Consistently there does appear to be hair cell losses in row 1 which correlates with the most apical section of the cochlea.

Using the semi quantitative analysis, there does not appear to be any appreciable loss of IHC or OHC in the biological control group throughout the cochlea (Figure 100). At row numbers 16 and 20 there were up to 20% of IHC which were unable to be counted due to cell distortion, mounting or dissection trauma. Cochlea from the biological control group show normal arrangement of three rows of outer hair cells and one row of inner hair cells. This result is consistent with the ABR threshold results for the biological control group which do not show any significant excursions from the initial mean value at week 0.

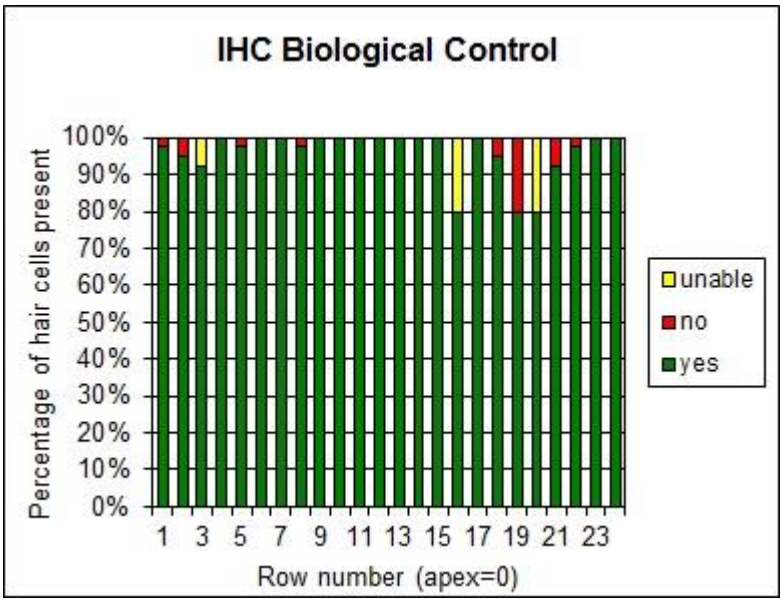


Figure 100: ***Cytocochleogram of biological control group inner hair cell rows from apex (row 0) to base.***

The innermost row of outer hair cells (OHC 1) shows loss of cells at rows 1, 5, 6, 8-9, 15, 19 and 21. These losses were spread throughout the cochlea from the apex to the base and none of the losses in a row reached more than 10%. This is shown as a cytocochleogram in Figure 103.

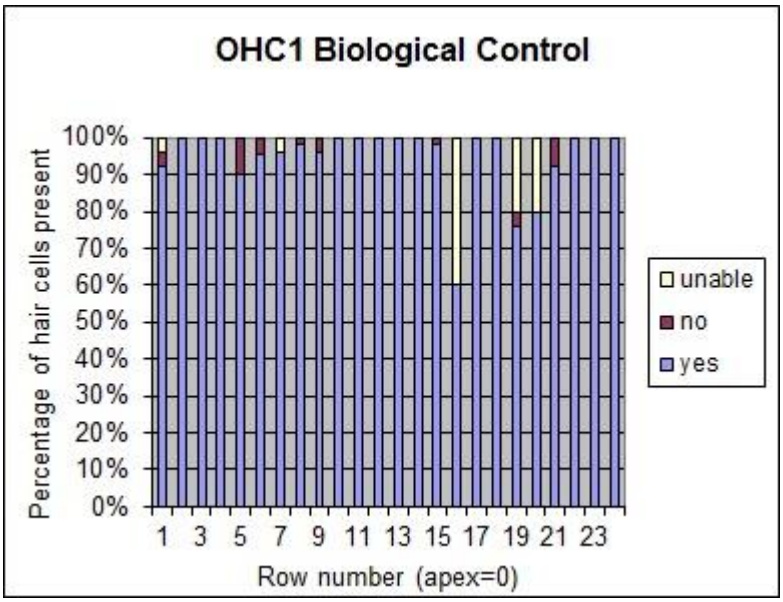


Figure 101: ***Cytocochleogram of biological control group OHC row 1 (innermost row) from apex (row 0) to base.***

The middle row of outer hair cells (OHC 2) shows loss of cells at rows 1-9, 11, 13-15, 18-24. These losses were spread throughout the cochlea from the apex to the base and none of the losses in a row reached more than 22% in row 1 and then 15% in row 5. This is shown as a cytocochleogram in Figure 104.

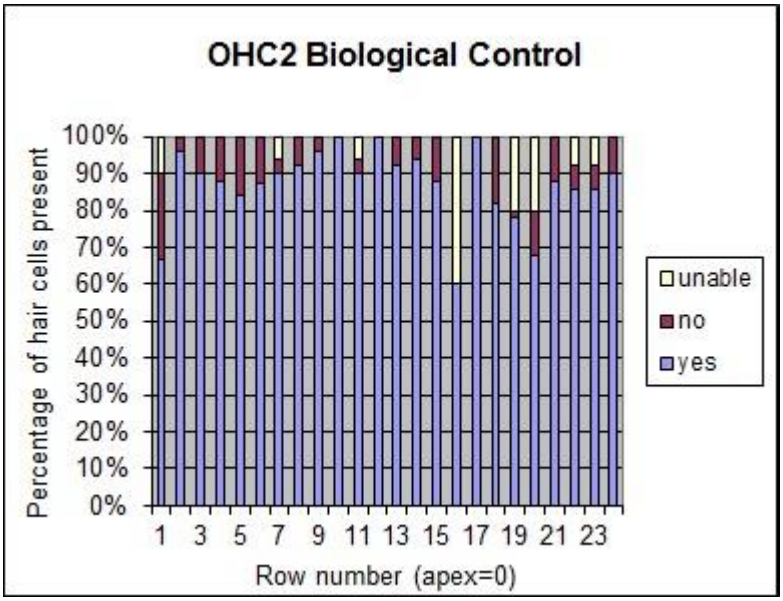


Figure 102: ***Cytocochleogram of biological control group OHC row 2 (middle row) from apex (row 0) to base.***

The outermost row of outer hair cells (OHC 3) show loss of cells at rows 1-11, 13-16, 19-24. These losses were spread throughout the cochlea from the apex to the base and the losses in a row reached more than 40% in row 1 and 22% in row 5. This is shown as a cytocochleogram in Figure 105.

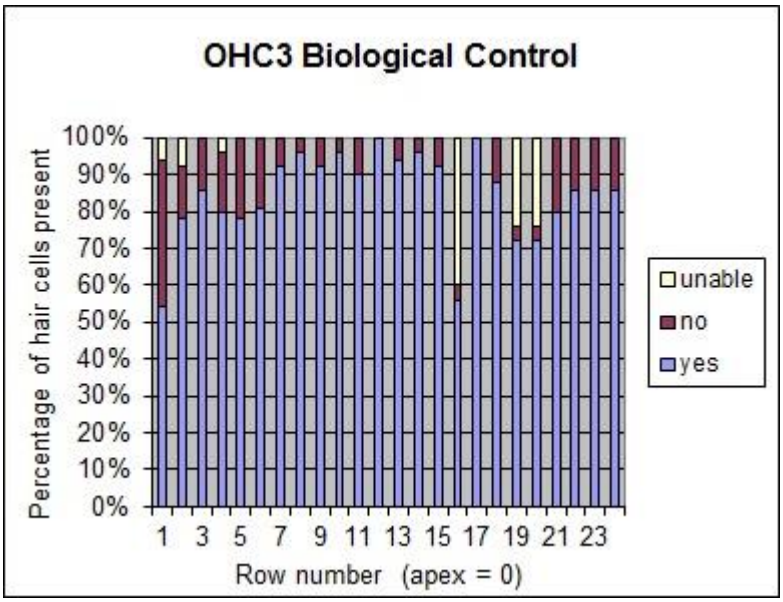


Figure 103: ***Cytocochleogram of biological control group outer hair cell row 3 (outermost row) from apex (row 0) to base.***

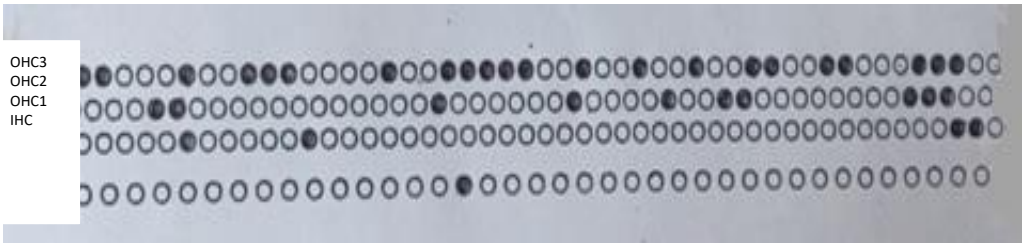


Figure 104: ***Schematic diagram of typical segment of cochlea (a row) from BC group showing the distribution of hair cells present ○ and absent ●. Template provided by Professor David Furness (see acknowledgements).***

6.1.2 Cytocochleogram of PLGA and pluronic pellet group

One full cochlea from a guinea pig in the pellet control group was prepared, dissected and a cytocochleogram was made. Hair cells were counted systematically from base to apex and marked off on a template (Figure 106). The inner hair cell (IHC) cytocochleogram shows loss of cells at rows 1-2, 5,8,18, 20% of row 19, 21-22 and 31. Most of these losses were less than 10% and were spread throughout the cochlea from the apex at row 1 to the base at row 35. There were several rows which were difficult to read: rows 3, 16, 20, at 80% of row 29. This is shown in the cytocochleogram in Figure 107.

On analysis of the outer hair cells, there appears to be an even spread of outer hair cell loss across the length of the cochlea with the outermost row of the outer hair cells (OHC 3) affected in all rows except two. (Figure 108,109,110). This is a greater amount of hair cell loss than in rows OHC 2 and OHC 1.

The rows which were unable to be read showed some consistency here with row 29 being the most obvious (up to 80% loss across all rows). Row 16 is also consistently affected across all of the rows and row 1 in the outer hair cell rows (Figure 108,109,110).

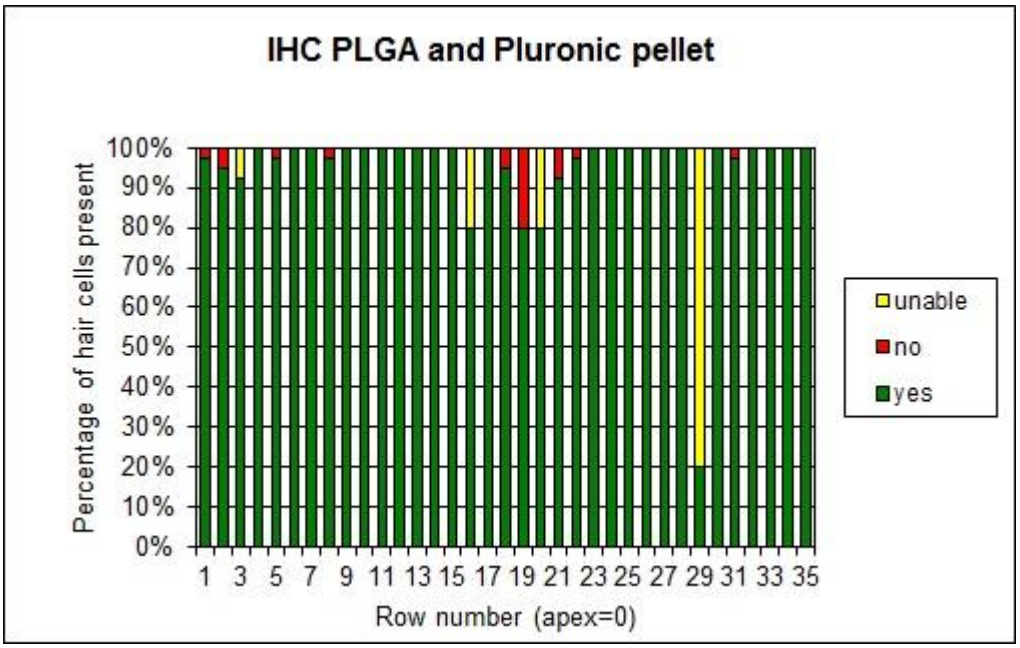


Figure 105: ***Cytocochleogram of PLGA and pluronic pellet control group IHC from apex (row 0) to base.***

The innermost row of outer hair cells (OHC 1) shows loss of cells at rows 1,5,6,8,9,15,19,21,25,27,30-31,35. The greatest loss was in row 25 (12%) followed by row 5 (10%). These losses were spread throughout the cochlea from the apex to the base. There were several rows which were difficult to read: row 1, 7, 40% of row 16, 19-20, 27-28, 80% of row 29, 35. This is shown as a cytocochleogram in Figure 108.

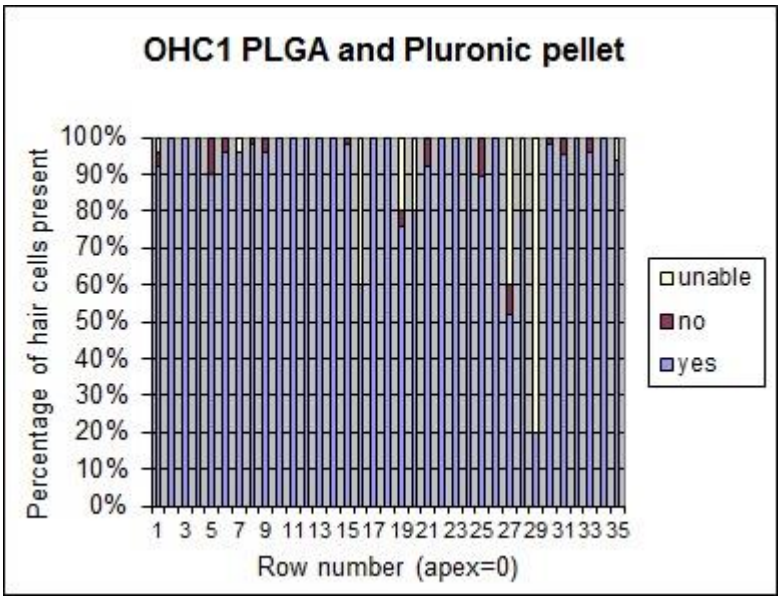


Figure 106: ***Cytocochleogram of PLGA and pluronic pellet control group innermost row of OHC from apex at 0 to base.***

The middle row of outer hair cells (OHC 2) shows loss of cells at rows 1-9, 11, 13-15, 18-24. These losses were spread throughout the cochlea from the apex to the base and none of the losses in a row reached 24% in row 1, 18% in row 18 and 15% in row 6. There were several rows which were difficult to read: row 1,7,11,16,19,20,22,23,27-28, 80% of row 29, 35. This is shown as a cytocochleogram in Figure 109.

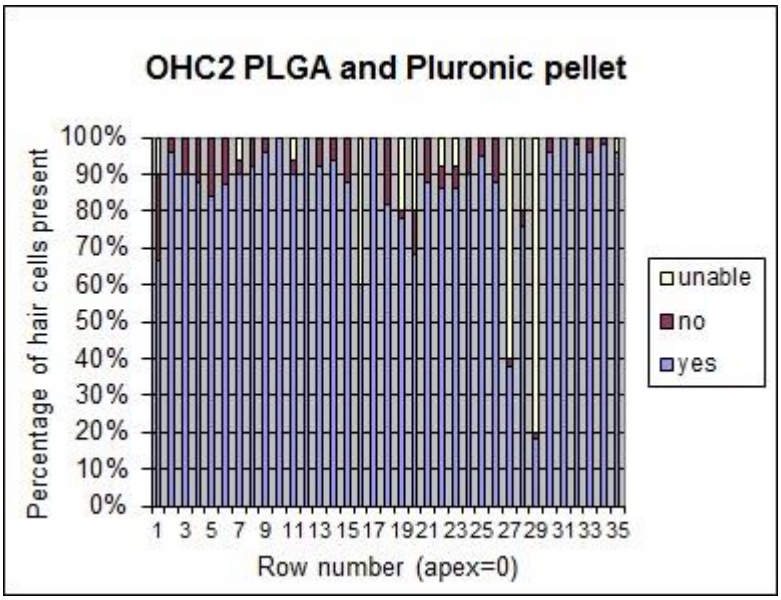


Figure 107: ***Cytocochleogram of PLGA and pluronic pellet control group middle row of OHC from apex at 0 to base.***

The outermost row of outer hair cells (OHC 3) show loss of cells to some degree in all rows expect 17 and 28. The greatest loss was 40% in row 1, 22% in row 5, and 20% in row 21. These losses were spread throughout the cochlea from the apex to the base. There were several rows which were difficult to read including rows 1, 2, 4, 16, 19, 60% of rows 27 and 28, 80% of rows 29 and 35. This is shown as a cytocochleogram in Figure 110.

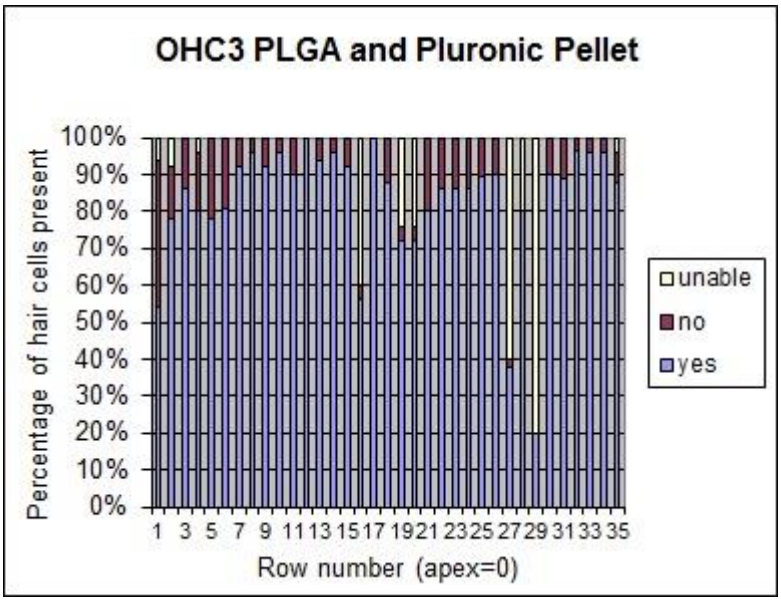


Figure 108: ***Cytocochleogram of PLGA and pluronic pellet control group outermost row of OHC from apex at 0 to base.***

Using the semi quantitative analysis, there does not appear to be any appreciable loss of IHC or OHC in the PLGA and pluronic control group throughout the cochlea. Cochlea from the PLGA and pluronic control group show normal arrangement of three rows of outer hair cells and one row of inner hair cells. These results are in keeping with the ABR threshold results for the PGLA and pluronic control group which do not show any significant excursions from the initial mean value at week 0.

6.1.3 Cytocochleogram of PLGA and pluronic pellet loaded with rifampicin and clindamycin

One full cochlea from a guinea pig in the pellet with rifampicin and clindamycin group was prepared, dissected and a cytocochleogram was made. Hair cells were counted systematically from base to apex and marked off on a template (Figure 106). The inner hair cell (IHC) cytocochleogram shows loss of cells at rows 1-2, 5, 8, 18, 20% of row 19, 21-22 and 31. Most of these losses were less than 10% and were spread throughout the cochlea from the apex at row 1 to the base at row 35. There were several rows which were difficult to read: 8% of row 3, 20% of row 16, 20% of row 20 and 80% of row 29. This is shown in the cytocochleogram in Figure 111.

There does not appear to be any difficulties reading the extreme apical region of the inner hair cells in the cochlea from the guinea pig loaded with pellets containing rifampicin and clindamycin. Inner hair cells are lost at the apex and predominantly the middle portion of the cochlea (Figure 111).

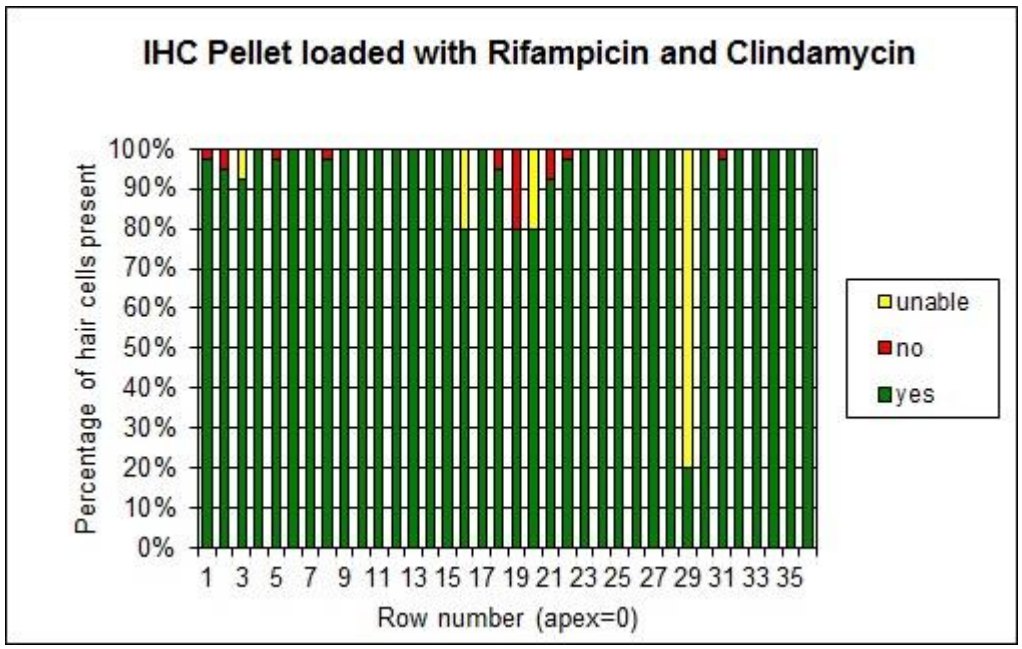


Figure 109: ***Cytocochleogram of PLGA and pluronic pellet loaded with rifampicin and clindamycin IHC from apex row 0 to base.***

The innermost row of outer hair cells (OHC 1) shows loss of cells at rows 1,5,6,8,9,14,19,21,25,27,30-31,33,36. The greatest loss was in row 25 (11%) followed by row 5 (10%). These losses were spread throughout the cochlea from the apex to the base. There were several rows which were difficult to read: row 1, 7, 40% of row 16, 19-20, 40% of row 27, 28, 80% of row 29, 35. This is shown as a cytocochleogram in Figure 112.

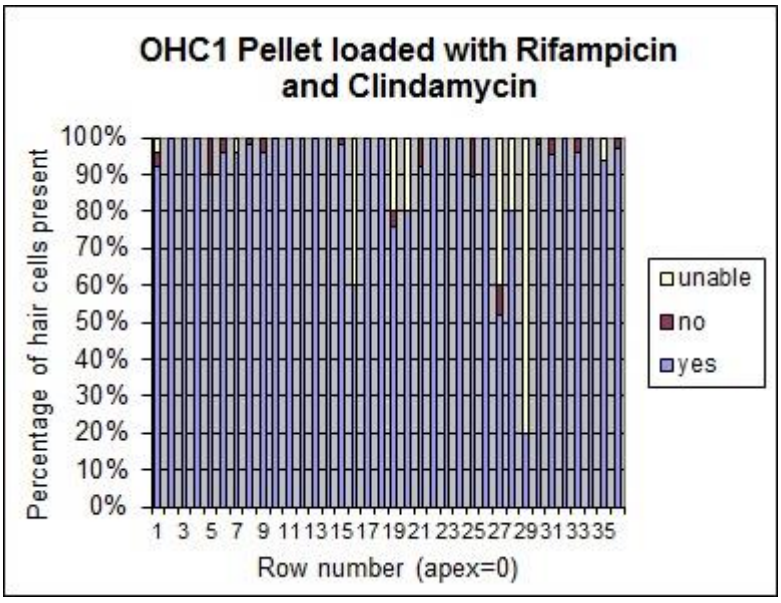


Figure 110: ***Cytocochleogram of PLGA and pluronic pellet loaded with rifampicin and clindamycin innermost row of OHC from apex row 0 to base.***

The middle row of outer hair cells (OHC 2) shows loss of hair cells in all rows with the exception of 10, 17 , 31 and 35. These losses were spread throughout the cochlea from the apex to the base and with a majority of row losses less than 10% with the greatest losses of 23% in row 1 and 18% in row 18. There were several rows which were difficult to read: rows 1, 7, 11, 16 (40%), 19, 20, 27(60%), 28, 80% of row 29, 35. This is shown as a cytocochleogram in Figure 113.

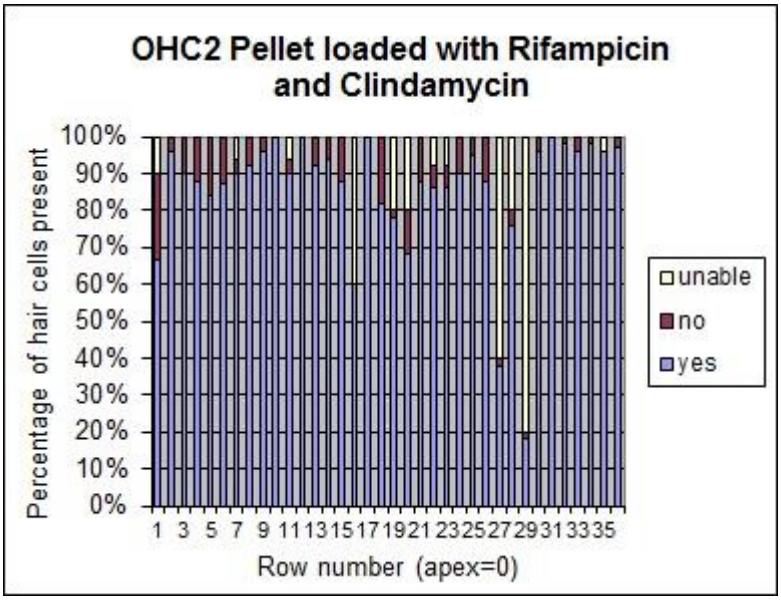


Figure 111: ***Cytocochleogram of PLGA and pluronic pellet loaded with rifampicin and clindamycin middle row of OHC from apex row 0 to base.***

The outermost row of outer hair cells (OHC 3) shows loss of cells to some degree in all rows expect 17, 28 and 29. The greatest loss was 40% in row 1, 22% in row 5, and 20% in row 6. These losses were spread throughout the cochlea from the apex to the base. There were several rows which were difficult to read including rows 1, 2, 4, 40% of row 16, 19, 20, 60% of row 27, 28, 80% of row 29, 35. This is shown as a cytocochleogram in Figure 114.

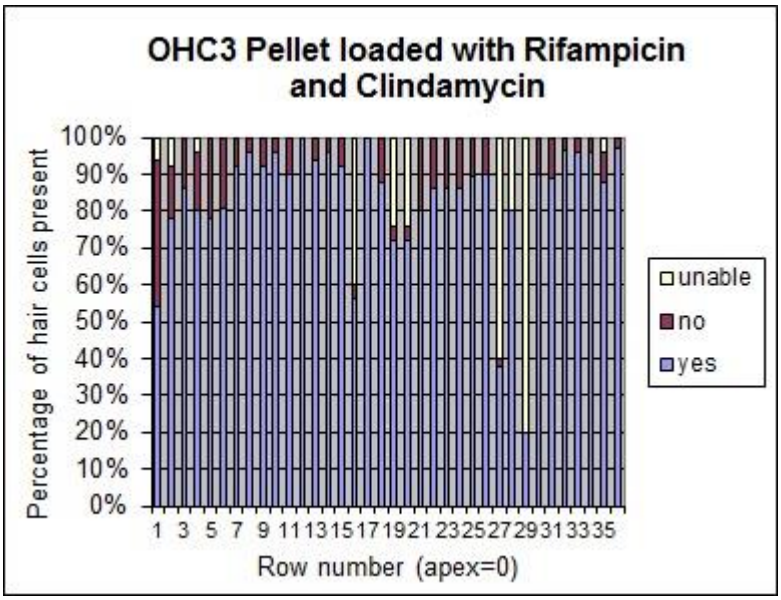


Figure 112: **Cytocochleogram of PLGA and pluronic pellet loaded with rifampicin and clindamycin outermost row of OHC from apex (row 0) to base.**

There does appear to be a pattern of OHC loss which is seen to a greater extent in the outermost hair cell row (OHC3) compared to the innermost row (OHC1) and with a trend towards the apex of the cochlea (Figure 114).

6.1.4 Summary of cytocochleogram results

Overall, there is no evidence of appreciable IHC or OHC loss in the biological control and PLGA and pluronic pellet control groups when analysing the cytocochleograms. This is consistent with the ABR recordings showing no significant elevation in ABR in these control groups. However, there does appear to be a small loss of outer hair cells in a graduation from the outermost row (OHC3) to the innermost row (OHC1) with the apex affected more than the base.

There is no significant loss of IHC and OHC to account for the ABR threshold elevation in the PLGA and pluronic pellet group loaded with rifampicin and clindamycin. The maximal hair cell loss from the cytocochleograms was 20% of the IHC and up to 40% of the OHC. These losses are sporadic and are insufficiently to attribute the ABR threshold elevations. Other studies of cytocochleograms correlating with ABR threshold elevations have shown consistent losses of IHC and OHC of up to 100% in an exponential manner (Wilmott *et al*., 2008) at an increased distance from the apex. The results of cytocochleogram studies therefore show that the ABR threshold elevation seen in the PLGA and pluronic pellet group loaded with rifampicin and clindamycin cannot be attributable to IHC or OHC loss. Immunofluorescence studies allow a detailed analysis of the IHC and OHC morphology to assess if the ABR threshold elevation associated with the antibiotic laden pellets can be accountable by subtle derangement in the IHC and OHC alignment or losses.

6.2 IHC and OHC morphological studies using immunofluorescence

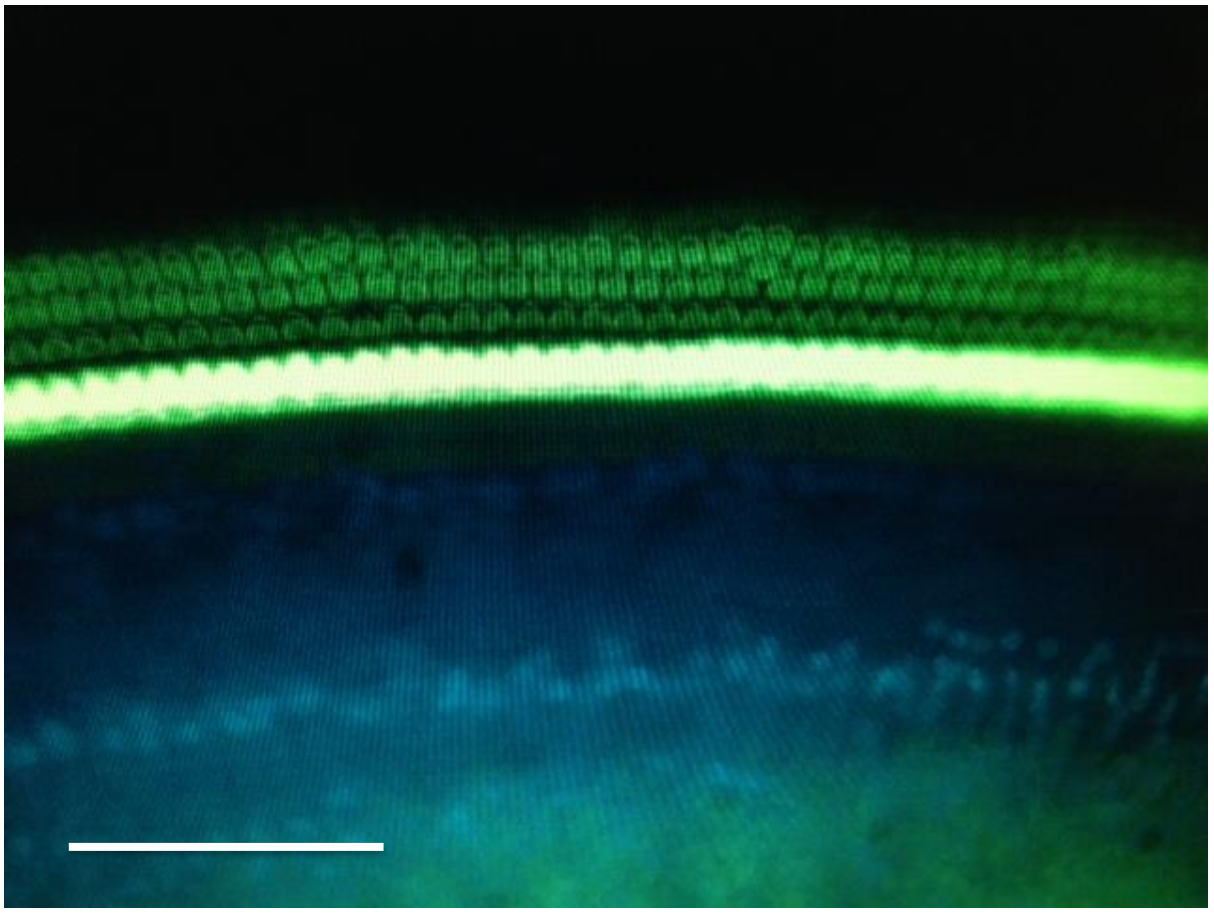


Figure 113: ***Preparation of Organ of Corti using DAPI and Phalloidin staining. Bar = 50µm in a biological control specimen.***

The immunofluorescence preparation allows appreciation of the normal organisation of the three outer hair cell rows and single inner hair cell row in the cochlea (Figure 115) and their morphology.

6.2.1 Surgical Control morphological studies of IHC and OHC

Sections of cochlea dissected and prepared for immunofluorescence taken from the apex show the three outer hair cell rows. There is occasional hair cell loss seen which is most apparent in the outermost row. The inverted V pattern of the kinocilium shows disorganisation (Figure 116) with a haphazard arrangement shown.

Apex

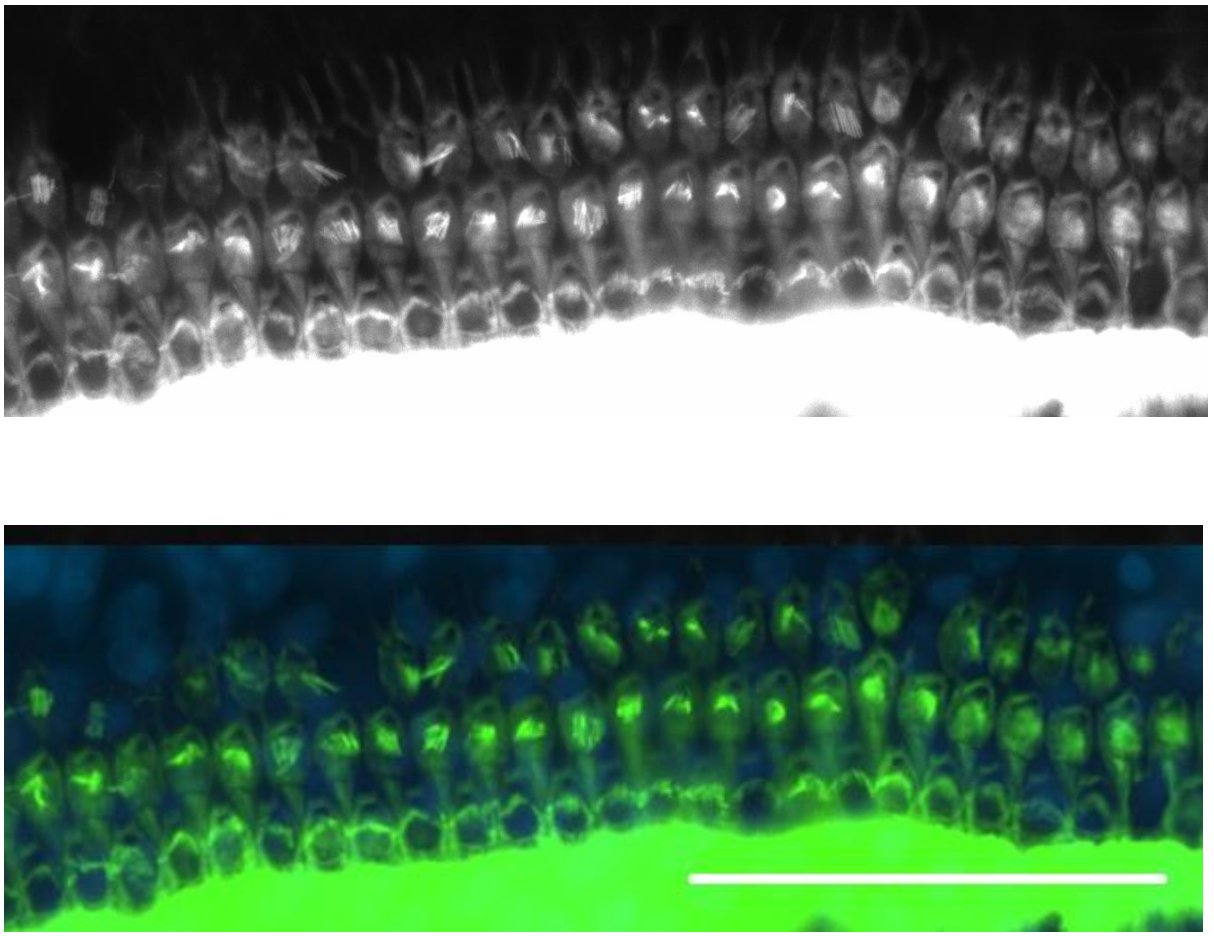


Figure 114: ***Surgical control apical section of cochlea without and with DAPI and Phalloidin immunofluorescence. Bar = 50µm***

The middle section of the cochlea from the surgical control group shows occasional hair cell loss and a clear organization of the hair cells. The detail of the kinocilium orientation is less obvious with the inverted V seen in a majority of the hair cells (Figure 117).

Middle

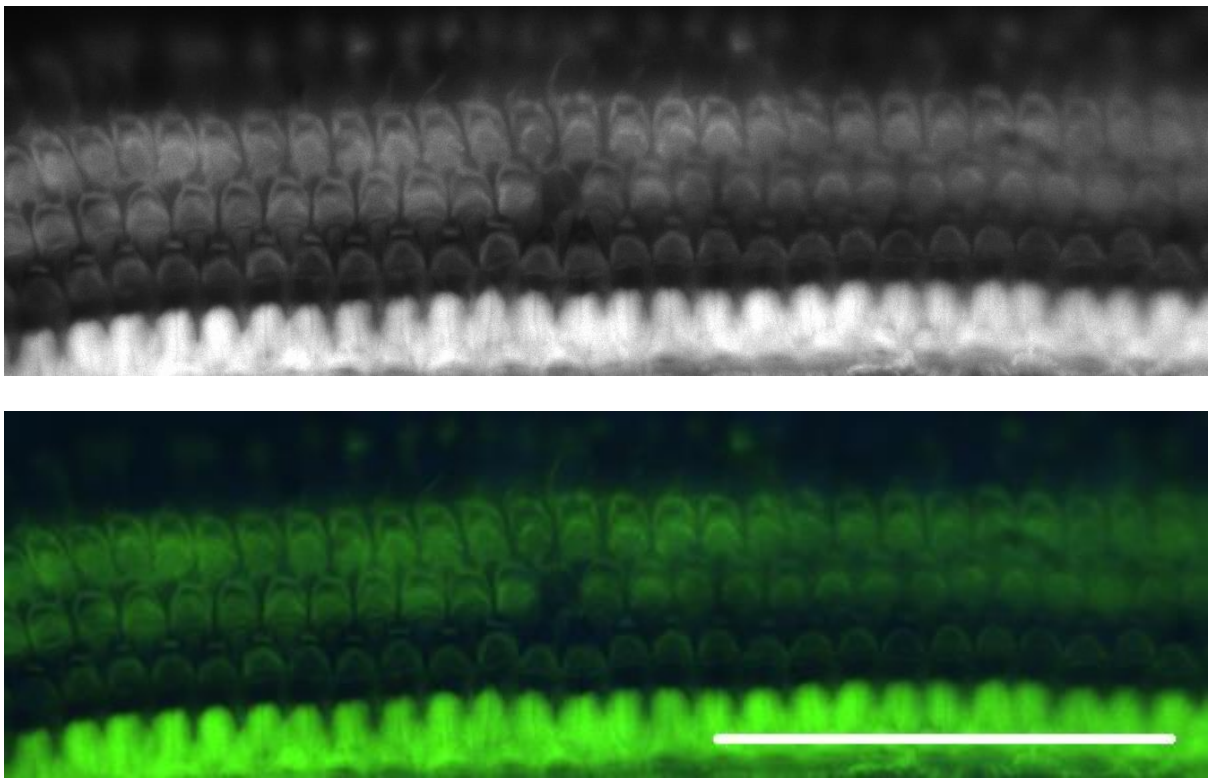


Figure 115: ***Surgical control middle section of cochlea without and with DAPI and Phalloidin immunofluorescence. Bar = 50µm***

Base

The basal section of the cochlea from the surgical control group shows occasional hair cell loss and a clear organization of the hair cells. The detail of the kinocilium orientation is less obvious with the inverted V seen in a majority of the hair cells (Figure 118).

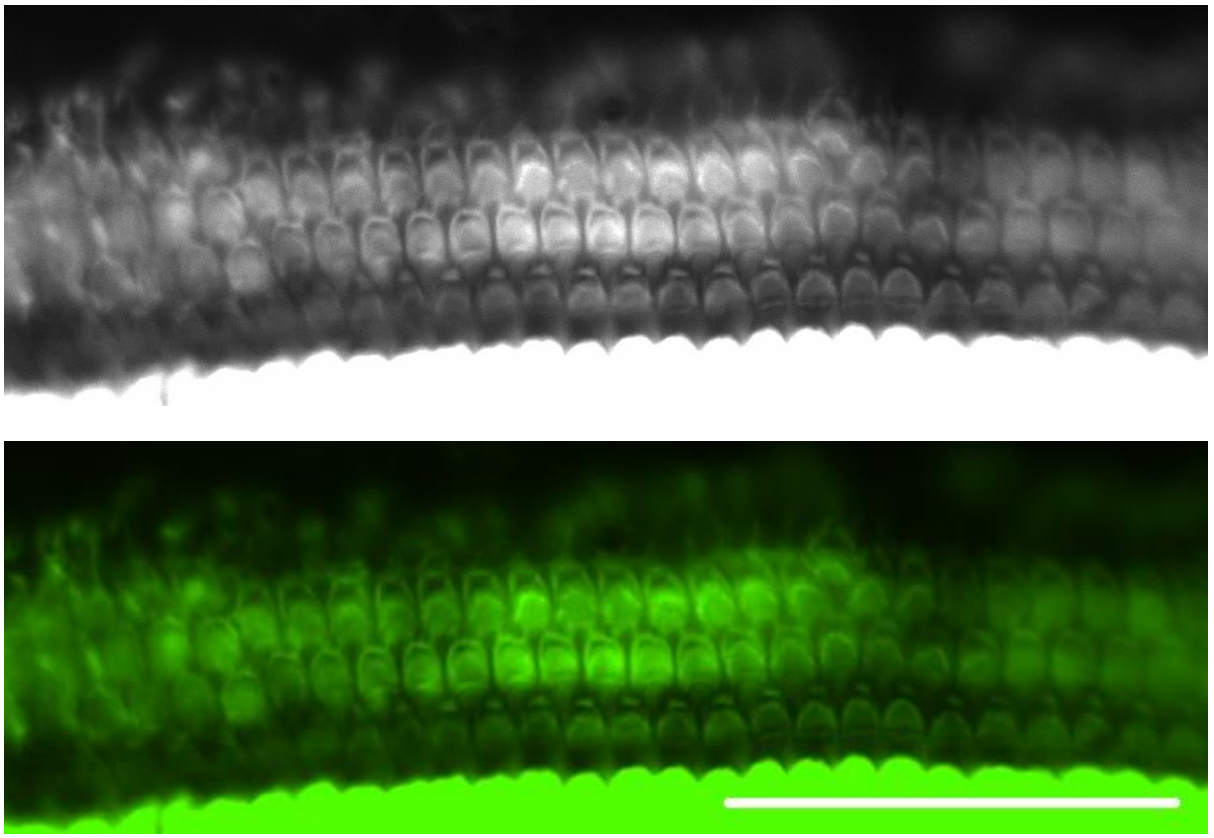


Figure 116: ***Surgical control basal section of cochlea without and with DAPI and Phalloidin immunofluorescence. Bar = 50µm***

6.2.2 PLGA and pluronic pellet control

Apex

Sections of cochlea dissected and prepared for immunofluorescence taken from the apex show the three outer hair cell rows. There is occasional hair cell loss seen which is most apparent in the middle and innermost rows (Figure 119). The inverted V pattern of the kinocilium shows disorganisation with a haphazard arrangement shown.

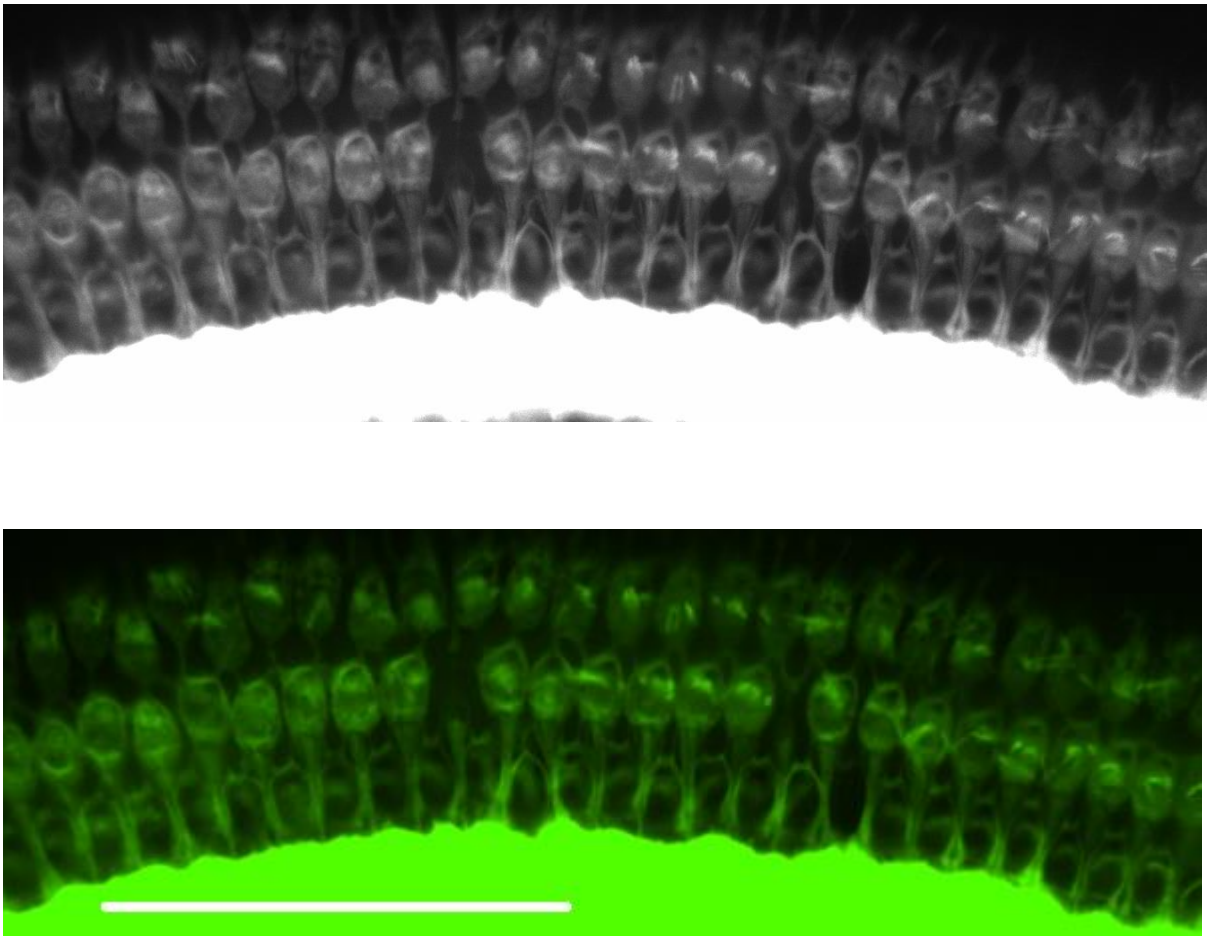


Figure 117: ***PLGA and pluronic pellet control apical section of cochlea without and with DAPI and Phalloidin immunofluorescence. Bar = 50µm***

Middle

Sections of cochlea dissected and prepared for immunofluorescence taken from the middle region show the three outer hair cell rows. There is occasional hair cell loss seen which is apparent in the outermost and innermost row. The inverted V pattern of the kinocilium shows disorganisation (Figure 120) with a haphazard arrangement shown.

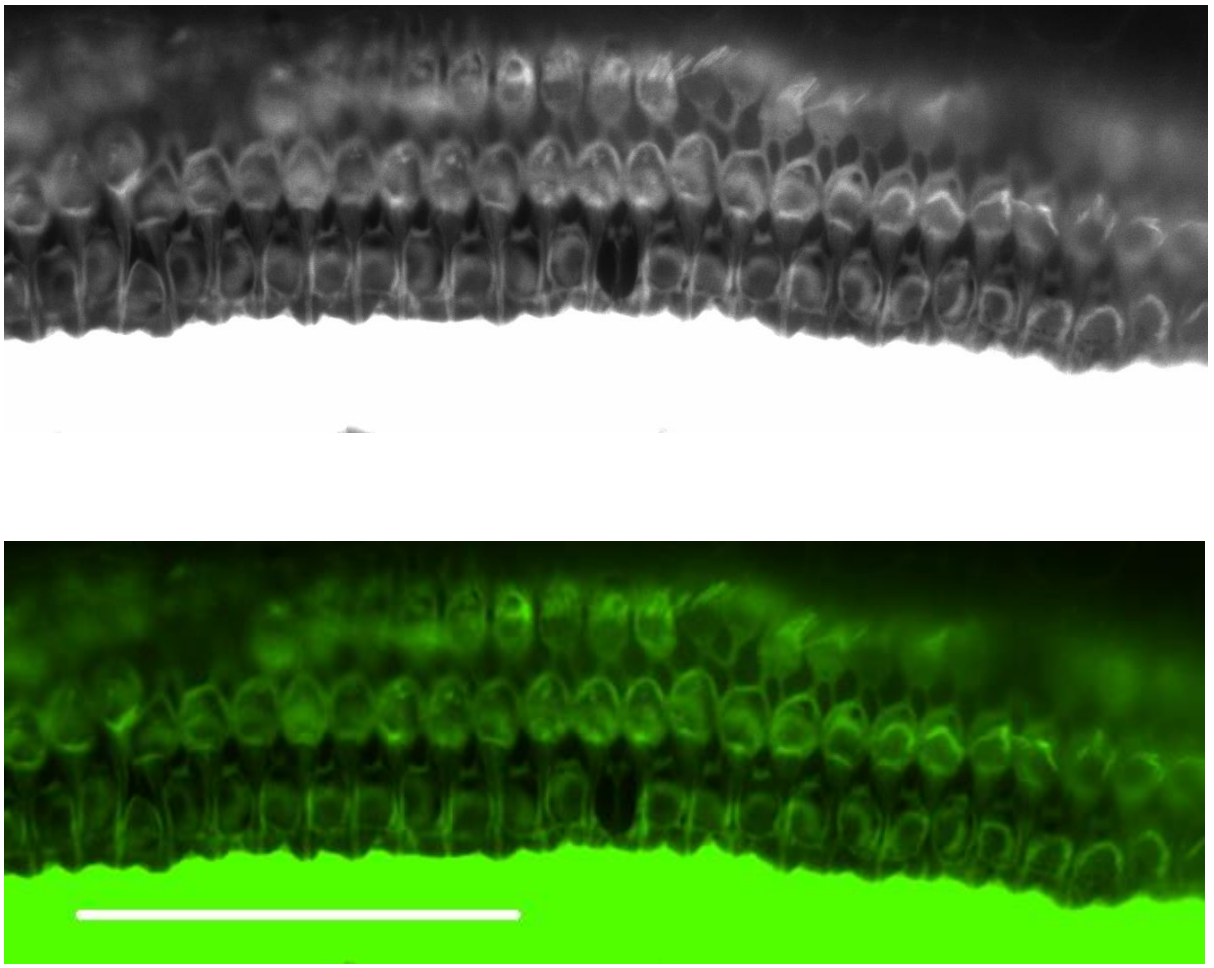


Figure 118: ***PLGA and pluronic pellet control middle section of cochlea without and with DAPI and Phalloidin immunofluorescence. Bar = 50µm***

Base

Sections of cochlea dissected and prepared for immunofluorescence taken from the basal region show the three outer hair cell rows. There is occasional hair cell loss seen which is apparent in the innermost row. The inverted V pattern of the kinocilium shows disorganisation and is difficult to appreciate with this specimen (Figure 121).

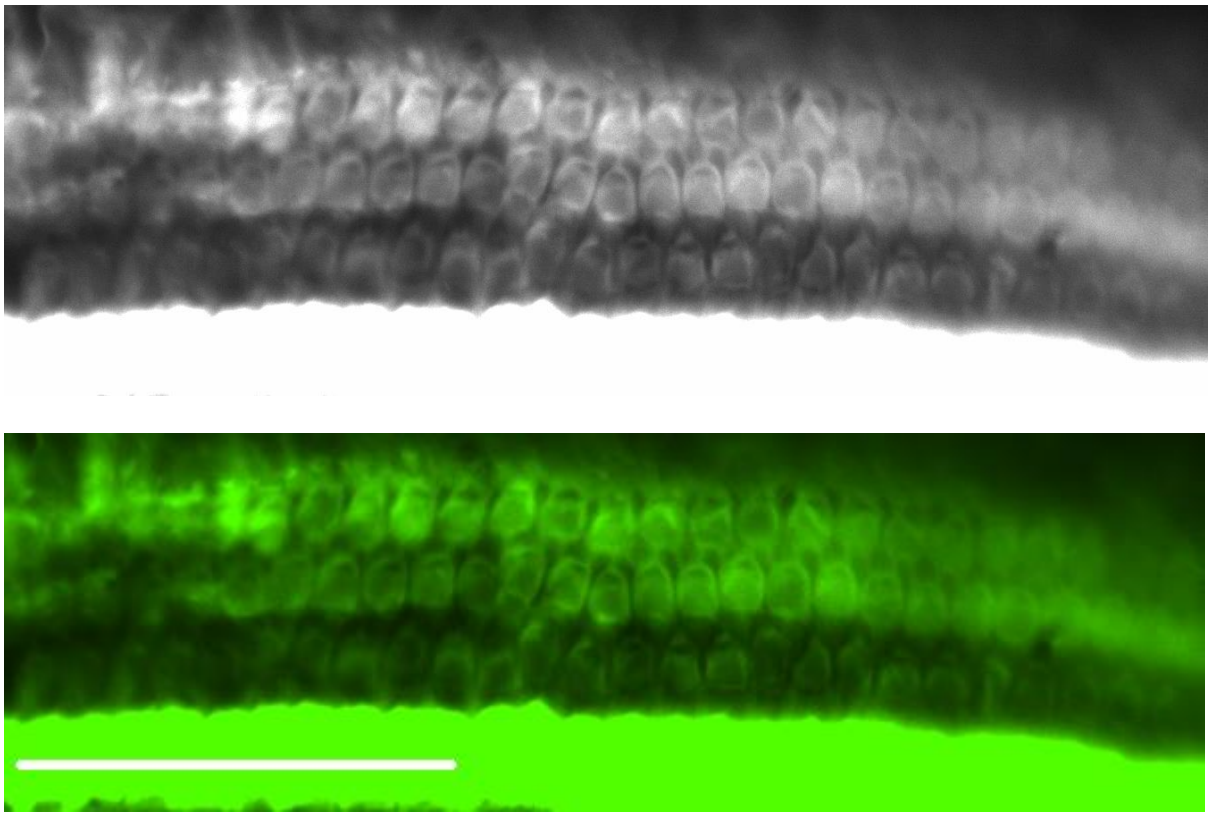


Figure 119: ***PLGA and pluronic pellet control basal section of cochlea without and with DAPI and Phalloidin immunofluorescence. Bar = 50µm***

6.2.3 PLGA and pluronic pellet loaded with rifampicin and clindamycin in combination

Apex

Sections of cochlea dissected and prepared for immunofluorescence taken from the apex show the three outer hair cell rows. There is occasional hair cell loss seen which is apparent in the outermost row. The inverted V pattern of the kinocilium shows disorganisation (Figure 122) with a haphazard arrangement shown, especially in the outermost row.

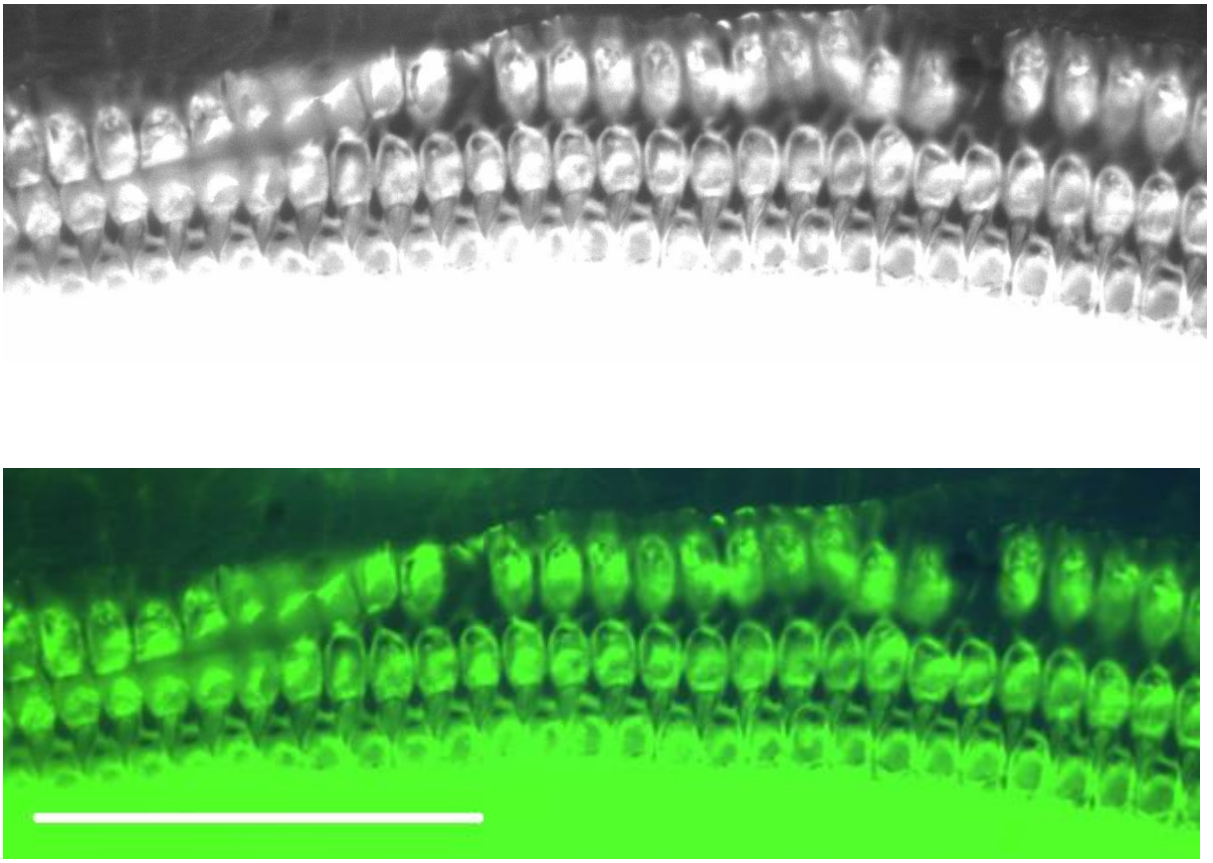


Figure 120: ***PLGA and pluronic pellet loaded with rifampicin and clindamycin apical section of cochlea without and with DAPI and Phalloidin immunofluorescence. Bar = 50µm***

Middle

Sections of cochlea dissected and prepared for immunofluorescence taken from the middle region show the three outer hair cell rows. There is occasional hair cell loss seen which is apparent in the outermost row. The inverted V pattern of the kinocilium shows disorganisation (Figure 123) with a haphazard arrangement shown in the middle and outer rows, but normal arrangement in the innermost row.

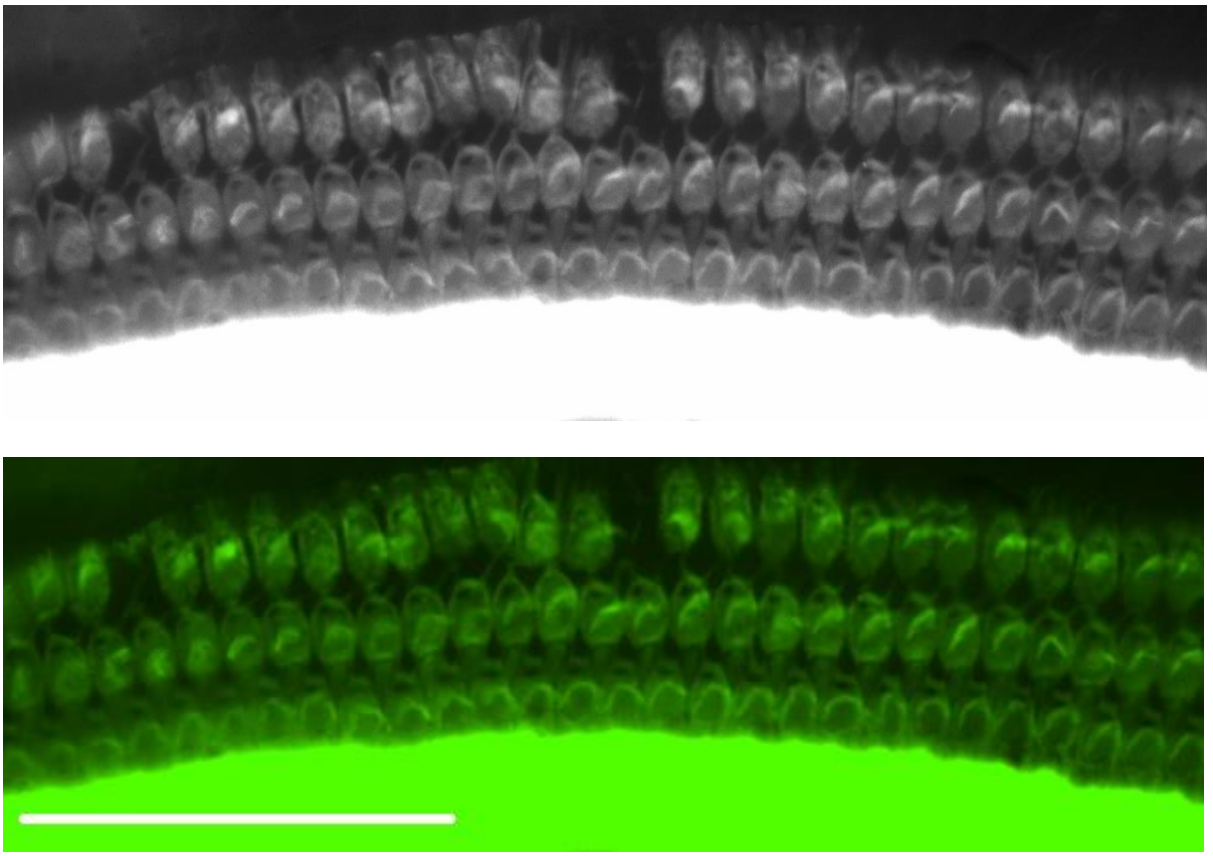


Figure 121: ***PLGA and pluronic pellet loaded with rifampicin and clindamycin middle section of cochlea without and with DAPI and Phalloidin immunofluorescence. Bar = 50µm***

Base

Sections of cochlea dissected and prepared for immunofluorescence taken from the basal region show the three outer hair cell rows. There is occasional hair cell loss seen which is apparent in the outermost row. The inverted V pattern of the kinocilium shows some disorganisation (Figure 124) but can be appreciated in the middle and innermost rows clearly.

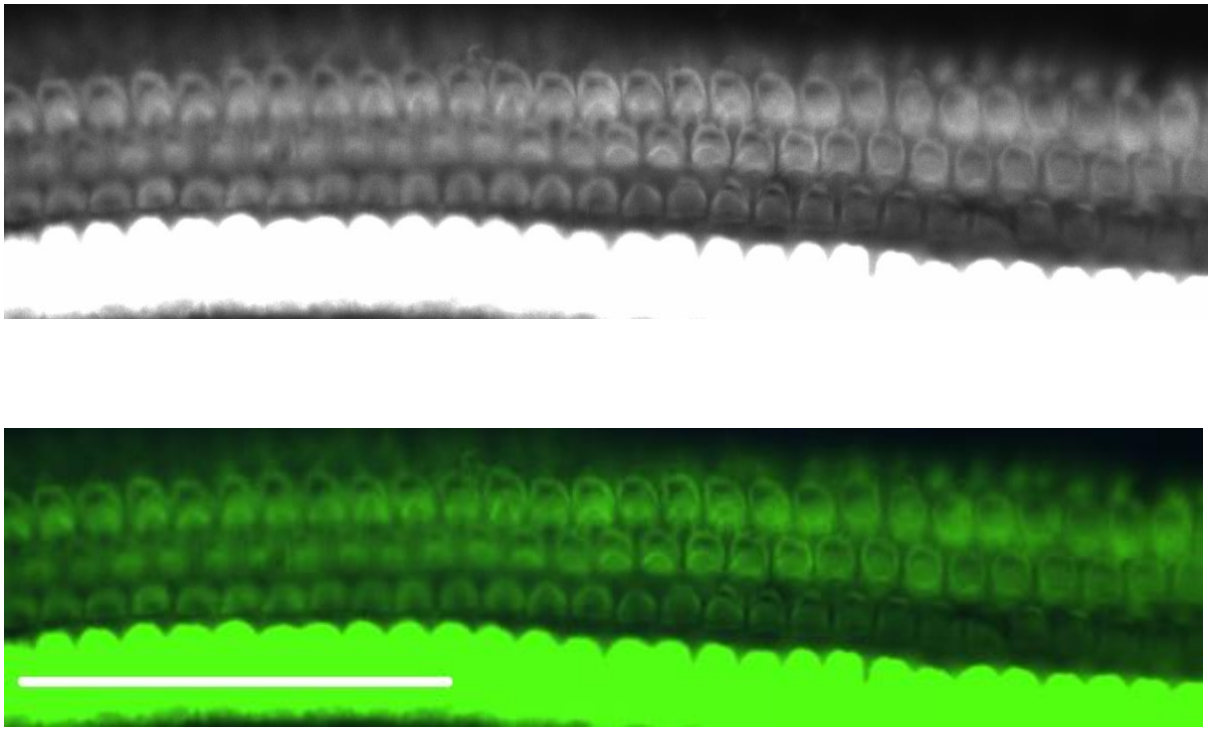


Figure 122: ***PLGA and pluronic pellet loaded with rifampicin and clindamycin basal section of cochlea without and with DAPI and Phalloidin immunofluorescence. Bar = 50µm***

6.2.4 Summary of immunofluorescence studies

In all of the immunofluorescence specimens, the microanatomy of the cochlea can be appreciated with three rows of outer hair cells and one row of inner. There are occasional hair cells losses in different rows and the kinocilium frequently shows disorientation instead of a neat inverted V pattern.

There does not appear to be any trend or appreciable difference between the control groups and pellet loaded with rifampicin and clindamycin. Therefore, the ABR threshold elevation seen in the experimental group with pellet loaded with antibiotics cannot be attributed to OHC or IHC loss or derangement. There does appear to be an increase in OHC derangement in the outermost row of the OHC. This is most likely caused by the sample preparation with dissection and placement of the coverslip.

The cytocochleogram and immunofluorescence studies show no OHC or IHC loss or derangement that are sufficient to account for the ABR threshold results. Any appreciable hair cell losses seen are not at the level where ABR thresholds would be affected. Other studies have shown that losses up to 100% consistently across the cochlea are required for ABR thresholds to be affected (Wilmott 2008).

The effect of the pellet in the middle ear and its potential to alter the conduction of sound 16 weeks after implantation should therefore be assessed using temporal bone histology studies. Any evidence of chronic inflammation and fibrosis from the surgery and pellet implantation would be of interest as antibiotic pellet implantation is a putative new treatment for OME. On a microscopic level, histology specimens may

contribute to information on the inner ear including the organ of Corti and relative sizes of the scala compartments. Pellet placement has the potential to affect the electrolyte balance of the endolymph and hence any evidence of hydrops would be of interest.

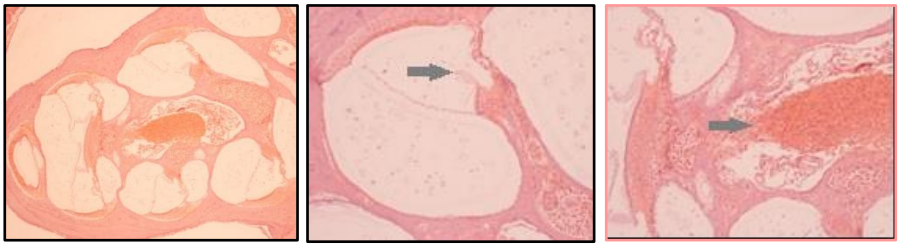
Chapter 7: Temporal bone histology results

7.1.1 Histology of surgical control group

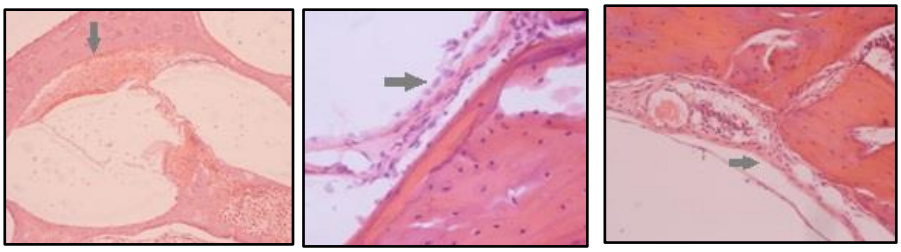
Middle ear Haematoxylin and Eosin (H and E) stained sections were analysed at the level of the modiolus. The epithelium around the surgical control sham procedure was identified and reviewed. This had a normal healthy appearance. There was still evidence, after 16 weeks of the epithelial disruption which had occurred to insert the pellet into the middle ear bulla (Figure 125).

The cochlea has a normal cross sectional appearance. Minor disruption of the Organ of Corti is seen in the preparations including displacement of the tectorial membrane and disruption of Reissner's membrane. The overall structure appears normal with no evidence of inflammatory cells and normal architecture of the stria vascularis and spiral ganglion. The cochlea has a normal cross sectional appearance in the apical, middle and basal regions.

SURGICAL CONTROL GROUP



a) Cochlea b) Organ of Corti c) Spiral ganglion



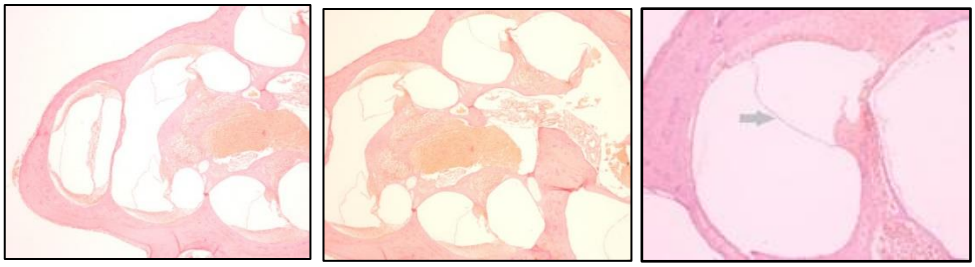
d) Stria vascularis e) Middle ear epithelium x 40 f) Middle ear epithelium x 20

Figure 125: ***Cochlea from surgical control guinea pig showing ultrastructure in a) Cochlea b) Organ of Corti c) spiral ganglion and d) stria vascularis and middle ear epithelium in e) and f).***

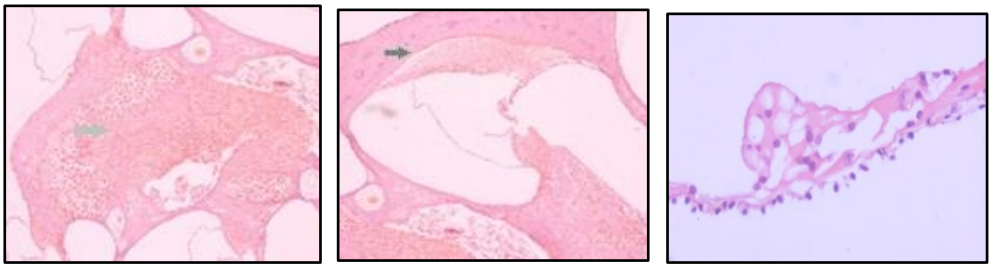
7.1.2 Histology of the pellet control group

The cochlea architecture has a normal appearance identifying the Organ of Corti, stria vascularis and spiral ganglion. Disruption of Reissner's and tectorial membranes are seen. The Organ of Corti also has a kinked appearance which is consistent in all the specimens (Figure 126 c).

PELLET CONTROL GROUP



a) Cochlea b) Cochlea c) Organ of Corti – intact Reissner's membrane (RM), disrupted tectorial



d) Spiral ganglion x 40 e) Stria vascularis x 20 f) Organ of Corti x40

Figure 123: ***Cochlea from PLGA and Pluronic guinea pig showing ultrastructure in a) Cochlea b) Cochlea c) Organ of Corti – intact Reissner's membrane, disrupted tectorial membrane d) spiral ganglion e) stria vascularis and f) Organ of Corti x 40.***

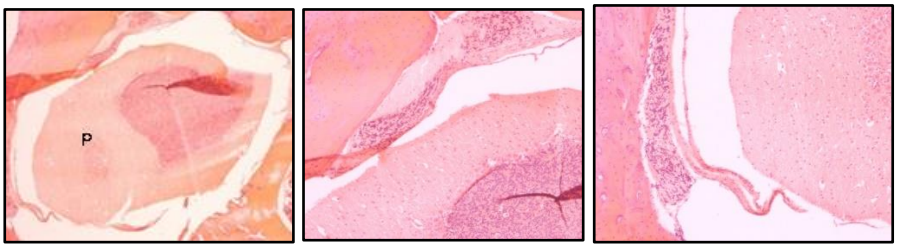
7.1.2 Histology of the pellet loaded with rifampicin and clindamycin

The remnant pellet in the middle ear microscopically has evidence of phagocytosis with macrophages located around the peripheries and a central remnant of the pellet which is intact (Figure 127 a,b and c). Evidence of acute inflammation is seen in the middle ear epithelium.

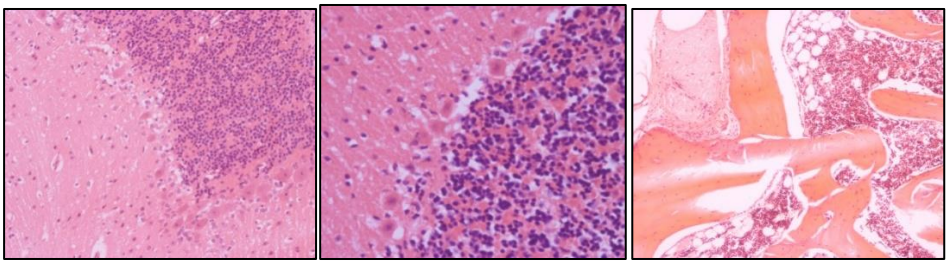
The cochlea has a normal architecture and the stria vascularis and spiral ganglion can clearly be identified with a normal appearance. The Organ of Corti is intact but with minor disruption of the Tectorial and Reissner's membrane seen. There did not appear to be any changes in the cochlea structure between cross sections of the apex, middle or base.

The middle ear epithelium shows disruption around the surgical site of pellet insertion. The bone wax remnant is also present (Figure 127 f).

PELLET WITH RIFAMPICIN AND CLINDAMYCIN



a) ME with pellet (P) x10 b) pellet (P) and ME epithelium x20 c) pellet and ME epithelium x 20



d) pellet margin and centre e) pellet margin and centre f) bone wax reaction

Figure 124: ***Cochlea from PLGA and pluronic guinea pig loaded with rifampicin and clindamycin showing ultrastructure in a) middle ear with pellet b) pellet and ME epithelium c) pellet and ME epithelium d) pellet margin and centre x 40 e) pellet margin and centre x 40 and f) bone wax reaction x 40.***

7.1.3 Discussion of histology results

The temporal bone histology results show that the surgical control and PLGA and pluronic pellet groups demonstrate normal architecture of the stria vascularis and spiral ganglion cells. The cochlea has a normal cross sectional appearance in the apical, middle and basal regions. The histology sections of the temporal bones loaded with PLGA and pluronic pellet with rifampicin and clindamycin demonstrate a kinked appearance of the Reissner's membrane. This is potentially associated with increased pressure in the endolymph compartment of the inner ear (Salt 2010) which can occur after alteration of the electrolyte balance between scala compartments.

The histology specimens from the temporal bones with rifampicin and clindamycin pellet demonstrate evidence of remnant pellet at 16 weeks with surrounding inflammatory cells. Macrophages are clearly seen surrounding the pellet remnant suggesting that the process of phagocytosis is occurring to eliminate the remnant pellet. At 16 weeks post implantation, this would bring a state of chronic inflammation to the middle ear which could potentiate epithelial secretions and mucous production as seen in the state of OME. The persistence of the PLGA and pluronic pellet in the middle ear after 16 weeks correlates with the ABR threshold elevation still recordable at 16 weeks and hence the remnant pellet maybe contributing to this audiometric effect.

After PLGA and pluronic pellet loaded with rifampicin and clindamycin implantation into the guinea pig middle ear, ABR testing has shown an initial pan threshold elevation with middle frequency recovery over time. ABR amplitude and latency testing has also

been recorded alongside cytocochleograms, immunohistochemistry and temporal bone histology. Analysis and discussion of these results in a cohesive manner for all experimental groups would help to theorise a possible mechanism underlying ABR threshold elevation.

Chapter 8: Discussion

Summary of Results:

- Controls (BC, SC, P) saw no ABR threshold elevation between 0 weeks and 16 weeks

- Pellets loaded with rifampicin and clindamycin saw a pan (8-30kHz) ABR threshold elevation between 0 weeks when the pellets were inserted into guinea pig models and week 1

- There was some partial mid frequency recovery by week 16 but persistent significant ABR threshold elevation at 8kHz and 30kHz

- There was no consistent significant changes in ABR amplitude and latency seen over all experimental groups

- Friedman's analysis and Holm Bonferroni correction were applied and this supported the statistical testing of the ABR threshold, amplitude and latency

- Cytocochleograms did not exhibit any appreciable frank outer or inner hair cell loss in the apex, middle or base of the cochleas

- Immunofluorescence did not show any derangement in stereocilia orientation

- Middle ear histology showed that pellet remnant produces a moderate inflammatory response at 16 weeks

- The guinea pig was a robust experimental middle ear model for pellet placement

The experimental results show an ABR threshold elevation on placement of antibiotic laden pellets in the guinea pig middle ear. This finding therefore does not support the translation of pellet placement as a vehicle for drug delivery in humans at present. Firstly, the limitations and caveats that apply to my data and its interpretation are discussed. Secondly, the meaning of the results is explored in detail.

8.1 Experimental limitations and homeostasis

8.1.1 Limitations of pellets

The pellets were manufactured in Nottingham University department of Trauma and Orthopaedics (please see acknowledgements) and then transferred to the University of Leicester before the animal experiments were commenced. They were transferred on a bed of ice and then stored in the fridge at approximately 5^{o}c. This process of transfer is unlikely to alter the components of the pellets in any form, but should be mentioned as a potential source of alteration of pellet behaviour from the *in vitro* work.

The pellets were made using moulds and a slight variation in their shape was noticed at implantation. This included irregular edges which may have affected the smooth implantation through the bulla wall and hence should be considered as a possible source of trauma to the middle ear cavity of the animals. The middle ear bulla fenestration could be widened sufficiently using a Schucknect pick to accommodate this variation.

8.1.2 Limitations of anaesthetic regimen

The initial experiments were performed using isoflurane anaesthetic administered using a face mask with subcutaneous midazolam injection. The face mask had to be securely held in position to minimise leakage, however, despite best efforts, this was not totally avoidable. This resulted in small variations in the quantity of isoflurane delivered between different animals. Preliminary readings of ABR thresholds using

isoflurane and midazolam were higher than using the anaesthetic combination of hypnorm and midazolam.

A majority of the experimental groups were all anaesthetized using the hypnorm and midazolam regimen. However, there was a final experimental subset of 9 animals in total which was performed after a time interval. This comprised of 5 guinea pigs with pellets laden with clindamycin alone and 4 guinea pigs with pellets laden with rifampicin. This was for the purposes of increasing the numbers in all of the experimental groups to n=8 to satisfy the original power calculation.

During this experimental interval, hypnorm as an anaesthetic was discontinued by the manufacturer. Efforts were made to locate the drug, but this was unsuccessful. As a result, the anaesthetic regimen had to be adapted again. This was described in the methods section 3.6.4 and changed to midazolam and flumazenil after consultation with the veterinary surgeon and Home Office Inspector. This was an unexpected and unavoidable change in the anaesthetic regimen.

As an anaesthetic agent, isoflurane is used safely without adverse reaction in animal models. The action of isoflurane has been compared to ketamine and other anaesthetic agents (Ruebhausen *et al*., 2012 and Cederholm *et al*., 2012) in rat and mouse models and a detailed study of isoflurane action in the guinea pig has been done comparing the effect on ABR amplitude and latency (Stronks *et al*., 2010). This demonstrated a dose dependent reduction in amplitude and increase in latency which was most pronounced at 2% isoflurane and peaks IV and V (see section 8.5.4 and 8.5.7). The experimental regimen used for the guinea pigs included isoflurane post ABR recording for the surgical procedures (section 3.8.2) at a dose of 1%. Therefore, the

impact of isoflurane on ABR amplitude and latency would be minimised and not easily detectable as the analysis of amplitude and latency focussed on measurements of ABR waves P1-3. Isoflurane is not associated with ABR threshold changes and therefore is not considered to be a confounding factor in the ABR results.

8.1.3 Importance of temperature homeostasis

Temperature is known to affect the ABR threshold, amplitude and latency. A reduction in core body temperature, defined as hypothermia if less than 35 ^{o}c, results in an elevation in ABR latency (Doyle *et al*., 1985). It is also known that hyperthermia can effect ABR recordings with a reduction in latency and an increase in amplitude of waves I and II (Katbamna *et al*., 1993). Experiments on rats have also shown that increases in temperature are associated with decreased ABR amplitude and with little recovery when the body temperature returns to the normal range (Gold *et al*., 1985, Takahashi *et al*., 1991).

Anaesthetised guinea pigs are prone to hypothermia due to their large surface area relative to their body mass making them prone to body heat loss (Kohn *et al*., 1997). During the ABR recordings and surgical experiments, care was taken to maintain the core body temperature of the anaesthetised guinea pigs by using a heated mat and foil blanket. A rectal probe was used to record temperature and was linked to an alarm which activated below a set temperature of 35.5 ^{o}c. Each ABR recording lasted approximately 45 minutes and the surgical procedure for pellet implantation also lasted a similar length of time. It was therefore important that guinea pig temperatures

were maintained during the experiments and in the post operative recovery period for accurate, consistent ABR readings and also to optimise animal welfare.

In addition to the impact of temperature changes on ABR recordings, other effects of hypothermia include cardiac arrhythmias, post anaesthetic tremors (Grahn *et al*., 1996) and a longer post anaesthetic recovery time. Death of the animals may also ensue. Lowering of core body temperature affects cell regulation and metabolism and has been shown in the guinea pig to alter ionic potentials in the Organ of Corti by suppressing the K^+ active transport system (Konishi *et al*., 1981). These effects on a cellular level may potentially explain the mechanism of ABR changes by altering the endolymph potential of the cochlea.

8.1.4 Importance of oxygen saturation homeostasis

During the procedures, oxygen was delivered to the anaesthetised animal via a facemask. The oxygen saturations were measured using a probe on the guinea pig's left foreleg. This was to ensure homeostasis of conditions and to optimise animal welfare. It is known that hypoxia, whilst potentially detrimental to the animal, can also influence the ABR recordings. Experiments have shown that hypoxia causes threshold shifts and increases in latency particularly in ABR waveform I (Attias *et al*., 1990). The mechanism of hypoxia causing ABR threshold and latency changes is via depression of the endocochlear potential (Freeman *et al*., 1995). It was therefore important to ensure oxygen levels were experimentally closely regulated and monitored.

8.2 Guinea pig animal welfare

8.2.1 Guinea pig housing

Before commencement of the guinea pig experiments, the animals had one week to acclimatise in the Clinical Research Facility (Animal House) in cages with four animals per cage. They were monitored daily by Animal House staff measuring their weight, inspecting for any surgical wounds and observing their general health. As they grew in size, some animals became dominant boars and were found to be scratching and biting the others in the cages. As a result, these large dominant boars were separated from the others. The animals which were injured were a mixture of experimental test groups (Table 58). There was a predominance of the injuries on the guinea pigs' left side which is the side of intervention. There is therefore potentially a connection with the experimental group creating a vulnerability which the dominant boars exploit. Complications were seen across all experimental groups: surgical control, PLGA and pluronic pellet or antibiotic laden pellets. The guinea pigs in cage 4 and 9 which were injured were housed alone for their safety. The guinea pig in cage 9 with a mark on its rump (surgical control number 10) was deemed to be the dominant boar and was also housed separately to protect the other two guinea pigs in cage 9. This was an intervention recommended by the NACWO and Animal House staff.

Mark / Cage	Nil	Head	Back	rump
1	SC1	BC9	P1	BC10
2	PA1	P2	SC2	PA2
3	P3	PA3	PA4	SC3
4	P5	P4	SC4	PA5
5	P6	SC6	PA6	SC5
6	P7	PA7	P8	PA8
7	SC7	BC1	SC8	BC2
8	SC9	PA9	P9	P10
9	PA10	BC3	BC4	SC10
10	BC5	BC6	BC7	BC8
11	PClind2	PClind1	PRif2	PRif1
12	PClind3	PRif3	PRif5	PRif4

Table 58: ***Table to show the guinea pigs housed at random (initially with 4 per cage)***

Key:
SC – surgical control
BC – biological control
P – PLGA and pluronic pellets
PA – PLGA and pluronic pellet loaded with antibiotics (rifampicin and clindamycin)
PClind – PLGA and pluronic pellet loaded with clindamycin
PRif – PLGA and pluronic pellet loaded with rifampicin
Red – trauma from scratches and bites
Green – corneal damage
Blue – wound infection

Inter-male aggression is well documented in guinea pigs (Sachser *et al*., 1994) with aggressive biting in the shoulder region a common form of behaviour (Grant *et al*., 1963). It has also been shown that inter-male aggression is affected by environment, particularly during puberty which is between 45-55 days (Slob *et al*., 1979). The experimental guinea pigs were housed together over this period, which may explain changes in their behaviour. However, 4 out of 5 of the guinea pigs with scratches and bites were from the experimental group of guinea pigs with pellets loaded with both rifampicin and clindamycin (Table 58). This does suggest a potential vulnerability caused by the experimental intervention with rifampicin and clindamycin laden pellets. The injuries sustained could also possibly originate from a vestibular disturbance which

would increase vulnerability to attack or the decreased hearing on the left side, preventing early warning, allowing the dominant boars to exploit this decreased reaction time and attack.

8.2.2 Complications of surgery: wound infection, haemorrhage, facial nerve injury

Post operatively, wound infections were identified in three of the animals, all presenting in the first post-operative week. On examination, there was swelling and fluctuance adjacent to the surgical wound. None of the guinea pigs with wound infections were given antibiotics as this may have impacted on the guinea pig's hearing threshold and hence on the integrity of the data. Therefore, they were managed conservatively and were seen to resolve. In total, three of the animals had a post operative wound infection (SC2, P6 and PA7) out of a cohort of 47 guinea pigs undergoing surgery (6.4%). The total number of guinea pigs undergoing a surgical procedure were 10 surgical controls, 10 pellet, 10 pellet with rifampicin and clindamycin, 8 rifampicin and 9 with clindamycin. Additional numbers were used in the SC, P and PA groups as the anaesthetic and surgical regimen was modified and developed.

Preventative measures were taken throughout the experiments to minimise wound infections. Pre operative preparation of the guinea pig skin was performed by shaving the fur in the mandibular region and applying chlorhexidine topically. This has also been used in other animal studies as disinfectant to reduce the rate of wound infection (Pinilla *et al*., 2001). Care was also taken during surgery to drape the animals and use an aseptic technique. The instruments used were sterilised in an autoclave at 121^{o}C

for 20 minutes and the pellets themselves were sterilised using an E-beam sterilisation technique (see section 3.12).

The ventral approach to the middle ear was performed on rats by Pinilla *et al*., 2001 and no reports of wound infection were reported, although the sample size in that study was only 6. As guinea pigs live in an open cage environment in groups of 4, there are multiple sources of contamination of the surgical wounds and therefore it is possible that contamination occurred post operatively during recovery and not during the surgical procedure itself. The scratches and bites elicited by the dominant boars in the cages tended to be on the left side of the animals. This trauma is a potential source of wound contamination as the epithelial layer of the skin was broken with the surgical incision. Minimising this contamination could be achieved via solitary housing, however, this is impractical and contrary to animal husbandry advice from the Animal House staff and NACWO unless there is a clear indication.

There were no reported cases of infection from the site of ABR electrode insertion. This was performed for each set of readings and the electrodes were clean, yet no skin preparation was used for their insertion. The size of the epithelium breach per electrode is very small compared to the cervical surgical incision which was approximately 2cms in diameter. This size discrepancy is likely to explain why ABR electrode insertion does not cause post procedural infection.

There were no reported cases of post-operative haematoma despite the cervical dissection. One reason for this low rate could be because the surgery was limited only to create access in the neck to the bulla and not aimed at resection of structures. There was therefore minimal disruption to the major vessels such as anterior facial vein or

large deep vessels which are branches of the internal carotid artery. Careful haemostasis was also achieved before closure of the neck wound. This was achieved using a combination of topical adrenaline (1:10 000) and bipolar diathermy on the coagulation setting of 10 Watts.

Facial nerve injury is possible from the cervical dissection to gain access to the middle ear bulla, however, no cases were seen. Damage would result in feeding difficulties due to injury to the facial musculature innervation and ocular complications from impaired eye closure. Two of the guinea pigs did have eye complaints (P2 and BC5) although the latter was on the non-intervention (right) side and appeared to be a cataract which has the possibility of a congenital origin. The other guinea pig had a corneal scratch on the left eye. There were no signs of facial nerve injury on examining this animal and therefore this was likely a traumatic injury potentially from the aggressive behaviours seen from the dominant boars (see section 8.2.1). Lacrilube eye ointment was applied to each guinea pig bilaterally during the experimental set up to prevent corneal injury.

Although there is a lack of weight gain seen in the cohort of guinea pigs with pellets loaded with rifampicin and clindamycin, there were no reported cases of facial nerve injury seen. If the left chorda tympani, which is a branch of the facial nerve supplying taste sensation to the anterior two thirds of the tongue, had been damaged, there is a compensatory contralateral right nerve which would not be affected, hence taste sensation overall would still be intact. The facial nerve branches which are vulnerable during the surgical approach to the middle ear bulla, however are distal to the chorda tympanic and hence alteration to taste sensation is unlikely without associated facial

palsy. Reduction in taste sensation is unlikely to be the explanation for the lack of weight gain seen.

Post operatively, no signs of vestibular disturbance were seen on examination of the guinea pigs. Vestibular dysfunction, however, was not formally measured. This can be done using short latency vestibular potentials evoked by RW stimulation. Recordings can be made from vertex-pinna electrodes measuring latency potentials V1-3 after 50μsec stimuli are presented to the RW. This response is lost after selective vestibular neurectomy (Bordure *et al.*, 1989) indicating that this is selective response from the vestibular system. This would be an interesting addition to the experimental design if the regimen were to be repeated. Access to the RW for stimulus presentation, however would involve access to the ME which would be a technical challenge on follow up. There is the potential for substances such as rifampicin and clindamycin to be vestibulotoxic as well as ototoxic, hence the importance of considering vestibular assessment in future experimental designs.

8.2.3 Complications of recovery

In the immediate post operative period, care was taken to position the guinea pigs prone with their heads supported by their front limbs. This ensured that there was equal pressure on the abdomen and that the nasal airway was patent. One animal did not survive the post operative 24 hours as it was found to have overheated as the cage was kept on a heated mat overnight. Upon review, the position of the cage was totally over the mat instead of allowing the animal a cooler area if it were partially on the mat. When it was reviewed the following morning, over 12 hours post procedure, its

breathing was laboured and there were copious secretions and hence it was humanely euthanized. This animal belonged to the cohort of guinea pig with pellet laden with clindamycin, therefore in the second cohort of experiments, an extra animal was used to ensure there was n=8 per experimental group. This guinea pig death was discussed at the Project License Review meeting held on February 6th 2017.

8.3 Technical challenges with ABR recordings

ABR recordings were made using the same equipment throughout, although before the final set of experiments, there was a change in room in the animal house. The recording equipment was carefully recalibrated after moving. This is unlikely to affect the recordings because of the recalibration. The final set of experiments (n=9) were performed using different ABR equipment and software due to updated laboratory equipment (TDT). Advantages of this updated technology and equipment included the increased speed of recordings and hence reduced anaesthetic time. This was advantageous to the animals as they had a shortened time for homeostatic regulation of oxygen saturations and temperature whilst under anaesthetic. Certain adaptations had to be made for analysis including the different mechanism for delivery of the sound to the ear via a tube. Adjustments were therefore made in the latency results from this cohort to allow for this alteration.

Minimising electromagnetic background noise was important to enable clear ABR recordings. There were several sources for background noise and signal distortion which had to be systematically minimised at the start of each recording. Firstly, the speculum delivering the signal to the EAC of the guinea pig could be blocked with secretions. This was carefully cleaned before recordings started for each animal. There was also the potential for incorrect positioning of the speculum which is designed to

channel the sound to the EAC. This can occur easily if the animal has any small movements and is overcome by repositioning, carefully lowering the speculum into the EAC whilst retracting the pinna using instrumentation to straighten the meatus and facilitate this placement. Insertion of the electrodes in the correct subcutaneous position was also a challenge. After electrode insertion, if the resistance was out of the desired range the electrode maybe inserted in the muscle instead of the correct subcutaneous plane and the electrodes were repositioned. Correct positioning became more difficult as the animals grew heavier and their skin became thicker.

Minimising the number of electronic instruments turned on during the recordings was also important to minimise electromagnetic background noise. Examples included fans in the room, heaters and additional computers which were not being used in the recordings.

On analysis of the ABR, it is evident that with the variability in standard errors seen, there is an electromagnetic background noise component that is difficult to eliminate. This is especially prominent in the measurement of amplitude and latency and can be attributed to the ABR waveform being distorted so the exact locations of P1, P2, P3 and N1 N2 and N3 are difficult to determine. Minimising background noise is also important in the threshold measurements, but exact readings to determine the start and peak of the waveforms is not required. The threshold values are therefore easier to read by the presence or absence of a waveform in contrast to the amplitude and latency values. The greatest variability was seen in the final cohort group: 5 guinea pigs implanted with pellets loaded with clindamycin and 4 guinea pigs with rifampicin. As a result, the amplitude and latency values could not reliably be used, although threshold values were easier to interpret in this cohort and hence were analysed.

8.4 Guinea pig dimensions and suitability as a middle ear experimental model

The guinea pig model was selected as the experimental model. This was initially due to its rodent status and the expertise of the animal house at guinea pig husbandry. In addition, the favourable measurements found from cadaveric work showed that guinea pigs had a relatively large middle ear ventral bulla volume (119 microlitres).

Surgical access to the guinea pig middle ear for pellet insertion was not possible via the transtympanic route for two reasons: 1) the fluting of the external auditory canal which restricted the diameter to 3mm at its widest point and 2) the limited surgical view and instrumentation which could be achieved down the EAC. The Retrobulla approach, although popular in animal models to access the oval window, was not chosen because of the limited access to the anterior aspect of the ventral bulla. Following the cadaveric studies, an anterobulla approach was selected. This has been previously performed in rat models, but is not well documented in guinea pigs (Pinilla 2001). On addition, a small hole was made in the ventral bulla using a Schucknect pick to allow for pellet insertion. This was a novel method of drug delivery to the middle ear which has not been previously reported in the guinea pig. It requires considerable surgical skill and has the potential complications of haemorrhage, wound infection and damage to the facial nerve. As this surgical approach was relatively unreported in the literature, careful surgical controls were performed to ensure that no damage to the hearing mechanism was caused by this technique. The one fatal procedural complication of overheating was a consequence of the post operative care and not with the anterobulla dissection technique.

The anterobulla approach, however, allowed careful surgical placement of the pellet into the middle ear away from the Eustachian tube opening and the ossicular chain. This careful positioning would not have been achieved through a transtympanic approach and hence may be considered a superior route for middle ear access.

The wound infection rates were 6.4% in total (Table 58). These all resolved without antibiotic treatment. Despite preventative measures to minimise wound infection, three animals were still affected. Potentially this could be related to the animal model selection as aggressive behaviour was seen between the animals which could result in potential contamination of the surgical wounds in the open cages. Separation of the animals would ensure this did not occur, but being housed together is companionship and environmental enrichment. Wound dressings are also unlikely to protect from wound infection as their adherence is only temporary. Neck ruffs could be worn post operatively, however, this may affect feeding and drinking and cause abrasion over the wound.

8.5 ABR results

Discussion of the ABR data has been separated in three parts: threshold, amplitude and latency. For each of these sections, the ABR results and comparison with relevant published data will be undertaken.

8.5.1 ABR threshold results

The ABR results for the experimental groups of biological control, surgical control and PLGA and pluronic pellet control groups suggest that the PLGA and Pluronic pellets do not contribute to any clinically significant threshold elevation. This was interesting as the model development involved significant surgical and experimental intervention in a small middle ear space also confirming that anterobulla access to the middle ear in the guinea pig is reproducible and safe.

The significant and sustained elevation of threshold seen with the antibiotic combination of rifampicin and clindamycin was unexpected and unusual in appearance. The partial mid frequency recovery and persistent elevation at 8 and 30 kHz seen at week 16 was also an unusual finding.

The ABR threshold results for pellets loaded with either rifampicin or clindamycin tested separately also resulted in unusual patterns of threshold elevation which are not as pronounced as the drugs used in combination. This suggests a possible synergistic effect between the two antibiotics when used together.

In order to understand the potential underlying mechanism of ABR threshold elevation in the pellet loaded with rifampicin and clindamycin group, other examples of

ototoxicity in the literature can be studied and their patterns of ABR threshold elevation.

Previous work on ototoxicity by other groups has shown variable defined patterns of hearing loss depending on the toxic insult. These can be thought of as a low frequency, high frequency or pan threshold hearing loss. The mechanisms of hearing loss also vary. Table 59 presents examples of this with molecular weights of the substances. An appreciation of these may help to elucidate the mechanism of threshold elevation seen with rifampicin and clindamycin.

Compound	**Mol weight g/mol**	**Hearing loss**	**Exposure/Source**	**Mechanism**	**References**
Heavy Metals					
Arsenic	75	Low frequency Up to 500 Hz	Parasite and microorganism inhibitor, coal power plant emissions	Apex of cochlea targeted	Bencko *et al*., 1977 Guo *et al*., 2007
Lead	207	High frequency (exposure time dependent) 4,6,8kHz	Battery manufacture	Dysfunction VIII nerve	Ghiasvand *et al*., 2016 Yamamura *et al*., 1989
Manganese	55	Low and high frequency affected	Battery manufacture Electroplating	Spiral ganglion cell damage	Ding *et al*., 2010 Muthaiah *et al*., 2016
Mercury	201	High frequency	Found in solder – manufacture of thermometers and detonators	Cochlea damage	Rice *et al*., 1992 Al-Batanony *et al*., 2013

Solvents and Asphyxiants					
Carbon disulphide	76	High frequency +/- low	Solvent for resin, waxes, lipids, oils Insecticides	Undetermined retro cochlear	Morata *et al*., 1989 Rebert *et al*., 1986 Carreres-Pons *et al*., 2017
Styrene Toluene	104 92	High frequency Worst mid frequency	Plastic, resin rubber manufacture	Oxygen free radical OHC damage, affect K+ recycling	Chen *et al*., 2007 Morata *et al*., 1991
Carbon monoxide	28	Pan thresholds, mostly high threshold	Exhaust fumes from motor vehicles	Organ of Corti damage-glutamate excitotoxicity IHC	Kanthasamy *et al*., 1994 Tawackoli *et al*., 2001
Clinical ototoxins					
Cisplatin	300	High frequency	Chemotherapy: breast, ovarian, colorectal cancer	Na+, K+ and Ca2+ APTase on lateral cochlear wall decreased Basal hair cell, stria vascularis apoptosis and spiral ganglion damage	Cheng *et al*., 2005 Xia *et al*., 2014 Rybak *et al*., 2007 Whitworth *et al*., 2007 Franceschi *et al*., 2011
Aminoglycoside antibiotics: Amikacin Gentamicin	777 478	High frequency 4kHz, 8kHz Basal cochlea – high frequency	Antibiotic treatment for TB, endocarditis, respiratory tract infections, osteomyelitis	Voltage gated sodium channel mediated Apoptosis Free radical mediated, OHC loss	Nekrassov *et al*., 2000 Vasconcelos *et al*., 2017 Jiang M *et al*., 2017 Sinswat *et al*., 2000

Bilirubin	585	High frequency	Neonatal period	Waves P5 - brainstem	Kaga *et al*., 1979 Ahlfors *et al*., 1986
Loop diuretics: Furosemide	331	High frequency loss	Diuretic	Na+ and K+ ion transporters in stria vascularis affected : oedema and cystic dilatation	Forge *et al*., 1982 Santos *et al*., 2017
Salicylate: Aspirin	108	High frequency	Antipyretic, analgesic	Increased membrane conductance of OHC	Stypulkowski *et al*., 1990 Jiang C *et al*., 2017
Experimental substances					
Rifampicin Clindamycin	823 425	Nil known	Tuberculosis therapy Osteomyelitis therapy		unknown
PLGA pluronic	150 000 12600	Nil known	Carrier vehicle		Nil reported

Table 59: ***Table to show compounds with their molecular weight, hearing loss profile and mechanisms of causation of ototoxicity.***

Aminoglycoside antibiotics such as amikacin cause permanent ABR threshold elevation (Nekrassov *et al*., 2000) in guinea pigs. This was seen at 4kHz and 8kHz. When a sodium channel antagonist vinpocetine was administered after the aminoglycoside, there was a protective effect suggesting that the ototoxicity mechanism is sodium channel mediated. Aminoglycosides enter the inner ear after crossing the blood-brain barrier and entering at the level of the stria vascularis. They enter the endolymph and the OHC. On a cellular level, they interact with the secondary messenger system of PIP_2 and release oxygen free radicals which in turn activates apoptosis of the OHC (Campo *et al*., 2013).

In the experimental cohort, there is both a high and low frequency ABR threshold elevation seen unlike amikacin. The experiments on guinea pigs did not show any IHC or OHC loss, therefore it is unlikely that the mechanism of ABR threshold elevation seen with rifampicin and clindamycin laden pellet is sodium-channel and apoptosis mediated.

Administration of another aminoglycoside antibiotic, gentamicin, intraperitoneally in guinea pigs has been shown to cause ototoxicity with threshold shift of 60dB at 18kHz using evoked brainstem response measurements (Sinswat *et al*., 2000). It has been proposed that post gentamicin, free radicals may mediate damage to the cochlea seen with loss of OHCs in the basal turn. Administration of dihydroxybenzoate which is an oxidoreductase enzyme concomitantly with the gentamicin reduces the threshold shift to less than 30 dB and also reduces the loss of outer hair cells. A possible mechanism proposed for hearing threshold elevation post gentamicin is therefore free radical damage resulting in OHC loss at the basal turn with corresponding high frequency loss. Aminoglycoside antibiotics have a physical form of a ring structure. This configuration is required for free radical generation.

Both amikacin and gentamicin have similar molecular weights to rifampicin and clindamycin. It is theoretically possible that after drug delivery to the middle ear from the pluronic and PLGA carriers, the molecules rifampicin and clindamycin cross the RW membrane and bind the sodium-potassium ATPase which alters the endocochlear potential. It is however, unlikely that the mechanism of ABR threshold elevation seen experimentally with rifampicin and clindamycin is similar to gentamicin. In the guinea pig experiments laden with PLGA and Pluronic pellets loaded with rifampicin and clindamycin there is an unusual low and high frequency ABR threshold elevation seen

at 16 weeks with partial mid frequency recovery (Figure 24). This occurs without OHC damage seen in the basal turn on the cytocochleograms (Figures 111,112,113) and immunofluorescence (Figures 122,123,124) unlike published work on gentamicin and amikacin (Campo *et al*., 2013) with OHC loss.

ABR threshold elevation has been recorded in infants with kernicterus. This is caused by unconjugated bilirubin crossing the blood brain barrier and being deposited in the brainstem, damaging the auditory pathway (Kaga *et al*., 1979). As a result, on ABR recording there is disruption to the P5 waveform (Kaga *et al*., 1979). There is no evidence of a similar neurotoxicity mechanism occurring in the experimental testing of pellets with rifampicin and clindamycin as there are no consistent amplitude and latency changes occurring.

Cisplatin is a chemotherapy agent which is known to be potentially ototoxic causing high frequency hearing loss. It is used as treatment for cancers including head and neck, breast, ovarian and colorectal. Cisplatin targets the hair cells in the basal region of the organ of Corti (Xia *et al*., 2014), cells in the spiral ganglion affecting the electromechanical coupling and also the spiral ligament and stria vascularis (Franceschi *et al*., 2011). The mechanism of action is platination of the DNA in the hair cells and stria vascularis with subsequent apoptosis. Hearing loss after cisplatin administration is also thought to occur via reactive oxygen species and subsequent inflammation (Sheth *et al*., 2017).

Cisplatin causes ABR threshold elevation (Cheng *et al*., 2005) and in experimental guinea pig models, this elevation in threshold corresponds to a reduction in the cochlear Na+ – K+ ATPase and Ca^{2+} ATPase in the lateral cochlear wall in a dose

dependent fashion. OHC loss in the basal and middle turns of the cochlea have also been identified in guinea pig models (Cardinal *et al*., 2000). This suggests that one of the mechanisms of developing ototoxicity is related to the ionic balance and physiology of the cochlea in the peripheral auditory system. However, other studies in humans with the monitoring of ABRs after cisplatin administration has shown latencies of wave P5 increased, suggestive of a central cause (De Lauretis *et al*., 1999). Therefore it is likely that cisplatin acts at multiple sites of the auditory pathway.

In relation to rifampicin and clindamycin, there is no convincing evidence that the central auditory pathway is affected as with cisplatin as there are no consistent increases in latency and amplitude of the ABR recordings and no evidence of IHC or OHC loss.

Loop diuretics, such as furosemide, act on the ascending limb of the loop of Henle inhibiting Na^+ and Cl^- resorption. They also act on the sodium and potassium transporters in the stria vascularis and hence alter the endolymph composition, decreasing the potential of the endolymph (Forge *et al*., 1982). The consequence of this is high frequency hearing loss. It is unlikely that rifampicin and clindamycin act in a similar manner as a pan threshold increase in ABR is initially seen with mid frequency recovery at 16 weeks.

Aromatic solvents such as toulene and styrene cause OHC death via reactive oxygen species and also affect the K+ ion transporters, altering the endolymph potential. These solvents have been shown experimentally to affect Hensen and Tectal cells and hence impact on K+ ion recycling from excitation of the hair cell and efflux to the endolymph (Chen *et al*., 2007). There is also evidence that Toluene causes

neurotoxicity altering acetylcholine receptors and voltage gated Ca^{2+} channels which affects the middle ear reflex (Maguin *et al*., 2009). This is a protective response to sudden loud noise mediated by stapedius and tensor tympani muscles. Rifampicin and clindamycin when loaded onto ME pellets for guinea pigs have not demonstrated any accompanying OHC loss with threshold elevation, therefore a similar mechanism is unlikely.

Non aromatic solvents such as carbon disulphide cause a central effect influencing sound transmission beyond the cochlea (Rebert *et al*., 1986). The exact mechanism of this is not well understood. Similar, central effects from rifampicin and clindamycin, however are unlikely as there is no supportive evidence of consistent amplitude and latency changes.

The permeability of the round and oval windows is a potential route for molecules to pass from the ME to the IE and is a possible mechanism of ototoxicity. The contribution of this in the context of rifampicin and clindamycin requires discussion.

8.5.2 Round window and oval window permeabilities

Intra tympanic molecules have been shown to pass to the inner ear. The main route for this is the round window (Salt *et al*., 2001), but the oval window is also a potential, less important gateway into the inner ear (Goycoolea *et al*., 1980). Systemic substances crossing the blood-brain barrier and entering the CSF also have the potential to enter into the inner ear via the cochlea aqueduct into the perilymph of the scala tympani.

The round window has three layers 1) outer epithelial layer 2) middle connective tissue layer and 3) inner absorptive layer in communication with the ST perilymph. The outer layer has adaptations which facilitate absorption including sparse microvilli, mitochondria and Golgi apparatus indicating an active transport mechanism (Bu *et al*., 2015).

There are many factors known to affect the round window permeability related to both the molecules and host factors. The molecular weight of the substance has a role in permeability. Low molecular weight molecules such as gentamicin and neomycin (Smith *et al*., 1979) pass through the RW whereas high molecular weight molecules such as albumin and thorotrast do not under normal conditions (Höft *et al*., 1969, Goycoolea *et al*., 1980). However, absorption of substances is still relatively low across the RW. When gentamicin and dexamethasone are applied to the round window, perilymph sampling shows that only 2.5% or 1.4% of the ME concentration is in the perilymph (Plontke *et al*., 2007). Other features of the molecules which may affect permeability include ionic charge, concentration, RW membrane thickness and charges associated with the molecules (Goycoolea *et al*., 2001).

Experimentally, perforations to the round window membrane increase the permeability (Kelso *et al*., 2015) A 12.5 micrometer syringe to make perforations experimentally enhances permeability by a factor of 35 and inflammation also increases RW permeability (Goycoolea *et al*., 1980) with albumin crossing the membrane in acute otitis media. In relation to the guinea pig experiments with rifampicin and clindamycin loaded on a PLGA and pluronic carrier pellet, inflammation is seen in the middle ear at 16 weeks from the histology slides (Figure 127) with macrophages surrounding the remnant pellet. It is possible that such chronic inflammation may affect the round window permeability which is apparent when the

antibiotics are present but not in controls. This is a possible explanation for ABR threshold elevation seen with rifampicin and clindamycin laden pellets. These localised effects may be exclusive to the Organ of Corti, sparing central disruption of the auditory pathway. This peripheral effect could also potentially explain the lack of significant amplitude or latency changes.

In relation to rifampicin with a molecular weight of 823 g/mol and clindamycin 425 g/mol, these are comparable to aminoglycoside antibiotics such as gentamicin with a molecular weight of 478g/mol and amikacin 777g/mol which are both known to cross with RW and cause ototoxicity. The mechanism of aminoglycoside ototoxicity is related to damage to the voltage gated sodium channels and also via free radical generation. It is possible that rifampicin and clindamycin could cause a similar effect on the basal end of the cochlea, potentially by binding to channels and hence causing high frequency hearing loss in the guinea pig. Perilymph sampling could help to investigate this as a plausible mechanism. Binding to voltage gated ion channels and alteration of the endocochlear potential can propagate across the whole of the cochlea and hence explain a pan threshold elevation which was seen initially at week 1 (Figure 24).

The molecular weights of PLGA 50:50 and pluronic F127 are 150 000g/mol and 12600g/mol. These are carrier molecules which are too large to pass through the RW membrane. As seen in the histology slides (Figure 127), they remain in the middle ear and hence may contribute to a chronic inflammatory reaction which may increase the permeability of the RW membrane. There high molecular weights also have the potential to cause an osmotic effect cross the RW and OW and hence alter the endolymph potentials. However, this would also be the case in the pellet control

groups, so it is likely there is another explanation for the threshold elevation mechanism when rifampicin and clindamycin are added to the pellets.

8.5.3 ABR amplitude results

Discussion of the ABR amplitude results is required and a comparison with relevant published literature.

As the results in Table 14 show, there are changes in ABR amplitude seen in control groups: biological control, surgical control and pellet without antibiotics in waves P2 and P3 all measured at week 1 and most pronounced at 94dB. These changes are amplitude decreases are an unexpected finding in the control groups. It is therefore difficult to conclude any meaningful changes in the amplitude of the guinea pig groups with antibiotic pellets. There is only one significant increase in amplitude seen with the pellets laden with both rifampicin and clindamycin at P2 week 16 at 84dB and also there are isolated significant decreases in amplitude seen in pellets laden with clindamycin for wave P1 at weeks 2 and 12 measured at 74dB. Other significant changes seen in weeks 2, 12 and 16 show that there is a decrease in amplitude for P3 at 94dB SPL and 74dB SPL (Table 20).

	P1	P2	P3
BC 16kHz	-	↓ week 1 94dB	↓ week 1 94dB
BC 24kHz	-	↓ week 1 94dB	↓ week 1 94dB, 84dB
SC 16kHz	-	↓ week 1 94dB	↓ week 1 94dB, 74dB
SC 24kHz	-	↓ week 1 94dB	↓ week 1 94dB, 74dB
P 16kHz	-	↓ week 1 94dB	↓ week 1 94dB, 74dB
P 24kHz	-	↓ week 1 94dB	↓ week 1 94dB, 74dB
PA 16kHz	-	-	↓ week 2 94dB ↓ week 2,16 74dB
PA24kHz	-	↑ week 16 84dB	-
PRif 16kHz	-	-	↓ week 2 74dB
PRif 24Hz	-	-	-
PClind 16kHz	↓ week 2 74dB	-	↓ week 12 74dB
PClind 24kHx	↓ week 12 74dB	-	-

Table 20 (repeated): *Summary of the changes in amplitude for waves P1-P3 measured at 16kHz and 24kHz for all experimental groups.*

The changes in amplitude seen in control groups could be explained by the level of background electromagnetic noise and difficulties in ABR recording. There are a number of sources of this including electronic equipment in the experimental room, aberrations in haemostasis of the guinea pig and misplacement of the recording electrodes into the deep muscular layer. Measures were taken to minimise the noise signal, but it was never completely eliminated. These included guinea pig warming with a foil blanket, heated mat, rectal temperature probe with an alarm warning system if temperature readings were out of range. Supplementary electric devices within the experimental test room which were not directly involved in the recording were turned off. Background noise may also disguise a subtle trend seen in the amplitude changes which are not possible to identify on analysis of the ABR recordings.

Due to the large variation in results seen in the error bars, Friedman's two way analysis was performed on the data (Table 21, 22, 23
. The results of this show no consistent significant alteration in amplitude, supporting the conclusion that amplitude is not consistently altered alongside ABR threshold elevation.

The Holm-Bonferroni correction has also been applied to the ABR amplitude results and show that there is no significant deviation from the null hypothesis that there is no alteration in ABR amplitude seen from weeks 0 to week 16. This supports the other statistical findings.

Consistent significant changes in ABR amplitude may indicate neurotoxicity on analysis of P1, P2 and P3. Therefore, the absence of this does not support any evidence of neurotoxicity from the rifampicin and clindamycin loaded pellets.

8.5.4 Factors causing ABR amplitude elevation

Guinea pig studies have shown a repeated dose dependent increase in amplitude of wave P1 on elevation in ABR thresholds. Studies using kanamycin in rats have shown an increase in ABR amplitude to precede ABR threshold elevation (Kuse *et al*., 2011). The administration of sildenafil a type 5 phosphodiesterase inhibitor to mice has also demonstrated an increase in ABR amplitude in P1 (Hong *et al*., 2008). These ABR amplitude elevations indicate decreased auditory function. Both of these studies (Kuse *et al*., 2011 and Hong *et al*., 2008) focus on ABR amplitude elevation in P1 and not P2.

Experimentally, one reading at week 16 (84dB) in the group of guinea pigs with pellets loaded with rifampicin and clindamycin showed ABR amplitude elevation. This is an isolated result in the 24kHz group and no trend in ABR amplitude elevation was identified. The ABR results testing pellets with rifampicin and clindamycin show ABR threshold elevation at week 1 without ABR amplitude elevation. This is unlike the study by Kruse *et al*., 2011 where amplitude changes preceded threshold changes, again supportive of there being no alteration in ABR amplitude.

Statistical testing using Friedman's two way analysis and also Holm Bonferroni correction also supported the findings of no significant consistent ABR amplitude elevation.

8.5.5 Factors causing ABR amplitude reduction

Experiments on rats have shown that increases in temperature are associated with decreased ABR amplitude and with minimal recovery on lowering the body temperature back to the normal range (Gold *et al*., 1985, Takahashi *et al*., 1991). This reinforces the requirements of monitoring guinea pig body temperature carefully during the experiments as aberrations can affect the ABR recordings. In the protocol, core body temperature was monitored using a rectal probe and maintained between 35.5 and 37.5 degrees celsius.

On analysis of the ABR trace, the first wave P1 is known to be generated by the auditory nerve (Buchwald *et al*., 1975). Decreases in suprathreshold P1 ABR amplitude have been associated with loss of auditory nerve fibres in mice after noise induced temporary threshold shifts (Kujawa 2009). This also correlates with ABR threshold elevation after noise-induced permanent hearing loss with damage to the inner hair cells and loss of auditory nerve fibres (Nordmann *et al*., 2000, Harding *et al*., 2002). In

the guinea pig experiments there are no such accompanying IHC losses seen and no consistent decrease in amplitude. Therefore, this mechanism of ototoxicity is unlikely.

Aminoglycoside antibiotics such as amikacin have shown P1 amplitude reduction in guinea pigs (Nekrassov *et al*., 2000) which appears to be voltage gated sodium channel mediated as antagonists to the sodium channels such as vinpocetine, prevent ototoxicity when administered after the amikacin. No consistent ABR amplitude decreases are seen experimentally which does not support this mechanism of ototoxicity.

Isoflurane anaesthetic has been shown to reduce ABR amplitude in guinea pigs at a dose of 2% and with the most prominent reduction seen in waves IV and V (Stronks *et al*., 2010). In the experimental regimen, isoflurane use was limited to surgery post initial ABR recordings at week 0 and was administered at a dose of 1%. Steps were taken to minimise the effect of isoflurane on the ABR readings. It is therefore unlikely isoflurane has any impact on ABR amplitude results in these experiments.

8.5.6 Explanation for no correlation of ABR amplitude changes

The two frequencies of 16kHz and 24kHz were selected for amplitude analysis in the guinea pig model as this is most likely to be representative of any changes seen. It is unlikely that amplitude changes were present at different frequencies.

Some agents such as isoflurane which are associated with a reduction in ABR amplitude have the most pronounced effect at waves P4 and P5. Therefore, it is possible that the potential ototoxic effect was not seen in these experimental

recordings as waves P1, P2 and P3 were selected to record amplitude values due to their relatively consistent clarity with limited background electromagnetic noise.

As discussed previously, it is unlikely that isoflurane contributes to any ABR threshold changes seen and therefore any ABR amplitude changes seen. Selection of waves P1,P2 and P3 for analysis was on the basis of being consistently clear to read and associated with neurotoxicity in other experimental scenarios (Nekrassov., *et al* 2000).

However, in relation to the guinea pig experiments, care was taken to ensure there were no temperature aberrations or excessive electromagnetic background noise. In addition, the changes seen in the groups of guinea pigs loaded with rifampicin and clindamycin were in the P2 group, not P1 as seen in the literature (Nekrassov *et al*., 2000).

Overall, the experimental results show no consistent significant alteration in ABR amplitude in waves P1, P2 and P3. This supports the ABR threshold elevation seen with pellets loaded with rifampicin and clindamycin being a peripheral effect and not associated with any neurotoxicity.

8.5.7 ABR latency results

Discussion of the ABR latency results is required and a comparison with relevant published literature.

As the results in section 5.4.16 show, there are changes in ABR latency seen in control groups: biological control, surgical control and pellet without antibiotics in waves P1, P2 and P3. These changes are all measured at week 1 and most frequently seen at 94dB. These changes are latency increases and are an unexpected finding in the control groups as there is no ABR threshold elevation in these groups. It is therefore difficult to conclude any meaningful changes in the latency of the guinea pig groups with antibiotic pellets. However, there is only one significant increase in latency seen with the pellets laden with both rifampicin and clindamycin at P2 week 2 at 84dB tested at a frequency of 24kHz and also there are isolated significant increases in latency seen in pellets laden with clindamycin for wave P1 at weeks 2 and P2 at 74dB and 94dB measured at 16kHz. Other significant changes seen for pellets loaded with rifampicin in week 2 is an increase in amplitude for P1 at 74dB measured at 24kHz (Table 42).

	P1	P2	P3
BC 16kHz	↑week 1 84dB	↑week 1 74dB,94dB	↑week 1 84dB
BC 24kHz	-	-	↑week 12 94dB
SC 16kHz	↑week 1 94dB ↑week 16 94dB	↑week 1 74dB, 94dB ↑week 4 84dB	↑week 1, 2 94dB ↑week1,2 84dB
SC 24kHz	↑week 1 94dB	-	-
P 16kHz	↑ week 2 94dB	↑ week 2 94dB	↓week 16 94dB
P 24kHz	-	-	↓week 4 94dB
PA 16kHz	-	-	-
PA24kHz	-	↑ week 2 84dB	-
PRif 16kHz	-	-	-
PRif 24Hz	↑week 2 74dB	-	-
PClind 16kHz	↑ week 2 74dB	↑ week 2 74dB, 94dB	-
PClind 24kHx	-	-	-

Table 42 (repeated): *Summary of the changes in latency for waves P1-P3 measured at 16kHz and 24kHz for all experimental groups.*

All of the changes in latency seen in the control groups: biological control, surgical control and pellet without antibiotics are in P1, P2 and P3 and showed increases across the weeks 1-16. These were pre dominantly seen at 16kHz. It is also interesting to note that changes in latency are pre dominantly increases, however when testing the pellet without antibiotics, at 94dB there were latency decreases seen at weeks 4 and 16 in ABR wave P3. Significant changes in ABR latency are unexpected in the control groups.

The significant changes identified with pellets loaded with both rifampicin and clindamycin were seen only in wave P2 at week 2 at 84dB at 24kHz frequency. When pellets are separately loaded with rifampicin or clindamycin, there is ABR latency elevation at week 2 in P1 at 74dB at both 16kHz and 24kHz and P2 waves at 16kHz at

both 74dB and 94dB (Table 42). This suggests that the elevation at week 2, 16kHz at 94dB may not be significant as it is also seen in the PLGA and pluronic pellet control group.

Inconsistencies in results could potentially be attributable to electromagnetic background noise and difficulties with measurements using poor quality traces. This can be seen with some of the graphs demonstrating latency results having large error bars. Due to this large variation, Friedman's two way analysis was performed on the data. The results of this show no consistent significant alteration in latency, supporting the conclusion that latency is not consistently altered alongside ABR threshold elevation.

The Holm-Bonferroni correction has also been applied to the ABR latency results and show that there is no consistent deviation from the null hypothesis supporting the statistical results.

Lack of consistent significant changes in ABR latency does not support any neurotoxicity for the guinea pigs loaded with rifampicin and clindamycin pellets on analysis of P1, P2 and P3.

8.5.8 Factors causing ABR latency elevation

Studies on infants with kernicterus have shown that alongside ABR threshold elevation, there are increases in ABR latencies for P1 and P5 (Kaga *et al*., 1979). This suggests that some of the damage to the auditory system from unconjugated bilirubin

is peripheral at the level of the cochlea and some centrally at the level of the brainstem.

Noise exposure in guinea pigs has shown results in ABR latency increases (Gourévitch *et al*., 2009). After exposure of guinea pigs to traumatic levels of noise 120dB SPL at 5kHz, the latencies of ABR were recorded and shown to be increased following acoustic trauma. However, there is a stabilisation identified after repeated insults meaning that the latency changes level off.

Aminoglycoside ototoxicity has been demonstrated to show increases in ABR latency in waves P1 and P5 (Hotz *et al*., 1990). In this study, 20 patients in intensive care were administered intravenous netilmicin and tobramycin. ABR recordings from the onset of treatment and at day 6 post commencement of treatment were compared. Shifts in ABR latency were observed in waves 1 and 5 with the effect of netilmicin noted to be the greatest. These results suggest that aminoglycosides cause ototoxicity at the level of the cochlear and the brainstem along the auditory pathway. Bedside recording of ABR latency changes in patients who are receiving aminoglycoside antibiotics has even been suggested as a non-invasive method for monitoring toxicity levels.

Aminoglycoside administration in the form of amikacin intramuscularly to guinea pigs has also shown ABR latency increases at 8kHz. This effect was seen after 160 days unlike the changes in ABR threshold and amplitude which were observed earlier (Nekrassov *et al*., 2000). This effect on ABR latency was also shown to be prevented by intravenous administration of sodium channel antagonist (vinpocetine) after amikacin was given. The longest experimental regimen used in this set of experiments was 112

days (16 weeks) and therefore, if latency changes were only to be seen after 160 days as per Nekrassov study in 2000, this would not be detected.

Chemotherapy agents such as cisplatin can cause ototoxicity and the ABR of patients has been used to detect the early stages of cochlea damage (De Lauretis *et al*., 1999). Two out of 9 patients in this study undergoing cisplatin treatment had a hearing loss and corresponding significant increase in P5 latency. This suggests an effect at the brainstem level, not peripherally at the level of the cochlea.

Isoflurane inhalational anaesthetic at 2% has been shown to increase ABR latency (Stronks *et al*., 2010). This effect is most pronounced at waves P4 and P5. The experimental measurements of latency changes were on waves P1, P2 and P3 as these were the most consistent and east to measure. Therefore latency changes only affecting P4 and P5 may not be identified, however this would be unusual.

8.5.9 Factors causing ABR latency reduction

Increases in temperature have been shown experimentally to decrease the ABR latency in dogs (Takahashi *et al*., 1991) which is most pronounced in P4 rather than P1. The explanation for this has been proposed that hyperthermia alters the conduction velocity of the central components of the auditory pathway more than the peripheral. Similar responses have also been seen in rats with induced hyperthermia (Gold *et al*., 1985) with decreased latency values on warming and reversibility on cooling. This again reinforces the importance of careful temperature monitoring and homeostasis throughout the experiments.

8.5.10 Explanation for no correlating ABR latency changes

Electromagnetic background noise results in ABR traces having less clarity and being difficult to interpret. Noise is minimised by turning of all non-essential electrical equipment and careful subcutaneous positioning of the electrodes. The range of variance seen in the measurements reflects these challenges (Table 42).

Latency wave analysis was performed for P1, P2 and P3. This is because the ability to interpret the latency of P4 and P5 became increasingly difficult and hence unreliable, especially if there was an increased degree of electromagnetic background noise. It is unusual to have an isolated change in latency in waveforms P4 and P5 without corresponding changes in P1, P2 and P3.

Review of ABR frequencies 16kHz and 24kHz was selected for latency analysis in the guinea pig model as this is mid-range for the guinea pig and is therefore more likely to be representative.

Overall, the experimental results show no consistent significant alteration in ABR latency in waves P1, P2 and P3. This supports the ABR threshold elevation seen with pellets loaded with rifampicin and clindamycin being and peripheral ototoxic effect and not centrally neurotoxic.

8.5.11 ABR threshold elevation without changes in amplitude and latency

The results show that there are no changes to ABR amplitude and latency which accompany the ABR threshold elevation for the guinea pigs loaded with rifampicin and clindamycin loaded middle ear pellets. This suggests that there is no central effect or neurotoxicity associated with the antibiotic pellets.

Multiple steps were taken experimentally to minimise background electromagnetic noise and produce clear traces from which to accurately measure ABR threshold, amplitude and latency. This was achieved by limiting electronic equipment at the time of recording and careful positioning of the subcutaneous electrodes.

Analysis of the ABR amplitude and latency results show no consistent significant excursions from week 0 values using t tests, Friedman's two way analysis of variance and Holm-Bonferroni correction. Therefore, there does not appear to be any corresponding decreased amplitude and increased latency with ABR threshold elevation for guinea pigs loaded with rifampicin and clindamycin pellets. This is evidence of a peripheral effect from the antibiotic pellets without any accompanying neurotoxicity of the auditory pathway.

8.5.12 Discussion of lack of weight gain from pellet loaded with rifampicin and clindamycin

Although rifampicin and clindamycin are not known to cause any gastrointestinal tract disturbance, the acute weight loss seen by administration of the PLGA pellet loaded with these antibiotics requires commentary (Figure 101). Other studies which have co-administered medication such as gentamicin and metformin subcutaneously have also shown a side effect of weight loss in guinea pigs (Oishi 2014). This weight loss was seen in 57% of animals and there were also premature deaths seen when using the combined drug regimen. It is therefore possible that the weight loss seen in the guinea pigs post insertion of middle ear pellets loaded with rifampicin and clindamycin is due to a synergistic effects of the combination of drugs.

Other experimental models in guinea pigs have shown weight loss in conjunction with ABR threshold elevation (Nekrassov *et al*., 2000), suggesting that there could be an impact on the animal's overall well being. There is a decrease in weight gain noticed post aminoglycoside (amikacin) administration and an overall increased mortality of this group. It is possible that hearing loss may suppress appetite or there may be a vestibular component causing nausea and decreased food intake. The plateau in weight seen in the initial period post implantation (Figure 99) between weeks 0 and 1 in the animals implanted with pellets loaded with rifampicin and clindamycin increases between weeks 1 and 2. By 16 weeks there is no appreciable difference in weight between the experimental groups. This suggests that the systemic impact on the animals causing the lack of weight gain is temporary and short lived. This recovery has a timescale similar to the partial recovery in ABR threshold elevation seen at the mid frequencies (Figure 24).

It is not possible to compare the weight trajectory over time of the guinea pigs with pellets loaded with either rifampicin or clindamycin separately with the other groups. This is beacuse their starting experimental weight was greater as they were older and purchased from another experimental group. Although clindamycin has been known to cause gastrointestinal tract disturbance as a side effect and has been associated with colitis (Rehg *et al*., 1980), there were no reports from the animal house staff of signs of this such as loose stool or abdominal distension. It is therefore unlikely that the weight loss seen in the guinea pigs treated with pellets loaded with rifampicin and clindamycin is attributable to gastrointestinal tract side effects.

Weight loss in rodent species has been linked to higher serum cortisol levels which are altered in different environments (Schumann *et al*., 2014). This is a potential mechanism for the lack of weight gain between weeks 1 and 2, seen in the experimental group of guinea pigs with pellets loaded with both rifampicin and clindamycin in combination. Future studies measuring post operative cortisol levels in the guinea pigs could investigate this.

8.6 Cytocochleogram studies

Analysis of the cytocochleograms was performed under supervision (see acknowledgements), however, the dissection and preparation of slides still yielded a degree of cell damage which rendered the cells unreadable. This is particularly evident at the apical region which is the most technically challenging to dissect due to the smaller dimensions. There was a tendency to damage this section on micro dissection. This is seen on the cytocochleograms with the first column (row 1) across the IHC and

OHC of the biological control group having cells which were not possible to count. It is therefore difficult to comment on the hair cells at the extreme apex.

Throughout the specimens, there were sections identified that were not possible to count. In the biological control group this was rows 16 and 20 consistently throughout all three rows of OHC and IHC. In the PLGA and pluronic pellet control group this was in rows 16, 19 and 29 and in the pellet with rifampicin and clindamycin this was in rows 1, 16, 19-20, 27-29 and 35.

This consistency throughout a sample group suggests micro dissection trauma or difficulties in mounting the specimen with the coverslip at the edges of the specimen. Overall, each cochlea was divided into approximately 8 pieces using the micro dissection technique of a mounted sample of razor blade on a wooden stick and held in place with adhesive described in section 3.11. It is at the edges of each specimen where the hair cells were the most difficult to read under the Nomarski microscope. Although there were areas of the cytocochleograms which were not possible to read, this has been seen in other cytocochleogram analyses (Mahendrasingham *et al*., 2011) and should therefore be deemed a normal limitation for this technique. A method of assessing the IHC and OHC without using the dissection and preparation including placing a coverslip over a curved specimen to flatten it out can be used. One such technique is scanning electron microscopy (Furness *et al*., 1986) (see future experiments).

Overall, the cytocochleograms did not show any appreciable inner or outer hair cell loss from the apex to the base in the biological control group and PLGA and pluronic pellet control group. In the experimental group with pellet insertion loaded with both

rifampicin and clindamycin, there was no appreciable IHC loss. However, there was a trend of increased OHC loss from rows 1-3 with the most seen in the outermost row (OHC3) and distributed throughout the cochlea but with an increase in hair cell loss in the apical region compared to the base. The proportion of hair cell loss seen from the OHC was still insufficient to attribute ABR threshold elevation. High percentages of loss up to 100% are requires to cause ABR threshold elevation (Wilmott *et al*., 2008). Therefore, on analysis of the cytocochleograms there is no evidence of IHC or OHC loss which would account for the ABR threshold elevation seen fin the guinea pigs with pellets loaded with rifampicin and clindamycin.

Hair cell loss in the apical region has previously been seen on other studies of ototoxicity such as after nicotine treatment (Abdel-Hafez 2014). In this study, outer hair cell loss was seen with changes in topography including stereocilia disorganization which is most pronounced in the basal region of the cochlea. Other studies have shown basal hair cell loss for example in gentamicin ototoxicity studies (King *et al*., 2013, Chen *et al*., 2009), cisplatin (Rybak *et al*., 2007) and noise (Chen *et al*., 2003). Both the aminoglycoside and cisplatin mediated ototoxicity target the outermost row of the outer hair cells first, followed by the middle and then the inner. The inner hair cells are more resilient, but with ongoing exposure to the ototoxic agent, will also be damaged (Chen *et al*., 2009; Rybak *et al*., 2007).

Studies have shown OHC apical hair cell loss (Abdel-Hafez *et al*., 2014) and the difficult dissection of the apical region may affect analysis of this area. It is worth noting that most of the apical cells which were difficult to analyse were in the biological control and pellet control groups though and not the pellet loaded with rifampicin and clindamycin antibiotic. It is worth commentary that this was the order the specimens

were analysed (BC, P then PA), suggesting that there may have been a technical improvement in the dissection and coverslip mounting when the pellet with rifampicin and clindamycin group was analysed. The effect of a challenging dissection of the apical region and preparation of the slides is therefore likely to be most pronounced in the control groups.

One of the limitations of cytocochleograms are the binary analysis of presence/absence of hair cells which is performed by assessing for the presence of the cell body and plate. This does not yield any detail on the hair cell morphology or function of the hair cells. It is useful to analyse cytocochleograms as an adjunct with other techniques to elucidate the presence/absence of ototoxicity mechanisms and should ideally not be interpreted in isolation.

8.7 Immunofluorescence studies

In the light of the results from Figures 116-124 there are a number of discussion points. Overall, there were no changes in IHC or OHC morphology seen on analysis of the pellet loaded with rifampicin and clindamycin guinea pig experimental group. ABR threshold elevation therefore cannot be attributable to changes in morphology or decreases in number of the IHC or OHC from analysis of the corresponding section of the cochlea using immunofluorescence.

Stereocilia morphology has been commented on in other studies showing disruption in association with ototoxicity. The technique of micro dissection and placing a coverslip over the cells before immunofluorescence staining produces a recognised

amount of stereocilia disruption. This technique therefore cannot be relied on for detailed stereocilia studies, although useful for inner and outer hair cell counts and an overall appreciation of the hair cell morphology.

The DAPI and Phalloidin staining show detail from the OHC rows including the orientation of the stereocilia bundle which is typically in an inverted V pattern in the OHC (Figure 118, 121). Some disruption to this organisation is seen throughout the specimens (Figure 117). It is difficult to comment on a trend here as there is the potential for damage to the stereocilia with the dissection, manipulation including staining and washings and coverslip placement. Other techniques would be better suited to visualise the hair cells including stereocilia disruption such as scanning electron microscopy (Furness 1986). This technique requires expertise, skill and the resources used are considerably more expensive.

Preparation of the immunofluorescence specimens required several stages and hence there was a defined learning curve and improvement seen in the quality of results as this skill was developed.

8.8 Histology studies

On review of the results in Figures 125-127 there are some interesting discussion points. After 16 weeks, there is considerable pellet remnant which histologically is surrounded by mononuclear cells and shows an inflammatory reaction (Figure 127). PLGA and pluronic have been shown in other studies to be inert however, as a foreign body in the middle ear, the pellet is a potential focus for infection and chronic inflammation. Instead of eradication of biofilms, insertion of a PLGA and pluronic pellet

may result in potentiation of chronic infection, the biofilm presence and hence propagation of OME.

A chronic inflammatory state may create a post-operative OME in the guinea pig ME after antibiotic pellets have been inserted. There are multiple steps involved in histology slide preparation (3.10) from perfusion-fixation to decalcification, dehydration and embedding the specimen in wax. The presence of any middle ear effusion which has formed as a sequelae of chronic inflammation from the antibiotic laden pellets is therefore unlikely to be detected. In addition, tympanometry and direct examination of the tympanic membrane for evidence of effusion was not performed. It is possible that an effusion was therefore present in the antibiotic laden pellet guinea pig middle ears and this impacted on the middle ear amplification and sound transduction to the IE hence causing an ABR threshold elevation.

The technique of sectioning the middle ear after paraffin embedding is delicate and although performed by expert hands (see acknowledgements), may still produce Organ of Corti disruption. This is seen with tectorial membrane inversion and shearing of Reissner's membrane. The high magnification view of the Organ of Corti show that this is consistently kinked in the specimens, which is attributable to the slide mounting technique and shows how delicate the slicing and mounting stage is. There are other imaging methods to assess the cochlea structure such as scanning electron microscopy, however, this would not produce any information on the middle ear epithelium and localised pellet remnant which is the focus for the histology study.

Creating cross sections taken parallel to the modiolus also produces a small degree of variation according to the orientation of mounting the temporal bones in wax. This

stage was observed and was undertaken by a specialist in the field (please see acknowledgements). Minor variations in the cross sectional slices were therefore seen.

There was a significant remnant pellet seen in the histology slides at week 16 (Figure 127). Future methods for cross sectional imaging of the temporal bones could accurately estimate the remnant pellet volume after 3 dimensional reconstruction. Magnetic resonance Imaging (MRI) could assist in pellet visualisation and computerised tomography (CT) for any bony disruption.

A microscope has been used to examine the inflammatory cells. This has an element of human error in the recognition and counting of cells. Several different slices were used for comparison between the pellet and pellet loaded with antibiotic groups. Bone wax is known to cause a foreign body reaction and granuloma formation post operatively (Baird *et al*., 2018). This was used in all surgical groups and therefore the effects of bone wax cannot account for the inflammation seen in the histology specimens from the pellet loaded with both rifampicin and clindamycin.

Examination of cross-sections of the cochlea taken at the level of the modiolus identifies an intact Reissner's membrane in several of the slides. This demonstrates that the slide preparation and fixation has been performed in a careful manner as this is a delicate structure prone to disruption after minimal trauma. There are also examples of a bulging Reissner's membrane suggestive of hydrops (Figure 124). This is seen in other conditions such as Meniere's disease which is associated with sensorineural hearing loss (Hallpike *et al*., 1938) and can be experimentally induced by surgical ablation of the endolymphatic sac in the guinea pig (Salt *et al*., 2010). There is no clear consensus on how the endolymphatic hydrops in Meniere's disease causes

SNHL although treatment for the condition aims at reducing the hydrops through pharmacology or surgical intervention (Foster *et al*., 2015). One theory is that rupture of Reissner's membrane from the build-up of increased pressure, contaminates the perilymph with the endolymph (Schuknecht *et al*., 1976) and causes disruption of the inner ear function resulting in vertigo and SNHL which is fluctuant in nature. It is potentially possible that a similar mechanism is occurring in the guinea pigs with pellets loaded with rifampicin and clindamycin. This could potentially explain the improvement seen in ABR threshold elevation in the mid frequency range over time (Figure 24) between post implantation at week 1 to week 16 as the endocochlear potential recalibrates. This theory does not fully explain only the mid frequency ABR threshold recovery seen and there is no histological evidence of stria vascularis damage to support this mechanism.

8.9 Potential sites of action of rifampicin and clindamycin

This section discusses possible sites of action of rifampicin and clindamycin and theories and to explain the observed results.

8.9.1 Stria vascularis

The stria vascularis is located on the lateral cochlea wall and if affected would be associated with an alteration of the endocochlear potential. A potential mechanism for stria vascularis to be affected is binding of the rifampicin and clindamycin molecules to the sodium-potassium ATPase pump and hence inhibiting its action. This is known to occur with loop diuretic furosemide (Forge *et al*., 1982) and cisplatin (Cheng *et al*., 2005). After a reduction of the endocochlear potential, the expectant ABR results would be threshold elevation and also a decreased amplitude and

increased latency across all frequencies. This is not seen and hence the stria vascularis is unlikely to be the site of action of rifampicin and clindamycin.

8.9.2 Spiral ganglion cells

Although the amplitude and latency results show some variability, there is no evidence of any pattern of change on analysis of P1, P2 and P3. This is supportive of no neurotoxicity seen after implantation of pellets laden with rifampicin and clindamycin which would show consistent changes in the ABR amplitude and latency throughout (P1-P3). Therefore, the ABR threshold elevation should be considered to be a peripheral effect from the ME pellets. Examination of the histology specimens does not show any appreciable spiral ganglion hair cell loss to support this as a site of action, however, loss of the nuclei may occur after a time delay.

8.9.3 OHC

There is no evidence from the immunofluorescence samples that there is any evidence of OHC loss or morphological changes. However, the cytocochleograms from guinea pigs with pellets laden with rifampicin and clindamycin do suggest subtle loss of outermost OHC from the apical region of the cochlea. The proportion of hair cells lost are insufficient to be accountable for ABR threshold elevation.

The outermost row of OHC (OHC3) is the most vulnerable to trauma by dissection and slide preparation with placing the coverslip. This could account for the subtle trend seen in OHC3 losses being greater than OHC1 losses. These losses are however insufficient to explain the ABR and partial mid frequency recovery seen at week 16. Immunofluorescence does not support any OHC losses or altered morphology. It is

therefore more likely a ME effect from the antibiotic laden pellets causing ABR threshold elevation.

8.9.4 IHC

Immunofluorescence studies show no appreciable inner hair cell loss or change in morphology and this is also seen on analysis of the cytocochleograms. Therefore IHC loss is unlikely to be the mechanism of ABR threshold elevation and supports an alternative explanation potentially at the site of the ME where the pellet is inserted.

8.9.5 Synaptopathy

Recent advances in the field of sensorineural hearing loss using guinea pig models has shown that noise induced hearing loss causes a loss of cochlear nerve hair cell synapses (Kujawa *et al*., 2015). This is accompanied with the clinical finding of temporary threshold shift in the ABR and hair cell loss. A similar mechanism has the potential in the guinea pigs implanted with pellets loaded with rifampicin and clindamycin. In this experimental group, there was no appreciable IHC and OHC loss, yet a threshold shift with some reversibility seen in the mid frequency range. This raises the possibility that the site of damage is the synapse.

After implantation of the pellet loaded with rifampicin and clindamycin, there is no appreciable IHC loss. There is still the potential for neurotrophin release from the IHC allowing spiral ganglion regeneration (Sugawara *et al*., 2005). Although synaptopathy is a possible explanation for ABR threshold elevation it is unlikely as there are no corresponding amplitude and latency changes seen.

8.10 Summary

8.10.1 Summary of experimental regimen

The experimental limitations of variability in pellet dimensions is unavoidable, however, the variation in size and be accommodated by adjustments to the bulla fenestration. The pellets are manufactured using a sterile technique and with E-beam sterilisation. Care was taken during storage and transfer to the site for experimental implantation to ensure correct storage at 5 degrees celsius.

Anaesthetic regimen alterations were unavoidable as Hypnorm was discontinued by the manufacturer. An alternative regimen was developed and implemented. Steps were taken to ensure delivery of 1% isoflurane via a face mask post ABR recording and the overall exposure to isoflurane was minimised. This is because a dose dependent impact of isoflurane on ABR results has been shown (Stronks *et al*., 2010).

Careful attention was paid to temperature and oxygen homeostasis as hypothermia and hypoxia are both know to influence ABR results (Kohn *et al*., 1997, Attias *et al*., 1990). An oxygen saturation probe and a thermometer which alarms if less than 35.5 degrees celsius were used to ensure this.

Guinea pig animal welfare was optimised with advice from the NACWO, Animal House staff and liaison with the Home office Vet. There was a 6.4% infection rate and one death from overheating. These complications have been discussed at the Licence review meeting 2017. Overall, the guinea pig model has proved robust for middle ear experimentation. The relatively large ventral bulla has allowed pellet placement away from the ossicular chain.

Of the animals experiencing trauma, 80% were in the PLGA and pluronic group loaded with rifampicin and clindamycin, exposing a potential vulnerability created by this intervention. This vulnerability may be explained by a unilateral increased hearing threshold, but there does appear to be a systemic upset which could potentially be disequilibrium or central vestibulotoxic effect. Intermale aggression is a component of guinea pig welfare which is common in the adolescent period (Slob *et al*., 1979).

Technical limitations which were unavoidable include changing the experimental room and ABR recording equipment as there was an interval between the experimental cohorts. Effects were made to minimise the electromagnetic background noise and to improve the signal transmission to the guinea pigs' ears. This included switching off unnecessary electrical devices, careful subcutaneous ABR recording electrode placement and cleaning the EAC from secretions.

8.10.2 Summary of experimental findings

ABR studies of threshold, amplitude and latency do not show any significant excursions from the mean in the biological control, surgical control and PLGA and pluronic pellet control groups. There is significant threshold elevation across all frequencies for the PLGA and pluronic pellet group loaded with rifampicin and clindamycin in combination with some partial mid frequency recovery at 16 weeks. Significant elevations of threshold are also seen with the guinea pigs loaded with pellet plus rifampicin or clindamycin groups. The threshold elevation results are evidence of impairment of auditory processing.

The results of ABR amplitude and latency show variability and hence Friedman's two way analysis and Holm-Bonferroni correction were implemented. There are no

consistent changes seen in amplitude and latency. Therefore, there is no evidence of central ototoxicity or neurotoxicity.

The cytocochleograms and immunofluorescence studies do not show any frank OHC or IHC damage or loss to explain the ABR results. The outermost row of the OHC is the most vulnerable to damage as the specimens are prepared for analysis. The middle ear histology slides show pellet remnant present after 16 weeks with a chronic inflammatory response around the pellet loaded with rifampicin and clindamycin in combination. Reissner's membrane also appeared to bulge in the histology cross sections.

8.10.3 Possible explanation for ABR threshold elevation

Insertion of the pellet loaded with rifampicin and clindamycin into the guinea pig middle ear has been shown in histology cross sections to cause a chronic inflammatory reaction and phagocytosis. This reaction may also create a middle ear effusion which has been undetected experimentally as the temporal bones are fixed, perfused, dissected and decalcified. No tympanometry was performed alongside ABR testing which may have detected OME with a Type B flat trace. The presence of a middle ear effusion has the potential to explain ABR threshold elevation without corresponding ABR latency and amplitude changes and some mid frequency recovery showing partial resolution.

The lack of IHC and OHC damage and loss would also be consistent with a middle ear effusion with its effects seen on the middle ear with cochlea sparing. The function of the middle ear with sound amplification and impedance mismatching is therefore affected.

Experimentally, guinea pig models of OME have shown a 40dB elevation in ABR threshold within 1 week of an injecting an insult to induce the effusion (Huang *et al*., 2005). Other studies have shown a faster onset of the effusion at 3 days (Dai *et al*., 2008) after injection into the ME to induce the inflammatory state. These ABR threshold elevation levels and timescales reported in other guinea pig models are consistent with the experimental findings seen. This suggests that introduction of rifampicin and clindamycin loaded PLGA and pluronic pellets into the ME of guinea pigs may induce an OME. This is plausible explanation for ABR threshold elevation at week 1 and with partial resolution by week 16 in the mid frequency range and is consistent with no changes in the amplitude and latency and no IHC or OHC loss. The histological evidence of ME inflammation seen after pellet insertion at 16 weeks is also compelling evidence to support this theory of OME generation.

Another potential explanation for ABR threshold elevation is endolymphatic hydrops. There is some histological evidence for this in cross sections (Figure 126c). The underlying mechanism is potentially an osmotic effect from the pellet loaded with antibiotics in the ME altering the endolymphatic potential. This could explain ABR pan threshold elevation and partial recovery from the recalibration. There is no damage to the IHC, OHC and cochlea which would be consistent with this theory.

The key results of the experiment after antibiotic laden pellet delivery to the ME are 1) ABR threshold elevation, 2) ME histological inflammation, 3) lack of evidence of any cochlea damage and 4) no evidence of neurotoxicity. A middle ear effusion is the most plausible explanation for these results.

8.11 Future studies

The experimental design was set up to assess for safety of the PLGA and pluronic middle ear pellets loaded with rifampicin and clindamycin. In accordance with the Russell and Birch principals which govern animal experimentation in the UK (1959), minimising the guinea pig numbers used for the *in vivo* experiments by testing a high dosage of both antibiotics was chosen. If there was no evidence of ototoxicity at the high doses of antibiotic, then safety can be assumed at lower clinical doses. Given ABR threshold elevation was detected, future experiments focusing on the dosage of antibiotics to determine when the critical level of drug for ototoxicity is reached would be valuable.

Investigation of the effects of other antibiotics loaded onto the PLGA and Pluronic pellet such as co-amoxiclav which have also shown potential success at eradication of biofilms in vitro would be interesting. Ototoxicity testing focusing on ABR threshold elevation and analysing the effect on IHC and OHC and middle ear epithelium would determine whether the results found with rifampicin and clindamycin are reproducible at similar doses of different antibiotics.

Three dimensional reconstructions of cross sectional imaging of the temporal bones taken at different time points and with different experimental groups would allow accurate estimation of the volume of the remnant pellet at different time points. This would be optimised by MRI imaging but CT scanning would also allow information on the temporal bone reactivity, middle ear ossicles and placement of the fenestration which allows insertion of the pellet into the middle ear bulla.

Scanning electron microscopy would allow for individual hair cells to be studied with a focus on morphology and also accurate counting. This technique is skilled and expensive but negates the need for micro dissection of the cochlea and placement of a coverslip. Both of these have the potential to create trauma with the outermost row of the OHC the most vulnerable. Eliminating slide preparation trauma and micro dissection trauma would ensure that any morphological changes seen in the OHC are attributable to the experimental intervention.

Removing the remnant pellet from the temporal bone specimens and analysing for any evidence of foreign body reaction including substrate for bacteria to grow would also be of interest. Microbiology culture of the pellet may also yield bacterial growth. In none of the temporal bone specimens was there evidence of OME or acute infection after pellet placement although tympanometry and inspection of the tympanic membrane to investigate this was not performed.

Overall, there is huge future potential in this technology of delivering drugs to the middle ear via pellets. On the basis of the results however, great care must be taken with future experimental design. The ABR threshold elevation is most likely attributable to OME, which is the clinical condition the pellets are designed to treat. Pellet design maybe favourably altered to reduce such potential inflammation in humans. Therefore, further studies must be undertaken before clinical application and translation to humans is considered.

References

ABDEL-HAFEZ AM, ELGAYAR SA, HUSAIN OA, THABET HS. Effect of nicotine on the structure of cochlea of guinea pigs. *Anat Cell Biol* 2014;47:162-70

ABDEL-HALIM RE. Contributions of Ibn Zuhr (Avenzoar) to the progress of surgery: a study and translations from his book Al-Taisir. *Saudi medical journal* 2005;26: 1333–9

ABDUL-AZIZ D, KOZIN ED, LIN BM, WONG K, SHAH PV, REMENSCHINEIDER AK, LANDEGGER LD, JULIANO AF, COHEN MS, LEE DJ. Temporal bone computed tomography findings associated with feasibility of endoscopic ear surgery. *Am J Otolaryngol* 2017;38:698-703

ABRAHAMS SW, LABBOK MH. Breastfeeding and Otitis Media: A Review of Recent Evidence *Curr Allergy Asthma Rep* 2011;11:508-512

AHLFORS CE, BENNETT SH, SHOEMAKER CT, ELLIS WG, DAVIS SL, WENNBERG RP, GOETZMAN BW. Changes in the auditory brainstem response associated with intravenous infusion of unconjugated bilirubin into infant rhesus monkeys. *Pediatr Res* 1986;20:511-5

AL-BATANONY MA, ABDEL-RASUL GM, ABU-SALEM MA, AL-DALATONY MM, ALLAM HK. Occupational exposure to mercury among workers in a fluorescent lamp factory. Quisna Industrial Zone, Egypt. *Int J Occp Environ Med* 2013;4:149-56

ALBUQUERQUE AA, ROSSATO M, OLIVEIRA JA, HYPPOLITO MA. Understanding the anatomy of ears from guinea pigs and rats and its use on basic otologic research. *Braz J Otorhinolaryngol* 2009;75:43-9

ALHO OP, OJA H, KOIVU M, SORRI M. Chronic otitis media with effusion in infancy. *Arch Otolaryngol Head Neck Surg* 1995;121:432-436

ALLEGRUCCI M, HU FZ, SHEN K, HAYES J, EHRLICH GD, POST JC, SAUER K. Phenotypic characterization of *Streptococcus pneumonia* biofilm development . *J Bacteriol* 2006;188:2325-35

AL-ZAHID S, DANIEL M, CHESSMAN R, ASHRAF W, FORTNUM H, SHAKESHEFF K, BIRCHALL R, BAYSTON R. The treatment of glue ear using biodegradable polymers to deliver high dose antibiotics and mucolytics to the infection site. *Int J Surg* 2011;9:496

ANGGARD E. Nitric oxide: mediator, murderer, medicine. *Lancet* 1994;343:1199-1206

Animals and Scientific Procedures Act 1986

ASHRY Y, KAWAI K, POE D. Utility of adjunctive procedures with balloon dilation of the Eustachian tube. *Laryngoscope Investig Otolaryngol* 2017;2:337-343

ASSAD JA ,SHEPARD GM, COREY DP. Tip-link integrity and mechanical transduction in vertebrate hair cells *Neuron* 1991;7:985-94

ATES M, CEVIK C, DOKUYUCU R, BERBER O, COLAK S, IZMIRLI M. The endothelial nitric oxide synthase (eNOS) polymorphism in otitis media with effusion (OME). *Eur Ann Otorhinolaryngol Head Neck Dis* 2017;134:3-5

ATTIAS S, SOHMER H, GOLD S, HARAN J, SHAHAR A. Noise and hypoxia induced temporary threshold shifts in rats studied by ABR. *Hear Res* 1990;45:247-52

BAIRD SM, THE BM, LIM KKM, CAMPBELL MC. Bone wax extrusion through postauricular wounds: A case series. *Laryngoscope* 2018;128:369-372

BAKALETZ LO. Bacterial biofilms in the upper airway- evidence for role in pathology and implications for treatment of otitis media. *Paediatr Respir Rev* 2012;13:154-159

BAKHOS D, AUSSEDAT C, LEGRIS E, AOUSTIN JM, NEVOUX J. Adult deafness: Towards new paradigm. *Presse Med* 2017;46:1033-1042

BARKER AB, LEIGHTON P, FERGUSON MA. Coping together with hearing loss: a qualitative meta-synthesis of the psychosocial experiences of people with hearing loss and their communication partners. *Int J Audiol* 2017;56:297-305

BARSHAK MB, DURAND ML. The role of infection and antibiotics in chronic rhinosinusitis. *Laryngoscope Investig Otolaryngol* 2017;23:36-42

BAYSTON R. Biofilms and prosthetic devices. Community structure and co-operation in biofilms (eds. Alison DG, Gilbert P, Lappin-Scott HM, Wilson M). Cambridge University Press 2000;295-308

BEERY QC, DOYLE WJ, CANTEKIN EI, BLUESTONE CD, WIET RJ. Eustachian tube function in an American Indian population. *Ann Otol Rhinol Laryngol Suppl* 1980;89:28-33

BÉKÉSY G V. Some biophysical experiments from fifty years ago. *Ann Rev Physiol* 1974;36: 1-18

BELFIELD K, BAYSTON R, BIRCHALL JP, DANIEL M. Do orally administered antibiotics reach concentrations in the middle ear sufficient to eradicate planktonic and biofilm bacteria? A review. *Int J Pediatr Otorhinolaryngol* 2015; 79:296-300

BENCKO V, SYMON K. Test of environmental exposure to arsenic and hearing changes in exposed children. *Environ Health Perspect* 1977;19:95-101

BENDELE AM, HULMAN JF, HARVEY AK, HRUBEY PS, CHANDRASEKHAR S. A passive role of articular chondrocytes in quinolone-induced arthropathy in guinea pigs. *Toxicol Pathol* 1990;18:304-312

BERNSTEIN JM. The role of IgE mediated hypersensitivity in the development of otitis media with effusion: a review. *Otolaryngol Head Neck Surg* 1993;109:611-20

BERRYHILL WE, GRAHAM MD. Chemical and physical labyrinthectomy for Ménière's disease. *Otolaryngol Clin North Am* 2002;35:675-682

BIBLE E, CHAU DY, ALEXANDER MR, PRICE J, SHAKESHEFF KM, MODO M. The support of neural stem cells transplanted into stroke-induced brain cavities by PLGA particles. *Biomaterials* 2009;30:2985-2994

BIRKENMEYER RD, KAGAN F. Lincomycin XI. Synthesis and structure of clindamycin, a potential antibacterial agent. *J Med Chemistry* 1970;13:616-619

BLAKLEY BW, HOCHMAN J, WELLMAN M, GOOI A, HUSSAIN AE. Differences in ototoxicity across species. *J Otolaryngol Head Neck Surg* 2008;37:700-3

BLUESTONE CD. State of the art: definitions and classifications. In: Liu DJ, Bluestone CD, Klien JO, Nelson JD (Eds). Recent advances in otitis media with effusion. Proceedings of the 3rd International Conference. Ontario: Decker and Mosby; 1984

BLUESTONE CD, GATES GA, KLEIN JO, LIM DJ, MOGI G, OGRA PL, PAPPRELLA MM, PARADISE JL, TOS M. Definitions, terminology and classification of otitis media. *Annals Otol Rhinol Laryngol* 2002;188:8-18

BOCK GR, STEEL KP. Use of albino animals for auditory research. *Hear Res* 1984;13:201-2

BOLINTINEANU DS, KAZNESSIS YN. Computation studies of protegrin antimicrobial properties: A review *Peptides* 2011;32:188-201

BORDURE P, DESMADRYL G, UZIEL A, SANS A. Short latency vestibular potentials evoked by electrical round window stimulation in the guinea pig. *Electroencephalography and Clin Neurophys* 1989;73:464-469

BOTTING J. Dispelling myths about penicillin: The importance of using the right model. *Laboratory Animals* 1997;26:37-39

BOUCHET V, HOOD DW, BRISSON JR, RANDLE GA, MARTIN A, LI Z, GOLDSTEIN R, SCHWEDA EK, PELTON SI, RICHARDS JC, MOXON ER. Host-derived sialic acid is incorporated into Haemophilus influenza lipopolysaccharide and is a major virulence factor in experimental otitis media. *Proc Natl Acad Sci* 2003;100:8898-903

BRAKE MK, JEWER K, FLOWERDEW G, CAVANAGH JP, CRON C, HONG P. Tympanocentesis results of a Canadian paediatric myringotomy population, 2018 to 2010. *J Otolaryngol Head Neck Surg* 2012;41:282-7

BRAUER M, GEHRING U, BRUNEKREEF B, DE JONGSTE J, GERRITSEN J, ROVERS M, WICHMANN HE, WIJGA A, HEINRICH J. Traffic related air pollution and otitis media. *Environ Health Perspect* 2006;114:1414-1418

BROWNELL W, BADER CR, BERTRAND D, DE RIBAUPIERRE Y. Evoked mechanical responses of isolated cochlear hair cells. *Science* 1985;227: 194-96

BROWNING GG (2008) Paediatric Otorhinolaryngology: Otitis media with effusion. In Gleeson M (Ed.) *Scott-Brown's Otorhinolaryngology: Head and Neck Surgery: Volume 1* (PP877-911). UK: Hodder Arnold

BROWNING GG, ROVERS MM, WILLIAMSON I, LOUS J, BURTON MJ. Grommets (ventilation tubes) for hearing loss associated with otitis media with effusion in children. Cochrane Database of Systematic Reviews 2010, Issue 10. Art. No: CD001801

BRUCKDORFER R. The basics about nitric oxide. *Mol Aspects Med* 2005;26:3-31

BU M, TANG J, WEI Y, SUN Y, WANG X, WU L, LIU H. Enhanced bioavailability of nerve growth factor with phytantriol lipid-based crystalline nanoparticles in cochlea. *Int J Nanomedicine* 2015;10:6879-89

BUCHWALD JS, HUANG CM. Far field acoustic response: origins in cat. *Science*. 1975;189:382-384

CAI T, MCPHERSON B. Hearing loss in children with otitis media with effusion: a systematic review. *Int J Audio* 2017;56:65-76

CAMPO P, MORATA TC, HONG O. Chemical exposure and hearing loss. *Dis Mon* 2013;59:119-138

CANNELL H. Phenobarbitone sodium anaesthesia for oral and immunological procedures in the guinea-pig. *Lab Anim* 1972;6:55-60

CANTEKIN EI, MANDEL EM, BLUESTONE CD, ROCKETTE HE, PARADISE JL, STOOL SE, FRIA TJ, ROGERS KD. Lack of efficacy of a decongestant-antihistamine combination for otitis media with effusion ("secretory" otitis media) in children. *N Eng J Med* 1983;308:297-301

CAPPER R, GUO L, PEARSON JP, BIRCHALL JP. Effect of nitric oxide donation on mucin production *in vitro. Clin Otolaryngol* 2003;28:51-54

CARDINAAL RM, DE GROOT JC, HUIZING EH, VELDMAN JE, SOMMRENBURG GF. Dose-dependent effect of 8 – day cisplatin administration upon the morphology of the albino guinea pig cochlea. *Hear Res* 2000;144:135-46

CARRERES-PONS M, CHALANSONNET M, VENET T, THOMAS A, NUNGE H, MERLEN L, COSNIER F, LLORENS J, CAMPO P. Carbon disulphide potentiates the effects of impulse noise on the organ of Corti. *Neurotoxicology* 2017;59:79-87

CASSELBRANT ML, BROSTOFF LM, CANTEKIN EI, FLAHERTY MR, DOYLE WJ, BLUESTONE CD, FRIA TJ. Otitis media with effusion in preschool children. *Laryngoscope* 1985;95:428-436

CASSELBRANT ML, MANDEL EM, FALL PA, ROCKETTE HE, KURS-LASKY M, BLUESTONE CD, FERRELL RE. The hereditability of otitis media: a twin and triplet study. *JAMA* 1999;8:2125-30

CEDERHOLM JM, FROUD KE, WONG AC, KO M, RYAN AF, HOUSLEY GD. Differential actions of isoflurane and ketamins-based anaesthetics on cochlear function in the mouse. *Hear Res* 2012;292:71-9

CELIN SE, BLUESTONE CD, STEPHENSON J, YIMAZ HM, COLLINS JJ. Bacteriology of acute otitis media in adults. *JAMA* 1991;266:2249-52

CESARANI A, CAPOBIANCO S, SOI D, GIULIANO DA, ALPINI D. Intratympanic dexamethasone treatment for control of subjective idiopathic tinnitus: our clinical experience. *Int. Tinnitus J.* 2002;8:111-114

CHANDRASEKHAR SS. Intratympanic dexamethasone for sudden sensorineural hearing loss: clinical and laboratory evaluation. *Otol Neurotol* 2001;22:18-23

CHAWDHARY G, PANKHANIA M, DOUGLAS S, BOTTRILL I. Current management of necrotising otitis externa in the UK: survey of 221 UK otolaryngologists. *Acta Otolaryngol* 2017;137:818-822

CHEN GD, FECHTER LD. The relationship between noise-induced hearing loss and hair cell loss in rats. *Hear Res* 2003;177:81-90

CHEN FQ, SCHACHT J, SHA SH. Aminoglycoside-induced histone deacetylation and hair cell death in the mouse cochlea. *J Neurochem* 2009;108:1226-1236

CHEN GD, CHI LH, KOSTYNIAK PJ, HENDERSON D. Styrene induced alterations in biomarkers of exposure and effects in the cochlea: mechanisms of hearing loss. *Toxicol Sci* 2007;98:167-77

CHEN GD, DECKER B, KRISHNAN MUTHAIAH VP, SHEPPARD A, SALVI R. Prolonged noise exposure-induced auditory thresholds in rats. *Hear Res* 2014;317:1-8

CHEN Y, WEN L, HU P, QIU J, LU L, QIAO L. Endoscopic intratympanic methylprednisolone injection treatment of refractory sudden sensorineural hearing loss and one case in pregnancy. *J Otolaryngol Head Neck Surg* 2010;39:640-645

CHENG PW, LIU SH, HSU CJ, LIN-SHIAU SY. Correlation of increased activities of Na+, K+-ATPase and Ca2+ ATPase with the reversal of cisplatin ototoxicity induced by D methionine in guinea pigs. *Hear Res* 2005;205:102-9

CHRISTENSEN GD, SIMPSON A, YOUNGER JJ, BADDOUR LM, BARRETT FF, MELTON DM, BEACHEY EH. Adherence of coagulase negative staphylococci to plastic tissue culture plates: a quantitative model for the adherence of staphylococci to medical devices. *J Clin Microbiol* 1986;22:996-1006

COATES H, VIJAYASEKRAN S. Bacterial biofilm in chronic supporative otitis media. *Otolaryngol Head Neck Surg* 2010;142:778

COHEN BJ AND LOEW FM (1984) Laboratory Animal Medicine: Historical Perspectives in Laboratory Animal Medicine (eds J.G. Fox, B.J. Cohen and F.M. Loew) Academic Press, Inc., Orlando, Florida

Collins, Douglas R. Atlas of Drug Reactions. New York NY: Churchill Livingstone 1985:123

COMMINS DJ, KOAY BC, BATES GI, MOORE RA, SLEEMAN K, MITCHELL B, BATES S. The role of Mucodyne in reducing the need for surgery in patients with persistent otitis media with effusion. *Clinical Otology* 2000;25:274-9

CONLEE JW, GILL SS, MCCANDLESS PT, CREEL DJ. Differential susceptibility to gentamicin ototoxicity between albino and pigmented guinea pig. *Hear Res* 1989;41:43-52

CRAWFORD A, EVANS MG, FETTIPLACE R. The actions of calcium on the mechano-electrical transducer current of turtle hair cells. *J Physiol* 1991; 434: 369-398

DAI C, GAN RZ. Change of middle ear transfer function in otitis media with effusion model of guinea pigs. *Hear Res* 2008; 243:78-86

DALHBERG G, DIAMANT M. Hereditary character of the cellular system in the mastoid process. *Acta Otolaryngol* 1945;33:378-89

DALY KA, HUNTER LL, GIEBINK GS. Chronic otitis media with effusion. *Pediatr Rev* 1999;20:85-93

DANIEL M, VAGHELA H, PHILPOTT C, THOMAS RSA, GANNON M, SPENCER H, HAGGARD M. Does the benefit of adenoidectomy in addition to ventilation tube insertion persist long term? *Clin Otol* 2006;31:580

DANIEL M, RAHMAN C, ASHRAF W, FERGIE N, SHAKESHEFF K, BIRCHALL JP, BAYSTON R. Development of an in-vitro model of *Staphylococcus Aureus* biofilm infection with a focus on reduced susceptibility to antibiotics. *J Hosp Infect* 2010;76 (Suppl 1):S4

DANIEL M, IMTIAZ-UMER S, FERGIE N, BIRCHALL JP, BAYSTON R. Bacterial involvement in otitis media with effusion. *Int J Pediatr Otorhinolaryngol* 2012;76:1416-22

DANIEL M, CHESSMAN R, AL-ZAHID S, RICHARDS B, RAHMAN C, ASHRAF W, MCLAREN J, COX H, QUTACHI O, FORTNUM H, FERGIE N, SHAKESHEFF K, BIRCHALL JP, BAYSTON RR. Biofilm eradication with biodegradable modified-release antibiotic pellets: a potential treatment for glue ear. *Arch Otolaryngol Head Neck Surg* 2012;138:942-9

DAVIES D. Understanding biofilm resistance to antibacterial agents. *Nat Rev Drug Discov* 2003;2:114-22

DE GROOT JC, MEEUWESEN F, RUIZENDAAL WE, VELDMAN JE. Ultrastructural localisation of gentamicin in the cochlea. *Hear Res* 1990;50:35-42

DE LAURETIS A, DE CAPUA B, BARBIERI MT, BELLUSSI L, PASSÀLI D. ABR evaluation of ototoxicity in cancer patients receiving cisplatin or carboplatin. *Scand Audiol* 1999;28:139-43

DEBOYSER D, GOETHALS F, KRACK G, ROBERFROID M. Investigation into the mechanism of tetracycline-induced steatosis: study in isolated hepatocytes. *Toxicol Appl Pharmacol* 1989;97:473-9

DEWEY C, MIDGLEY E, MAW R. The relationship between otitis media with effusion and contact with other children in a British cohort studied from 8 months to 3 ½ years. The ALSPAC Study Team. Avon Longitudinal Study of Pregnancy and Childhood. *Int J Pediatr Otorhinolaryngol* 2000;15:33-45

DING D, ROTH J, SALVI R. Manganese is toxic to spiral ganglion neurons and hair cells in vitro. *Neuro Toxicity* 2010;32:233-41

DONLAN RM. Biofilms: microbial life on surfaces. *Emerg Infect Dis* 2002;8:881-890

DONLAN RM, COSTERTON JW. Biofilms: survivial mechanisms of clinically relevant microorganisms. *Clin Microbiol Rev* 2002;15:167-193

DOYLE WJ, FRIA TJ. The effects of hypothermia on the latencies of the auditory brain-stem response (ABR) in the rhesus monkey. *Electroencephalogr Clin Neurophysiol* 1985;60:258-66

DUAH V, HUANG Z, DEMASON C, POLEY M, PRECIADO D. Younger patients with COME are more likely to have mucoid middle ear fluid containing mucin MUC5B. *Int J Pediatr Otolaryngol* 2016;90:133-137

DURLACH HCN. Binaural phenomena: Handbook of Perception 1978:365-466

ENT UK. OME (glue ear)/adenoid and grommet: position paper. 2009
www.entuk.org.uk/position_papers/documents/OME

EGGERMONT JJ. Electrophysiological study of the normal and pathological human cochlea. I. Presynaptic potentials. *Rev of Laryngol, Otol and Rhinol* 1976;97(Suppl):487-95

EHRLICH GD, VEEH R, WANG X, COSTERTON JW, HAYES JD, HUFZ, DAIGLE BJ, EHRLICH MD, POST JC. Mucosal biofilm formation on middle ear mucosa in the chinchilla model of otitis media. *JAMA* 2002; 287:1710-5

FAY RR. Hearing in vertebrates: a psychophysics data book. Hill Fay Associates; Winnetka, III:1988

FEE WE. Aminoglycoside ototoxicity in the human. *Laryngoscope* 1980;90:1-19

FENG L, WARD JA, LI SK, TOILA G, HAO J, CHOO DI. Assessment of PLGA-PEG-PLGA copolymer hydrogel for sustained drug delivery in the ear. *Curr Drug Deliv* 2014;11:279-86

FERGIE N, BAYSTON R, PEARSON JP, BIRCHALL JP. Is otitis media with effusion a biofilm infection? *Clin Otolaryngol* 2004;29:38-46

FETTIPLACE R, CRAWFORD AC, EVANS MG. The hair cell's mechanical transducer channel. *Ann N Y Acad Sci* 1992; 656: 1-11

FETTIPLACE R (1992). The role of calcium in hair cell transduction: Sensory Transduction. Chapter 22 Rockefeller University Press

FETTIPLACE R. Hair cell transduction, tuning and synaptic transmission in the mammalian cochlea. *Compr Physiol* 2017;7:1197-1227

FLECKNELL PA, MITCHELL M. Midazolam and fentanyl-fluanisone: assessment of anaesthetic effects in laboratory rodents and rabbits. *Lab Anim* 1984;18:143-6

FLEMMING HC, WINGENDER J. The biofilm matrix . *Nat Rev Microbiol* 2010;8:623-33

FORGE A. A tubulo-cisternal endoplasmic reticulum system in the postassium transporting marginal cells of the stria vascularis and effects of the ototoxic diuretic ethacrynic acid. *Cell Tissue Res* 1982;226:375-387

FORGE A. Outer hair cell loss and supporting cell expansion following chronic gentamicin treatment. *Hear Res* 1985;19:171-82

FORGE A, Schacht J. Aminoglycoside antibiotics. *Audiol Neurootol* 2000;5:3-22

FOSTER CA. Optimal management of Ménière's disease. *Ther Clin Rick Manag* 2015;11:301-7

FRANCESCHI CM, TOCHETTO T, SILVERIA AF, FANTINEL MR, ALGARVE TD. Cisplatin effects on guinea pigs: cochlear histology and genotoxicity. *Braz J Otorhinolaryngol* 2011;77:728-35

FREEMAN S, GOITEIN K, ATTIAS J, FURST M, SOHMER H. Effect of hypoxemia and ethacrynic acid on ABR and distortion product emission thresholds. *J Neurol* Sci 1995;131:21-9

FREEMANTLE N, SHELDON TA, SONG F, LONG A. The treatment of persistent glue ear in children. Effective Healthcare Bulletin No 4. York: University of York, NHS Centre for Reviews and dissemination, 1992

FURNESS DN, HACKNEY CM. Morphological changes to the stereocilia bundles in the guinea pig cochlea after kanamycin treatment. *Br J Audiol* 1986;20:253-9

FURNESS DN, HACKNEY CM. High-resolution scanning-electron microscopy of stereocilia using the osmium-thiocarbohydrazide coating technique. *Hear Res* 1986;21:243-9

FURNESS DN, HACKNEY CM, HYND AN. Rotated stereociliary bundles and their relationship with the tectorial membrane in the guinea pig cochlea. *Acta Otolaryngol (Stockh)* 1990;109:66-75

FU Y, ZHAO H, ZHANG T, CHI F. Intratympanic dexamethasone as initial therapy for idiopathic sudden sensorineural hearing loss: clinical evaluation and laboratory investigations. *Auris Nasus Larynx* 2011;38:165-171

GAN CW, CHOOI WH, NG HC, WONG YS, VENKATRAMAN SS, LIM LH. Development of a novel biodegradable drug-eluting ventilation tube for chronic otitis media with effusion. *Laryngoscope* 2013;123:1770-7

GAN RWC, OVERTON P, BENTON C, DANIEL M. Hearing aids for otitis media with effusion: Do children use them? Int J Pediatr Otorhinolaryngol 2017;99:117-119

GAO X, WANG Y, CHEN K, GRADY BP, DORMER KJ, KOPKE RD. Magnetic assisted transport of PLGA nanoparticles through a human round window membrane model. *J Nanotechnol Engin Med* 2010;1:1-6

GATES GA, VERY CA, PRITHODA T, COOPER JC. Effectiveness of adenoidectomy and tympanostomy tubes in the treatment of chronic otitis media with effusion. *NEJM* 1987;317:1444-1451

GEISLER CD. A model of stereociliary tip-link stretches. *Hear Res* 1993;65: 79-82

GEISLER CD AND PICKLES (1998). From sound to synapse. Physiology of the mammalian ear. Oxford University Press

GHIASVAND M, MOHAMMADI S, ROTH B, RANJBAR M. The relationship between Occupational Exposure to Lead and Hearing Loss in a Cross-Sectional Survey of Iranian Workers. *Front Public Health* 2016;4:19

GIL-CARCEDO LM, MARTIN MC, CARRANZA MA, BENITO JI. Surgical approach to the middle ear of the guinea pig. *Acta Otorrinolaryngol Esp* 1991;42:399-403

GILLESPIE PG. Molecular machinery of auditory and vestibular transduction. *Curr Opin Neurobiol* 1995; 5:449-455

GLEESON M. Scott-Brown's Otorhinolaryngology. In: *Head and Neck Surgery (Seventh Edition).* Hodder Arnold, London, UK (2008)

GOKSU N, HAZIROQLU R, KEMALOGLU Y, KARADEMIR N, BAYRAMOGLU I, AKYILDIZ N. Anatomy of the guinea pig temporal bone. Ann Otol Rhinol Laryngol 1992;101:699-704

GOLD S, CAHANI M, SOHMER H, HOROWITZ M, SHAHAR A. Effects of body temperature elevation on auditory nerve-brain-stem evoked responses and EEGs in rats. *Electroencephalogr Clin Neurophysiol* 1985;60:146-53

GORECKA-TUTEJA A, JASTRZĘBSKA I, SKLADZIEN J, FYDEREK K. Laryngopharyngeal reflux in children with chronic otitis media with effusion. *J Neurogastroenterol Motil* 2016;22:452-8.

GOURÉVITCH B, DOISY T, AVILLAC M, EDELINE JM. Follow-up of latency and threshold shifts of auditory brainstem responses after single and interrupted acoustic trauma in guinea pig. *Brain Res* 2009;1304:66-79

GOYCOOLEA MV. Clinical aspects of round window membrane permeability under normal and pathological conditions. *Acta Otolaryngol* 2001;121:437-47

GOYCOOLEA MV, PAPARELLA MM, JUHN SK, CARPENTER AM. Oval and round window changes in otitis media. Potential pathways between middle and inner ear. *Laryngoscope.* 1980;90:1387–1391

GOYCOOLEA MV, PAPARELLA MM, GOLDBERG B, CARPENTER AM. Permeability of the round window membrane in otitis media. *Arch Otolaryngol* 1980;106:430-3

GOYCOOLEA MV, MUCHOW DC. Sustained release of antimicrobials in the middle ear using a biodegradeable support. *Ann Otol Rhinol Laryngol Suppl* 1994;163:46-8

GOYCOOLEA MV, MUCHOW DC, SIRVIO LM, WINANDY RM. In search of missing links in otology II. Development of an implantable middle ear drug delivery system: initial studies of sustained ampicillin release for the treatment of otitis media. *Laryngoscope* 1991;101:727-32

GOYCOOLEA MV, LUNDMAN L. Round window membrane structure, function and permeability: a review. MICROSC. RES. TECH 1997;36:201-211

GRAHN DA, HELLER M, LARKIN J, HELLER H. Appropriate thermal manipulations eliminate tremors in rats recovering from halothane anesthesia. J Appl Physiol 1996;81:2547–2554

GRANT EC, MACKINTISH JH. A comparison of the social postures of some common lab animals. *Behaviour* 1963;21:246-259

GRATTON MA, SCHMIEDT RA, SCHULTE BA. Age related decreases in endocochlear potentials are associated with vascular abnormalities in the stria vascularis. *Hear Res* 1996;94:116-124

GREEN CJ. Neuroleptanalgesic drug combinations in the anaesthetic management of small laboratory animals. *Lab Anim* 1975;9:161-78

GREENE NT, MATTINGLY JK, JENKINS HA, TOLLIN DJ, EASTER JR, CASS SP. Cochlear Implant electrode effect on sound energy transfer within cochlea during acoustic stimulation. *Otol Neurotol* 2015;36:1554-61

GREENWOOD GJ. Neomycin ototoxicity; report of a case. AMA *Arch Otolaryngol.* 1959;69:390-397

GRIFFIN GH, FLYNN C, BAILEY RE, SCHULTZ JK. Antihistamines and/or decongestants for otitis media with effusion (OME) in children. Cochrane Database of Systematic Reviews. 2006;4:CD003423

GUAN X, GAN RZ. Effect of middle ear fluid on sound transmission and auditory brainstem response in guinea pigs. *Hear Res* 2011;277:96-106

GUINAN J AND PEAKE W. Middle ear characteristics of anaesthetised cats. *J Acoust Soc Am* 1967;41: 1237-61

GUO JX, HU L, YAND PZ, TANABE K, MIYATALRE M, CHEN Y. Chronic arsenic poisoning in drinking water in Inner Mongolia and its associated health effects. J Environ Sci Health Part A Toxic/Hazard. *Subst Environ Eng* 2007;42:1853-1858

HALL-STOODLEY L, HU FZ, GIESEKE A, NISTICO L, NGUYEN D, HAYES J, FORBES M, GREENBERG DP, DICE B, BURROWS A, WACKYM PA, STOODLEY P, POST JC, EHRLICH GD, KERCHNER JE. Direct detection of bacterial biofilms on the middle ear mucosa of children with chronic otitis media. *JAMA* 2006;296:202-211

HALL-STOODLEY L, STOODLEY P. Evolving concepts of biofilm infections: microreview on modelling pathogenesis. *Cell Microbiol* 2009;11:1034-43

HALLPIKE CS, CAIRNS HWB. Observations of the pathology of Meniere's syndrome. *Proc Roy Soc Med* 1938;31:1317-1336

HARDING GW, BOHNE BA, AHMAD M. DPOAE level shifts and ABR threshold shifts compared to detailed analysis of histopathological damage from noise. *Hear Res* 2002;174:158-171

HARKNESS JE. Rodent drug doses. In Exotic animal formulary: a supplement to AAHA's practitioner guides to exotic animal medicine. Bauck L, Boyer TH, Brown SA, Harkness JE, Jenkins JR. American Animal Hospital Association, Lakewood, Colorado 1995:37-46

HARRIS GG. Brownian motion in the cochlear partition. *J Acoust Soc Am* 1968; 44:176-86

HASHIMOTO I, ISHIYAMA Y, YOSHIMOTO T, NEMOTO S. Brain-stem auditory evoked potentials recorded directly from human brainstem and thalamus. *Brain* 1981;104:841-59

HEERINGA AN, VAN DIJK P. The dissimilar time course of temporary threshold shifts and reduction of inhibition in the inferior colliculus following intense sound exposure. *Hear Res* 2014;312:38-47

Heffner HE, Heffner RS. Hearing ranges of laboratory animals. *J Am Assoc Lab Anim Sci* 2007;46:20-2

HEFFNER RS, KOAY G, HEFFNER HE. Hearing in American leaf-nosed bats. III: Artibeus jamaicensis. *Hear Res* 2003;184:113-22

HEMILÄ S, NUMMELA S, REUTER T. What middle ear parameters tell about impedance matching and high frequency hearing. *Hear Res* 1995;85:31-44

HEMLIN C, BRAUNER A, CARENFELT C, WRETLIND B. Nasopharyngeal flora in otitis media with effusion. A comparative semiquantitative analysis. *Acta Otolaryngol* 1991;111:556-61

HENRY KR. Auditory brainstem volume-conducted responses: origins in the laboratory mouse. *J Am Aud Soc* 1979;4:173-8

HENTZER E. Ultrastructure of the middle ear mucosa. *Acta Otolaryngol Suppl.* 1984;414:19-27

HICKOX AE, LARSEN E, HEINZ MG, SHINOBU L, WHITTON JP. Translational issues in cochlear synaptopathy. *Hear Res* 2017;349:164-171

HILL SL 3RD, DIGGES EN, SILVERSTEIN H. Long term follow-up after gentamicin application via Silverstein MicroWick in the treatment of Ménière's disease. *Ear Nose Throat J* 2006;85:494,496,498

HILTON JM, LEWIS MA, GRATI M, INGHAM N, PEARSON S, LASKOWSKI RA, ADAMS DJ, STEEL KP. Exome sequencing identifies a missense mutation in Isl1 associated with low penetrance otitis media in dearisch mice. *Genome Biol* 2011;21:R90.doi:10.1186/gb-2011-12-9-r90

HIROSE K, LIBERMAN MC. Lateral wall histopathology and endocochlear potential in the noise damaged mouse cochlea. *J Assoc Res Otolaryngol* 2003;4:339-352

HO HG, LIN HC, SHU MT, YANG CC, TSAI HT. Effectiveness of intratympanic dexamethasone injection in sudden-deafness patients as salvage treatment. *Laryngoscope* 2004;114:1184-1189

HÖFT J. The permeability of the round window membrane and its changes by pantocaine (tetracaine). *Arch Klin Exp Ohren Nasen Kehlkopfheilkd* 1969;193:128-37

HOLM S. A simple sequential rejective multiple test procedure. *Scandanavian Journal of Statistics* 1979;6:65-70

HOMOE P, BJARNSHOLT T, WESSMAN M, SORENSEN HC, JOHANSEN HK. Morphological evidence of biofilm formation in Greenlanders with chronic supporative otitis media. *Eur Arch Otorhinolaryngol* 2009;266:1533-8

HONRUBAI V, WARD PH. Properties of the summating potential of the guinea pig's cochlea. J Acoust Soc Am 1969;45: 1443-50

HORI K, MATSUMOTO S. Bacterial adhesion: From mechanism to control *Biochem Engin J* 2010;48:424-434

HORIE RT, SAKAMOTO T, NAGAKAWA T, ISHIHARA T, HIGAKI M, ITO J. Stealth nanoparticles strategy for enhancing the efficacy of steroids in mice with noise-induced hearing loss. *Nanomedicine (Lond)* 2010:5;1331-40

HORIE RT, SAKAMOTO T, NAKAGAWA T, TABATA Y, OKAMURA N, TOMIYAMA N, TACHIBANA M, ITO J. Sustained delivery of lidocaine into the cochlea using poly lactic/glycolic acid micro particles. *Laryngoscope* 2010;120:377-83

HORVÁTI K, BACSA B, KISS E, GYULAI G, FODOR K, BALKA G, RUSVAI M, SZABÓ E, HUDECZ F, BÓSZE S. Nanoparticle encapsulated lipopeptide conjugate of antitubercular drug isoniazid: *in vitro* intracellular activity and *in vivo* efficacy in a guinea pig model of tuberculosis. *Bioconj Chem* 2014;17:2260-8

HOSKISON E, DANIEL M, AL-ZAHID S, BAYSTON R, BIRCHALL JP. Drug delivery to the ear. *Ther Deliv* 2013;4:1-10

HOSOKAWA S, SUGIYAMA K, TAKAHASHI G, TAKEBAYASHI S, MINETA H. Prognostic factors for idiopathic sudden sensorineural hearing loss treated with hyperbaric oxygen therapy and intravenous steroids. *J Laryngol Otol* 2017;131:77-82

HOSPITAL EPISODE STATISTICS HES

HOTZ MA, ALLUM JH, KAUFMANN G, FOLLATH F, PFALTZ CR. Shifts in auditory brainstem response latencies following plasma-level-controlled aminoglycoside therapy. *Eur Arch Otorhinolaryngol* 1990;247:202-5

HUANG P, MA Z, CHEN X, LI M, CAO Y, CAI J. The curative effect of pulmonary surfactant on otitis media with effusion in guinea pigs. *Lin Chuang Er Bi Yan Hou Ke Za Zhi*. 2005;19:605-6

HUDSPETH AJ. Mechanoelectrical transduction by hair cells in the acousticolateralis sensory system. *Ann Rev Neurosci* 1983;6:187-215

HUDSPETH AJ AND LEWIS RS. A model for electrical resonance and frequency tuning in saccular hair cells of the bull-frog, Rana catesbeiana. *J Physiol* 1988; 400: 275-297

HUDSPETH AJ AND GILLESPIE PG. Pulling strings to tune transduction: adaptation by hair cells. *Neuron* 1994;12: 1-9

HUTH ME, RICCI AJ, CHENG AG. Mechanisms of aminoglycoside ototoxicity and targets of hair cell protection. *Int J Otolaryngol* 2011;937861-5739

HUTTON DA, FOGG FJ, KUBBA H, BIRCHALL JP, PEARSON JP. Heterogeneity in the protein cores of mucins isolated from human middle ear effusions: evidence for expression of different mucin gene products. *Glycoconjucate J* 1997;15:283-291

ICHIMAYA I, SUZUKI M, MORGI G. Age related changes in the murine cochlear lateral wall. *Hear Res* 2000;134:116-22

ILOMÄKI JH, KARHUKETO T, VASAMA JP, KÄÄRIÄINEN J, RAUTIAINEN M. The endoscopic study of human middle ear mucociliary transport. *Eur Arch Otolaryngol* 2016;273:1711-5

INGHAM NJ, THORNTON SK, COMIS SD, WITHINGTON DJ. The auditory brainstem response of aged guinea PIGS. ACTA OTOLARYNGOL 1998;118:673-80

IMAIMURA S, ADAMS JC. Distribution of gentamicin in the guinea pig inner ear after local or systemic application. *J Assoc Res Otolaryngol* 2003;4:176-195

INOUE M, ATES N, VOSSEN JM, COENEN AM. Effects of neuroleptanalgesic fentanyl-fluanisone (Hypnorm) on spike-wave discharges in epileptic rats. *Pharmacol Biochem Behav* 1994;48:547-51

ISHII T, TORIYAMA M, SUZUKI JI. Histopathological study of otitis media with effusion. *Ann Otol Rhinol Laryngol* 1980;89:83-86

JACKSON CG, GLASSCOCK ME 3RD, DAVIS WE, HUGHES GB, SISMANIS A. Medical management of Meniere's disease. *Ann Otol Rhinol Laryngol* 1981;90:142-147

JACKSON LE, SILVERSTEIN H. Chemical perfusion of the inner ear. *Otolaryngol Clin North Am* 2002;35:639-653

JACOBSON GP, YEH HS. The auditory brainstem response in surgical monitoring: the pathological significance of a reduced P1-P5 interwave interval. *Clin Electroencephalog* 1985;16:83-7

JAMAL M, AHMAD W, ANDLEEB S, JALIL F, IMRAN M, NAWAZ MA, HUSSAIN T, ALI M, RAFIQ M, KAMIL MA. Bacterial biofilm and associated infections. J Clin Med Assoc 2017;S1726-4901

JANG CH, CHO YB, CHOI CH. Structural features of tympanostomy tube biofilm formation in ciprofloxacin-resistant *Pseudomonas* otorrhoea. *Int J Pediatr Otorhinolaryngol* 2007;71:591-5

JERO J, KARMA P. Bacteriological findings and persistence of middle ear effusion in otitis media with effusion. *Acta Otolaryngol Suppl* 1997;529:22-6

JERO J, MHATRE AN, TSENG CJ, STERN SE, COLING DE, GOLDSTEIN JA, HONG K, ZHENG WW, HOQUE AT, LALWANI AK. Cochlear gene delivery through an intact round window membrane in mouse. *Hum Gene Ther* 2001;12:539-48

JIANG C, LUO B, MANOHAR S, CHEN GD, SALVI R. Plastic changes along auditory pathway during salicylate-induced ototoxicity: Hyperactivity and CF shifts. *Hear Res* 2017;347:28-40

JIANG M, TAGHIZADEH F, STEYGER PS. Potential mechanisms underlying inflammation – enhanced aminoglycoside-induced cochleotoxicity. *Front Cell Neurosci* 2017;11:362

JOHN EO, RUSSELL PT, NAM BH, JINN TH, JUNG TT. Concentration of nitric oxide metabolites in middle ear effusion. *Int J Pediatr Otorhinolaryngol* 2001;30:55-8

JOHNSON IJM, BROOKS T, HUTTON DA, BIRCHALL JP, PEARSON JP. Compositional differences between bilateral middle ear effusions in Otitis Media with Effusion: Evidence for a different aetiology? *Laryngoscope* 1997;107:684-89

JOHNSTONE BM AND BOYLE AJ. Basilar membrane vibration examined with the Mössbauer technique. *Science* 1967;158: 389-90

JONES EA, THOMAS LR, DAVIS NC. The significance of secretory IgA in middle ear fluid *Ann Allergy* 1979;42:236-240

JUDKINS RF, LI H. Surgical anatomy of the rat middle ear. *Otolaryngol Head Neck Surg* 1997;117:438-47

KAGA K, KITAZUMI E, KODAMA K. Auditory brainstem responses of kernicterus infants. *Int J Pediatr Otorhinolaryngol* 1979;1:255-64

JUFAS N, MARCHIONI D, TARABICHI M, PATEL N. Endoscopic Anatomy of the Protympanum. *Otolaryngol Clin North Am* 2016;49:1107-19

KAJI C, WATANABE K, APICELLA MA, WATANABE H. Antimicrobioal effect of fluoroquinolones for the eradication of nontypable *Haemophilus influenzae* isolates within biofilms. *Tohoku J Exp Med* 2008;214:121-8

KAKEHATA S, SASAKI A, OJI K, FUTAI K, OTA S, MAKINAE K, SHINKAWA H. Comparison of intratympanic and intravenous dexamethasone treatment on sudden sensorineural hearing loss with diabetes *Otol Neurotol* 2006;27:604-608

KANTHASHAMY A, BOROWITZ J, PAVLAKOVIC G, ISOM G. Dopaminergic neurotoxicity of cyanide: neurochemical, histological and behavioural characterization. *Toxicol Appl Pharmacol* 1994;126:156-163

KATBAMNA B, BANKAITIS AE, METZ DA, FISHER LE. Effects of hyperthermia on the auditory-evoked brainstem responses in mice. *Audiology* 1993;32:344-55

KELSO CM, WATANABE H, WAZEN JM, BUCHER T, QIAN ZJ, OLSON ES, KYSAR JW, LALWANI AK. Microperformations significantly enhance diffusion across round window membrane. *Otol Neurotol* 2016;36:694-700

KEMP DT. Stimulated acoustic emissions from within the human auditory system. *J Acoust Soc Am* 1978;64: 1386-91

KHANNA SM, LEONARD DG. Basilar membrane tuning in the cat cochlea. *Science* 1982;215: 305-306

KIANG NYS, LIBERMAN MC, SEWELL WF, GUINAN JJ. Single unit clues to cochlea mechanisms. *Hear Res* 1986;22:171-82

KING EB, SALT AN, EASTWOOD HT, O'LEARY SJ. Gentamicin administration on the stapes footplate causes greater hearing loss and vestibulotoxicity than round window administration in guinea pigs. *Hear Res* 2013; 304:159-66

KIVEKAS I, CHAO WC, FAQUIN W, HOLLOWELL M, SILVOLA J, RASOOLY T, POE D. Histopathology of balloon-dilation Eustachian tuboplasty. *Laryngoscope* 2015;125:436–441.

KOBEL M, LE PRELL CG, LIU J, HAWKS JW, BAO J. Noise-induced cochlear synaptopathy: past findings and future studies. *Hear Res* 2017;349:148-154

KOHN DF, WIXSON SK, WHITE WJ, BENSON GJ. 1997. Anesthesia and analgesia in laboratory animals. Academic Press.ISBN 9780080527222

KONISHI T, SALT AN, HAMRICK PE. Effects of hypothermia on ionic movement in the guinea pig cochlea. *Hear Res* 1981;4:265-278

KONRAD-MARTIN D, DILLE MF, MCMILLAN G, GRIEST S, MCDERMOTT D, FAUSTI SA, AUSTIN DF. Age-related changes in the auditory brainstem response (ABR). *J Am Acad Audiol* 2012;23:18-35

KUBBA H, PEARSON JP, BIRCHALL JP. The aetiology of otitis media with effusion: a review. *Clin Otolaryngol* 2000;25:181-194

KUJAWA SG, LIBERMAN MC. Adding insult to injury: cochlear nerve degeneration after temporary noise-induced hearing loss. *J Neurosci* 2009;29:14077-14085

KUJAWA SG, LIBERMAN MC. Synaptopathy in the noise-exposed and aging cochlea: Primary neural degeneration in acquired sensorineural hearing loss. *Hear Res* 2015;330:191-9

KUJAWSKI OB, POE DS. Laser eustachian tuboplasty. *Otol Neurotol* 2004;25:1–8

KURABI A, BEASLEY KA, CHANG L, MCCANN J, PAK K, RYAN AF. Peptides actively transported across the tympanic membrane: functional and structural properties. *PLoS One* 2017;12:1-17

KURATA K, YAMAMOTO M, TSUKUDA R, SUZUKI T, SATO S. A characteristic of aspiring-induced hearing loss in auditory brainstem response of conscious rats. *J Vet Med Sci* 1997;59:9-15

KUSE H, OGAWA T, NAKAMURA N, NAKAYAMA Y, NAKAKARUMAI A, KOMORI C, TSUDA Y, MATSUSHIMA K, NAKAMURA A, TAMURA K. Changes in auditory brainstem response (ABR) in Kanamycin-induced auditory disturbance in model rats. *J Toxicol Sci* 2011;36:835-841

KUSUNOKI T, CUREOGLU S, SCHACHERN PA, BABA K, KARIYA S, PAPARELLA MM. Age-related pathological changes in the human cochlea: a temporal bone study. *Otolaryngol Head Neck Surg* 2004;131:897-903

LAFOND JF, SHIMOJI M, RAMASWAMY B, SHUKOOR MI, MALIK P, SHAPIRO B, DEPIREUX DA. Middle ear histopathology following magnetic delivery to the cochlea of prednisolone-loaded iron oxide nanoparticles in rats. *Toxicol Pathol* 2018;46:101-106

LANDRY RM, AN D, HUPP JT, SINGH PK, PARSEK MR. Mucin-Pseudomonas aeriginoas interactions promote biofilm formation and antibiotic resistance. *Molecular Microbiology* 2006;59:142-151

LAVIGNE P, LAVIGNE F, SALIBA I. Sustained Inner Ear steroid delivery via bioabsorbable stent: a tolerability and feasibility study on guinea pigs. *Otolaryngol Head Neck Surg* 2016;155:649-53

LEFF S. Bullied children are picked on for their vulnerability. *BMJ* 1999;318:1076

LEHRER RI, GANZ T. Cathelicidins: a family of endogenous antimicrobial peptides. *Curr Opin Hematol* 2002;9:18-22

LEICHTLE A, HERNANDEZ M, PAK K, WEBSTER NJ, WASSERMAN SI, RYAN AF. The Toll-like receptor adaptor TRIF contributes to otitis media pathogenesis and recovery. *BMC Immunol* 2009;10:1-12

LEMKE LE, MCGEE DH, PRIESKORN DM, WALL GM, DOLAN DF, ALTSCHULER RA, MILLER JM. Safety of ciprofloxacin and dexamethasone in the middle ear. *Arch Otolaryngol Head Neck Surg* 2009;135:575-80

LEUNG C, CHIBBA A, GOMEZ-BIAGI RF, NITZ M. Efficient synthesis and protein conjugation of β-(1→6)-D-*N*-acetylglucosamine oligosaccharides from the polysaccharide intercellular adhesion. *Carbohydrate Research* 2009;344:570-575

LI F, YU J, YANG H, WAN Z, BAI D. Effects of Ambroxol on alginate of mature pseudomonas aeruginosa biofilms. *Curr Microbiol* 2008;57:1-7

LIBERMAN MC AND BEIL DG. Hair cell condition and auditory nerve response in normal and noise damaged cochleas. *Acta Otolaryngol* (Stockh) 1979;71:166-76

LIBERMAN MC, KUJAWA SG. Cochlear synaptopathy in acquired sensorineural hearing loss: manifestations and mechanisms. *Hear Res* 2017;349:138-147

LIGHT JP, SILVERSTEIN H. Transtympanic perfusion: indications and limitations. *Curr Opin Otolaryngol Head Neck Surg* 2004;12:378-383

LIN CY, WU JL, SHIH TS, TSAI PJ, SUN YM, MA MC, GUO YL. N-acetyl cysteine against noise induced temporary threshold shift in male workers. *Hear Res* 2010;269:42-49

LIN HW, FURMAN AC, KUJAWA SG, LIBERMAN MC. Primary neural degeneration in the guinea pig cochlea after reversible noise-induced threshold shift. *J Assoc Res Otolaryngol* 2011;12:605-616

LINDEN SK, SUTTON P, KARLSSON NG, KOROLIK V, MCGUCKIN MA. Mucins in the mucosal barrier to infection. *Mucosal Immunol* 2008;1:183-97

LITOVITZ T, SCHMITZ BF. Ingestion of cylindrical and button batteries: an analysis of 2382 cases. *Pediatrics* 1992;89:747-57

LIU H, FENG L, TOLIA G, LIDDELL MR, HAO J, LI SK. Evaluation of intratympanic formulations for inner ear delivery: methodology and sustained release formulation testing. *Drug Dev Ind Pharm* 2014;40:896-903

LUO W, YI H, TAYLOR J, LI JD, CHI F, TODD NW, LIN X, REN D, CHEN P. Cilia distribution and polarity in the epithelial lining of the mouse middle ear cavity. *Sci Rep* 2017;7:45870

MACK D, BECKERB P, CHETTERJEEC I, DOBINSKYA S, KNOBLOCHA JKM, PETERSB G, ROHDEA H, HERRMANNE M. Mechanisms of biofilm formation in *Staphylococcus epidermidis* and *Staphylococcus aureus*: functional molecules, regulatory circuits and adaptive responses. *Int J of Med Microbiol* 2004;294:203-212

MAGUIN K, CAMPO P, PARIETTI-WINKLER C. Toluene can perturb the neuronal volate-dependent Ca^{2+} channels involved in the middle ear reflex. *Toxicol Sci* 2009;107:473-81

MAHENDRASINGHAM S, MACDONALD JA, FURNESS DN. Relative time course of degeneration of different cochlear structures in the CD/1 mouse model of accelerated aging. *JARO* 2011;12:437-453

MANDEL EM, CASSELBRANT ML, ROCKETTE HE, FIREMAN P, KURS-LASKY M, BLUESTONE CD. Systemic steroid for chronic otitis media with effusion in children. *Paediatrics* 2002;110:1071-1080

MANDEL EM, DOYLE WJ, WINTHER B, ALPER CM. The incidence, prevalence and burden of OM in unselected children aged 1-8 years followed by weekly otoscopy through the common cold season. *Int J Pediatr Otorhinolaryngol* 2008;72:491-499

MANLEY GA. Comparative Auditory Neuroscience: Understanding the Evolution and Function of Ears. J Assoc Res Otolaryngol 2017;18:1-24

MARTINES F, BENTIVEGNA D, MAIRA E, SCIACCA V, MARTINES E. Risk factors for otitis media with effusion: case control study in Sicilian schoolchildren. *Int J Pediatr Otorhinolaryngol* 2011;75:754-9

MATSUDA K, UEDA Y, TONO T, HARUTA A, TUYAMA K, KOMUNE S. Increase in glutamate-aspartate transporter (GLAST) mRNA during kanamycin-induced cochlear insult in rats. *Hear Res* 1999;133:10-16

McCall AA, Swan EE, Borenstein JT, Sewell WF, Kujawa SG, McKenna MJ. Drug delivery for treatment of inner ear disease: current state of knowledge. *Ear Hear* 2010;31:156-65

McClure JT and Rosin E. Comparison of amikacin dosing regimens in neutropenic guinea pigs with Escherichia coli infection. *American Journal of Veterinary Research* 1998;59:750-755

Meech RP, Campbell KC, Hughes LP, Rybak LP. A semiquantitative analysis of the effects of cisplatin on the rat stria vascularis. *Hear Res* 1998;124:44-59

Mehraei G, Hickox AE, Bharadwaj HM, Goldberg H, Verhulst S, Liberman MC, Shinn-Cunningham BG. Auditory brainstem response latency in noise as a marker of cochlear synaptopathy. *J Neurosci* 2016;36:3755-64

Melcher JR, Kiang NY. Generator of the brainstem auditory evoked potential in cat.III: Identified cell populations. *Hear Res* 1996;93:52-71

Melino S, Santone C, Di Nardo P, Sarker B. Histatins: salivary peptides with copper(II)- and zinc (II)- binding motifs: perspectives for biomedical applications. *FEBS J* 2014;281;657-72

Metson R, Pletcher SD, Poe DS. Microdebrider eustachian tuboplasty: a preliminary report. *Otolaryngol Head Neck Surg* 2007;136:422–427

MIKULEC AA, HARSTOCK JJ, SALT AN. Permeability of the round window membrane is influenced by the composition of applied drug solutions and by common surgical procedures. *Otol Neurotol* 2008;29:1020-1026

MILLER A, HALL F, AHSAN S. Chronic otitis media with effusion following radiation therapy. *Ear Nose Throat J*. 2016;95:10-11

MILLER BJ, JAAFAR M, ELHASSAN HA. Laser Eustachian tuboplasty for Eustachian tube dysfunction: a case series review. *Eur Arch Otorhinolaryngol* 2017;274:2381-2387

MORATA TC. Study of the effects of simulatenous exposure to noise and carbon disulphide on workers' hearing. *Scand Audiol* 1989;18:53-8

MORATA TC, FIORINI AC, FISCHER FM, COLACIOPPO S, WALLINGFORD KM, KRIEG EF, DUNN DE, GOZZOLI L, PADRÃO MA, CESAR CL. Toluene-induced hearing loss among rotogravure printing workers. *Scand J Work Environ Health* 1997;23:289-98

MRC MULTICENTRE OTITIS MEDIA STUDY GROUP. Adjuvant adenoidectomy in persistent bilateral otitis media with effusion: hearing and revision surgery outcomes through 2 years in the TARGET randomised trial. *Clin Otolaryngol* 2012;37:107-16

MUKHERJEA D, JAJOO S, WHITWORTH C, BUNCH JR, TURNER JG, RYBAK LP, RAMKUMAR V. Short interfering RNA against transient receptor potential vanilloid 1 attentuates cisplatin-induced hearing loss in the rat. J Neurosci 2008;28:13056-65

MULHERAN M, DEGG C, BURR S, MORGAN DW, STABLEFORTH DE. Occurence and risk of cochleotoxicity in cystic fibrosis patients receiving repeated high-dose aminoglycoside therapy. *Antimicrob Agents Chemotherap* 2001;45:2502-2509

MÜNKER G. Inner ear hearing loss in acute and chronic otitis media. *Adv Otorhinolaryngol* 1981;27:138-43

MURAKAMI S, SOTSU M, NAKAMURA N. Circadian variation in the latency of auditory brainstem response *No To Shinkei* 1992;44:615-20

MURILLO-CUESTA S, CONTRERAS J, CEDIEL R, VARELA-NIETA I. Comparison of different aminoglycoside antibiotic treatments to refine ototoxicity studies in adult mice. *Lab Anim* 2009; 009046

MURPHY TF, KIRKHAM C. Biofilm formation by non typeable Haemophilus influenza: strain variability, outer membrane antigen expression and role of pili. *BMC Microbiol* 2002;2:7

MUSICANT AD, CHAN JC, HIND JE. Direction dependant spectral properties of cat external ear: new data and cross-species comparisons. *J Acoustic Soc Am* 1990; 87:757-781

MUTHAIAH VPK, CHEN GD, DING D, SALVI R, POTH JA. Effect of manganese and manganese plus noise on auditory function and cochlear structures. *Neurotoxicology* 2016;55:65-73

NADELL CD, XAVIER JB, LEVIN SA, FOSTER KR. The Evolution of Quorum sensing in bacterial biofilms. PLoS Biol 2008;6:e14.doi:10.1371/journal.pbio.0060014

NATIONAL INSTITUTE OF CLINICAL EXCELLENCE OME Guidelines 2008

NEILSON LJ, HUSSAIN SS. Management of granular myringitis: a systemic review. *J Laryngol Otol* 2008;122:3-10

NEKRASSOV V, SITGES M. Vinpocetine protects from aminoglycoside antibiotic-induced hearing loss in guinea pig *in vivo*. Brain Res 2000;868:222-9

NEUT D, VAN DER MEI HC, BULSTRA SK, BUSSCHER HJ. The role of small-colony variants in failure to diagnose and treat biofilm infections in orthopaedics. *Acta Orthopaedica* 2007;78:299-308

NGAN EM, MAY BJ. Relationship between the auditory brainstem response and auditory nerve thresholds in cats with hearing loss. *Hear Res* 2001;156:44-52

NIELSEN AT, TOLKER-NIELSEN T, BARKEN KB, MOLIN S. Role of commensal relationships on the spatial structure of a surface-attached microbial consortium. *Environ Microbiol* 2000:2:59-68

NISTICO L, KREFT R, GIESEKE A, COTICCHIA JM, BURROWS A, KHAMPANG P, LIU Y, KERSCHNER JE, POST JC, LONERGAN S, SAMPATH R, HU FZ, EHRLICH GD, STOODLEY P, HALL-STOODLEY L. Adenoid reservoir for pathogenic biofilm bacteria. *J Clin Micro* 2011;49:1411-1420

NORDMANN AS, BOHNE BA, HARDING BW. Histopathological differences between temporary and permanent threshold shift. *Hear Res* 2000;139:13-30

NOZAWA N, IMAMURA S, FUJIMORI I, HASHIMOTO K, SHIMOMURA S, HISAMATSU K, MURAKAMI Y. Age-related alterations in the auditory brainstem responses and the compound action potentials in guinea pigs. *Laryngoscope* 1998;106:1034-9

OBRINGER E, CHEN JL. Acute mastoiditis caused by *Streptococcus pneumoniae*. *Pediatr Ann* 2016;45:e176-9

O'CONNOR KN, CAI H, PURIA S. The effects of varying tympanic-membrane material properties on human middle-ear sound transmission in a three-dimensional finite-element model. *J Acoust Soc Am* 2017;142:2836

OHASHI Y, NAKAI Y. Current concepts of mucociliary dysfunction in otitis media with effusion. *Acta Otolaryngol Suppl* 1991;486:149-61

OISHI N, KENDALL A, SCHACHT J. Metformin protects against gentamicin-induced hair cell death *in vitro* but not ototoxicity *in vivo*. *Neur Let* 2014;583:65-69

OTTO AC, BROWN RD, GAGE-WHITE L, HUPETZ S, ANNIKO M, PENNY JE, HENLEY CM. Effects of cisplatin and thiosulfate upon auditory brainstem responses of guinea pigs. *Hear Res* 1988;35:79-86

PALUCH-OLES J, MAGRYS A, KOZIOL-MONTEWAKA M, NIEDZIELSKI A, NIEDZWIADEK J, NIEDZIELSKA G, KOTOWSKI M. The phenotype and genetic biofilm formation characteristics of coagulase-negative *Staphlococci* isolates in children with otitis media. *Int J Pediatr Otorhinolaryngol* 2011;75:126-130

PARADISE JL, ROCKETTE HE, COLBORN DK, BERNARD BS, SMITH CG, KURS-LASKY M, JANOSKY JE. Otitis media in 2553 Pittsburgh-area infants: prevalence and risk factors during the first two years of life. *Paediatrics* 1997:99;318-333

PARISA A, REZA NA, JALAL SS, MOHAMMAD K, HOMA ZK. Horizontal localization in simulated unilateral hearing loss. *J Audiol Otol* 2017;22:39-44

PARSEK MR, SINGH PK. Bacterial biofilms: an emerging link to disease pathogenesis. *Ann Rev Microbiol* 2003;57:677-701

PASSALI D, BELLUSSI L, MASIERI S. Transtympanic Iontophoresis: personal experience. *Laryngoscope* 1984;94:802-806

PAU HW. Does balloon dilatation represent a breakthrough for Eustachian tube disorders - even in children? *HNO* 2015;63:681-2

PAWLOWSKI KS, SI E, WRIGHT CG, KOULICH E, HOSSEINI K, ROLAND PS. Ototoxicity of topical azithromycin solutions in the guinea pig. *Arch Otolaryngol Head Neck Surg* 2010;136:481-7

PEARSON MM, LAURENCE CA, GUINN SE, HANSEN EJ. Biofilm formation by *Moraxella catarrhalis* in vitro: roles of UspaA1 adhesin and the Hag hemagglutinin*. Infect Immun.* 2006;74:1588-96

PEDRERO-ESCALAS MF, JIMENEZ-ANTOLIN J, LASSALETTA L, DIAZ-SAEZ G, GAVILÁN J. Hospital clinical trial: Homeopathy (Agraphis nutans 5CH, Thuya occidentalis 5CH, Kalium Muriaticum 9CH and Arsenicum iodatum 9CH) as adjuvant, inchildren with otitis media with effusion*. Int J Pediatr Otorhinolaryngol* 2016;88:217-23

PERTOVAARA A, HAAPALINNA A, SIRVIÖ J, VIRTANEN R. Pharmacological properties, central nervous system effects and potential therapeutic applications of atipamezole , a selective alpha 2 adrenoceptor antagonist. *CNS Drug Reviews* 2005;11:273-88

PICHICHERO ME, REED MD. Variations in amoxicillin pharmoacokinetic/ pharmacodynamic parameters may explain treatment failures in acute otitis media. *Paediatr. Drugs* 2009;11:243-249

PIERI L, SCHAFFNER R, SCHERSCHLICHT R, POLC P, SEPINWALL J, DAVIDSON A, MOHLER H, CUMIN R, DA PRADA M, BURKARD WP, KELLER HH, MULLER RK, GEROLD M, PIERI M, COOK L, HAEFELY W. Pharmacology of midazolam Arzneimittelforschung 1981;31:2180-201

PINILLA M, RAMIREZ-CAMACHO R, JORGE E, TRINIDAD A, VERGARA J. Ventral approach to the rat middle ear for otologic research. *Otolaryngology Head and Neck Surgery* 2001;124:515-517

PITKÄRANTA A, JERO J, ARRUDA E, VIROLAINEN A, HAYDEN FG. Polymerase chain reaction-based detection of rhinovirus, respiratory syncytial virus and coronavirus in otitis media with effusion. *J Pediatr* 1998;133:390-4

PIU F, WANG X, FERNANDEZ R, DELLAMARY L, HARROP A, YE Q, SWEET J, TAPP R, DOLAN DF, ALTSCHULER RA, LICHTER J, LEBEL C. OTO-104: a sustained release dexamethasone hydrogel for the treatment of otic discorders. *Otol Neurotol* 2011;32:171-9

PLONTKE SK, MYNATT R, GILL RM, BORGMANN S, SALT AN. Concentration gradient along the scala tympani after local application of gentamicin to the round window membrane. *Laryngoscope* 2007;117:1191-8

PLONTKE SK, LOWENHEIM H, MERTENS J, ENGEL C, MEISNER C, WEIDNER A, ZIMMERMANN R, PREYER S, KOITSCHEV A, ZENNER HP. Randomized, double blind placebo controlled trial on the safety and efficacy of continuous intratympanic dexamethasone delivered via a round windowcatheter for severe to profound idiopathic sensorineural hearing loss after failure of systemic therapy. *Laryngoscope* 2009;119:359-369

POIRRIER AL, VAN DEN ACKERVEKEN P, KIM TS, VANDENBOSCH R, NGUYEN L, LEFEBVRE PP, MALGRANGE B. Ototoxic drugs: a difference in sensitivity between mice and guinea pigs. *Toxicol Lett* 2010;193:41-9

POST JC, HILLER NK, NISTICO L, STOODLEY P, ERLICH GD. The role of biofilms in otolaryngologic infections: update 2007. *Curr Opin Otolaryngol Head Neck Surg* 2007;15:347-51

POST JC, STOODLEY P, HALL-STOODLEY L, EHRLICH GD. The role of biofilms in otolaryngologic infections. *Curr Opin Otolaryngol Head Neck Surg* 2004; 12:185-90

PREYER S, HEMMERT W, ZENNER HP, GUMMER AW. Abolition of the receptor potential response of isolated mammalian outer hair cells by hair bundle treatment with elastase: a test of the tip link hypothesis. *Hear Res* 1995;89: 187-193

QUREISHI , LEE Y, BELFIELD K, BIRCHALL JP, DANIEL M. Update on otitis media – prevention and treatment. *Infect Drug Resist* 2014;10:15-24

RAMASWAMY B, ROY S, APOLO AB, SHAPIRO B, DEPIREUX DA. Magnetic nanoparticle mediated steroid delivery mitigates cisplatin induced hearing loss. *Front Cell Neurosci* 2017;11:268

RANDRUP TS, OVESEN T. Balloon Eustachian tuboplasty: a systemic review. *Otolaryngol Head Neck Surg* 2015;152:383-92

RASK-ANDERSEN H, SCHART-MORÉN N, STRÖMBÄCK K, LINTHICUM F, LI H. Special Anatomic Considerations in Otosclerosis Surgery. *Otolaryngol Clin North Am* 2018;51:357-374

RAUCH SD, HAPLIN CF, ANTONELLI PJ, BABU S, CAREY JP, GANTZ BJ, GOEBEL JA, HAMMERSCHLAG PE, HARRIS JP, ISAACSON B, LEE D, LINSTROM CJ, PARNES LS, SHI H, SLATTERY WH, TELIAN SA, VRABEC JT, REDA DJ. Oral vs intratympanic corticosteroid therapy for idiopathic sudden sensorineural hearing loss: a randomized trial. *JAMA* 2011;305:2071-9

RAVI R, SOMANI SM, RYBAK LP. Mechanism of cisplatin ototoxicity: antioxidant system *Pharmacol Toxicol* 1995;76:386-394

RAYNER MG, ZHANG Y, GORRY MC, CHEN Y, POST JC, EHRLICH GD. Evidence of bacterial metabolic activity in culture negative otitis media with effusion. *JAMA* 1998;279:296-9

REBERT CS, BECKER E. Effects of inhaled carbon disulphide on sensory-evoked potentials of Long-Evans rats. *Neurobehav Toxicol Teratol* 1986;8:533-41

REDDY MS, MURPHY TF, FADEN HS, BERNSTEIN JM. Middle ear mucin glycoprotein: purification and interaction with nontypable *Haemophilus influenza* and *Moraxella catarrhalis*. *Otolaryngol Head Neck Surg* 1987;116:175-80

REHG JE. Cecal toxin(s) from guinea pigs with clindamycin-associated colitis, neutralized by Clostridium sordelli antitoxin. *Infect Immun* 1980;27:387-90

RICE DC, GILBERT SG. Exposure to methyl mercury from birth to adulthood impairs high-frequency hearing in monkeys. *Toxicol Appl Pharmacol* 1992;115:6-10

ROSE AS, PRAZMA J, RANDELL SH, BAGGETT HC, LANE AP, PILLSBURY HC. Nitric oxide mediates mucin secretion in endotoxin-induced otitis media with effusion. *Otolaryngol Head Neck Surg* 1997;116:308-16

ROSENFELD RM, POST JC. Meta –analysis of antibiotics for the treatment of otitis media with effusion. *Otolaryngology and Head and Neck Surgery* 1992;106:378-86

ROSENFELD RM, SCHWARTZ SR, CANNON CR, ROLAND PS, SIMON GR, KUMAR KA, HUANG WW, HASKELL HW, ROBERTSON PJ. Clinical practice guideline: acute otitis externa. Clinical practice guideline: acute otitis externa. Otolaryngol Head Neck Surg 2014;150:S1-S24

ROVERS MM, STRAATMAN H, ZIELHUIS GA, INGELS K, VAN DER WILT GJ. Seasonal variation in the prevalence of persistent otitis media with effusion in one-uear-old infants. Paediatr Perinat Epidemiol 2000;14:268-74

RUEBHAUSEN MR, BROZOSKI TJ, BAUER CA. A comparison of the effects of isoflurane and ketamine anaesthesia on auditory brainstem response (ABR) thresholds in rats. *Hear Res* 2012;287:25-9

RUSSELL JD, GILES SJ. Persistend otitis media with effusion: a new experimental model. Laryngoscope 1998;108:1181-4

RUSSELL WMS, BURCH RL. The principles of humane experimental technique 1959

RYBAK LP, RAVI R AND SOMANI SM. Mechanism of protection by diethyldithiocarbamate against cisplatin ototoxicity: Antioxidant system. *Fundam Appl Toxicol* 1995;26:293-300

RYBAK LP, RAMKUMAR V. Ototoxicity mini review. *Kidney Int* 2007;72:931-935

RYBAK LP, WHITWORTH CA, MUKHERJEA D, RAMKUMAR V. Mechanisms of cisplatin induced ototoxicity and prevention. *Hear Res* 2007; 226: 157–167.

SAAFAN ME, IBRAHIM WS, TOMOUM MO. Role of adenoid biofilm in chronic otitis media with effusion in children. *Eur Arch Otorhinolaryngol* 2012;270:2417-25

SACHSER N, LICK C, STANZEL K. The environment, hormones and aggressive behaviour: A 5 year study in guinea pigs. *Psychoneuroendocrinology* 1994;19:697-707

SADE J. Middle ear mucosa. *Arch Otolaryngol* 1966;84:137-143

SALIH WH, BUYTAERT JA, AERTS JR, VANDERNIEPEN P, DIERICK M, DIRCKX JJ. Open access high-resolution 3D morphology models of cat, gerbil, rabbit rat and human ossicular chains. *Hear Res* 2001;284:1-5

SALT AN, MA Y. Quantification of solute entry into cochlear perilymph through the round window membrane. *Hear Res* 2001;154:88–97

SALT AN, KING EB, HARSTOCK JJ, GILL RM, O'LEARY SJ. Marker entry into vestibular perilymph via the stapes following application to the round window niche of guinea pigs. *Hear Res* 2012;283:14-23

SALT AN, PLONTKE SK. Endolymphatic hydrops: pathophysiology and experimental models. *Otolaryngol Clin North Am* 2010;43:971-983

SALT AN, PLONTKE SK. Endolymphatic hydrops: pathophysiology and experimental models. *Otolaryngologic Clinics of North America.* 2010;43:971-83

SAMELLI AG, RONDON-MELO S, RABELO CM, MOLINI-AVEJONAS DR. Association between language and hearing disorders- risk identification. *Clinics (Sao Paulo).* 2017;72:213-217

SANTOS F, NADOL JB. Temporal bone histopathology of furosemide ototoxicity. *Laryngoscope Investig Otolaryngol* 2017;25:204-207

SANTOS PM, HALL RA, SNYDER JM, HUGHES LF, DOBIE RA. Diuretic and diet effect on Ménière's disease evaluated by the 1985 committee on Hearing and Equilibrium Guidelines. *Otolaryngol Head Neck Surg* 1993;109:680-689

SASSEN ML, BRAND H, GROTE JJ. Risk factors for otitis media with effusion in children 0-2 years of age. *Am J Otolaryngol* 1997;18:324-30

SENSI P. History of the development tof rifampicin. *Rev Infect Dis* 1983; 5 Suppl 3: S402-6

SCHACHT J, WEINER N. Aminoglycoside-induced hearing loss: a molecular hypothesis. *ORL Journal for Oto-rhino-laryngology and its related species* 1986;48:116-23

SCHILDER AG, CHONMAITREE T, CRIPPS AW, ROSENFELD RM, CASSELBRANT ML, HAGGARD MP, VENEKAMP RP. Otitis Media. *Nat Rev Dis Primers* 2016;8:16063

SCHILDER AG, MAROM T, BHUTTA MF, CASSELBRANT ML, COATES H, GISSELSSON-SOLEN, HALL AJ, MARCHISIO P, RUOHOLA A, VENEKAMP RP, MANDEL EM. Panel 7: Otitis Media: Treatment and complications. *Otolaryngol Head Neck Surg* 2017;156:S88-S105

SCHUBERT ML. Gastric secretion. *Curr Opin Gastroenterol* 2014;30:578-82

SCHUKNECHT HF. Pathophysiology of endolymphatic hydrops. *Arch Otorhinolaryngol* 1976;212:253-62

SCHUKNECHT HF, GACEK MR. Cochlear pathology in presbyacusis. *Ann Otol Rhinol Laryngol* 1993;102:1-16

SCHUMANN K, GUENTHER A, JEWGENOW K, TRILLMICH F. Animal Housing and welfare: effects of housing conditions on body weight and cortisol in a medium sized rodent (*Cavia Aperea*). *J Appl Anim Welf Sci*

SCOTTISH INTERCOLLEGIATE GUIDELINES NETWORK (SIGN). *Diagnosis and management of Childhood Otitis Media in Primary Care.* Scottish intercollegiate guidelines network, Edinburgh 2006; 66

SELVADURI DK, ETHERIDGE S, JONES P, MULHERAN M, COOK JA. Pharmacological protection of auditory function against noise and hypoxia with MK 801. *Clin Otolaryngol Allied Sci* 2000;25:570-6

SHAPIRO B, DORMER K, RUTEL IB. A two-magnet system to push therapeutic nanoparticles. *AIP Conf Proc.* 2010;1311:77-88

SHAPIRO B, KULKARNI S, NACEV A, SARWAR A, PRECIADO D, DEPIREUX DA. Shaping magnetic fields to direct therapy to ears and eyes. *Annu Rev Biomed Eng* 2014;16:455-81

SHAPRIO GG, BIERMAN CW, FURUKUWA CT. Treatment of persistent Eustachian tube dysfunction with aerosolized nasal dexamethasone versus placebo. *Annals of Allergy* 1982;49:81-5

SHEA PF, RICHEY PA, WAN JY, STEVENS SR. Hearing results and quality of life after streptomycin/dexamethasone perfusion for Ménière's disease. *Laryngoscope* 2012;122:204-211

SHETH S, MUKHERJEA D, RYBAK LP, RAMKUMAR V. Mechanisms of cisplatin-induced ototoxicity and otoprotection. *Front Cell Neurosci* 2017;11:338

SHULMAN A, GOLDSTEIN B. Intratympanic drug therapy with steroids for tinnitus control: a preliminary report. *Int Tinnitus J* 2000;6:10-20

SIMPSON SA, LEWIS R, VAN DER VOORT J, BUTLER CC. Oral or topical nasal steroids for hearing loss associated with otitis media with effusion in children. *Cochrane Database of Systemic Reviews* 2011, Issue 5. Art No: CD001935

SINCLAIR MD. A review of the physiological effects of alpha 2-agonists related to the clinical use of medetomidine in small animal practice. *Can Vet J* 2003;44:885-97

SINWAT P, WU WJ, SHA SH, SCHACHT J. Protection from ototoxicity of intraperitoneal gentamicin in guinea pig. *Kidney Int* 2000;58:2525-32

SLINGER R, CHAN F, FERRIS W ET AL. Multiple combination antibiotic susceptibility testing of nontypable *Heamophilus Influenze* biofilms. *Diagn Microbiol Infec Dis* 2006;56:247-53

SLINGER R, DUVAL M, LANGILL J, BROMWICH M, MACCORMICK J, CHAN F, VACCANI JP. Direct molecular detection of a broad range of bacterial and viral organisms and *Streptococcus pneumonia* vaccine serotypes in children with otitis media with effusion. *BMC Res Notes* 2016;9:247

SLOB AK, VREEBURG JT, VAN DER WERFF TEN BOSCH JJ. Body growth, puberty and undernutrition in the male guinea pig. *Br J Nutr* 1979;41:231-7

SMIEJA M. Current indications for the use of clindamycin : A critical review. *Can J Infect Dis* 1998;9:22-28

SMITH A, BUCHINSKY FJ, POST JC. Eradicating chronic ear, nose and throat infections: a systemically conducted literature review of advances in biofilm treatment. *Otolaryngol Head Neck Surg* 2011;144:338-47

SMITH SJ, RAHMAN CV, CLARKE PA, RITCHIE AA, GOULD TW, WARD JH, SHEKESHEFF KM, GRUNDY RG, RAHMAN R. Surgical delivery of drug releasing poly(lactic-co-glycolic acid)/poly(ethylene glycol) paste with in vivo effects against glioblastoma. *Ann R Coll Surg Engl* 2014;96:495-501

SOLZBACHER D, HANISCH FG, VAN ALPHEN L, GILSDORF JR, SCHROTEN H. Mucin in middle ear effusions inhibits attachment of *Haemophilus influenza* to mucosal epithelial cells. *Eur Arch Otorhinolaryngol* 2003;260:141-7

SONG BB, ANDERSON DJ, SCHACHT J. Protection from gentamicin ototoxicity by iron chelators in guinea pig *in vivo*. *J Pharmacol Exp Ther* 1997;282:369-77

SOULI M, GIAMARELLOU H. Effects of slime produced by clinical isolates of coagulase-negative *Staphylococci* on activities of various microbial agents. *Antimicrob Ag Chemother* 1998:42;939-941

SPICER SS, GRATTON MA, SCHULTE BA. Expression patterns of ion transport enzymes in spiral ligament fibrocytes change in relation to strial atrophy in the aged gerbil cochlea. *Hear Res* 1997;111:93-102

SPOENDLIN H. Primary structural changes in the organ of Corti after acoustic overstimulation. *Acta Otolaryngol (Stockh)* 1971;71:166-76

STARNER TD, SHROUT JD, PARSEK MR, APPELBAUM PC, KIM G. Subinhibitory concentrations of azithromycin decrease nontypable. *Haemophilus influenzae* biofilm formation and diminish established biofilms. *Antimicrob Agents Chemother* 2008;52:137-45

STEVENS SM, BROWN LN, EZELL PC, LANG H. The mouse round-window approach for ototoxic agent delivery: a rapid and reliable technique for inducing cochlear cell degeneration. *J Vis Exp* 2015;105:53131

STRONKS HC, AARTS MC, KLIS SF. Effects of isoflurane on auditory evoked potentials in the cochlea and brainstem of guinea pigs. *Hear Res* 2010;260:20-9

STYPULKOWSKI PH. Mechanisms of salicylate ototoxicity. *Hear Res* 1990;46:113-45

SUGAWARA M, CORFAS G, LIBERMAN MC. Influence of supporting cells on neuronal degeneration after hair cell loss. *J Assoc Res Otolaryngol* 2005;6:136-147

SUGIMOTO S, OKUDA K, MIYAKAWA R, SATO M, ARITA-MORIOKA K, CHIBA A, YAMANAKA K, OGURA T, MIZUNOE Y, SATO C. Imaging of bacterial multicellular behavious in biofilms in liquid by atmospheric scanning electron microscopy. *Sci Rep* 2016;6:25889

SURYANARAYANAN R, SRINIVASAN VR, O'SULLIVAN G. Transtympanic gentamicin treatment using Silverstein MicroWick in Meniere's disease. *J Laryngol Otol* 2009;123:45-49

SZYMANSKI A, BHIMJI SS. *Anatomy, Head, Ear.* StatPearls Publishing; 2018

SZYMANSKI MD, BAIN DE, KIEHL K, PENNINGTON S, WONG S, HENRY KR. Killer whale (orcinus orca) hearing: auditory brainstem response and behavioural audiograms. *J Acoust Soc Am* 1999;106:112005;11534-41

TAKAHASHI H, TANAKA R, SEKIHARA Y, HONDO H. Auditory brainstem response during systemic hyperthermia. *Int J Hyperthermia* 1991;7:613-20

TAKEUCHI K, MAJIMA Y, HIRATA K, HATTORI M, SAKAKURA Y. Quantification of tubotympanal mucociliary clearance in otitis media with effusion. *Ann Otol Rhinol Laryngol* 1990;99:211-4

TAMURA T, KITA T, NAKAGAWA T, ENDO T, KIM TS, ISHIHARA T, MIZUSHIMA Y, HIGAKI M, ITO J. Drug delivery to the cochlea using PLGA nanoparticles. *Laryngoscope* 2005:115:2000-5

TASKER A, DETTMAR PW, PANETTI M, KOUFMAN JA, BIRCHALL JP, PEARSON JP. Reflux of gastric juice and glue ear in children *Lancet* 2002;359:493

TAWACKOLI W, CHEN GD, FECHTER LD. Disruption of cochlear potentials by chemical asphyxiants. Cyanide and carbon monoxide. *Neurotoxicol Teratol* 2001;23:157-65

TAWFIK SA, IBRAHIM AA, TALAAT IM, EL-ALKAMY SS, YOUSSEF A. Role of bacterial biofilm in development of middle ear effusion. *Eur Arch Otorhinolaryngol* 2016;273:4003-4009

TOLKER-NIELSEN T, BRINCH UC, RAGAS PC, ANDERSEN JB, JACOBSEN CS, MOLIN S. Development and dynamics of Pseudomonas sp. Biofilms. *J Bacteriol* 2000;182:6482-9

TOS M. Pathogenesis and pathology of chronic secretory otitis media. *Ann Otol and Rhinol Laryngol Supp*. 1980:89:91-7

TOS M, POULSON G, BORCH J. Etiologic factors in secretory otitis. *Arch Otolaryngol* 1979;105:582-588

TROPITZSCH A, ARNOLD H, BASSIOUNI M, MULLER A, ECKHARD A, MULLER M, LOWENHEIM H. Assessing cisplatin induced ototoxicity and otoprotection in whole organ culture of the mouse inner ear in simulated microgravity. *Toxicol Let* 2014; 227:203-212

TRAVIS SM, CONWAY BA, ZABNER J, SMITH JJ, ANDERSON NN, SINGH PK, GREENBERG EP, WELSH MJ. Activity of abundant antimicrobials of the human airway. *Am J Respir Cell Mol Biol* 1999;20:872-9

TRULL FL. More Regulation of Rodents. *Science* 1994;284: 1463

TURNER JG, PARRISH JL, CASPARY DM. Hearing in laboratory animals: strain differences and nonauditory effects of noise. *Comp Med* 2005; 55:12-23

UBELL ML, KHAMPAMG P, KERSCHNER JE. Mucin gene polymorphism in otitis media patients. *Laryngoscope* 2010;120:132-138

UNDERWOOD M, BAKALETZ L. Innate immunity and the role of defensins in otitis media. *Curr Allergy Asthma Rep*. 2011;11:499-507

VAN BEETHOVEN L. The Heiligenstadt testament 1802. English translation in: The Beethoven Compendium: A Guide to Beethoven's Life and Music, edited by B. Cooper. New York: Thames and Hudson, 1991

VAN HOECKE H, DE PAEPE AS, LAMBERT E, VAN BELLEGHEM JD, COOLS P, CAN SIMAEY L, DESCHAGHT P, VANEECHOUTTE M, DHOOGE I. Haemophilus influenza biofilm formation in chronic otitis media with effusion. *Eur Arch Otorhinolaryngol* 2016;273:3553-3560

VAN ROZENDAAL BA, VAN GOLDE LM, HAAGSMAN HP. Localization and functions of SP-A and SP-D at mucosal surfaces. *Pediatr Pathol Mol Med* 2001;20:319-39

VAN RUIJVEN MW, DE GROOT JC, KLIS SF, SMOORENBURG GF. The cochlear targets of cisplatin: an electrophysiological and morphological time-sequence study. *Hear Res* 2005;205:241-248

VAN WIJCK F, STEACKER H, LEFEBVRE PP. Topical steroid therapy using the Silverstein Microwick in sudden sensorineural hearing loss after failure of conventional treatment. *Acta Otolaryngol* 2007;127:1012-1017

VARSAK YK, SANTA MARIA PL. Mouse model of experimental Eustachian tube occulation: a surgical technique. *Acta Otolaryngol* 2016;136:12-7

VASCONCELOS KA, FROTA SMMC, RUFFINO-NETTO A, KRITSKI AL. The importance of audiometric monitoring in patients with multidrug resistant tuberculosis. *Rev Soc Bras Med Trop* 2017;50:646-651

VENEKAMP RP, BURTON MJ, VAN DONGEN TM, VAN DER HEJDEN GJ, VAN ZON A, SCHILDER AG. Antibiotics for otitis media with effusion in children. Cochrane Database Syst Rev 2016;CD009163

VAN ZON A, VAN DER HEIJDEN GJ, VAN DONGEN TM, BURTON MJ, SCHILDER AG. Antibiotics for otitis media with effusion in children. Cochrane Database Syst Rev 2012;CD009163

WALKER RE, BARTLEY J, FLINT D, THOMPSON JMD, MITCHELL EA. Determinants of chronic otitis media with effusion in preschool children: a case-control study. *BMC Pediatr* 2017;17:4

WANG DE, LAM DJ, BELLMUNT AM, ROSENFELD RM, IKEDA AK, SHIN JJ. Intranasal steroid use for otitis media with effusion: ongoing opportunities for quality improvement. *Otolaryngol Head Neck Surg* 2017;157:289-296

WANG X, FERNANDEZ R, TSIVKOVSKAIA N, HARROP-JONES A, HOU HJ, DELLAMARY L, DOLAN DF, ALTSCHULER RA, LEBEL C, PIU F. OTO-201: nonclinical assessment of a sustained-release ciprofloxacin hydrogel for the treatment of otitis media. *Otol Neurotol* 2014;35:459-69

WARREN RL, RAMAMOORTHY S, CIGANOVIĆ N, ZHANG Y, WILSON TM, PETRIE T, WANG RK, JACQUES SL, REICHENBACH T, NUTTALL AL, FRIDBERGER A. Minimal basilar membrane motion in low-frequency hearing. *Proc Natl Acad Sci USA* 2016;26:113

WÄSTERSTRÖM SA, BREDBERG G, LINDQUIST NG, LYTTKENS L, RASH-ANDERSEN H. Ototoxicity of kanamycin in albino and pigmented guinea pigs: a morphologic and electrophysiologic study. *Am J Otol* 1986;7:11-8

WEBSTER P, WU S, GOMEZ G, APICELLA M, PLAUT AG, ST GEME 3RD JW. Distribution of bacterial proteins in biofilms formed by non-typable *Haemophilus influenza. J Histochem cytochem* 2006;54:829-42

WENZEL GI, WARNECKE A, STÖVER T, LENARZ T. Effects of extracochlear gacyclidine perfusion on tinnitus in humans: a case series. *Eur Arch Otorhinolaryngol* 2010;267:691-699

WIERZBICKA M, PUSZCZEWICZ M, BARTOCHOWSKA A, SZYFTER W. The otologic manifestation of Wegener's granulomatosis-review of contemporary achievements in diagnostics and treatment. *Otolaryngol Pol* 2012;66:254-8

WILLIAMSON I, BENGE S, BARTON S, PETROU S, LETLEY L, FASEY N, HAGGARD M, LITTLE P. A double-blind randomised placebo-controlled trial of topical intranasal corticosteroids in 4 to 11 year old children with persistent bilateral otitis media with effusion in primary care. *Health Technol Assess* 2009;13:1-144

WILLIAMSON I. Otitis media with effusion in children. Clin Evid (Online) 2011;12:0502

WILMOTT JF, VANDENBOSCHE J, SHIMIZU T, DING DL, SALVI R. Effects of exposing C57BL/6Jmice to high- and low-frequency augmented acoustic environments: auditory

brainstem response thresholds. Cytocochleograms, anterior nucleus morphology and the role of gonadal hormones. Hear Res 2008;235:60-71

WILSON WR, BYL FM, LAIRD N. The efficacy of steroids in the treatment of idiopathic sudden hearing loss. A double-blind clinical study. *Arch Otolaryngol* 1980;106:772-6

WITHNELL RH, GOWDY LE. An analysis of the acoustic input impedance of the ear. *J Assoc Res Otolaryngol* 2013;14:611-22

WOODFORD N, LIVERMORE DM. Infections caused by gram-positive bacteria: a review of the global challenge. *J Infect* 2009;59:S4-16

WHO. Treatment of TB guidelines. 2010 ISBN 978-92-4-154783-3

WYSOCKI J. Topographical anatomy of the guinea pig temporal bone. *Hear Res* 2005;199:103-10

XIA L, CHEN Z, SU K, YIN S, WANG J. Comparison of cochlear cell death caused by cisplatin, alone and in combination with furosemide. *Toxicol Pathol* 2014;42:376-385

XIA L, CHEN Z, YIN S. Ototoxicity of cisplatin administered to guinea pigs via the round window membrane*. J Toxicol Soc* 2012; 37:823-30

XIONG M, HE Q, WANG J. Oxidative stress in spiral ganglion cells of pigmented and albino guinea pigs exposed to impulse noise. *Acta Otolaryngol* 2011;131:914-20

XU Q, KAUR R, CASY JR, ADLOWITZ DG, PICHICHERO ME, ZENG M. Identification of streptococcus pneumonia and Haemophilus influenza in culture-negative middle ear

fluids from children with acute otitis media by combination of multiplex PCR and multilocus sequencing typing. *Int J Pediatr Otorhinolaryngol* 2011;75:239-44

YAMAMOTO M, KURATA Y, CHIBA S. Effects of aminoglycoside antibiotics on the auditory brainstem response and post rotatory nystagmus in rats. *Fundam Appl Toxicol* 1992;18:499-503

YAMAMURA K, TERAYAMA K, YAMAMOTO N, KOHYAMA A, KISHI R. Effects of acute lead acetate exposure on adult guinea pigs: electrophysiological study of the inner ear. *Fundam Appl Toxicol* 1989;13:509-15

YANG R, SABHARWAL V, OKONKWO OS, SHLYKOVA N, TONG R, LIN LY, WANG W, GUO S, ROSOWSKI JJ, PELTON SI, KOHANE DS. Treatment of otitis media by transtympanic delivery of antibiotics. *Sci Transl Med* 2016;8:356

YIN H, KANASTY RL, ELTOUKHY AA, VEGAS AJ, DORKIN JR, ANDERSON DG. Non-viral vectors for gene based therapy. *Nat Rev Genet* 2014;15:541-555

YLIKOSKI J. Guinea pig hair cell pathology from ototoxic antibiotics. *Acta Otolaryngol (Stockh)* 1974; Suppl 326:5-22

YOO MH, CHO YS, CHOI J, CHOUNG YH, CHUNG JH, CHUNG JW, HAN GC, JEON EJ, JUN BC, KIM DK, KIM KS, LEE JH, LEE KY, LEE SH, MOON IS, PARK HJ, PARK SN, RHEE J, SEO JH, YEO SG. Microbiological results fom middle ear effusion in pediatric patients receiving ventilation tube insertion; multicentre registry study on the effectiveness of

ventilation tube insertion in pediatric patients with chronic otitis media with effusion: part 1. *Clin Exp Otorhinolaryngol* 2018;28:21053

YOON JY, YANG KJ, PARK SN, KIM DK, KIM JD. The effect of dexamethasone/cell penetrating peptide nanoparticles on gene delivery for inner ear therapy. *Int J Nanomedicine* 2016;11:6123-6134

YORGASON JG, LUXFORD W, KALINEC F. *In vitro* and *in vivo* models of drug ototoxicity: studying the mechanisms of a clinical problem. *Expert Opin Drug Metab Toxicol* 2011;7:1521-34

YOSHIOKA M, NAGANAWA S, SONE M, NAKATA S, TERANISHI M, NAKASHIMA T. Individual differences in the permeability of the round window: evaluating the movement of intratympanic gadolinium into the inner ear. *Otol Neurotol* 2009;30:645-648

ZERNOTTI ME, PAWANKAR R, ANSOTEGUI I, BADELLINO H, CROCE JS, HOSSNY E, EBISAWA M, ROSARIO N, BORGES MS, ZHANG Y, ZHANG L. Otits media with effusion and atopy: is there a causal relationship? World Allergy Organ J 2017;10:37

ZHANG X, CHEN G, WEN L, YANG F, SHAO AL, LI X, LONG W, MU L. Novel multiple agents loaded PLGA nanoparticles for brain delivery via inner ear administration : in vitro and in vivo evaluation. *Eur J Pharm Sci* 2013;48:595-603

ZHAO S, ZHAO J, DONG S, HUANGFU X, LI B, YANG H, ZHAO J, CUI W. Biological augmentation of rotator cuff repair using bFGF-loaded electrospun poly (lactide-co-glycolic) fibrous membranes. *Int J Nanomedicine* 2014;14:2373-85

ZHENG JL, GAO WQ. Differential damage to auditory neurons and hair cells by ototoxins and neuroprotection by specific neurotropins in rat cochlear organotypic cultures. *Eur J Neurosci* 1996;8:1897-1905

ZHENG JL, STEWART RR, GAO WQ. Neurotropin-4/5, brain derived neurotropic factor and neurotrophn-3 promote survival of cultured vestibular ganglion neurons and protect them against neurotoxicity of ototoxins. *J Neurosci* 1995;28:330-340

ZIELHUIS GA, STRAATMAN H, RACH GH, VAN DEN BROEK P. Analysis and presentation of data on the natural course of otitis media with effusion in children. *Int J Epidemiol* 1990;19:1037-44

ZOU J, SAULNIER P, PERRIER T, ZHANG Y, MANNINEN T, TOPPILA E, PYYKKÖ I. Distribution of liquid nanocapsules in different cochlear cell populations after round window membrane permeation. *J Biomed Mater Res B Appl Biomater* 2008;87:10-8

ZOU J, LÄHELMÄ J, KOVISTO J, DHANASINGH A, JOLLY C, AARNISALO A, WOLFF J, PYYKKÖ I. Imaging cochlear implantation with round window insertion in human temporal bones and cochlear morphological variation using high-resolution cone beam CT. *Acta Otolaryngol* 2015;135:466-72